The effects of oncolytic Maraba virus (MG1) in malignant melanoma

Edward John Lloyd Armstrong

The Institute of Cancer Research, University of London

A thesis submitted for the degree of Doctor of Philosophy

January 2022

Declaration

This thesis was completed under the supervision of Dr Vicki Jennings, Professor Alan Melcher and Professor Kevin J. Harrington. The work described here was conducted at The Institute of Cancer Research (ICR), Chester Beatty Laboratories, 237 Fulham Road, London, SW3 6JB.

I, Edward John Lloyd Armstrong, confirm that the work presented in this thesis is my own. Where information has been derived from other sources, I confirm that this has been indicated within the thesis.

Signature: E. Armstrong

Date: 1st January 2022

1 Chapter 1: Preface

1.1 Abstract

Despite recent advances in the targeted and immunological treatment of melanoma, the incidence of this malignancy is increasing and is responsible for approximately 60000 global deaths annually, highlighting the ongoing need for novel treatments. Oncolytic viruses (OV) have demonstrated the capacity for selective infection, replication and killing of tumour cells and the subsequent activation of anti-tumour immunity. Maraba virus (MG1) is a promising OV currently being investigated within phase I/II clinical trials.

This thesis investigates the anti-tumoural effects of MG1 using both *in vitro* melanoma cell line models and within an immunocompetent *in vivo* murine model. The ability of MG1 to reach the tumour, replicate within it and exert anti-tumour survival benefits using different routes of administration and in different *in vivo* models was explored. In addition, the ability of MG1 infection to induce immunogenic cell death in melanoma cell lines and the changes in the tumour immune microenvironment *in vivo* was examined. Finally, in an attempt to enhance OV therapeutic outcomes, rational combination treatments of MG1 with additional immunotherapeutic agents were investigated.

The results discussed here demonstrate that oncolytic MG1 was able to selectively infect, replicate inside and kill melanoma tumour cells, both *in vitro* and *in vivo*. Furthermore, *in vivo*, the tumour tropic properties of MG1 were illustrated, even despite the production of anti-viral neutralising antibodies. MG1 could generate hallmarks of immunogenic cell death and alter the tumour immune microenvironment, at an immune cell, cytokine and RNA level. Intratumoural MG1 monotherapy was able to extend murine survival in a 4434, but not B16-F1, murine *in vivo* melanoma model. These survival gains could be enhanced through combining MG1 with an anti-PD-1 checkpoint inhibitor antibody.

1.2 Acknowledgements

I would like to thank my senior supervisors, Professor Alan Melcher and Professor Kevin Harrington, for giving me the opportunity to work on such an interesting and varied project, in addition to their guidance throughout my PhD. I would also like to express my gratitude to my assistant supervisor, Dr Vicki Jennings, for all her practical advice and support in supervising my laboratory work and for her constructive feedback during the writing of my thesis. I am also grateful to Dr Matthew Chiu for helping with *in vivo* experiments, for his collaboration in writing a literature review and for providing general support and friendship during the project. To Dr Shane Foo, who introduced me to the laboratory and taught me the basics of tissue culture, viral plaque assays, MTT assays and the conduct of performing responsible experiments with animals; to Eva Crespo-Rodriguez, for teaching me western blotting and other laboratory techniques; to Dr Emmanuel Patin, for teaching me to understand flow cytometry including sample preparation, compensation and data analysis; to Dr Malin Pedersen, Dr Martin McLaughlin and David Mansfield for ensuring the smooth running of the laboratory including ensuring the restocking and availability of consumables; to Harriet Whittock and Holly Baldock for providing animal care and assisting with tumour measurements; and to all the other members of the Harrington-Melcher laboratory.

I most gratefully acknowledge The Wellcome Trust for providing funding which has enabled me to undertake this PhD project, and to the ICR for the institutional and pastoral support provided to PhD students.

I am indebted to my family including my mother Veronica, my brother Jonathan and my partner Paula, for their unwavering support, understanding and patience throughout my PhD.

Finally, I would like to dedicate this thesis to my children, Master Emmanuel Armstrong and Miss Isabel Armstrong, for making everything I do worthwhile, and to the memory of my late father, Richard.

1.3 Statement of Impact

The global impact of COVID-19 has been profound, and its effects have not only been devastating for public health but impacted virtually every aspect of work and life. There have been major disruptions to research, which have impacted me directly. During the final year of my PhD, the ICR was closed completely for three months, with staff, including myself, placed on the furlough scheme. After a phased return to a COVID-secure environment, the services available for wet laboratory research were restricted due to social distancing measures. One aspect that affected me significantly was the limited access to the animal unit that prohibited me from repeating or initiating new *in vivo* experiments. In this thesis, I have therefore highlighted experiments which, if given more time and in the absence of COVID, would have benefited in strengthening my conclusions. Whilst both myself and my supervisors believe this disruption has not prevented me submitting an acceptable thesis, we thought this was worth highlighting and hope these issues can be taken into consideration when assessing my work.

Student: E. Armstrong

Supervisor: Alan Melcher

1.4 Table of Contents

1.5 List of Tables

1.6 List of Figures

1.7 Table of Abbreviations

ACK	Ammonium-chloride-potassium
ACT	Adoptive cell therapy
ADCC	Antibody-dependent cell-mediated cytotoxicity
ADV	Adenovirus
AE	Adverse events
AJCC	American Joint Committee on Cancer
APC	Antigen presenting cells
B2M	β_2 microglobulin
BiTE	Bispecific T cell engager
BRAF	V-raf murine sarcoma viral oncogene homologue B1
CAR-T	Chimeric antigen receptor T cell
CAR	Coxsackie and adenovirus receptor
CAV	Coxsackievirus
CCL	Chemokine (C-C motif) ligand
CD	Cytosine deaminase
CD	Cluster of differentiation
CDKN2A	Cyclin-dependent kinase inhibitor 2A
CEA	Carcinoembryonic antigen
cGAS	Cyclic GMP–AMP synthase
CI	Confidence Interval
CRAF	RAF proto-oncogene serine/threonine-protein kinase C
CRR	Complete response rate
CRT	Calreticulin
CTL	Cytotoxic T lymphocytes
CTLA-4	Cytotoxic T-lymphocyte-associated protein 4
CXCL	Chemokine (C-X-C motif) ligand

CXCR	Chemokine (C-X-C motif) receptor
DAF	Decay-accelerating factor
DAMP	Danger-associated molecular patterns
DC	Dendritic cells
DCT	Dopachrome tautomerase
DMSO	Dimethyl sulfoxide
DNA	Deoxyribonucleic acid
DTIC	Dacarbazine
ECM	Extracellular matrix
ELISA	Enzyme-linked immunosorbent assay
EMA	European Medicines Agency
FACS	Fluorescence activated cell sorting
FBS	Foetal bovine serum
FC	Flurocytosine
FDA	Food and Drug Administration
FGF	Fibroblast growth factor
FLUC	Firefly luciferase
FMG	Fusogenic membrane glycoprotein
FU	Fluorouracil
G-CSF	Granulocyte colony-stimulating factor
GDP	Guanosine diphosphate
GFP	Green fluorescent protein
GPCR	G-protein coupled receptor
GrzB	Granzyme B
GTP	Guanosine triphosphate
GITRL	Glucocorticoid-Induced tumour necrosis factor receptor ligand
GM-CSF	Granulocyte-macrophage colony-stimulating factor

GNA-11	Guanine nucleotide-binding protein subunit alpha-11
GNAC	Guanine nucleotide-binding protein G(q) subunit alpha
HCC	Hepatocellular carcinoma
HER	Human epidermal growth factor receptor
HFF	Human foreskin fibroblast
HLA	Human leukocyte antigen
HMGB	High motility group box
HPV	Human papillomavirus
HR	Hazard ratio
HSV	Herpes simplex virus
HVEM	Herpesvirus entry mediator
HRAS	Harvey Rat sarcoma virus
ICAM	Intra cellular adhesion molecule
ICB	Immune checkpoint blockade
ICD	Immunogenic cell death
ICI	Immune checkpoint inhibitors
ICOS	Inducible costimulatory
ICR	Institute of Cancer Research
ICV	Infected cell vaccine
IDO	Indoleamine 2, 3 dioxygenase
IFN	Interferon
IGF	Insulin-like growth factor
IHC	Immunohistochemistry
IL	Interleukin
IM	Intramuscular
IO	Immune oncology
IP	Intraperitoneal

IPRES	Innate anti-PD-1 resistance
IPS-1	Interferon-beta promoter stimulator 1
IRF	Interferon regulatory factor
IT	Intratumoural
IV	Intravenous
JAK	Janus-kinases
KIT	v-kit Hardy-Zuckerman 4 feline sarcoma viral oncogene homolog
KRAS	Kirsten rat sarcoma
LAG-3	Lymphocyte-activation gene 3
LDLR	Low-density lipoprotein receptor
LFA-3	Lymphocyte function-associated antigen 3
LLC	Lewis lung carcinoma (otherwise known as 3LL)
MAGE	Melanoma-associated antigen
MAPK	Mitogen-activated protein kinase
MAVS	Mitochondrial antiviral signalling protein
MDA-5	Melanoma differentiation associated protein 5
MDSC	Myeloid derived suppressor cells
MET	Mesenchymal-epithelial transition factor
MEK	Mitogen-activated protein kinase
MG1	Maraba virus
MHC	Major histocompatibility complex
MOI	Multiplicity of infection
mRNA	Messenger ribonucleic acid
MV	Measles virus
NAbs	Neutralising antibodies
NDV	Newcastle disease virus
NF1	Neurofibromatosis type 1

NFκB	Nuclear factor kappa-light-chain-enhancer of activated B cells
NGS	Next generation sequencing
NIS	Sodium iodide symporter
NK	Natural killer
NKT	Natural killer T cells
NO	Nitric oxide
NRAS	Neuroblastoma RAS viral oncogene homolog
NSCLC	Non-small cell lung cancer
NTRK	Neurotrophic tyrosine receptor kinase
ORR	Objective response rate
OS	Overall survival
OV	Oncolytic virus
PAMP	Pathogen-associated molecular pattern molecules
PBMC	Peripheral blood mononuclear cells
PBS	Phosphate-buffered saline
PCR	Polymerase chain reaction
PD-1	Programmed cell death protein 1
PD-L1	Programmed death-ligand 1
PFA	Paraformaldehyde
PFS	Progression free survival
pfu	Plaque forming unit
PIK3CA	Phosphatidylinositol-4,5-iphosphate 3-kinase catalytic subunit
PKR	Protein kinase R
PRR	Pattern recognition receptor
PSA	Prostate-specific antigen
PTEN	Phosphatase and tensin homolog
RAC1	Ras-related C3 botulinum toxin substrate 1

RANTES	Regulated on activation, normal T cell expressed and secreted
RB	Retinoblastoma
RET	Rearranged during transfection
RIG-I	Retinoic acid-inducible gene 1
RLU	Relative light units
RNA	Ribonucleic acid
ROS	Reactive oxygen species
RT3D	Reovirus type 3 Dearing
SD	Standard deviation
SFV	Semliki Forest virus
SHP	SH2 domain-containing protein tyrosine phosphatase
STAT1	Signal transducer and activator of transcription 1
STEAP	Six transmembrane antigen of the prostate
STING	Stimulator of interferon genes
STK	Serine/threonine kinase
TAA	Tumour-associated antigens
TAM	Tumour-associated macrophages
TAN	Tumour-associated neutrophils
TBK	TANK-binding kinase
TCGA	The Cancer Genome Atlas
TERT	Telomerase reverse transcriptase
TGF	Transforming growth factor
TIGIT	T cell immunoreceptor with Ig and ITIM domains
TIL	Tumour infiltrating lymphocytes
TIM-3	T-cell immunoglobulin and mucin-domain containing-3
TK	Tyrosine kinase
TKI	Tyrosine kinase inhibitor

TLS	Tertiary lymphoid structures
TME	Tumour microenvironment
TNBC	Triple negative breast cancer
TNF	Tumour necrosis factor
TNM	Tumour node metastases
TP53	Tumour protein p53
TRAIL	TNF-related apoptosis-inducing ligand
T-VEC	Talimogene laherparepvec
UKCCCR	United Kingdom Co-ordinating Committee on Cancer Research
UV	Ultraviolet radiation
VEGF	Vascular endothelial growth factor
VSV	Vesicular stomatitis virus
VV	Vaccinia virus

Chapter 2:

Introduction

2 Chapter 2: Introduction

2.1 Melanoma

2.1.1 Melanoma background

Melanoma skin cancer is the 5th most common cancer overall in the UK with an annual incidence of 16,200 cases per year. This is the equivalent of 32 cases per 100,000 people, and accounts for 4% of all new cancer cases. Since the 1990s, the incidence of melanoma has more than doubled due to a combination of increased ultraviolet radiation exposure and advancing life expectancy. Other risk factors include having a pale skin type, a family or personal history, a high number of melanocytic or dysplastic naevi and immunosuppression.[1]

Approximately 10% of cases are diagnosed at an advanced stage and whilst the outcome for some patients has improved, there continues to be a significant mortality attributed to melanoma, with 2285 deaths in the UK in 2016 and 59,782 deaths globally.[1]

There are four main types of cutaneous melanoma including superficial spreading, nodular, lentigo maligna and acral lentiginous which account for approximately 70%, 15%, 10% and <5% of all melanoma cases respectively. Of note, acral lentiginous melanoma is proportionally more common in people with dark skin types, is not related to sun exposure and usually occurs on the soles of the feet, palms of the hands or under the nails. Non-cutaneous melanomas include mucosal and ocular subtypes and are both rare, but tend to have a particularly poor prognosis.[1]

Survival for melanoma skin cancer is strongly related to stage of the disease at diagnosis with patients diagnosed at Stage I, II and III having a 100%, 98% and 94% one-year survival respectively. This compares to 53% of patients diagnosed with advanced disease, which, prior to the last decade, had a

median overall survival (mOS) of approximately eight months and typically less for patients with brain metastases.[1, 2]

2.1.2 Melanoma staging

The 8th edition of the AJCC melanoma staging system [3] is presented in Appendix 9.1.

2.1.3 Melanoma treatment in context

The traditional treatments for advanced melanoma included chemotherapeutic agents and outdated immunotherapies. The alkylating agent dacarbazine (DTIC) was widely used as a single agent for the treatment of advanced melanoma.[4, 5] Response rates with DTIC range from 5% to 12% in clinical trials, but responses are generally short-lived.[2, 5] Treatment with the immunotherapeutic agent IL-2 could lead to tumour responses in 5–10% of patients, sometimes with durable outcomes, but were frequently associated with notable toxicity.[2, 4-6] Prior to 2010, no treatment for advanced melanoma had been shown to improve patient overall survival (OS) in a phase III randomised controlled trial.[2, 4]

2.1.4 Molecular landscape of melanoma and targeted therapy

The advent of next-generation sequencing (NGS) and other high-throughput genomic profiling platforms has enabled a better understanding of the molecular landscape of melanoma. This understanding has subsequently led to the development of targeted therapies which have resulted in the longer survival of melanoma patients.

2.1.4.1 BRAF

The most significant mutation to have been identified are *BRAF* mutations which occur in 40-50% of patients with cutaneous melanoma.[7-9] Mutations in *BRAF* lead to the activation of the MAP kinase signalling pathway and a resultant upregulation in the promotion of cellular growth and the inhibition of apoptosis.[10, 11] The most common *BRAF* mutation is a substitution of glutamic acid for valine at amino acid 600 (V600E) accounting for 70–88% of all *BRAF* mutations.[7]

Gaining this understanding of the importance of *BRAF* mutations has led to the development of *BRAF* and *MEK* inhibitors which have both been shown in phase III trials to increase survival as single agents when compared to chemotherapy.[12, 13] Several subsequent trials have shown the superiority of combining these agents together [14-16] and therefore this approach has become a standard of care in the treatment of patients with *BRAF* mutant metastatic melanoma. Furthermore, in patients with high-risk, resected melanoma the combination of dabrafenib and trametinib has shown an improvement in both progression free survival (PFS) and OS when compared with placebo.[17]

2.1.4.2 NRAS

The *RAS* family includes three primary proto-oncogenes: *NRAS*, *KRAS*, and *HRAS*, that regulate cell proliferation and apoptosis. *NRAS* mutations occur in approximately 20% of melanoma patients[7, 9] with the majority of *NRAS* mutations involving a point mutation leading to the substitution of glutamine to leucine at position 61.[7] As with *BRAF*, *NRAS* mutations activate the MAPK, and PI3K signalling pathways resulting in cell growth and proliferation and dysregulation of cell cycle control mechanisms.[18] However, NRAS signals through activation of CRAF as opposed to BRAF thereby negating the potential for a BRAF targeted approach to treatment.[18-20]

NRAS-mutated melanoma is distinct from BRAF-mutated melanoma both in terms of its clinical presentation and prognostic features. Patients presenting with NRAS-mutated melanomas are usually older than 55 years of age with a more chronic pattern of ultraviolet exposure compared to patients with BRAF-mutated melanoma.[21] They are more common in non-sun exposed skin [22] and are associated with an aggressive clinical course and poor prognosis.[23, 24] Despite binimetinib (a MEK inhibitor), leading to a modest improvement in mPFS when compared to DTIC in NRAS mutated melanoma, survival was not prolonged [25] and therefore further clinical trials are needed in this cohort of patients.

2.1.4.3 NF1

The neurofibromatosis type 1 (*NF1*) tumour suppressor gene protein negatively regulates the MAPK pathway by converting active RAS-GTP to inactive RAS-GDP and therefore mutations and or loss of NF1 leads to MAPK pathway activation.[26] *NF1* mutations have been identified in 14% of melanomas, especially those which are BRAF or NRAS wild-type.[7] *NF1* mutations are shown to be associated with a high mutational burden and therefore there is good rationale for the use of immunotherapeutic agents in this cohort of patients.[9, 27]

2.1.4.4 KIT

KIT is a proto-oncogene tyrosine kinase receptor found on the cell membrane. The ligand for the KIT receptor is a cytokine named stem cell factor. Binding of this ligand activates dimerisation of the KIT protein and initiates signalling pathways affecting cell growth, proliferation, survival, and tumour cell migration.[9] Mutations in *KIT* occur in only 1–3% of all melanomas but are more commonly found in acral or mucosal melanomas and in areas of chronic sun damage.[28] Several KIT inhibitors including imatinib, nilotinib and dasatinib have shown activity in the treatment of *KIT*-mutant melanoma in phase II trials but responses are often short lived.[29-36]

2.1.4.5 Other mutations

Other mutations have been identified in genes encoding CDKN2A, p53, PTEN, RAC1, myc and TERT promoter regions. Of note, GNAQ/GNA11 mutations occur in 80-90% of uveal melanomas [7, 9] but unfortunately, trials of small molecule targeted treatments in this subset of patients have thus far been disappointing.[37] However, tebentafusp, a bispecific T cell engager (BiTE) drug, which has affinity to the gp100 protein, has recently shown to improve OS in previously untreated metastatic uveal melanoma patients with the HLA-A*02:01 subtype.[38]

2.1.5 Melanoma and the tumour immune microenvironment

Testing for and characterising the mutations discussed above is clearly important in identifying driver mutations that have led to, and have the potential for future, practice changing treatments.

However, as shown by *Alexandrov et al.*, advanced sequencing techniques have now enabled a whole repertoire of somatic mutations to be identified by sequencing and comparing whole genomes from individual cancer samples with normal DNA from the same individuals.[39] This has led to the establishment of mutation signatures and an understanding of the prevalence and variability of somatic mutations between different tumour types (Figure 1).[39]

Figure 1: Signatures of mutational processes in human cancer

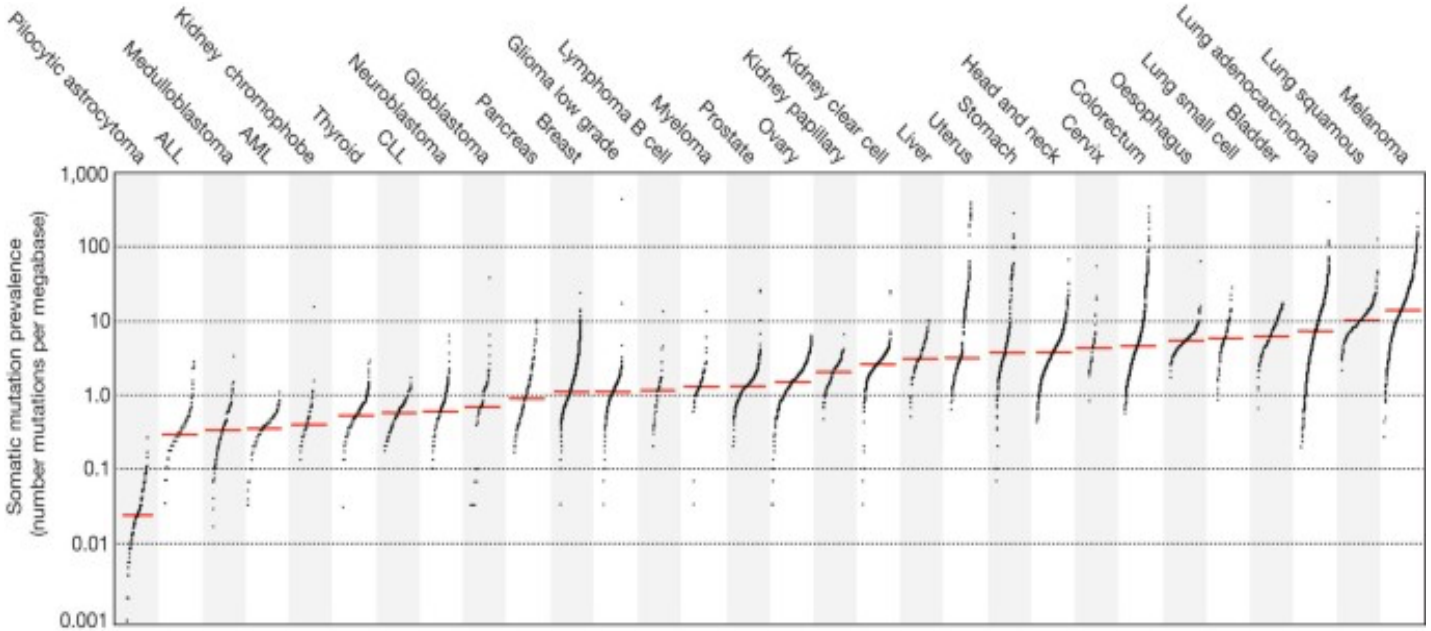

Figure adapted from Alexandrov, L.B., et al., *Signatures of mutational processes in human cancer.* Nature, 2013. 500(7463): 415-421 [39]

As illustrated, melanoma has shown the highest prevalence of somatic mutations of any major cancer type with over ten mutations per megabase of DNA.[39] It is implied, that this high mutational burden generates a high number of neoantigens, against which the immune system can mount a specific response.[40, 41] In view of this, melanoma is considered to be highly immunogenic [41] with immunosurveillance playing a prominent role in its development, progression and potential for treatment opportunities.[40]

2.1.6 Cancer immunosurveillance and immunoediting

Evading immune destruction was included as a hallmark of cancer by Hanahan and Weinburg in 2011,[42] however the recognition of the interaction between cancer and the immune system dates back over 100 years. In the 1890s, the sarcoma surgeon, William Coley, noted a patient's spontaneous tumour regression following a severe infection.[43] This led Coley to treat over 1000 cancer patients with bacteria and bacteria products, known as Coley's toxins.[44] In time, these became overlooked due to the lack of consistent outcomes and were soon superseded by the development of more effective treatments including radiotherapy and chemotherapy.[45]

The concept that the cancer and the immune system could interact was proposed by Ehrlich in the early 20th century who experimented in attempting to generate immunity to cancer by injecting weakened cancer cells.[46] These ideas were refined into the cancer immunosurveillance theory by Burnet and Thomas in the 1950s and stated that the emergence of malignant cells can be identified and suppressed by the host's immune system, and that cancer develops when this immunity is weakened.[47, 48] Although it is recognised that certain cancers are more common in the immunosuppressed, the hypothesis was questioned given that athymic nude mice do not show an increased incidence of tumours compared to wild-type animals and, in addition, that tumours can arise in the presence of a functioning immune system.[45, 49, 50]

The cancer immune-editing concept was proposed by Dunn in 2002 and recognised that through interactions between immune cells, tumour cells and the tumour microenvironment, the immune system can play a role in both suppressing tumour growth but also enabling tumour progression. This acts through three dynamic processes of elimination, equilibrium and escape.[45, 51]

In the first phase, termed elimination, the immune system recognises tumour cells as abnormal, leading to their destruction. If at this stage, all the nascent transforming cells are successfully destroyed, then then whole cancer editing process is complete.

However, if some malignant cell variants survive the elimination process, they enter into a phase of equilibrium with the immune system. In this state, the immune system is able to exert a control on tumour cell growth but is unable to fully eradicate it. During this dynamic equilibrium, many of the original tumour cell variants are destroyed, however, new variants arise which harbour different mutations and gradually, through survival selection pressure, these cells progressively acquire increased immune resistance. This equilibrium phase can persist over many years and may account for the clinical scenario where patients undergo prolonged periods of remission before cancer relapse.

Finally, the escape phase is marked when a new population of tumour clones have developed with mechanisms that enable the avoidance of immunological detection and the ability to proliferate despite an immunologically intact host environment.[45, 51]

2.1.7 Melanoma and the immune system

As our appreciation of the immune editing process has evolved, so too has our understanding of the constituent parts of immunology, including the innate and adaptive immune systems, and what role these play in helping or hampering the development of cancer, including melanoma.

2.1.7.1 Innate immunity

2.1.7.1.1 Macrophages

Macrophages are innate immune cells that differentiate from circulating monocytes following their extravasation into tissues. Upon differentiation, macrophages sense and respond to infections and inflammation and are involved in tissue homeostasis and repair.[52] In oncological patients and preclinical models, tumour-associated macrophages (TAMs) correlate with a poor prognosis and reduced overall survival.[53, 54]

Activated macrophages are commonly described as either pro-inflammatory M1-type or anti-inflammatory M2-type. During carcinogenesis, anti-tumour macrophages often display an M1-like polarisation characterised by the secretion of pro-inflammatory cytokines IL-1, IL-6 and TNF-α that are involved in the elimination of more immunogenic cancer cells.[55] In addition, anti-tumour macrophages also contribute to the anti-tumour response through their antigen-presenting capacity.[40] However, as the tumour progresses, the macrophages tend towards a pro-tumourigenic M2-like polarisation that enables tumour progression through the promotion and stimulation of angiogenesis by vascular endothelial growth factor (VEGF) secretion [56], cancer cell proliferation through epidermal growth factor release [57] and the suppression of anti-tumour effector immune cells.[54, 58]

2.1.7.1.2 Macrophages and melanoma

In a murine BRAF mutant model of melanoma, it has been shown that tumour progression is associated with a transition from an M1 to an M2 polarised macrophage population and that, ongoing tumour survival and proliferation is dependent on the presence and secretion of transforming growth factor beta (TGF-β) from M2 macrophages.[59] Furthermore, studies of tissue collected from patients treated with BRAF inhibitors found that a high number

of macrophages before treatment predicts for early relapse and a shorter PFS.[60]

2.1.7.1.3 Neutrophils

As the most abundant innate immune cell, neutrophils play an important role in the recognition of inflammation and infection. Following their recruitment to affected tissue, they can counter pathogens by means of phagocytosis, degranulation and though the deposition of neutrophil extracellular traps.[61] In patients, an elevated level of tumour-associated neutrophils (TANs) or a high neutrophil:lymphocyte ratio have been associated with an adverse prognosis in different malignancies.[62-65] Indeed, a circulating blood neutrophilia is used in the prognostic scoring of advanced renal cell carcinoma, thereby directly influencing treatment decisions.[66]

The recruitment of TANs to the tumour microenvironment (TME) is mediated mainly through CXCR2 ligands including CXCL1, CXCL2 and CXCL5,[54, 67] which are secreted by cancer and stromal cells, and also through TGF-β which has also been associated with recruitment and reprogramming to pro-tumour TANs.[68]

The exact function of neutrophils in malignancy is unclear as they appear to have both anti- and pro-tumour effects. In human colorectal cancer, high levels of TANs have been associated with better prognosis by enhancing the effector function of $CD8^+$ T cells.[69] Neutrophils can also exert a tumouricidal function enhancing radiotherapy effectiveness particularly when given concurrently with granulocyte colony-stimulating factor (G-CSF).[70]

Conversely, TANs may contribute to inflammation during cancer initiation and progression, thereby promoting tumour growth.[54, 71] In addition, the secretion of neutrophil elastase promotes invasion, cancer cell proliferation and angiogenesis,[71, 72] which is further stimulated through the release, by neutrophils, of factors including VEGF.[56]

TANs can also have immunosuppressive effects on effector T cells through increasing PD-L1 expression [73] and may mediate the development of lung premetastatic niches which enable tumour cells to survive and proliferate at metastatic sites.[54, 56, 74]

2.1.7.1.4 Neutrophils and melanoma

Although the role of neutrophils in melanoma is poorly understood, their existence in human primary melanoma has been correlated with a poor prognosis.[64] In murine melanoma models, the depletion of TANs has been shown to slow tumour growth,[75] however their presence may be necessary to complement antibody-mediated killing of tumour cells in the context of immunotherapy treatment.[40, 76]

2.1.7.1.5 NK cells

NK cells are innate immune cells that display cytolytic activity in response to infected or transformed cells.[54, 77] NK cells have a wide array of inhibitory and stimulatory receptors on their cell surface that are used for immune surveillance. The inhibitory receptors on NK cells exert an anti-tumour effect through the targeting of tumour cells aberrantly lacking major histocompatibility class I (MHC-I) and marking them for programmed cell death.[78] In this regard, the presence of NK cell infiltration in colorectal, gastric, kidney and lung cancer tumours correlates with a favourable outcome.[79-83]

In murine cancer models, aberrant cell proliferation, DNA damage and RAS pathway activation lead to the tumour cell production of ligands that are recognized by the NKG2D transmembrane receptor on NK cells, resulting in NK cell activation.[54] Upon activation, NK cells mediate tumour killing through the release of cytotoxic perforin and granzyme [84] and can also trigger apoptotic pathways in tumour cells through the production of TNF-α or

via direct cell-to-cell contact through activation of the TRAIL and FASL pathways.[54]

2.1.7.1.6 NK cells and melanoma

Although NK cell numbers are generally low in melanoma,[85] an increased level of NK cells in stage III melanoma is associated with longer survival.[86] In addition, the expression of NKG2D on NK cells is associated with a better prognosis in patients with BRAF-mutant melanoma.[87] NK cells expressing granzyme B and CD16, the latter of which is critical in antibody-dependent cell-mediated cytotoxicity (ADCC),[88] has also been shown to correlate with an improved response to anti-PD-1 therapy.[40, 89]

2.1.7.1.7 Dendritic cells

Dendritic cells (DCs) are specialised antigen-presenting cells (APCs) that represent the interface between innate and adaptive immunity. They present endogenous and exogenous antigens to T cells in the context of MHC molecules and as such, while they may not act directly upon tumour cells, they do have an important role to play in initiating and modulating T cell responses to tumours.[54]

Immature $CD1a^+$ DCs are effective in phagocytosing antigens but are poor stimulators of T cell activity. Mature dendritic cells, characterised by the expression of markers including CD80, CD83 and CD86, are potent activators of T cells, and are associated with a stronger T-cell response.[90] Immature dendritic cells are more likely to infiltrate the tumour, whereas mature dendritic cells remain confined to the tumour margins and peri-tumoural areas from where they generate an ongoing immune response and contribute to increased T cell activation at the tumour margin. Mature DCs have been associated with improved patient survival in different cancer types, further demonstrating their contribution to the promotion of anti-tumour immunity.[40]

In addition to their maturation status, the dendritic cell lineage also contributes to the DC response to tumours, with conventional dendritic cells (cDCs) being of myeloid lineage, and plasmacytoid dendritic cells (pDCs) being of lymphoid lineage. cDCs, characterised by CD141 expression in humans, are the main dendritic cell APC and activate tumour-specific $CD8^+$ T cells through antigen cross-presentation.[91] By contrast, the production of IFN-α by pDCs may promote regulatory T cell (Treg) expansion and therefore pDCs can limit the anti-tumour immune response.[92]

2.1.7.1.8 Dendritic cells and melanoma

In primary melanoma, cDCs are thought to promote an anti-tumour immune response as they have been found to be elevated in patients without nodal metastasis. Conversely, pDCs have been associated with a poor outcome in primary melanoma.[64] A poor outcome from melanoma also correlates with a downregulation of genes in the β-catenin pathway [93] and, as has been shown in murine models, this may impair cDC trafficking and subsequent $CD8^+$ T cell immunity.[40]

Several phase I and II clinical trials have investigated the use of autologous DCs pulsed with tumour antigens, with the aim of increasing tumour antigen cross-presentation in order to initiate an anti-tumour T-cell response. This showed promising but limited success, especially in melanoma.[94, 95] It was discussed that the *ex vivo* DC antigen loading may have impacted the subsequent DC function when returned *in vivo*. A more recent phase II study in 39 melanoma patients showed that the combination of an intradermal autologous DC vaccine combined with ipilimumab resulted in an overall response rate (ORR) of 38% with eight complete and seven partial responses [96] and therefore, the use of DC vaccines in conjunction with checkpoint blockade is an interesting strategy to pursue.[54]

2.1.7.2 Adaptive immunity

2.1.7.2.1 T cells

T cells are components of the adaptive immune system that act as helpers, regulators and effectors of immunity. Depending on the immunological context, T cells can acquire differing phenotypes and consequently these subsets can have opposing effects on the immune response and cancer survival.[82]

2.1.7.2.1.1 $CD8^+$ T cells

$CD8^+$ T cells are considered the primary effectors of the anti-tumour response through their ability to deliver cytotoxic activity towards cells that present a particular epitope on MHC-I. Upon recognition of target cells, $CD8^+$ T cells can cause target tumour cell death by releasing cytotoxic granules containing granzyme B and perforin on to the surface of target cells and also by inducing apoptosis pathways through the binding between the target cell Fas receptors with the $CD8^+$ membrane FasL.[40]

The presence of $CD8^+$ T cells in the TME has been correlated with improved survival in a range of human cancers including melanoma [97, 98], lung [99], colorectal [100], renal [101], ovarian [102], breast [103] and bladder cancer [104] among others.[55] As $CD8^+$ T-cell effector function relies on cell-to-cell contact, the activity of $CD8^+$ T cells is impacted by their location in relation to tumour cells. Typically, the highest proportions of $CD8^+$ T cells can be found at the margins of solid tumours, but they also comprise a significant share of tumour-infiltrating lymphocytes (TILs).[105]

Another important role of the $CD8^+$ T-cell population is their potential to provide long-lasting anti-tumour immunity.[106] Furthermore, the high expression of immune checkpoint receptors including PD-1 and CTLA-4 [107] on $CD8^+$ cells

allows them to be good targets for reactivation through the use of immune checkpoint antibodies.[40]

2.1.7.2.1.2 CD8$^+$ T cells and melanoma

As mentioned, the presence of CD8$^+$ T cells have been found to be a predictive indicator of improved outcomes in melanoma. In addition, in stage III melanoma, higher levels of CD8$^+$ T cells expressing the CD56 marker of activation predicts for prolonged overall survival. Furthermore, tumour-resident CD8$^+$ T cells have been associated with improved responses to anti-PD-1 therapy. At present, however, whilst the prognostic significance of activated tumoural CD8$^+$ T cells is evident, it is still to be determined whether the identification of such immune patterns in tumour samples can act as a biomarker to help guide therapy decisions in metastatic or adjuvant melanoma patients.[87, 108]

In mice, CD8$^+$ T cells have been found to confer immune protection following rechallenge with melanoma [109] and it is suggested that tumour-resident CD8$^+$ T cells could play an important role in maintaining an immune equilibrium with melanoma cells to prevent tumour escape.[110]

2.1.7.2.1.3 Helper CD4+ T cells

Helper CD4$^+$ T cells (Th) are also activated following antigen presentation, but in contrast to CD8$^+$ T cells, they are restricted to recognising antigens presented by MHC class II present on APCs.[40] They proliferate upon recognition of tumour-associated antigens and have been located within the immune microenvironment in melanoma tumours among others.[111] Several functionally distinct subtypes of CD4$^+$ helper T cells exist, including Th1, Th2 and Th17.

Th1 cells activate the immune response to intracellular pathogens through secretion of high amounts of proinflammatory cytokines such as IL-2, TNF-α,

and IFN-γ, leading to the promotion of the $CD8^+$ T cell cytotoxic response and the anti-tumoural activity of macrophages and NK cells.[112, 113] Separate studies described that Th1 numbers and the expression of Th1 genes are associated with a better prognosis in certain malignancies.[100, 114]

Conversely, Th2 cells can suppress the Th1 response and activate regulatory macrophages and B cells through the increased secretion of immunosuppressive cytokines including IL-10 and IL-4. A high Th2 to Th1 ratio has been associated with reduced survival in certain malignancies.[115, 116]

Th17 cells release the cytokine IL-17 and are considered to be pro-inflammatory as it has been shown in both murine and human data that Th17 cells recruit $CD8^+$ T cells and NK cells to the site of the tumour. In addition, the presence of Th17 cytokines correlate with both the presence of Th1 cells and patient survival.[40]

2.1.7.2.1.4 Helper $CD4^+$ T cells and melanoma

In general, Th1 is regarded as the predominant anti-tumour $CD4^+$ T cell subset and this observation is supported in melanoma. For instance in melanoma lymph node metastases, a higher expression of Th2 than Th1 cytokine genes were identified, indicating that melanoma progression and the predominant Th subtype may be connected.[117] In addition, studies in murine melanoma models have found that Th17 cells, through the production of IFN-γ, can play a role in tumour eradication.[118]

2.1.7.2.1.5 Regulatory T cells

$CD4^+FoxP3^+CD25^+$ regulatory T cells (Tregs) suppress the activity of $CD8^+$ T cells, antigen-presenting cells and other immune cells. This is mediated through the expression of inhibitory ligands including CTLA-4, inhibitory

cytokines including IL-10 or by depriving T cells of essential growth factors such as IL-2 and amino acids.[40, 119]

Given their role in the suppression of $CD8^+$ T cell activity, it has been demonstrated in multiple tumour types that Tregs cells contribute to the early establishment and progression of tumours in murine models and that their absence results in the delay of tumour progression.[120, 121]

Furthermore, in human studies, it has been found that a high tumour infiltration of Tregs, or a low ratio of effector T cells to Treg cells, is associated with reduced patient survival in different cancer types.[122] Due to their ability to act in both a cell-to-cell-dependent manner and also through the release of immunosuppressive cytokines, Treg tumour localisation is not as strongly predictive of patient outcome as it is for $CD8^+$ T cells.[54, 123]

2.1.7.2.1.6 Regulatory T cells and melanoma

In melanoma, as with other malignancies, $FoxP3^+$ $CD25^+$ Tregs have been associated with a poorer prognosis and a reduced number of tumoural $CD8^+$ and $CD4^+$ T cells and therefore, they have been targeted in an attempt to improve outcomes.[87]

In preclinical murine models, the anti-CD25 antibody clone PC-61 partially depletes Treg cells in the blood and peripheral lymphoid organs and has shown the capacity to inhibit tumour growth and improve survival when administered before or soon after tumour implantation.[120, 124] However, the use of anti-CD25 antibodies to reduce Tregs as a therapeutic intervention against established tumours has generally failed to delay tumour growth or prolong survival.[120, 121]

Early-phase clinical studies in patients with advanced melanoma have investigated using an human anti-CD25 antibody.[125, 126] These results demonstrated a variable effect on circulatory Treg cell numbers, however they

have not shown clear evidence that Treg cells in the TME are depleted effectively, and have therefore had a disappointing resultant effect on anti-tumour activity, with no survival benefits observed.[121]

However, more recently it has been proposed that one mechanism by which anti-CTLA-4 antibodies may function is through the reduction of intratumoural Treg cells.[121, 127, 128] These authors therefore, developed an antibody, αCD25-m2a, that was optimised to bind to the Treg FcγR and through ADCC resulted in superior intratumoural Treg depletion. In murine models this optimised antibody had a greater therapeutic effect compared to its unoptimised counterpart and also showed a potent synergy when combined with anti-PD-1 blockade.[121]

Furthermore, our group has demonstrated that in a murine BRAF mutant melanoma model, adding this optimised anti-CD25 antibody as a triplet treatment can further enhance the therapeutic effects of the doublet combination of an intratumoural oncolytic herpes virus (HSV) and oral BRAF targeted agent.[129] This triple combination was also associated with a marked increase in tumoural $CD8^+$ T cell infiltration. Whether depleting Tregs can have a beneficial effect in human clinical trials requires further exploration.

2.1.7.2.2 B cells

Upon activation in the germinal centres in lymphoid organs, B cells expressing high-affinity antibodies differentiate into antibody-secreting plasma cells and memory B cells that mediate humoral immunity.[54] Although B cells only comprise a small percentage of the immune infiltrate in cancer, they have a broad range of functions in the TME and various impacts on tumour outcome.[40, 82, 130]

B cells are able to produce anti-tumour antibodies that can localise within the TME. These infiltrating B cells often cluster in tertiary lymphoid structures (TLSs) [131] and these have been shown to correlate with favourable patient

outcomes including in ovarian, colorectal and pancreatic cancer.[40] Tumour infiltrating B cells have also been found to proliferate in response to, and have clonality against tumour antigens suggesting that B cells represent part of an ongoing anti-tumour immune response.[40, 132] However, B cells are generally regarded as playing a role in promoting tumour progression and B cell functions that are normally part of a robust immune response can actually be detrimental in the context of the TME.[40, 130]

For instance, studies in murine models have shown that the lack of mature B cells decreases tumour progression and the adoptive transfer of B cells can restore chronic inflammation, angiogenesis and tumour growth.[54] Mechanistically, this may occur by increasing the immunosuppressive environment through IL-10, IL-35 and TGF-β secretion. Furthermore, as a result of immunoglobulin deposition in the tissue microenvironment, B cells can indirectly stimulate angiogenesis and chronic inflammation.[54]

2.1.7.2.3 B cells and melanoma

B cells have not been studied as extensively as their T cell counterparts, however, in one study in patients with metastatic melanoma, immunohistochemical staining of patient samples demonstrated that a high density of intratumoural B cells and plasma cells correlated with improved survival.[85]

Conversely, plasma cells have correlated with poor survival in primary melanoma and it has been speculated that the production of IgA by plasma cells may impede the immune response to melanoma by physically blocking immune cell access to the tumour.[132, 133] In metastatic melanoma the release of IGF-1 by B cells may also have a mechanistic role in the resistance to BRAF and MEK inhibitors.[40, 134]

Currently therefore, it appears that B cells have conflicting roles in the immune response to melanoma and a better understanding of their function in malignancy is necessary to realise any potential therapeutic interventions.

To summarise, whilst much remains to be identified, we have developed an understanding of the constituent parts of the immune system and what roles this plays in the development of malignancy, including melanoma. Indeed, as will be discussed, it is arguably within the field of melanoma, that this understanding has resulted in the most significant advancements in therapies that harness the immune system for improved patient outcomes.

2.1.8 Melanoma and immunotherapy

The identification of immune checkpoint molecules and their role in regulating the tumour immune response has been pivotal in the development of novel therapies in many tumour types, in particular for the treatment of melanoma.[135] The generation of an immune signal requires the presentation of tumour antigens by major histocompatibility complex (MHC) class I or II molecules on antigen presenting cells. The simultaneous binding of CD28 on the T cell surface with a costimulatory B7 ligand on the APC leads to subsequent anti-tumour T cell activation.[2, 127, 136]

To counter this activation, the intracellular CTLA-4 protein translocates to the T cell surface where it binds to the B7 ligand with a higher avidity than CD28 thereby generating an opposing signal that inhibits T cell proliferation. CTLA-4 therefore acts as a negative regulator of the T cell response.[2, 136, 137]

The programmed death 1 (PD-1) receptor also acts as a negative regulator of anti-tumour T cell effector function, predominantly within peripheral tissues. The binding of the PD-1 receptor to its tumour cell surface ligand PD-L1 triggers the dephosphorylation of SHP-2 and inhibition of intracellular signals involved in T cell activation.[138, 139] Inflammation-induced PD-L1

expression in the TME leads to PD-1-mediated T cell exhaustion, inhibiting the cytotoxic T cell anti-tumour response.[135, 140, 141]

This understanding of the mechanisms of checkpoint control over the T cell anti-tumour response has enabled the development of immune checkpoint antibodies, that, put simply, act by blocking the inhibition of T cell activation. These have since become a standard of care in the treatment of melanoma, both in the advanced and adjuvant treatment settings.

The first phase III immunotherapy trial to show a survival advantage in advanced melanoma compared ipilimumab (a humanised anti-CLTA-4 antibody), administered with or without a glycoprotein 100 (gp100) peptide vaccine, with gp100 alone in patients with previously treated metastatic melanoma. Ipilimumab resulted in a mOS of 10.0 months among patients receiving ipilimumab plus gp100, as compared with 6.4 months among patients receiving gp100 alone (HR 0.68; P<0.001). The mOS with ipilimumab alone was 10.1 months (HR in the comparison with gp100 alone, 0.66; P=0.003). No difference in OS was detected between the two ipilimumab groups (HR 1.04; P=0.76).[142]

Following this success, ipilimumab plus DTIC was compared to DTIC alone in patients with treatment-naive metastatic melanoma. OS was significantly longer in the group receiving ipilimumab plus DTIC than in the group receiving DTIC plus placebo (11.2 months vs. 9.1 months, HR 0.72; P<0.001), with higher survival rates in the ipilimumab plus DTIC group at one year (47.3% vs. 36.3%), two years (28.5% vs. 17.9%), and three years (20.8% vs. 12.2%) However, grade 3 or 4 adverse events occurred in 56.3% of patients treated with ipilimumab plus DTIC, as compared with 27.5% treated with DTIC and placebo (P<0.001).[143]

Attempting to harness inhibition of the PD-1/PD-L1 axis, the Checkmate 066 trial compared nivolumab (a humanised IgG4 anti-PD-1 antibody) with DTIC in previously untreated patients with advanced BRAF wild-type melanoma.

The overall rate of survival at one year was 72.9% in the nivolumab group, as compared with 42.1% in the DTIC group (HR, 0.42; P<0.001) with an improved mPFS of 5.1 months with nivolumab versus 2.2 months with DTIC (0.43; P<0.001). The ORR was 40.0% in the nivolumab group versus 13.9% in the DTIC group (P<0.001). The survival benefit with nivolumab versus DTIC was observed across prespecified subgroups, including subgroups defined by PD-L1 status. Grade 3 or 4 drug-related adverse events occurred in 11.7% of the patients treated with nivolumab and 17.6% of those treated with DTIC.[144]

Pembrolizumab (another humanised IgG4 anti-PD-1 antibody) was evaluated in the phase III Keynote 006 study in patients with untreated advanced melanoma. Two different pembrolizumab schedules were compared with ipilimumab.

The results showed an improved one-year survival rate of 74.1%, 68.4%, and 58.2% respectively, for two-weekly pembrolizumab (HR 0.63; P=0.0005) and three-weekly pembrolizumab (HR 0.69; P=0.0036) versus ipilimumab and a PFS at six months of 47.3%, 46.4% and 26.5% respectively (HR 0.58; P<0.001). In addition, response rates were 33.7%, 32.9%, for the two pembrolizumab schedules and 11.9% for ipilimumab (P<0.001). Encouragingly, treatment-related adverse events of grade 3 to 5 severity were lower in the pembrolizumab groups (13.3% and 10.1%) than in the ipilimumab group (19.9%).[145]

Subsequent results following almost five years of follow up have continued to demonstrate the superiority of pembrolizumab versus ipilimumab with a mOS of 32.7 months in the combined pembrolizumab groups and 15.9 months in the ipilimumab group (HR 0.73, p=0.00049).[146]

In the same year as Keynote 006, the data from the Checkmate 067 trial were published investigating nivolumab plus ipilimumab, nivolumab alone, or ipilimumab alone in previously untreated patients with metastatic melanoma. The mPFS survival was 11.5 months with nivolumab plus ipilimumab and 6.9

months with nivolumab alone as compared with 2.9 months with ipilimumab (HR 0.42; P<0.001) and (HR 0.57; P<0.001) respectively.

Treatment-related adverse events of grade 3 or 4 occurred in 59% of the patients in the nivolumab-plus-ipilimumab group, in 21% of those in the nivolumab group, and in 28% of those in the ipilimumab group.[147] Subsequent results at three years demonstrated the mOS had not been reached in the nivolumab-plus-ipilimumab group compared to 37.6 months in the nivolumab group, and with 19.9 months in the ipilimumab group (HR for nivolumab plus ipilimumab vs. ipilimumab, 0.55; P<0.001)(HR for nivolumab vs. ipilimumab, 0.65; P<0.001).[148] With further follow up, the OS at five years was 52% in the nivolumab-plus-ipilimumab group and 44% in the nivolumab group, as compared with 26% in the ipilimumab group.[149]

Thus, at present, both the anti-CTLA-4 and anti-PD-1 antibody combination of ipilimumab with nivolumab, in addition to the anti-PD-1 monotherapy treatments, continue as current standard of care options in the first line treatment of metastatic melanoma. In those patients with BRAF positive disease, trials are currently on-going to establish whether an initial targeted or immunotherapeutic approach, or an upfront combination of both, is preferred.[150]

The immunotherapy agents discussed above have also been evaluated in the adjuvant setting.

In one phase III trial, patients were given ipilimumab or placebo every three weeks for four doses, then every three months for up to three years. The median recurrence-free survival was 26.1 months in the ipilimumab group versus 17.1 months in the placebo group (HR 0.75; p=0.0013), however, adverse events led to the discontinuation of treatment in 52% of patients who started ipilimumab.[151]

In the subsequent Checkmate 238 trial, adjuvant nivolumab was compared to ipilimumab and showed a one-year recurrence-free survival of 70.5% and

60.8% respectively (HR 0.65; P<0.001). Nivolumab was also associated with lower treatment related adverse events and fewer treatment discontinuations.[152] The four-year recurrence-free survival rate continued to demonstrate an advantage in the nivolumab group compared to ipilimumab.[153]

Pembrolizumab has also been evaluated in the adjuvant setting in patients with resected stage III melanoma. Patients received pembrolizumab or placebo for one year and pembrolizumab was associated with significantly longer recurrence-free survival of 75.4% compared to 61.0% respectively (HR 0.57; P<0.001) with grade 3-5 adverse events occurring in 14.7% versus 3.4% of patients.[154] Pembrolizumab is also being considered for use in the adjuvant setting for patients with stage IIB and IIC tumours following encouraging data from the phase III Keynote 716 study.[155]

2.1.9 Resistance to immunotherapy

Despite the progress observed with cancer immunotherapy detailed above, many patients still fail to benefit from treatment. This could be due to primary immune resistance, and in those patients who initially respond, relapse may subsequently occur due to an acquired resistance.[45] Although not an exhaustive list of all potential mechanisms, these have been categorised and discussed below.

2.1.9.1 Primary resistance to immunotherapy

2.1.9.1.1 Factors intrinsic to the tumour cell

Several mechanisms have been identified within tumour cells which may contribute to immunotherapy resistance. A common oncogenic driver in tumour cells is aberrant signalling through the MAPK pathway. This can lead to increased production of VEGF and IL-8, whose function includes the promotion of angiogenesis. These factors can have an inhibitory effect on T-

cell tumour infiltration and therefore immune resistance.[156] This was found in melanoma tumour biopsies, where increased levels of VEGF were noted in patients not responding to treatment with anti–CTLA-4 and anti–PD-1 immunotherapy, in comparison to those patients that did respond.[157] To support this further, in both murine models and human biopsy samples, treatment with BRAF inhibition has resulted in VEGF downregulation and increased T-cell recruitment [158] and in a murine model of melanoma, anti-VEGF therapy can increase T cell tumour infiltration.[159]

VEGF expression can also have a role in T cell activation through its effects on DC maturation. DC maturation results in the increased expression of markers necessary for stimulation of naïve T cells.[160] In human melanoma tumours the density of DCs correlates with the density of activated T cells and these have been identified as an independent factor of prognosis.[161] As VEGF can have inhibitory effects on DC maturation [162, 163] this further supports a primary resistance pattern in tumours expressing VEGF.

In addition, the loss of the *PTEN* tumour suppressor gene, results in unopposed signalling through the PI3K pathway and can result in increased PD-L1 tumour cell expression.[164] This can result in the inhibition of the T cell-mediated anti-tumour response and treatment with a PI3K inhibitor can improve the efficacy of both anti-PD-1 and anti-CTLA-4 antibodies in murine melanoma models. Furthermore, it was shown that in patients, PTEN loss correlates with decreased T-cell infiltration at tumour sites and inferior outcomes with anti-PD-1 antibody treatment.[165]

Another molecule effecting the negative regulation of T-cell function and immune resistance is indoleamine 2,3-dioxygenase (IDO).[166] IDO overexpression increases the enzymatic conversion of tryptophan to kynurenine which suppresses T-cell proliferation and activity, as well as increasing tumour-infiltrating myeloid-derived suppressor cells (MDSC) and Treg cells.[156, 167] Murine experiments combining inhibitors of IDO with CTLA-4 blockade demonstrate a synergy leading to rejection of tumours in a T cell dependent manner and leading to enhanced effector T cell activity. This

thereby suggests the immunosuppressive role of IDO in the context of immune checkpoint inhibition.[168]

A further mechanism of primary resistance to immunotherapy was identified by transcriptomic analysis of melanoma tumours from patients failing to respond to anti-PD-1 treatment. This showed an innate anti-PD-1 resistance signature, or IPRES, with a concurrent increased expression of genes involved in the regulation of mesenchymal transition, cell adhesion, extracellular matrix remodelling, angiogenesis, and wound healing.[169] These findings imply that attenuating the biological processes that underlie IPRES may improve anti-PD-1 responses in melanoma and other cancer types.

The interferon-gamma (IFN-γ) pathway has favourable effects on the anti-tumour immune response to checkpoint blockade.[45, 170, 171] IFN-γ produced by tumour-specific T cells, including in response to anti-CTLA-4 therapy,[172] can induce an effective anti-tumour immune response. However, resistance to immune checkpoint blockade may be mediated by mutations or epigenetic changes in the interferon receptor signalling pathway.[170] It has been demonstrated that for effective anti-CTLA-4 therapy, IFN-γ signalling is critical, as murine melanoma models with IFN-γ receptor 1 (IFNGR1) knockdown have impaired tumour rejection upon anti-CTLA-4 therapy.[170] Furthermore, the analysis of tumours from patients who failed to respond to ipilimumab revealed an increased number of alterations in the IFN-γ pathway.[170] These mutations prevent IFN-γ mediated signalling along the Janus kinase 2 (JAK2)/signal transducer and activators of transcription (STAT1) and interferon regulatory factor (IRF) pathway and consequently, tumour cells are able to escape from IFN-γ mediated T-cell attack, thereby resulting in primary resistance to anti-CTLA-4 therapy.[170] Additionally, mutations in this pathway result in a lack of IFN-γ driven PD-L1 expression and therefore, subsequently blocking of PD-L1 or PD-1 with checkpoint antibodies would be ineffective, as these patients would harbour a primary resistance to such therapy.[173]

Levels of tumour cell expression of PD-L1 have also been shown to impact on immunotherapy resistance. In patients with NSCLC and urothelial cancer,[174-176] PD-L1 expression is used as a predictive biomarker to decide treatment choices. In melanoma, a lower PD-L1 expression is associated with a lower mutational burden and whilst not directly used to determine treatment, a negative PD-L1 level is associated with worse patient outcomes and correlates with primary immunotherapy resistance.[146, 147, 156, 177]

2.1.9.1.2 Factors extrinsic to the tumour cell

In addition to factors intrinsic to the tumour cell, extrinsic factors within the TME can also give rise to resistance mechanisms which contribute to the inhibition of the anti-tumour immune response.

Myeloid-derived suppressor cells (MDSCs) are immature myeloid cells not found in healthy individuals but can be identified within the TME,[178] where an increased population of MDSCs has been identified in promoting angiogenesis, tumour cell invasion and metastases.[178, 179] Through the release of nitric oxide (NO), reactive oxygen species (ROS) and arginase-1,[180] and the expression of membrane inhibitory ligands including PD-L1, MDSCs have an immunosuppressive effect on T cell function and can promote the development of Treg cells.[181, 182] The increased presence of MDSCs correlates with reduced survival in certain human cancers.[183-186] and the depletion of MDSCs has been associated with improved survival outcomes in murine studies.[40, 187] In ipilimumab treated patients, increased MDSC levels correlated with the severity of metastatic disease and in addition, the presence of MDSCs is associated with a decreased efficacy from immune checkpoint blockade.[188]

As previously discussed, TAMs are another subset of cells that affect responses and resistance to immunotherapy.[40, 45] Clinical studies have shown an association between higher frequencies of TAMs and poor

prognosis in human cancers [189] possibly by PD-L1 driven suppression of T cell responses.[190] Moreover, TAMs secrete cytokines including IL-10 and TGF-β that induce immunosuppression impairing the activity of effector T cells [40] and the depletion of M2 macrophages in murine melanoma tumour models has been successful in limiting tumour growth.[191]

In addition, the presence of Treg cells in the TME is likely to contribute to tumour immune resistance.[192] In human melanoma samples there can be an accumulation and over-representation of Treg cells including in metastatic lesions.[193] Moreover, in murine models, the depletion of Tregs from the TME can restore anti-tumour immunity and the response to anti-CTLA-4 therapy is associated with an increase in the T effector to Treg ratio.[128, 194] These data suggest that tumours in which immunotherapy is unable to deplete Tregs or increase the ratio of T effectors to Tregs, are likely to harbour a pattern of resistance to treatment.[45]

Moreover, tumour T cell recruitment and treatment resistance can be affected by the differential expression of chemokines and their receptors. In murine melanoma models, it has been shown than the high expression of both the CXCR3 receptor along with its ligand CXCL9 are key immune chemoattractants which can increase $CD4^+$ and $CD8^+$ T-cell infiltration.[195, 196] An association between high $CD8^+$ T-cell expression and increased levels of CXCL9 and CXCL10 was also identified in human tumour samples.[156, 197]

Conversely, tumours can secrete ligands including CCL5, CCL7 and CXCL8 which, through binding to their receptors CCR1 or CXCR2 expressed on MDSCs, can attract MDSCs into the TME.[198] In addition, tumour secretion of the TGF-β cytokine enhances angiogenesis and the stimulation of Tregs, and increased levels of TGF-β are associated with poor prognosis in multiple tumour types.[199, 200] The expression of CXCR4 on cancer cells and their interaction with the CXCL12 ligand is also involved in tumour progression, angiogenesis, metastasis and the enrichment of Tregs thereby leading to a

resistant TME which locally suppresses the anti-tumour immune response.[45, 201, 202]

A further proposed mechanism under investigation is the role the gut microbiome may play in influencing patient responses or resistance to immunotherapy. Studies that have analysed the gut microbiome from metastatic melanoma patients has shown a correlation between a higher $CD8^+$ T cell density and a better response to both anti–PD-1 and anti CTLA-4 antibody treatment with a more diverse gut microbiome, including its specific bacterial composition.[203] Murine experiments have demonstrated how the adoptive transfer of memory T cells specific for the commensal gut bacteria *bacteroides fragilis* can restore sensitivity to ipilimumab.[156, 204] In the clinical arena, early stage clinical trials have been investigating the potential for faecal microbiota transplantation (FMT) in immunotherapy refractory melanoma patients.[205] Favourable changes in immune cell infiltrates and gene expression profiles in both the gut and tumour microenvironment have been observed [205] although further studies are needed to identify effective therapies that could be widely adopted using this approach.

2.1.9.2 Acquired resistance to immunotherapy

In addition to primary resistance to immunotherapy discussed above, acquired resistance can occur when, following an initial response, a selection of subpopulations of tumour cells develop that can evade the immune system, through changes in the tumour cells themselves or in the immune cell tumour recognition.[156]

One identified mechanism of acquired resistance involved mutational changes in the beta-2-microglobin subunit of the MHC class I molecule.[206] β_2 microglobulin (B2M) is necessary for the cell surface expression and stability of MHC class I and in murine models an absence of B2M results in limited MHC class I presentation of tumour antigens and a subsequent reduced number of anti-tumour $CD8^+$ T cells.[207, 208]

An analysis of tumour samples from five patients who initially responded to immunotherapy were found to harbour a loss B2M expression not present on the corresponding pre-treatment samples.[206] Furthermore, in a patient relapsing following almost two years of treatment with pembrolizumab, sequencing of resistant cells identified a new mutation in B2M and resulted in a loss of MHC class I expression at the tumour cell surface, therefore enabling the tumour to evade effector T cell recognition.[171] In the same paper, the authors also identified two patients whose biopsy samples, prior to and at the time of relapse on pembrolizumab, demonstrated a new mutation resulting in the loss of *JAK1* or *JAK2*. These mutations resulted in the tumour cells lacking a response to IFN-γ, including a reduction in the expression of PD-L1 and MHC class I and a failure to up-regulate transcripts involved in antigen presentation and T-cell chemotaxis.[171]

Other proposed mechanisms of acquired resistance include mutations in or a reduced expression of tumour neoantigens, leading to reduced MHC presentation and rendering cytotoxic T-cells unable to identify their target.[45] Furthermore, the upregulation of other immune checkpoint markers such as lymphocyte activation gene 3 (LAG-3), T-cell immunoglobulin and mucin domain 3 (TIM-3) and T cell immunoreceptor with Ig and ITIM domains (TIGIT) may increase T-cell exhaustion resulting in the acquisition of immunotherapy resistance.[209] Upregulation of these markers have been identified in patients relapsing on checkpoint inhibitors and on-going trials of antibodies to these targets are investigating their potential in the clinical arena.[45, 156, 209, 210] Of note, a recent publication has demonstrated that the combination of relatlimab (an anti-LAG-3 antibody) with nivolumab leads to an improved mPFS versus nivolumab alone (10.1 months vs 4.6 months respectively, HR 0.75, P=0.006) in the first line treatment of advanced melanoma.[211] Whether this subsequently results in an improvement in survival is unknown at this stage.

It is likely that, over a chronological spectrum, multiple potential immune evasive mechanisms exist that enable tumours to escape immune system

recognition. Given that many patients continue to demonstrate either primary or acquired resistance to immune checkpoint blockade, it will be important to determine these mechanisms and thereby realise novel approaches that further the progress already made with current immunotherapies, in order deliver durable outcomes for patients with advanced melanoma. One such approach under investigation includes the development and integration of oncolytic viral treatments into the compendium of potential therapies.

2.2 Oncolytic viruses (OVs)

2.2.1 OV background

Although better known for treating Napoleon Bonaparte's haemorrhoids, the eminent French anatomist, Baron Guillaume Dupuytren observed, in 1829, the spontaneous regression of a patient's advanced breast cancer following a febrile illness.[212] Whether this was viral in nature would, at the time, have been impossible to know given that viruses were only first identified in 1892.[213] Not long after, reports occurred in the medical literature including a clinical case of leukaemia that went into remission after a presumed influenza infection [214], and a series of cervical cancer patients whose tumours showed temporary shrinkage after inoculation with live-attenuated rabies virus vaccine.[215]

Subsequently, in 1922, pre-clinical research found that certain tumours were more susceptible to viruses than normal cells, and that viruses could preferentially replicate in tumour cells [216], thereby furthering an interest in the potential of viruses as anti-cancer agents. These observations led, in the 1940s, to a clinical trial which evaluated injecting Hodgkin lymphoma patients with hepatitis B virus.[217] Of 21 treated patients, seven had an improvement in symptoms and a tumour size decrease was seen in four patients. Unfortunately, 13 patients developed viral hepatitis, of which one patient died.[218]

Further oncology clinical trials during the 1950-60s, investigated numerous viruses, though, due to lack of efficacy, safety concerns and the development of more effective cytotoxic chemotherapy regimens, interest in using viruses as oncological therapy waned.[219] However, the subsequent progress in genetic engineering techniques have enabled an improvement in the efficacy and safety of candidate viruses. In addition, the recognition of the interplay between the immune system and cancer has further enhanced the potential benefits of OVs. Proponents of OVs point to their dual mechanism of action;

firstly, as capable of selectively infecting, replicating within and lysing tumour cells, and secondly their capacity to promote an anticancer immune response, leading to the immune destruction even of uninfected cancer cells.[220, 221] In addition, no traditional chemotherapy, immunotherapy or small molecule inhibitor can target tumour cells and then amplify at the site of action and spread to other sites of tumour growth.[222]

The terminology classifying OVs together, belies the wide range of variation that exists between different agents within this grouping (Figure 2). This variation includes both DNA and RNA viruses, naturally occurring and genetically modified viruses and those known to cause human pathology and those that do not. However, despite this variation, common key desirable characteristics of any oncolytic virus include an acceptable safety profile, specificity for the targeted cancer, a potency to kill infected cells and the generation of anti-tumour immunity.[222]

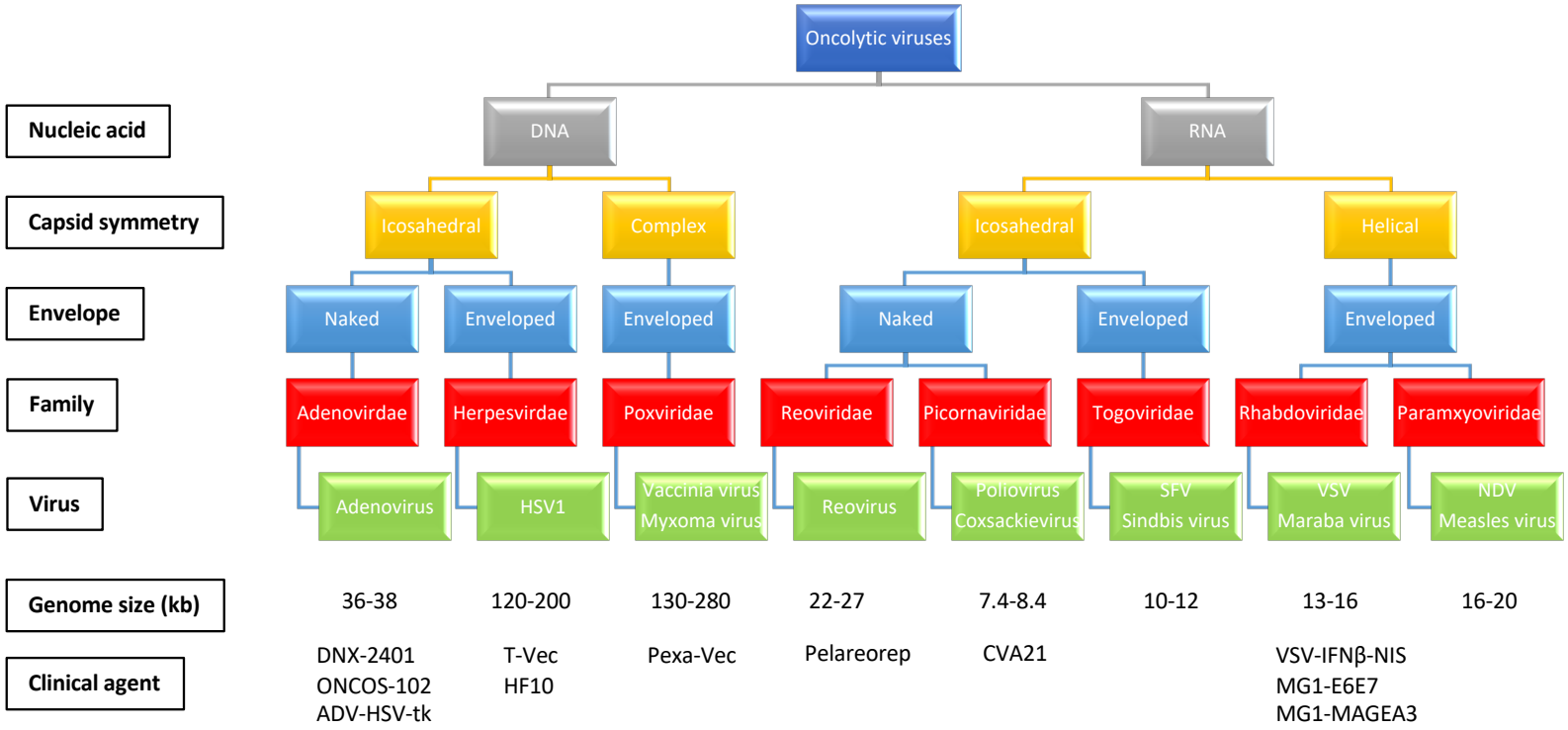

Figure 2: OV classification

OV classification and viruses currently undergoing or that have undergone clinical trials in combination with ICIs. SFV: Semliki Forest virus; VSV: Vesicular stomatitis virus; NDV: Newcastle disease virus

2.2.2 OV safety

The aforementioned early virotherapy trials undertaken in the 1950s and 1960s recorded deaths and severe adverse reactions which are now presumed to have been secondary to OV replication in normal tissues, notably the brain, in immunocompromised cancer patients.[223]

Necessarily therefore, recent oncolytic viral studies have had an excellent safety record with few serious adverse events reported from human trials.[224] The most common adverse effects reported in recent OV trials are transient fever and flu-like symptoms.[225] However, as the numbers of patients participating in trials grows, so will the insight into rare treatment related adverse events.

Viral cytotoxicity is necessary for direct oncolytic activity, however off-target infection and killing of normal cells by poorly targeted OVs can cause unwanted pathology through non-selective cell lysis in normal tissue. Furthermore, as the OV replicates and amplifies in tumour cells, there is a potential for progeny viruses to acquire mutations potentially enabling the infection of normal host cells. OVs are therefore finely balanced between retaining enough virulence to substantially decrease tumour burden versus being sufficiently tumour selective to not cause harm to the patient.[222]

The transmission of an OV from a treated patient to a caregiver, family member, health worker or other species is a potential risk of using infectious agents and is clearly highly undesirable.[222]

In an OV-treated patient, pre-existing antiviral immunity can be a considerable barrier to efficacy. However, pre-existing antiviral immunity in patient contacts provides reassuring protection against onward virus transmission. Conversely, by circumventing this particular barrier by using OVs engineered for antibody evasion or selected for low host baseline seroprevalence, the risk

of spread within in the human population, unchecked by pre-existing herd immunity, is greater.[222]

An alternative strategy often used to avoid initial antibody neutralization, is to utilise OVs derived from zoonotic animal viruses. Additional regulatory scrutiny is warranted for these viruses to address the additional risks to agriculture and the wider environment.[222]

Fortunately, in reality, to date there has been no instance in which transmission of an OV from a patient to a caregiver, other contact or other species has been demonstrated, and there are no examples of long-term OV persistence or shedding in a treated patient.[222]

2.2.3 OV mechanisms of tumour tropism

The hallmarks of malignant cells that distinguish them from normal host tissue include a sustained proliferation, insensitivity to growth inhibition signals, resistance to cell death, replicative immortality, angiogenic induction, and the capacity to invade and metastasise.[42]

These characteristics, however, can generally leave tumours more vulnerable than normal tissues to viral attack, and this susceptibility can be exploited in the development of OVs. As with any oncology drug, the concept of a virus with mechanisms giving selective tropism for malignant cells, whilst sparing normal tissue, has obvious appeal. Several of these mechanisms are discussed below.

2.2.3.1 Exploiting tumour cell receptors

OVs can exploit a tropism for receptors that are specifically over-expressed on tumour cells.

Coxsackie virus has a natural tropism for melanoma cells over-expressing the decay-accelerating factor (DAF) and intercellular adhesion molecule-1 (ICAM-1).[226] Furthermore, enterovirus B targets integrin $\alpha_1\beta_2$, which is over-expressed on ovarian cancer cells [227] and measles virus is thought to derive its tumour selectivity through its binding to the CD46 receptor which is often over-expressed on tumour cells.[228] In addition, poliovirus infects cells expressing the CD155 receptor [229] which is abundant on the cells of many solid tumour types, and oncolytic HSV can gain tumour cell entry through attachment to the HSV entry mediator (HVEM) receptors on melanoma cells.[230]

In addition to these natural tropisms, viruses can be genetically modified to enhance their tumour selectivity. For instance, adenovirus (serotype 5) has been edited to divert its affiliation away from its normal coxsackie and adenovirus receptor (CAR), which is low or absent on tumour cells, and instead reprogrammed towards cell surface integrins or other adenoviral receptors which are expressed on tumour cells.[231, 232]

2.2.3.2 Exploiting the anti-apoptotic nature and replication of tumour cells

The death of the host cell will limit ongoing viral replication within it, therefore to maximise replication viruses can encode proteins that inhibit apoptosis.[233] Genetically removing the genes encoding these viral proteins ensures that normal cells infected by virus retain intact apoptotic pathways, whereas within tumour cells that are inherently resistant to apoptosis, the virus can replicate unchecked, thereby making tumour cells highly susceptible to such OVs.[222]

The tumour suppressor protein, p53, mediates apoptosis and cell cycle arrest following DNA damage or viral infection. Tumour cells often develop mutations in this pathway allowing unchecked cellular proliferation. During adenovirus infection of normal cells, the viral E1B gene inactivates the host cell p53 gene thereby enabling viral replication. The oncolytic adenovirus ONYX015 has a

deletion of its E1B gene, resulting in an adenovirus that specifically replicates in tumour cells which have a p53 mutation, while normal cells with intact p53 are spared. This method therefore mitigates the adenoviral pathogenicity whilst also enhancing its tumour selectivity.[234]

2.2.3.3 Defects in anti-viral responses

2.2.3.3.1 Interferon response

Viral infection within normal cells results in the release of type 1 IFN, the effect of which is to protect surrounding cells from further viral propagation. Malignant cells often have a defective IFN signalling pathway and therefore, a greater susceptibility to viral infection.

Exploiting this, the *Rhabdoviridae* vesicular stomatitis virus (VSV) and modified Maraba virus (MG1) [235] and the *Paramyxoviridae* Newcastle disease virus (NDV) [236] are restricted to cells with defective IFN responses, thereby establishing them as potential OVs given their tumour selectivity. In addition, other viruses have been modified to render them specific to tumour cells with a defective IFN response for instance, HSV [237], adenovirus [238], vaccinia virus (VV) [239] and influenza virus.[240]

2.2.3.3.2 Double-stranded RNA-dependent protein kinase

The intracellular dsRNA-dependent protein kinase (PKR) enzyme prevents the translation of viral transcripts. However, tumour cells harbouring a *Ras* mutation have a defective PKR response following viral infection. Viruses including reovirus can exploit this defective PKR activity and replicate in tumour cells specifically [241-243].

2.2.3.4 Other mechanisms of tumour tropism

Other mechanisms of OV tumour selectivity include the deletion of viral thymidine kinase (TK) in VV. TK is required by the virus for generating the deoxynucleotide triphosphates required for synthesis of progeny virus genomes. Therefore, the deletion of the TK gene from the viral genome ensures that the virus is dependent on human TK for its replication. By virtue of this, viral replication is restricted to cells with an upregulation of human TK, as occurs within cancer cells.[244] In addition, the Toca-511 retrovirus encodes the drug activating enzyme cytosine deaminase (CD). As retrovirus integration is dependent on the S-phase of the cell cycle, this virus is selectively amplified in rapidly proliferating tumour tissue.[245] Viruses can also be engineered such that essential viral genes are under the control of tumour specific promoters. Hence, viral replication occurs specifically in tumour cells.[246] Finally, improved tumour tropism can be optimised by encoding microRNAs into the viral genome to minimise off target pathology in normal tissues.[247]

2.2.4 OV delivery

A major factor distinguishing OVs from traditional drugs is that they self-amplify and spread after delivery so their peak concentration may not be reached until sometime after the treatment is administered. OV therapy begins with the administration of the virus to the patient just as with any other drug. Several approaches can be taken, each with advantages and limitations, to deliver a sufficient quantity of virus to sites of tumour growth to initiate a productive, anti-tumour infection.[222]

2.2.4.1 IV delivery

Intravenous (IV) delivery of an OV seems advantageous in the setting of metastatic disease, allowing the virus to potentially access all sites of disease via the circulation. In a clinical setting, systemic delivery may be a more

practically applicable than intratumoural (IT) inoculation. However, attempts at systemic delivery have shown limited success given the administered virus is immediately diluted in the circulating blood volume.[222] In addition, IV virus can be sequestered by the reticuloendothelial system or neutralised by serum proteins including antibodies and complement. The virus must then be able to extravasate and navigate the extracellular matrix to reach and infect any cancer cells.[248]

Despite these challenges, the ability of an IV OV to infect the endothelial cells of the tumour vasculature could enable subsequent widespread intratumoural spread and may cause intravascular coagulation and disruption of the tumour blood supply. To enable better extravasation, strategies including the application of focused ultrasound to create localised pores within the tumour architecture are being developed.[222, 249]

2.2.4.2 IT delivery

IT administration has the advantage of directly delivering a high concentration of the OV into the injected tumour but may not result in the spread of the virus to distant sites of metastasis. However, systemic viral spread can occur following IT administration if the initially infected tumour cells amplify the virus and release progeny into the bloodstream. In human patients, tumours often develop in and metastasise to visceral organs making IT delivery difficult, although with advanced interventional radiology techniques, many more tumours may be accessible for IT administration.[222]

2.2.4.3 Other routes of delivery

Intraperitoneal virus administration has been used in studies aiming to impact ovarian cancer and other disseminated intraperitoneal malignancies, while intrapleural administration has been pursued for mesothelioma therapy. Intravesical viral treatment is convenient for early-stage bladder cancer, requiring only that the input virus is stable in urine. In addition, immediately

after brain cancer surgery, in an attempt to control residual disease, virus is often instilled directly into the resection cavity.[222] Finally, OV within the context of an isolated limb perfusion circuit, for example in patients with multiple subcutaneous deposits of melanoma or angiosarcoma affecting a particular limb, may be an attractive option in certain patients and is currently under investigation within clinical trials.[250]

2.2.5 Neutralising antibodies

A significant barrier to widespread OV delivery is the rapid neutralisation in seropositive patients who have previously been exposed to the same virus, either naturally through past infection, through prior vaccination, or from a previous treatment dose, resulting in the clearance of circulating virus particles. Antibodies and complement proteins can coat the virus blocking its ability to interact with its cellular receptor and accelerating the Fc receptor-mediated clearance of virus by splenic macrophages and hepatic Kupffer cells.[251]

In preclinical models, antibody neutralisation reduces the efficacy of systemically administered OVs including measles, VSV and VV.[252] This is particularly problematic when pre-existing seroprevalence exists, or for subsequent treatments beyond the first dose. One approach to counter this is using immunosuppressive drugs such as cyclophosphamide which, when administered concurrently with an OV, has been shown to suppress or delay the development of humoral and cytotoxic antiviral T-cell responses.[253] Moreover, engineering or switching the viral coat proteins, or by substituting the surface glycoproteins to avoid initial immune recognition has been attempted.[254] In addition, using animal pathogens as OVs has an appeal due to their low pre-existing seroprevalence in the human population. Furthermore, zoonotic viruses may be capable of infecting both rodent and human tumour cells which allows for more informative preclinical testing in immunocompetent mouse cancer models.[222]

2.2.6 OVs and the immune system

OVs were initially developed owing to their direct cytotoxic activity against tumour cells. However, it is increasingly recognised that OVs have the potential to induce both innate and adaptive anti-tumour immune responses.

Following oncolytic viral infection, host cells use varying mechanisms to shut down viral replication to avoid pathogenicity. Viral pathogen-associated molecular patterns (PAMPs) are recognised by host pattern recognition receptors (PRRs) resulting in the induction of chemokines and cytokines including type I IFNs.[221] This activates and recruits innate immune cells, including neutrophils, macrophages, NK cells, and APCs to respond at the site of viral infection. APCs can present viral and tumour associated antigens (TAAs) in order to initiate an adaptive anti-tumoural immune response.[221]

Therefore, OVs that have the potential to revert an immunosuppressive, cold, microenvironment into an immune activated, hot microenvironment are an interesting strategy for cancer immunotherapy.

2.2.6.1 Innate immune responses

The innate immune response can vary depending on the type of infecting virus. RNA viruses are recognized by retinoid acid-inducible receptors (retinoic acid-inducible gene 1 (RIG-1) and melanoma differentiation-associated protein 5 (MDA-5)). DNA viruses are detected by cytosolic double-stranded DNA sensors including cyclic guanosine monophosphate–adenosine monophosphate synthase (cGAS).[221, 255]

These pathways ensure rapid antiviral innate immune responses that may compromise the replication and killing activity of OVs. However, strategies to block the generation of a strong antiviral innate responses may hamper the subsequent development of the adaptive immune response to both virus and tumour.[256] The objective, therefore, is an OV that balances effective viral

replication and cytotoxicity with optimal innate response and adaptive immune priming.

2.2.6.2 Immunogenic cell death and adaptive immune responses

OVs can contribute to cancer immunity by triggering tumour immunogenic cell death (ICD). The hallmarks of ICD involve the release from dying tumour cells of specific damage-associated molecular patterns (DAMPs) including high-mobility group box 1 (HMGB1), adenosine triphosphate (ATP), annexin 1, calreticulin and type I IFN.[257, 258] OVs have been shown *in vitro* to be capable of inducing tumour ICD, resulting in increased activation of both anti-tumour innate and adaptive immune responses.[257, 259, 260]

Further investigations have demonstrated the importance of an intact immune system for the efficacy of oncolytic virotherapy by comparing OVs in immunodeficient and immunocompetent mouse models. In one study, HSV type 1 had an anti-tumour effect in immunocompetent mice which was lost in immunodeficient athymic mice, highlighting the necessary role of the endogenous population of $CD8^+$ cytotoxic T lymphocyte (CTL).[261] The dependence on the immune system for an anti-tumour effect has been a consistent finding, supported through further murine studies using other OVs including NDV [262], Maraba virus (MG1) [263], reovirus [264] and Sendai virus [265].

In addition, clinical data has shown that OVs can instigate an innate and adaptive anti-tumour immune response in patients. In a phase Ib trial, tumour biopsies were taken prior to and during a course of treatment with an IT oncolytic HSV, talimogene laherparepvec (T-VEC). Immunohistochemical analysis comparing the paired samples showed an increased infiltration by immune cells and a clear increase in cells expressing PD-L1 in eight out of ten injected tumours and in two out of four non-injected tumours. Changes in immune infiltrates in the on-treatment biopsies from some patients included an

influx of $CD4^+$ and $CD8^+$ T cells as well as $CD56^+$ NK cells and $CD20^+$ B cells.[266] Increases were also observed in the density of immunosuppressive Treg cells however, the magnitude of effector T cell increases was much larger relative to Treg cells, resulting in an overall decrease in the Treg to Teff ratio in tumours following T-VEC.[266]

2.2.7 Enhancing oncolytic viral therapy

Whilst OVs have demonstrated the capability to selectively infect and lyse tumour cells and additionally generate an anti-tumour immune response, thus far they have not significantly improved patient survival. This may be, in part, due to the immune system counterbalancing localised oncolytic viral infection and inflammation through the recruitment of MDSCs and Tregs into the TME which serve to inhibit the anti-tumoural immune responses.[166, 267] Greater therapeutic gains may be realised through strategies that enhance individual OVs and through treatment combinations with other agents that have complementary mechanisms of action, as discussed below.

2.2.7.1 Enhancing the cytotoxic potential of OVs

2.2.7.1.1 Enhancing OV amplification and spread

After a virus has infected a tumour cell, its potency is in part driven by its subsequent propagation. Local spread may occur by intercellular fusion, by direct transfer of virus from infected to adjacent cells, or by release and local migration of progeny virions through the interstitial space.[222]

An advantage with direct cell-to-cell transfer of viruses is the avoidance of neutralisation by antiviral antibodies in the interstitial fluid.[268] Viruses can be engineered with genes encoding fusogenic membrane glycoproteins (FMGs) which create large, non-viable multinucleated syncytia through intercellular fusion. This facilitates superior cell-to-cell viral transfer and, in addition, the syncytia may increase antigen presentation and amplification of

the anti-tumour immune response.[269] This strategy has been adopted in developing HSVs encoding fusogenic gibbon ape leukaemia virus glycoproteins, and has shown superior efficacy when compared with the corresponding parental viruses [270-272] and is now being investigated within early stage clinical trials.[273]

As mentioned, viruses in the extracellular matrix are more susceptible to antibody neutralisation and their passage between cells can be hampered by the collagenous matrix of protein fibrils, adhesive proteins and proteoglycans.[222] Therefore, disturbing the ECM can facilitate better viral spread throughout the tumour and can be achieved using conventional chemoradiotherapy.[274] An alternative approach is to encode a matrix-degrading enzyme into the viral genome. For example, hyaluronidase and relaxin encoding oncolytic adenoviruses have been shown to spread more efficiently in murine melanoma models.[222, 275, 276]

2.2.7.1.2 OVs encoding cytosine deaminase

Regardless of how well an OV infection spreads throughout a tumour, a proportion of the cancer cells will escape infection. To target these remaining cells, one adopted strategy is to encode enzymes that can convert prodrugs into active metabolites.

The cytosine deaminase (CD) enzyme converts the inert prodrug 5-flurocytosine (5-FC), into the commonly used cytotoxic agent 5-fluorouracil (5-FU), that irreversibly inhibits thymidylate synthase.[277] Therefore, treatment with a CD encoded OV along with 5-FC results in higher local production of 5-FU in the OV-infected tumour compared to normal tissue, as CD is not found in mammalian cells. This approach thereby ameliorates toxicity and enhances the therapeutic index of the drug. CD has been incorporated into the retrovirus vocimagene amiretrorepvec, Toca 511, however, unfortunately did not yield positive phase III data in patients with glioma.[278]

2.2.7.1.3 OVs encoding the sodium iodide symporter

In a similar fashion, the transgene encoding the sodium iodide symporter (NIS) glycoprotein has been incorporated into oncolytic viral genomes. The symporter concentrates iodide into thyroid follicular cells for thyroxine production. Therefore, the expression of NIS in virally infected tumour cells increases their avidity for iodide and creates the possibility for combinations with radiolabelled iodine for tumour imaging or therapy.[251] Two NIS-expressing OVs, a prostate targeted oncolytic adenovirus and a measles virus, have advanced to human clinical trials.[279, 280]

2.2.7.2 Enhancing immunogenic potential of OVs

In addition to their cytotoxic potential, OVs are able to prompt the immune-mediated killing of uninfected tumour cells and have therefore been manipulated to maximise their immune enhancing properties.

2.2.7.2.1 OVs encoded to express cytokines

OVs have been engineered to express type I IFN to better stimulate an immune response. IFN-β inhibits tumour cell proliferation, suppresses angiogenesis and directly promotes the proliferation of NK cells and antigen specific $CD8^+$ T cells.[281] VSV-IFN-β showed significant therapy against a murine mesothelioma model following local viral delivery.[282] The IFN-β expressed from VSV added significantly to therapy compared with VSV alone, dependent in part on host $CD8^+$ T cell responses. In addition, virally mediated IFN-β also offered extra safety by providing protection from off-target viral replication in non-tumour tissues thereby enhancing the viral therapeutic index.[283] VSV has also been encoded with the IL-15 cytokine to activate both NK and T cells and has improved survival compared to VSV alone in a murine model of colorectal cancer. Other cytokines, including IL-12 and IL-18, have been encoded into adenovirus and result in improved tumour control *in vivo* and an increased infiltration of NK and $CD8^+$ T cells.[284]

Similarly, granulocyte macrophage-colony stimulating factor (GM-CSF) has been integrated into adenovirus, HSV, VV and measles viruses. The virally infected tumour cells release GM-CSF thereby stimulating the recruitment of antigen presenting dendritic cells [285] and can result in tumour responses both in virally injected and non-injected lesions [286] that are dependent on $CD4^+$ and $CD8^+$ T cells.[287]

2.2.7.2.2 OVs encoding bispecific T-cell engagers

Bispecific T cell engagers (BiTEs) are a novel class of immunotherapeutic molecules that consist of tandem antibody fragments that target both CD3 on T cells and a tumour-associated antigen, respectively.[288] Through this mechanism, T cells are recruited to tumour cells irrespective of T cell receptor specificity or antigen presentation.[289] BiTEs have recently been expressed from oncolytic VV [290] and measles virus backbones, and their localised expression demonstrated therapeutic efficacy against established tumours in fully immunocompetent mice, and were associated with increased intratumoural T cell infiltration and induction of protective anti-tumour immunity.[291]

2.2.7.2.3 OVs and adoptive cell therapy

The development of adoptive cell therapy (ACT) as an effective cancer treatment strategy gives the opportunity for combination with OVs. One of the challenges to achieving durable responses with ACT is enhancing the trafficking to and survival of donor T cells in the tumour. OVs may provide a mechanism to recruit and activate the donor T cells in the tumour. For instance, an OV could be engineered to express cytokines that mediate T cell recruitment and survival and could then be used in tandem with *ex vivo* expanded tumour infiltrating lymphocytes (TILs) to drive cytotoxic T cell activity within the tumour. Another approach could be to modify an OV reactive T cell with a tumour-specific chimeric antigen receptor (CAR) T cell. The subsequent

CAR T cells would have a dual tumour and viral specificity and therefore could be locally activated within the tumour on recognition of the administered tumour tropic OV. Demonstrating the breadth of potential modifications that can be made to OVs to generate an anti-tumour immune response, an adenovirus was encoded with the triple combination of the IL-12, an anti-PD-L1 antibody and a BiTE specific for the tumour expressed CD44 molecule. The BiTE enabled specific CAR T cells to target CD44 expressing tumour cells and to produce a more rapid and sustained disease control in a lung cancer model compared to using any of the three mechanisms alone.[292]

2.2.7.2.4 OVs encoded with costimulatory molecules

Another strategy to boost the anti-tumour immune response has been to modify OV by encoding T cell costimulatory molecules to enhance cancer-specific T cell activation and DC maturation.[293] For instance, VV encoding the costimulatory molecules B7.1, intercellular adhesion molecule 1 (ICAM-1), and lymphocyte function-associated antigen 3 (LFA-3), has shown activity in animal models and phase I clinical trials.[294] In addition, NDV expressing the inducible costimulatory (ICOS) ligand has demonstrated enhanced tumour T cell activation and infiltration.[295] Furthermore, virally expressed costimulatory members of the TNF receptor superfamily, including OX40, CD40, and 4-1BB have shown evidence of immune activation in diverse range of malignancies.[293, 296]. Lastly, the ligand of the glucocorticoid-induced tumour necrosis family receptor (GITR-L) has been encoded into an adenovirus backbone (Ad-GITR-L) and the local release of this ligand in infected tumour cells can inhibit the suppressor function of $CD25^+$ Treg cells, attract $CD8^+$ cells and inhibit tumour growth in a murine B16 melanoma model.[297]

2.2.7.2.5 OVs expressing cloned tumour antigens thereby acting as vaccine vectors

OVs armed with relevant tumour associated antigens have also provided a promising therapeutic approach by further amplifying tumour-specific

immunity. This has included encoding the tumour associated antigens carcinoembryonic antigen (CEA), prostate-specific antigen (PSA), or human dopachrome tautomerase which is overexpressed in a range of malignancies. Oncolytic vaccine vectors have been developed in a range of viruses including VV, adenovirus, VSV and Maraba virus among others.[298]

The obstacles with this approach however include the heterogeneity of tumours and the resultant variability in antigen expression, thereby potentially diminishing the immunogenicity of any individual virally expressed antigen. In addition, inducing efficacious immune responses against tumour antigens is challenging, as these tend to be autologous in nature but have already become tolerated by the immune system during tumour equilibrium and escape. In addition, the immune response to the presence of the replicating OV may dominate over the response to the virally generated tumour antigens.[293, 299]

2.2.8 Oncolytic viruses and clinical use

As of 2021, there have been three approved OVs, of which, only T-VEC, has FDA and EMA approval for use in advanced melanoma.[1] T-VEC is a modified HSV-1 with deletions in the HSV neurovirulence factor genes *ICP34.5* and *ICP47*.[300]

The deletion of *ICP34.5* attenuates the viral pathogenicity and enhances tumour-selective replication. The deletion of the *ICP47* gene results in enhanced tumour antigen presentation by infected cancer cells and increases the expression of the HSV *US11* gene which partially enhances the oncolytic activity of T-VEC.[300] Furthermore, the human GM-CSF gene has been inserted into the deleted *ICP34.5* genomic site. GM-CSF promotes dendritic

[1] Deriving from the enterovirus genus of the *picornaviridae* family of RNA viruses, ECHO-7 was previously approved in Latvia for use in patients with melanoma. However, its efficacy has not been proven within rigorous clinical trials and, in May 2019, the registration licence for ECHO-7 was suspended.

cell accumulation at sites of inflammation and enhances antigen presenting cell function.[230]

T-VEC was approved for clinical use based on the results of the phase III OPTiM (Oncovex [GM-CSF] Pivotal Trial in Melanoma) trial.[301] In this study, intralesional T-VEC injection resulted in a statistically significant improvement in durable ORR when compared to GM-CSF alone (16.2% vs 2.1%, P<0.001), in patients with unresectable stage IIIB or IV melanoma. Furthermore, an anenestic response was also noted, as 15% of measurable non-injected visceral lesions reduced in size by ≥50% following T-VEC treatment. The final analyses revealed a mOS difference of 23.3 months vs. 18.9 months in the T-VEC and GM-CSF arms, respectively (HR 0.79; $P = 0.051$) while also exhibiting a tolerable safety profile with low rates of grade 3 or 4 adverse events.[302] T-VEC was also found to alter the tumour immune microenvironment by reducing the number of $CD4^+$ Tregs, and MDSCs.[303]

Oncolytic adenoviruses were some of the earliest OVs to enter clinical trials and have shown promising results. ONYX015, is an E1A/E1B-deleted virus has been tested and approved for treatment of head and neck cancer in China under the name H101. In a phase III trial, cisplatin was given with or without IT H101 and the response rate from combination therapy was 79% compared with 39% with chemotherapy alone.[304] Due to the termination of sponsor funding and difficulty in collecting on-going patient data, the trial was suspended prior to any assessment of overall survival and is therefore not approved beyond China.[305]

Another E1A deleted adenovirus, tasadenoturev, DNX-2401, has shown encouraging responses in clinical trials. A dose-escalation phase I study showed that DNX-2401 was safe and capable of viral replication and tumour control in recurrent high-grade glioma patients. 72% of patients (18 out of 25) displayed a reduction in tumour size and 20% (5 patients) survived beyond 3 years.[306]

Pexa-Vec, JX-594, is an oncolytic VV that has also been engineered to express human GM-CSF. It has been well tolerated in early stage clinical trials including in patients with hepatocellular carcinoma (HCC)[307] and colorectal cancer.[308] However, in the phase III PHOCUS trial,[309] it failed to improve survival in patients with advanced HCC. It is currently under investigation in combination with nivolumab in patients with advanced HCC (ClinicalTrials.gov: NCT03071094).

PROSTVAC is another modified VV and contains transgenes for both PSA and the T cell costimulatory molecules ICAM-1 (intercellular adhesion molecule 1), B7.1, and LFA-3. In a prime-boost regimen it has shown promise within phase I and II trials [310] and showed no additional or unexpected toxicity when tested alongside ipilimumab.[311]

Wild-type coxsackievirus A21 (Cavatak) has been tested in six phase I or II clinical trials in a range of malignancies including NSCLC and bladder cancer. In addition, it has shown an overall response rate of 28% in a cohort of patients with advanced melanoma demonstrating activity in both injected and uninjected lesions.[312]

In addition, clinical trials using PVS-RIPO, a polio virus attenuated to mitigate the neurovirulence of the wild-type virus, but with a tropism for the upregulated CD155 receptor on malignant cells, has reported activity in patients with recurrent glioblastoma.[313] In addition, 21% of patients remained alive 36 months following treatment, a figure notably higher than might be expected with historical controls.

Other early stage clinical trials have been undertaken using other viruses including, but not limited to, measles virus, reovirus, NDV, VSV and Maraba virus.[225]

In summary, although to date only one OV is widely licensed for use in advanced melanoma, the multitude of recent early stage clinical trials have demonstrated a manageable safety profile and interesting potential. As

discussed next, combining OVs as adjunctive therapy alongside immune checkpoint inhibitors is garnering particular interest.

2.2.9 OVs and immune checkpoint inhibition

As discussed previously, ICI treatment has significantly improved patient outcomes in multiple tumour types, including melanoma. Nevertheless, many patients still fail to respond to ICI treatment. On the basis of their ability to self-amplify within tumour cells and mediate anti-tumour immune activity, OVs represent a potential therapeutic platform to potentiate responses in patients and tumour types that currently respond poorly to immune checkpoint blockade (ICB). When deployed with ICIs, OVs may increase the response to, and reverse the resistance to, ICB and to favourably alter components of the anti-tumour immune response.[220] *In vivo* experiments have demonstrated that the combination of OV with checkpoint blockade can improve survival when compared to either agent given alone, and through depletion experiments, demonstrate that this is dependent on the enhanced recruitment of effector T cells to the TME. These beneficial outcomes have been consistently shown in multiple murine models and across a breadth of different OVs. A comprehensive review of the pre-clinical and clinical studies combining ICB with OVs has been recently published by our group (Table 1).[314]

Particular note should be given to two clinical trials that have combined T-VEC with checkpoint antibody therapy. The first, (ClinicalTrials.gov: NCT01740297) investigated T-VEC in combination with ipilimumab within a phase Ib/II trial for patients with previously untreated unresectable stage IIIB-IV melanoma. The initial phase of the study recruited 19 patients in total and documented no dose-limiting toxicities. The ORR was 50% with 44% of patients having a durable response lasting more than six months.[315]

In the subsequent phase II part of the trial, 198 patients were randomised to receive T-VEC plus ipilimumab (n = 98), or ipilimumab alone (n = 100). Thirty-eight patients (39%) in the combination arm and 18 patients (18%) in the

ipilimumab arm had an objective response (p = 0.002). Importantly, responses were not only limited to injected sites, as distant non-injected tumours also showed anenestic responses with visceral lesions reducing in size in 52% of patients in the combination arm and 23% of patients in the ipilimumab arm. The study was not powered for formal evaluation of PFS data, however, a descriptive analysis reported a median PFS of 8.2 months in the combination arm and 6.4 months in the ipilimumab arm (HR, 0.83; p = 0.35).[316]

A second trial, MASTERKEY-265/KEYNOTE-034 (ClinicalTrials.gov: NCT02263508) evaluated T-VEC in combination with pembrolizumab for patients with advanced melanoma. The phase Ib aspect of this trial recruited 21 patients and confirmed that treatment was well tolerated, with no dose-limiting toxicities occurring and no increased toxicities above single agent therapy. In terms of early efficacy signals, the trial demonstrated an ORR of 62%, with a complete response rate (CRR) of 33% in patients receiving T-VEC plus pembrolizumab combination therapy.[266] This exceeds an overall response rate of approximately 33% in previous trials of pembrolizumab alone [145] although cross-trial comparisons are imperfect as the need to select patients who had tumour lesions amenable to viral injection may have skewed the population toward those with a good prognosis. Nevertheless, the trial also reported a >50% size reduction in 82% of injected, 43% of non-injected non-visceral, and 33% of non-injected visceral lesions.[266]

Previous data has suggested low response rates to single-agent pembrolizumab in patients with baseline low $CD8^+$ T cell tumour infiltrates or a negative IFN-γ gene signature.[317] This trial however, noted clinical responses in 9 out of 13 patients with a baseline low $CD8^+$ T cell density and 3 out of 5 patients with a low IFN-γ gene signature. The initial run-in phase of the trial with T-VEC alone led to an increase in systemic circulating $CD4^+$ and $CD8^+$ T cells and increased $CD8^+$ T cell infiltration into the sampled tumours. There was also an associated increase in T cell PD-1 expression and an upregulation of tumoural PD-L1, and this was proposed to be limiting the potential anti-tumour activity from treatment with T-VEC alone. It was inferred therefore, that the addition of pembrolizumab to T-VEC would block this PD-

1/PD-L1 signalling axis and that administering T-VEC prior to pembrolizumab would promote a tumour environment conducive to checkpoint blockade.

These data support the concept that oncolytic virotherapy can convert ‘cold’ tumours to ‘hot’, priming for more effective ICB and resulting in clinical activity beyond what would be expected with either therapy alone.[266] The subsequent phase III trial reported in September 2021. Despite a numerical mPFS difference between the pembrolizumab plus T-VEC group (14.3 months) compared to the pembrolizumab plus placebo group (8.5 months) (HR 0.86), this was not significant (p=0.13). In addition, although the mOS data was immature, it was not expected to achieve statistical significance.[318] Whilst the results for the overall population were disappointing in not reaching its primary endpoint, subsequent analysis may identify subgroups or biomarkers that may help to identify specific patients that may derive benefit from this combination. The trial perhaps highlights the pressing need to identify other potential OV agents, to better understand the immunological effects of OVs and how they can be optimally used, either alone or in rational combinations with other immunomodulatory therapies.

Table 1: Clinical trials combining OVs with immune checkpoint inhibitors

Virus	Clinical Trial Number	Genomic Modifications	ICI Combination	Disease model	Estimated Enrolment	Phase
Herpesvirus	NCT01740297	T-VEC (deletion in ICP34.5 and ICP47 and addition of GM-CSF)	Ipilimumab	Melanoma	217	Ib/II
	NCT02263508	T-VEC (deletion in ICP34.5 and ICP47 and addition of GM-CSF)	Pembrolizumab	Melanoma	713	1b/III
	NCT03153085	HF10 (deletion in UL43,49.5,55 and 56 and overexpression in UL53 and 54)	Ipilimumab	Melanoma	28	II
	NCT02272855	HF10 (deletion in UL43,49.5,55 and 56 and overexpression in UL53 and 54)	Ipilimumab	Melanoma	46	II
	NCT03259425	HF10 (deletion in UL43,49.5,55 and 56 and overexpression in UL53 and 54)	Nivolumab	Melanoma	7	II
Vaccinia Virus	NCT03206073	Pexa-Vec (addition of GM-CSF and β-galactosidase)	Durvalumab, Tremelimumab	Colon	35	I/II
	NCT03071094	Pexa-Vec (addition of GM-CSF and β-galactosidase)	Nivolumab	HCC	30	I/IIa
	NCT02977156	Pexa-Vec (addition of GM-CSF and β-galactosidase)	Ipilimumab	Solid tumours	66	I
Adenovirus	NCT02798406	Tasadenoturev (deletion of E1A)	Pembrolizumab	Glioblastoma	49	II
	NCT03003676	ONCOS-102 (addition of GM-CSF)	Pembrolizumab	Melanoma	24	I

	NCT03004183	ADV/HSV-tk	Pembrolizumab	TNBC, mNSCLC	57	II
Reovirus	NCT02620423		Pembrolizumab	Pancreas	11	I
VSV	NCT02923466	VSV-IFNβ-NIS	Avelumab	Solid tumours, Colon	93	I
	NCT03647163		Pembrolizumab	Solid tumours, NSCLC, HNSCC	23	I
Maraba	NCT02879760	MG1-MAGEA3	Pembrolizumab	NSCLC	75	I/II
	NCT03618953	MG1-E6E7	Atezolizumab	HPV associated malignancies	75	I/Ib
	NCT03773744	MG1-MAGEA3	Pembrolizumab	Melanoma, Squamous skin cancer	40	Ib
Coxsackie	NCT02307149	Coxsackie A21	Ipilimumab	Melanoma	59	Ib
	NCT02565992	Coxsackie A21	Pembrolizumab	Melanoma	50	Ib

Table adapted from Chiu, M., Armstrong, E. J. L. et al., Combination therapy with oncolytic viruses and immune checkpoint inhibitors. Expert Opin Biol Ther, 2020. 20(6): p. 635-652. [314] VSV: Vesicular stomatitis virus; HCC: Hepatocellular carcinoma; TNBC: Triple-negative breast cancer; NSCLC: non-small cell lung cancer; HNSCC: Head and neck squamous cell carcinoma; HPV: Human papilloma virus

2.3 Maraba virus

2.3.1 Background

Maraba virus was first isolated from Amazonian phlebotomine sand flies in Brazil and, to date, has not been detected outside South America.[319] Maraba virus belongs to the vesiculovirus genus of the *Rhabdoviridae* family although it is genetically distinct from VSV.[320] No Maraba virus related pathogenicity has been reported in humans and only one case of seroconversion against viral antigens has been documented in the literature. Furthermore, unlike VSV, Maraba does not pose an environmental risk to livestock.[321]

The virion consists of a bullet-shaped enveloped particle (Ø: 70 nm x L: 170 nm) containing an 11-kb single-stranded negative-sense RNA genome (Figure 3). Its genome consists of a 3′ leader sequence and a 5′ trailer sequence separated by five open reading frames, each encoding one viral protein: nucleocapsid (N), phosphoprotein (P), matrix (M), glycoprotein (G), and polymerase (L).[321, 322]

Figure 3: Structure and genome of Maraba virus

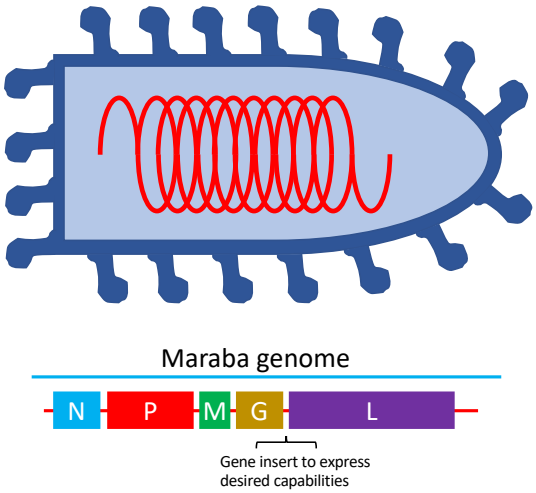

Maraba virus replication (Figure 4) occurs exclusively within the host cell cytoplasm. It utilises the ubiquitous low-density lipoprotein receptor (LDLR) to attach to host cells and cell entry is facilitated by endocytosis. After endocytosis, the intracellular endosome undergoes acidification and this drop in pH triggers a conformational change in the glycoprotein that mediates fusion between the viral envelope and the endosomal membrane. The viral nucleocapsid is then able to enter the cell cytoplasm and commence viral replication.[322]

As a negative sense RNA virus, the viral RNA must first be transcribed by viral RNA polymerase into positive sense mRNA which is then translated into viral proteins using the host ribosomes. In addition, the viral RNA polymerase uses the positive sense mRNA as a template to synthesise copies of genomic negative-sense RNA. Replication is complete when the viral proteins and genomic RNA are assembled together into complete virions and the progeny virus exits the cell by budding through the host cell plasma membrane.[322]

Figure 4: Replicative lifecycle of Maraba virus

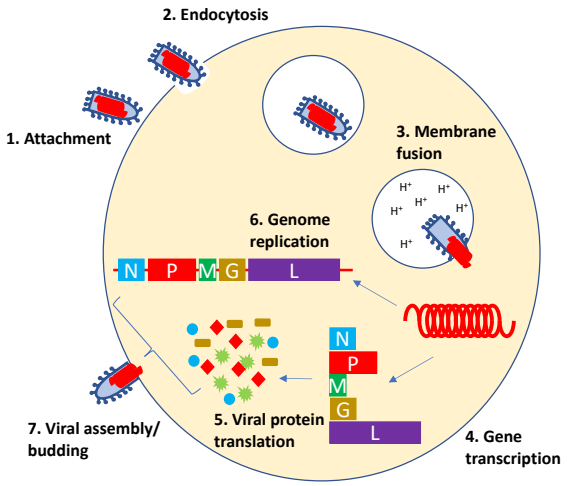

Figure adapted from Lichty, B.D., et al., *Vesicular stomatitis virus: re-inventing the bullet.* Trends Mol Med, 2004. **10**(5): p. 210-6 [322]

The wild-type Maraba virus has been genetically modified in order to enhance its replication within malignant cells. Two single mutations have been introduced, specifically the L123W and Q242R substitutions in the sequence of the M and G proteins, respectively. The resulting strain, named MG1, has demonstrated faster replication, a larger burst size and an increased killing potency in tumour cells. Conversely, MG1 was strongly attenuated in normal non-malignant cells due to the inability of MG1 to block type I IFN-mediated antiviral immunity. Given that a deficient or defective IFN signalling pathway is frequently acquired during oncogenesis, this further highlights the tumour tropic nature of MG1.[320]

Taking into consideration its enhanced tumour tropism, its cytoplasmic replicative cycle mitigating the risk of genotoxicity, and its lack of human pathogenicity, demonstrates that MG1 virus has characteristics suited for potential use as oncolytic virotherapy.[321]

2.3.2 MG1 cytotoxicity

In vitro, MG1 has demonstrated oncolytic activity against multiple adherent cancer cell lines of human, canine, and murine origins (Table 2).[323] Additionally using an ovarian cancer model, it was demonstrated that MG1 was able to infect, replicate, and induce cell death killing activity against detached cells in suspension and against three-dimensional spheroids.[324] When tested against a range of sarcoma cell lines, MG1 has also shown superior cytotoxicity when compared to the VSVΔM51, HSV-1 N212, vvDD and reovirus OVs.[321]

Ex vivo, MG1 can infect, replicate and have a cytotoxic effect against tissue from human tumour biopsies. These samples included prostate cancer, head and neck squamous cell carcinoma and a range of sarcomas subtypes.[325-327] Given the often poor prognosis in patients with bone and soft tissue

malignancies, MG1 therapy could represent a promising therapeutic prospect for these challenging cancers.

In vivo, MG1 can be delivered directly to the tumour but can also be safely administered systemically, thereby enabling the treatment to reach not only localised but also disseminated sites of disease. This has been shown in a murine syngeneic subcutaneous CT26 colorectal carcinoma model, in which, systemically administered MG1 successfully infected the tumour bed and replicated *in situ*, leading to complete tumour regression and durable cures. Additionally, IV MG1 was able to reach and showed superior efficiency in eliminating CT26 lung metastases when compared to VSV OV.[320, 321] Multiple publications have subsequently shown the oncolytic activity of MG1 in other syngeneic or xenograft models, including ovarian, lung, skin, breast, prostate, sarcoma and haematological cancers.[320, 326, 328-330]

MG1 has also demonstrated synergistic oncotoxic benefits when administered in combination with other agents. For instance, the co-treatment of mice bearing syngeneic subcutaneous breast tumours using intratumoural MG1 alongside intraperitoneal paclitaxel led to a survival extension compared to either agent given as monotherapy.[329] Mechanistically, paclitaxel impaired tumour cell IFN-β production, thus enabling increased MG1 replication and oncolysis.[321, 329]

Table 2: Cell lines susceptible to MG1 oncolysis *in vitro*

Origin	Cancer type	Cell line	References
Canis familiaris	Sarcoma	• D17	[326]
Homo sapiens	Breast cancer	• BT549 • HS587T • MCF7 • MDA-MB-231 • MBA-MB-435 • NCI/ADR-RES • T47D	[320, 329, 330]
	Central nervous system cancer	• SF268 • SF295 • SF539 • SNB19 • SNB75 • U118 • U343 • U373	[320, 331]
	Colon cancer	• COLO205 • HCT116 • HCT15 • HT29 • SW620	[320, 328]
	Leukaemia, lymphoma	• A.301 • Jurkat • OCI-Ly18	[332]

	Lung cancer	• A549 • HOP62 • HOP92 • NCI-H226 • NCI-H23	[320, 331]
	Ovarian cancer	• ES2 • HEYA8 • iOvCa105 • iOvCa131 • iOvCa142 • iOvCa147 • OVCAR3 • OVCAR4 • OVCAR8 • SKOV3	[320, 324, 331, 333]
	Pancreatic cancer	• PANC-1	[320]
	Prostatic cancer	• DU145 • LNCaP • PC3	[320, 327]
	Renal cancer	• 786-O • ACHN • SN12C • TK10	[320]
	Sarcoma	• 143B • RD-ES • SW982 • U2OS	[320, 326]

	Skin cancer	• A431 • M14 • MALME3M • SKMEL28 • UACC257 • UACC62	[320]
Mus musculus	Central nervous system cancer	• GL261	[320]
	Colon cancer	• CT26 • CT26lacZ	[320, 328]
	Leukaemia, lymphoma	• EL4 • L1210	[332]
	Lung cancer	• TC1	[334]
	Mammary gland cancer	• E0771 • EMT6 • 4T1	[320, 329]
	Prostatic cancer	• TRAMP-C1 • TRAMP-C2	[327]
	Skin cancer	• B16 • B16F10 • B16lacZ	[263, 323, 328]

Table adapted from Pol, J.G. *et al*. *Development and applications of oncolytic Maraba virus vaccines.* Oncolytic Virother, 2018. 7: p. 117-128. [321]

2.3.3 MG1 and the immune system

The therapeutic efficacy of MG1 not only relies on its oncolytic activity but also on its ability to induce an anti-tumour immune response.

To determine this experimentally, MG1 was inactivated by ultraviolet light for two minutes (MG1-UV2min) to render it replication incompetent and then compared to live, replication-competent MG1. In a syngeneic B16lacZ melanoma model, the MG1-UV2min was equally effective in reducing lung metastases as live MG1, albeit that this held true only at high doses, as the efficacy of non-replicating MG1 gradually dropped with lower doses, unlike its replicative counterpart that retained its full potency.[321, 328]

Nevertheless, the absence of detectable MG1 from the responding lung lesions further indicated that the *in vivo* efficacy of MG1 could be attributed to an immune-mediated effect, rather than solely on viral oncolysis. In addition, within 24 hours post MG1 administration, the authors observed a splenomegaly resulting from an increase in innate populations of NK and dendritic cells. This immune cell expansion lasted up to five days and was accompanied by an enhancement of effector NKs secreting IFN-γ or granzyme B. The activation of this NK cell immune response appeared critical for the therapeutic efficacy as selective depletion of NKs abolished tumour growth control.[321, 328]

The ability of MG1 to stimulate an anti-tumour immune response is also of interest within the neoadjuvant setting.[263, 330] The biological stress responses to surgery are immunosuppressive and can therefore promote cancer progression.[335] This has been illustrated in experiments showing a shorter survival in untreated tumour-bearing mice undergoing surgery, who experience a postoperative increase in malignant lesions compared to unoperated controls.[336]

However, the neoadjuvant administration of MG1 in a B16lacZ melanoma and a 4T1 breast cancer murine model, decreased the post-operative metastatic burden compared to surgery alone and thereby improved overall survival in the B16lacZ lung metastasis model.[263]

Neoadjuvant MG1 also demonstrated benefits against a murine model of triple-negative breast cancer. IT administration of MG1 prior to tumour resection led to the development of an adaptive immunological response that protected 20% of the animals against a subsequent tumour rechallenge. This benefit was found to depend upon viral replication as UV-inactivated MG1 did not provide protection against tumour recurrence. Interestingly, the IV delivery of MG1 appeared more efficient in generating immunological memory than IT injection as 40% of animals were protected against rechallenge.[330]

In analysing these changes further, transcriptomic data revealed that pathways linked to immune responses were enriched during MG1 infection. This involved an increased expression of chemokines including CCL5 and CXCL11 as well as activation of STAT1, NFκB and IRF3. *In vivo*, MG1-infected tumours displayed greater T cell infiltration at the time of surgery compared to controls. This T cell infiltration was dependent on CXCR3 and its associated chemokine ligands CXCL9, CXCL10, and CXCL11. *Ex vivo*, the restimulation of splenocytes led to IFN-γ release in MG1-treated mice thereby indicating tumour-specific reactivity.[330]

In addition, MG1 infection upregulated PD-L1 protein level expression in three breast cancer cell lines *in vitro*. This gave the rationale for combining neoadjuvant MG1 with post-operative dual anti-CTLA-4 and anti-PD-1 checkpoint blockade in triple negative breast cancer models. The combination treatment significantly extended survival, compared to control or either treatment given alone with a complete response in 60%–90% of the animals depending on the model.[330] Altogether, these preclinical findings indicate the potential role for MG1 as an immune based virotherapy adjunct in the neoadjuvant setting.[321]

The immunogenicity of MG1 has also been used to improve the efficacy of cancer cell vaccines against leukaemia [332] and metastatic solid cancers.[328] *In vitro*, although MG1 could infect several lymphoma and leukaemia cell lines, it was ineffective against an *in vivo* L1210 murine leukaemia model. However, when mice with the same model were given an infusion of MG1-infected γ-irradiated leukaemia cells, named iLOV, 60% of the animals had a complete response. In addition, the prophylactic infusion of iLOV cells resulted in complete protection against the subsequent leukaemia challenge, and notably, injecting uninfected cells was ineffective, thereby suggesting the importance of MG1-induced cancer immunogenic cell death for effective iLOV cell vaccine treatment.[332]

A similar approach has been utilised in a B16 melanoma and CT26 colon cancer model. The administration of an infected cell vaccine (ICV) consisting of MG1 expressing IL-12 (MG1-IL12-ICV) was superior in controlling pulmonary metastases when compared to MG1-ICV control.[328] In addition, in a peritoneal carcinomatosis model of B16 melanoma, MG1-IL12-ICV extended survival and this benefit was dependent on both NK cells and $CD8^+$ T lymphocytes as their selective depletion abolished anti-tumour activity.[328]

Given that the systemic administration of cytokines as a traditional treatment in melanoma is often accompanied with severe adverse events, MG1 guided local delivery of elevated levels of IL-12 into the TME may be a safe and effective method to enhance anti-tumour immune immunity.[321]

To expand on this concept, MG1 has been used as a successful oncolytic vaccine vector by encoding the viral genome with transgenes that overexpress tumour antigens to potentiate the anti-tumour immune response.

This approach was investigated by inserting the melanoma associated tumour antigen dopachrome tautomerase (DCT) between the G and L gene sections of the MG1 genome. By itself, MG1-DCT did not prime a detectable adaptive T-cell response against the melanoma antigen. However, beneficial effects

were observed when a prime-boost strategy was adopted, by using an initial administration of a replication-defective (E1/E3 deleted) adenovirus also encoded to express DCT (Ad-DCT) prior to subsequent MG1-DCT.[323]

The Ad-DCT:MG1-DCT prime-boost extended the median survival when compared to Ad-DCT-treated mice, curing 20% and 30% of the animals bearing brain and lung metastases, respectively. Of note, the DCT-specific adaptive response increased with this prime-boost approach with 30% of circulating $CD8^+$ T-lymphocytes reacting against the DCT epitope, compared to 20% with VSV-DCT or 6% with Ad-DCT alone. Furthermore, this prime-boost method was also able to stimulate reactivity against the melanoma-associated antigen gp100, which was not encoded by the viral vaccine, thereby suggesting that oncolytic virotherapy can lead to treatment-induced antigen cross presentation. The benefits observed were largely $CD8^+$ mediated as the anti-tumour activity was negated by $CD8^+$ depletion and an anti-tumour memory was induced that protected cured animals from subsequent tumour rechallenge.[323]

The prime-boost vaccination strategy has since been adapted for the treatment of human papillomavirus (HPV) positive tumours [325, 334] and prostate cancer.[327] Both the replication-defective adenovirus and MG1 virus were encoded with transgenes expressing the E6 and E7 antigens of the HPV serotypes 16 and 18. When Ad-E6/E7:MG1-E6/E7 was used in a prime-boost method against an HPV expressing TC1 lung carcinoma murine model, 60% of circulating $CD8^+$ T-cells showed E7 antigen reactivity and 75% of mice achieved complete tumour regression with the establishment of long-term immune memory. This response was associated with a local increase in the expression of genes involved in antigen presentation, antiviral innate immunity and T-cell activation, in comparison to untreated tumours.[321, 325]

Moreover, the replication-defective adenovirus and MG1 virus were encoded with a transgene encoding the human six-transmembrane antigen of the prostate (hSTEAP). In this instance, $CD8^+$ T cell responses against the STEAP antigen were detected in 40% of subjects. When administered for the

treatment of subcutaneous TRAMP-C2 prostate tumours, the Ad-hSTEAP:MG1-hSTEAP viral vaccine vector significantly slowed tumour growth and extended median survival. Transcriptional profiling and immunohistochemical analysis showed an increased expression of receptors and ligands involved in T cell activation, function and migration. In addition, genes involved in antigen processing and presentation were also enriched.[321, 327]

In summary, these preclinical data highlight the ability of the MG1 OV to exert tumour tropic oncolysis and to generate a significant tumour-specific immune response leading to therapeutic efficacy as well as immune memory protecting from cancer recurrence. On this basis, the MG1 platform has been progressed into the clinical area.

2.3.4 MG1 in clinical use

Building upon the encouraging signals from pre-clinical studies, three human clinical trials have been initiated to evaluate MG1 using a prime boost strategy.

The first phase I/II trial is evaluating Ad:MG1-MAGEA3 in patients with incurable solid tumours expressing the tumour antigen melanoma-associated antigen 3 (MAGE-A3) (ClinicalTrials.gov: NCT02285816).[337]

Patients received two infusions, three days apart, of MG1-MAGEA3 alone (Arm A) at a dose of $1x10^{10}$, or were administered with intramuscular 1×10^{10} pfu of Ad-MAGEA3 alone (Arm B), or were treated with Ad-MAGEA3 followed two weeks later with systemic MG1-MAGEA3 (Arm C). Treatment related toxicities included hypoxia/dyspnoea, vomiting, headache, diarrhoea, nausea, anorexia, chills, fatigue, fever, flu-like symptoms, hypophosphatemia, headache, and hypotension. A transcriptomic analysis of tumour biopsies identified a modulation of numerous pro-inflammatory genes. Furthermore, markers of NK cells and activated antigen-presenting cells were detected, namely CD56, CD68, CD80, HLA-A, HLA-B and TLR3. Several inflammation

supporting chemokines and cytokines were induced, such as CCL2, CCL5, CX3CL1, CXCL10, IL-6, and TNF whereas conversely, the immunosuppressive TGF-β appeared downregulated. Anti-tumour immunity was evidenced in three out of the six patients evaluated, with over 1% of total circulating $CD8^+$ T cells reacting against MAGE-A3 in one participant. Moreover, patient blood samples taken during the trial detected the presence of MG1-MAGEA3 genomes two weeks following treatment, thereby confirming the ability of the virus to replicate in humans.[337]

A second phase I/II clinical trial has recruited patients to receive the Ad-MAGEA3:MG1-MAGEA3 treatment, combined with pembrolizumab, in patients with previously treated metastatic non-small-cell lung cancer (ClinicalTrials.gov: NCT02879760).

The third phase I clinical trial is investigating the prime-boost effects of Ad-E6/E7:MG1-E6/E7 in combination with atezolizumab in patients with advanced HPV associated tumours (ClinicalTrials.gov: NCT03618953).

In summary, the little clinical data available validate the feasibility of the Ad:MG1 oncolytic vaccination and its potential ability to stimulate adaptive anti-tumour cell response in cancer patients.[321] Furthermore, the current trials have shown a reassuring safety profile and therefore, MG1 is well positioned for further investigation to identify how it can be used to improve patient cancer outcomes.

2.4 Conclusion

To conclude, the last decade has seen the development of immune checkpoint inhibitors and a marked improvement in the treatment outcomes for patients with advanced melanoma. However, many patients still fail to respond, or relapse, and the most effective combination treatments can be associated with significant immune related adverse events. Therefore, there is still an unmet need to understand the biological principles that underpin the interaction

between the tumour and the immune system and how this might be harnessed to find novel treatments or combinations which lead to further improving the survival of, or mitigating treatment toxicity in, these patients.

OVs represent a promising therapeutic platform given their ability to preferentially replicate in tumour cells, self-amplify and lyse tumour cells and in doing so, modulate the TME to optimise both innate and adaptive immune-mediated tumour eradication, both at locoregional and systemic sites of disease.

OVs can also be genetically manipulated to boost their anti-tumour effects and represent attractive combination partners when delivered with ICB as they have favourable safety profiles, promote the recruitment of effector lymphocytes and can induce the upregulation of PD-1/PD-L1 expression thereby increasing the responsiveness of checkpoint antibodies. Given the ability for cancers to evade immune control, OVs therefore show great promise as an additional approach to cancer treatment.

The Maraba virus MG1 has demonstrated potent oncolytic activity against multiple cancer cell lines and has been shown to generate both innate and adaptive anti-tumoural immune responses. Given its zoonotic lifecycle, there is no widespread pre-existing immunity in the general population. In addition, it can be administered both locally and systemically, allows genome modifications and transgene insertions and has been successfully combined with other anti-cancer therapies.

In murine models, MG1 has demonstrated oncolytic activity in a range of tumour subtypes and has been taken forward into several early stage clinical trials. Despite the wide variety of OVs, the above characteristics make MG1 an exciting prospect, warranting further investigation, as a potential novel method in the treatment of cancer.

2.5 Study Aims

The aims of this study are to examine the MG1 virus as a potential anti-cancer agent for the treatment of melanoma, by investigating both the direct cytotoxicity and the generation of anti-tumour immunity. In addition, this study aims to determine whether MG1 efficacy can be enhanced by combining with other standard of care cancer treatments such as immune checkpoint inhibitors.

Specific aims of the project are to:

1. Investigate the cytotoxicity of MG1 against murine and human melanoma cell lines.
2. Characterise the immune effects of MG1 treatment in melanoma.
3. Test the efficacy of IT and IV delivery of MG1 in different murine melanoma *in vivo* models.
4. Determine whether the efficacy of MG1 virus can be effectively enhanced through novel combinations including with ICB.

Chapter 3:

Materials and Methodology

3 Chapter 3: Materials and Methodology

3.1 Cell culture and storage

3.1.1 Cell lines acknowledgement

Melanoma cell lines and Vero cells were donated from colleagues within the Professor Melcher and Professor Harrington laboratories at the ICR, London, in 2018. The murine melanoma cell lines used were B16-F1 and B16-F10 (BRAF V600E wild-type) in addition to 4434 and 21015 (BRAF V600E mutant). The human melanoma cell lines used were Mel888, A375 and Mel624 (BRAF V600E mutant, NRAS wild-type), DO4 (BRAF V600E wild-type, NRAS mutant) and MeWo (BRAF V600E wild-type, NRAS wild-type). Murine pancreatic cell lines were donated by colleagues within the Professor Sadanandam laboratory at the ICR, Sutton, in 2018.

3.1.2 Cell culture

All melanoma cell lines, and Vero cells were cultured in Dulbecco's Modified Eagle's Medium (DMEM) (Sigma) with 10% heat-inactivated foetal bovine serum (FBS) (Sigma), 1% L-glutamine (Sigma) and 0.5% penicillin-streptomycin (60 mg/L and 100 mg/L respectively) (Sigma). All pancreatic cell lines were cultured in Roswell Park Memorial Institute (RPMI) media (Sigma) with 10% heat-inactivated foetal bovine serum (FBS), 1% L-glutamine and 0.5% penicillin-streptomycin (60 mg/L and 100 mg/L respectively). All media and reagents were supplied by Laboratory Support Services, ICR, London, unless stated otherwise. All cell lines were cultured in a humidified atmosphere of 5% CO_2 in air at 37°C within a cell incubator (Heracell™ 150i, Thermo Fisher). Routine maintenance of cell lines was performed under aseptic conditions within a microbiological safety cabinet (BioMAT Class II Microbiological Safety Cabinets, Medical Air Technology Ltd). Cells were maintained in vented plastic tissue culture flasks (75 cm² and 175 cm²)

(Corning®). 50 mL or 15 mL sterile polypropylene tubes (BD Falcon) were used for harvesting and washing cells. Cells were plated in 6-, 24- and 96-well plates for assays as indicated (Corning®). Adherent cells were harvested near confluence by washing with phosphate buffered saline (PBS) followed by trypsin–EDTA (Sigma). Cells were pelleted by centrifugation at 400g for five minutes using an Heraeus Megafuge 2.0R centrifuge unless stated otherwise. Viable cell counts were obtained using 0.2% (v/v) trypan blue in PBS, with an improved Neubauer haemocytometer (Weber Scientific). Every three months, all cell lines were tested for, and found to be free from, mycoplasma infection using the e-Myco™ PCR Kit (iNtRON Biotechnology, South Korea). The user instruction manual details the technique used, but in summary, the process initially required suspending at least $1x10^5$ cells in 100 µL of sterile PBS. Samples were heated at 90°C for 10 minutes and vortexed for 5-10 seconds. Samples were centrifuged for two minutes at 1400g. 10 µL of sample was added to each tube of e-Myco™ Mycoplasma PCR Detection Kit and then resuspended after the addition of 10 µL sterile water, equating to a 20 µL PCR reaction volume. 35 PCR denaturation, annealing and extension cycles were conducted using a QuantStudio™ PCR machine (Thermo Fisher) before sample detection on a 2% agarose gel (Thermo Fisher).

3.1.3 Cryopreservation

Cell pellets were resuspended in freezing medium 90% (v/v) FBS; 10% (v/v) dimethyl sulfoxide (DMSO) (Sigma) and stored in 1 mL cryovials (Nunc®). Cryovials were immediately placed at –80°C in a slow-cooling insulating box and stored within an ultra-low temperature freezer at –80°C (Haier). When required, cells were thawed in a 37°C water bath, washed in a large volume of DMEM or RPMI to remove DMSO, resuspended in growth medium and placed into a culture flask.

3.2 MG1 virus

3.2.1 Viruses

MG1-green fluorescent protein (MG1-GFP) and MG1-firefly luciferase (MG1-FLUC) were originally produced and provided by Ottawa Hospital Research Institute (Ottawa, Canada).[320]

3.2.2 Viral storage

Viral stocks were stored in PBS at -80°C. Required dilutions for assays were made in PBS or either DMEM or RPMI complete growth media. Each virus was amplified (3.2.3) and aliquoted into 200 µL Eppendorf tubes (Sigma) for longer term storage at -80°C.

3.2.3 Viral propagation

Vero cells were infected with 0.1 MOI (multiplicity of infection) of MG1-GFP or MG1-FLUC. After 24 hours, supernatants were collected and centrifuged at 400g for 10 minutes using a Heraeus Megafuge 2.0R centrifuge at 400g for 10 minutes to pellet the cellular debris for disposal. The supernatants were aspirated and filtered through Sartorius™ Minisart® 0.2 µm high flow syringe filters (Thermo Fisher) prior to centrifugation at 8000g for one hour using a Beckman Coulter Optima XPN ultracentrifuge. The viral pellet was resuspended in PBS and aliquots were stored as per section 3.2.2.

3.2.4 Viral titre using plaque assay

Virus titre was determined by plaque assay using Vero cells. Vero cells were plated at $1x10^{5}$ cells/well in 12-well plates. After 24 hours, serial dilutions of between $2x10^{-4}$ and $2x10^{-9}$ of cell lysates or stock MG1 were prepared in virus serum-free dilution medium (DMEM, 2mM L-glutamine). The medium was removed from the Vero cells and replaced with 200 µL virus serum-free dilution medium followed by 100 µL of diluted viral samples, in duplicates. After one

hour incubation at 37°C, the supernatant medium was removed and the wells overlaid with a 1:1 solution of 3% CMC (sodium carboxymethyl cellulose) (Sigma) and 10% DMEM. After 48 hours incubation at 37°C, plates were carefully aspirated, washed with PBS, fixed with 1% PFA (1% (w/v) paraformaldehyde (Sigma) in PBS) and stained with 0.2% crystal violet (Sigma) for five minutes. Plates containing plaques were counted manually. The average of duplicate wells was used to calculate viral titre, using the following calculation:

Viral titre (pfu/mL) = average number of plaques / dilution

3.3 Cell infection

Cells were plated at a density of $5x10^5$ cells/well in 6-well plates with 4 mL of growth medium and infected with MG1-GFP at MOI concentrations of 10, 1.0, 0.1, 0.01 and 0.001 in addition to an uninfected PBS control. Live images of MG1-GFP infected cells were acquired using an EVOS Fl cell imaging system microscope (Thermo Fisher) at 24 and 48 hours post-infection.

For flow cytometry analysis, cells were plated and infected in the same method with MG1-GFP at an MOI of 0.1 and 10, then harvested at 24 and 48 hours. $1x10^5$ cells from each sample were added to individual FACS tubes (BD Falcon) and cells were washed with 2 mL of FACS buffer (PBS; 1% (v/v) FCS; 0.1% (w/v) sodium azide (Sigma)). Cell pellets were re-suspended in 100 µL FACS buffer before the addition of a viability dye (eBioscience fixable viability dye eFluor 780). Cells were incubated in the dark for 30 minutes at 4°C and then washed with 4 mL FACS buffer. Finally, cells were fixed with 1% PFA and stored at 4°C prior to acquisition on a BD LSR II flow cytometer.

3.4 Cell replication assay

B16-F1, B16-F10, 4434 and 21015 cells were seeded in 12-well plates at a density of $1x10^5$ cells/well in 1 mL of growth medium. Each well was infected with MG1-FLUC at MOI 0.1 or 1.0. The cells were incubated at 37°C and the

supernatants collected using a wide tip Pasteur pipette at 0, 4, 8, 18, 24, 48 and 72 hours. Cell-free supernatants were collected following centrifugation and were used to determined viral titre by viral plaque assay (section 3.2.4).

3.5 Cell viability assays

3.5.1 3-(4,5-dimethylthiazol-2-yl)-2,5-diphenyltetrazolium bromide (MTT) assay

Cell viability was quantified using MTT assay. Cells were plated in a clear-walled 96-well plate at a density of 2000 cells/well in 200 uL growth medium. The following day, cells were infected with MG1-GFP at MOI concentrations of 10, 1.0, 0.1, 0.01, 0.001 and an uninfected PBS control. The plates were incubated for 24 or 48 hours before 20 µL of MTT reagent (Thermo Fisher) at 5 mg/mL concentration was added to each well for four hours in the dark at 37°C. The medium was gently aspirated and 200 µL DMSO added to each well. Optical density was determined using SpectraMax 384 plate reader (Molecular Devices) at a wavelength of 550 nm. Results were normalised to the control population of untreated cells.

3.5.2 Adenosine triphosphate (ATP) release assay

To measure ATP release, cells were seeded into 12-well plates with $1x10^5$ cells per well in 1 mL growth medium and incubated overnight. The following day, the medium was aspirated and replaced with 1 mL of fresh growth medium before the addition of MG1-GFP at MOI concentrations of 0.01, 1.0 and uninfected control. The supernatants were collected using a wide tip Pasteur pipette following 24 and 48 hours and centrifuged. 100 µL of each supernatant was distributed into a 96-well solid white polystyrene microplate (Fisher Scientific) and 25 µL of CellTiter-Glo® Luminescent assay (Promega) was added to each well. The plate was allowed to incubate in the dark for 10 minutes at 37°C and the luminescent signal was recorded using a SpectraMax 384 plate reader (Molecular Devices) and results were normalised to the control population of untreated cells.

3.6 Enzyme-linked immunosorbent assay (ELISA)

The concentration of supernatant IFN-β was determined using the mouse IFN-β ELISA kit (R&D systems) and splenocyte IFN-γ release was assessed with the IFN-γ ELISA kit (R&D systems). HMGB1 was assessed using HMGB1 ELISA kit (Tecan). Samples were tested according to the manufacturer's protocol. Briefly, flat-bottomed 96-well plates were coated with 100 µL of the optimised dilution of capture antibody, sealed and incubated overnight at room temperature. Antibody coated plates were washed three times with 400 µL for each well of PBST wash buffer (0.05% (v/v) Tween20 (Sigma) in PBS). 300 µL of block buffer (1% BSA (Sigma) in PBS) was added for one hour at room temperature. The plates were washed a further three times with wash buffer before 100 µL of serially diluted recombinant protein standards and sample supernatants were added in duplicate for two hours. Plates were washed a further three times before 100 µL of optimally diluted detection antibody was added and incubated at room temperature for a further two hours. After a further three washes, 100 µL of optimally diluted streptavidin-HRP was added to each well and incubated in the dark for 20 minutes at room temperature. Plates were washed a further three times and 100 µL of substrate solution added to each well prior to a further 20 minute incubation in the dark. Finally, 50 µL of stop solution was added to each well and the optical density of each well determined using a SpectraMax 384 plate reader (Molecular Devices) correcting for optical imperfections in the plate by subtracting readings acquired at 570 nm from those at 450 nm.

3.7 Western Blotting

3.7.1 Buffers

2x loading buffer

> 100 mM Tris HCl pH 6-8 (Sigma) 4% (w/v) SDS (Sigma); 0.2% (w/v) bromophenol blue (Sigma); 20% (v/v) glycerol (Sigma); 200 mM dithiothreitol (DTT) (Sigma) in ddH20

Running buffer

> 25 mM Tris base; 250 mM glycine (Sigma); 0.1% (w/v) SDS (Sigma) in ddH20

3.7.2 Method

Cell lysates for western blot were obtained directly on the culture surface of 7cm petri dishes (Sigma) with RIPA buffer (Thermo Fisher) containing protease (Roche) and phosphatase inhibitors (PhosSTOP™, Roche) and subjected to protein quantification (BCA, Thermo Scientific) prior to western blot analysis. Samples were mixed with an equal volume of 2x loading buffer and heated at 95°C for five minutes. To verify protein size, 30 µL of each sample and 2 µL of Odyssey® Protein Molecular Weight Marker (LI-COR® Biosciences) were loaded on to 10% Criterion™ TGX™ Precast Midi Protein Gel (Bio-Rad). Gels were run in Bio-Rad Mini Trans-Blot® cell containing running buffer at 100 V/gel for approximately 90 minutes until the loading dye had run to the bottom of the gel. The gels were then removed from the cassettes and briefly washed with running buffer. Protein transfer was completed in a Trans-Blot Turbo Transfer System (Bio-Rad) and transferred to Trans-Blot Turbo Midi 0.2 µm nitrocellulose transfer membranes. These membranes were washed with PBS and then blocked in a 1:1 mixture of Odyssey blocking buffer (LI-COR® Biosciences) and TBST (0.05% Tween 20 in tris buffered saline) for one hour. Primary antibodies were added in a 1:1 mixture of blocking buffer and TBST and incubated for 24 hours. Primary antibodies were removed by four TBST washes, each lasting 15 minutes.

Secondary antibodies were added in blocking buffer and TBST as above and incubated for one hour at room temperature. Secondary antibodies were removed with four further 15 minute TBST washes. Nitrocellulose membranes were read on a LI-COR® Odyssey infrared imager and analysed using LI-COR® Image Studio software. (Antibody specifics are detailed within Appendix 9.2)

3.8 *In vivo* experiments

3.8.1 Mice

Five- to six-week-old female C57Bl/6 mice (Charles River, UK) were selected for use in all *in vivo* experiments. These were conducted at the ICR Biological Services Unit and were approved by the ICR local Ethical Review Committee and standards of care were based upon the UKCCCR Guidelines for the welfare and use of animals in cancer research.[338]

3.8.2 Tumour implantation, treatment and monitoring

B16-F1 or 4434 murine melanoma tumours were established by 100 µL subcutaneous (SC) injection of $5x10^5$ and $4x10^6$ cells respectively into the right flank of each mouse. Tumour measurements were taken twice weekly in three dimensions using Venier callipers and the tumour volume estimated using the formula: length x width x height (mm) x 0.5236. For systemic IV treatments, a total volume of 100 µL was injected via the tail vein with a 27-gauge needle (BD Biosciences). In contrast, a total volume of 50 µL was used for IT administration via insulin needles with a 28-gauge diameter (BD Biosciences). Humane endpoint was defined as a tumour diameter greater than 15 mm in any dimension.

3.8.3 Imaging of MG1-FLUC in B16-F1 and 4434 tumours and other organs after IV administration

Right flank B16-F1 or 4434 tumours were established in C57Bl/6 mice using the technique described (3.8.2). $1x10^7$ pfu of MG1-FLUC was administered IV to each mouse. At time points of 6, 18, 24 and 30 hours following viral treatment, the mice were anaesthetised using inhaled isoflurane (4-5% concentration at induction and 3% for maintenance at flow rate of 0.8-1.0 L/min) and then 200 µL (at a concentration of 9.375 mg/mL) of D-luciferin (Sigma) was administered via intraperitoneal injection. Mice were imaged using the IVIS® Spectrum *in vivo* imaging system. After imaging, the mice were sacrificed and the tumour, along with other organs including the spleen, liver, lung and brain were harvested and imaged *ex vivo* in the IVIS system.

3.8.4 Identification of neutralising antibodies

Tumour-naïve C57Bl/6 mice received IV MG1-FLUC at a dose of $1x10^6$ pfu. Mice were sacrificed and blood harvested by intracardiac puncture at 48 hours, 72 hours, 7 days and 14 days. Whole blood was placed into 1.5 mL plasma collection tubes (Thermo Fisher) and centrifuged at 400g for 10 minutes in a Heraeus Megafuge 2.0R centrifuge to separate the plasma which was then transferred to sterile Eppendorf tubes and heated at 56°C for 30 minutes to inactivate complement proteins. MG1-FLUC with an MOI of 0.1 was added to each plasma sample and incubated at 37°C for four hours. The presence of replication active MG1 within each plasma/MG1-FLUC mix was then assessed via plaque assay (section 3.2.4).

Mice harbouring subcutaneous 4434 tumours were also systemically injected with either PBS or $1x10^6$ pfu of MG1-GFP virus. Five days later, all mice were challenged with IV $1x10^6$ pfu MG1-FLUC and the tumours and organs were harvested for IVIS imaging 48 hours later.

3.8.5 Combination therapy with MG1-FLUC and anti-PD-1 antibody

Five- to six-week-old female C57Bl/6 mice were implanted with $4x10^6$ subcutaneous 4434 cells on the right flank. Treatment commenced on day 21 when the tumours were approximately 150 mm^3 in volume. Six mice per group were treated with either IT PBS + IP isotype (InVivoMab mouse IgG2b isotype control, clone MPC-11; 2BScientific), IT MG1-FLUC ($1x10^7$ pfu) + IP isotype, IP anti-PD-1 (InVivoMab rat anti-mouse PD-1 (CD279), clone- RMP1-14 monoclonal antibody, IgG2a κ; 2BScientific) + IT PBS or IT MG1-FLUC + IP anti-PD-1. 200 µg of isotype control or anti-PD1 antibody was administered twice a week for a maximum of four weeks or until mice reached humane end point. Tumour measurements were recorded twice weekly.

3.9 *Ex vivo* sample preparation

3.9.1 Tumour processing – homogenisation

B16-F1 or 4434 tumours were implanted into C57Bl/6 mice and received planned treatment within each specified experiment. At the desired timepoints, the tumours were collected and placed into homogeniser tubes (Precellys, Fisher Scientific) containing 500 µL of lysis buffer (one protease inhibitor cocktail tablet (Sigma) in 50 mL PBS). The tubes were inserted into the homogeniser (Precellys 24, Bertin Technologies) and homogenised at 5500 rpm for 15 seconds, then at 6000 rpm for three cycles of 20 seconds. After leaving the tubes on ice for 10 minutes, they were centrifuged at 1400g for 15 minutes at 4°C. The supernatant was aspirated and transferred into new Eppendorf tubes. The lysates underwent three freeze-thaw cycles between -80°C and room temperature.

Plaque assays (section 3.2.4) were performed for each sample and quantified according to the weight of the tumour harvested. The spleens and other organs collected also underwent processing and plaque assay quantification.

Sample supernatants were also tested via ELISA for the presence of IFN-β (section 3.6).

3.9.2 Tumour processing – proteome cytokine array

Methodology followed that described in the Proteome Profiler™ Mouse XL Cytokine Array Kit (RnD Systems). Tumours were harvested and homogenised as previously described. On the completion of the homogenisation process, Triton™ X-100 (Sigma) was added to a final concentration of 1%. Samples were frozen at -80°C, thawed, and centrifuged at 400g for five minutes to remove cellular debris. Quantitation of sample protein concentrations were calculated using a total protein assay.

Nitrocellulose membranes with pre-plated capture antibodies were added to 2 mL of array block buffer and incubated for one hour. The block buffer was aspirated, and the prepared sample (200 µg) added to the membrane and incubated overnight at 4°C on a rocking platform shaker. Membranes were rinsed three times with wash buffer for 10 minutes prior to the addition of 1.5 mL of diluted detection antibody cocktail. Membranes were then incubated for one hour at room temperature and washed a further three times prior to the addition of 2 mL of streptavidin-HRP. After a 30 minute incubation and wash phase, the Chemi Reagent Mix was added for one minute and the nitrocellulose membrane placed in an autoradiography film cassette and exposed to X-ray film for one minute. Images from the membrane were analysed with Image Lab™ software version 5.2.1.

3.9.3 Tumour processing – differential gene expression evaluation through RNA analysis

4434 tumours were explanted from animals and stored in RNAlater (Thermo Fisher) at -20°C prior to RNA extraction. Samples were homogenised as described previous and RNA extraction performed using RNeasy kit (Qiagen, USA) as per manufacturer protocol. Extracted RNA was quantified using NanoDrop spectrophotometer (Thermo Fisher) and quality assessed using

BioAnalyzer 2100 (Agilent, Santa Clara, USA). Samples were stored at -80°C before subsequent analysis.

Total RNA was used to prepare cDNA libraries using the Illumina TruSeq Stranded Total RNA with Ribo-Zero Gold Preparation kit (Illumina, USA). RNA integrity number (RIN) values for the samples ranged from 9.7 to 10. Briefly, 750 ng of total RNA was rRNA depleted, followed by enzymatic fragmentation, reverse-transcription, and double-stranded cDNA purification using AMPure XP magnetic beads (Beckman Coulter, USA). The cDNA was end repaired, 3′ adenylated, with Illumina sequencing adaptors ligated onto the fragment ends, and the stranded libraries were pre-amplified with PCR. The library size distribution was validated and quality inspected using an Agilent 2100 Bioanalyzer. The quantity of each cDNA library was measured using the Qubit 3.0 (Thermo Fisher, USA). The libraries were pooled and sequenced to a target read depth of 30 M reads per library using single-end 76 cycle sequencing with the High Output 75-cycle kit (Illumina) on the Illumina NextSeq 500.

The generated FASTQ files were assessed for quality using FastQC. Genome alignment was performed using HISAT2, SAMtools and StringTie to generate counts per gene. In-house R scripts and the Spliced Transcripts Alignment to a Reference (STAR) sequence aligner, and gene counts for mapped reads were determined. Differential expression was performed using the R-package DESeq2. GO-term enrichment was performed using the TopGO package. Immune cell deconvolution used the mMCP-counter package. Data visualisation was performed using ggplot2 or complex Heatmap packages.

This work was conducted with assistance from Dr Martin McLaughlin, Radiotherapy and Imaging Division at the Institute of Cancer Research, London.

3.9.4 Tumour processing – flow cytometry

4434 tumours were collected at the desired timepoints, placed on ice, blotted dry and weighed. Following mechanical dissociation with scissors, they were placed in a digestion solution of 1 mL RPMI containing 40 µL 0.25% trypsin (Sigma), 20 µL collagenase (25 mg/mL in PBS) (Sigma), 2 µL dispase (200 mg/mL) (Sigma) and 10 µL DNase (20 mg/mL) (Sigma) and incubated at 37°C for 30 minutes before being passed through a 0.7 µM filter and rinsed with RPMI supplemented with 10% FCS and 5mM EDTA (Sigma). Samples were resuspended in PBS with 5% FCS, blocked with anti-CD16/32 antibody (BioLegend) on ice for 10 minutes and washed twice. Antibodies had been diluted in FACS buffer (as shown in Appendix 9.3), were added to the samples and incubated together in the dark for 30 minutes before washing twice. For intracellular epitopes, samples were fixed and permeabilized after staining for extracellular epitopes, using the FoxP3/Transcription factor fixation/permeabilization kit (eBioscience) in accordance with the manufacturer protocol; subsequent staining was performed using the permeabilization buffer from this kit. After fixation, samples were washed twice and fixed using 1% formaldehyde in PBS before acquisition on a BD LSR II flow cytometer. The sample was divided equally into staining panels and each sample was acquired entirely. Counts were normalised to tumour weight and corrected for the number of panels into which the sample was divided.

3.9.5 Spleen processing – flow cytometry

Spleens were collected at the desired timepoints, placed on ice, blotted dry and weighed. The spleens were homogenised into a single cell suspension through a 0.7 uM filter using RPMI into a 50 mL falcon tube. After centrifugation at 400g for five minutes, the medium was discarded. To lyse red blood cells, the resulting cell pellet was resuspended in 5 mL of ammonium-chloride-potassium (ACK) lysing buffer (Thermo Fisher) for two minutes. 15 mL RPMI medium was added to the falcon tubes, before filtering through a second 0.7 uM cell filter. After centrifugation, the cell pellet was

resuspended in 1 mL of FACS buffer and stained/fixed in a similar process as described (section 3.9.3) prior to acquisition on the BD LSR II flow cytometer.

3.10 Flow cytometry

3.10.1 Immunophenotyping the 4434 model of melanoma

Following sample preparation as described, FACS acquisition was conducted using the BD LSR II flow cytometer (BD Biosciences). Acquired data were analysed using FlowJo software version 0.9 (BD Biosciences). Photomultiplier tube voltages were set using fully stained samples and compensation was performed using single-stained UltraComp eBeads (Invitrogen). Gating was performed using "fluorescence minus one" and isotype controls as detailed (Appendix 9.3). Conjugated antibodies and isotypes were obtained from BioLegend (San Diego, USA) unless otherwise stated (Appendix 9.3). Cell viability was assessed using the eBioscience fixable viability dye eFluor 780.

3.10.2 GFP expression following MG1-GFP infection

Cells were seeded in 12-well plates with $1x10^5$ cells/well and incubated overnight at 37°C. The following day, the cells were treated with either PBS or MG1-GFP MOI 0.1 or 10. The cells were harvested 24 or 48 hours later and then washed twice with PBS prior to centrifugation. The cell pellets were resuspended in FACS buffer containing viability dye (1:1000) for 30 minutes. After washing twice with PBS, the cells were fixed with 1% PFA for 20 minutes before flow cytometry acquisition.

3.10.3 PD-L1 expression following MG1-GFP infection

Cells were seeded in 12-well plates with $1x10^5$ cells/well and incubated overnight at 37°C. The following day, the cells were treated with either PBS or MG1-FLUC MOI 0.01. After a further 24 hours had elapsed, the cells were harvested, washed twice with PBS then centrifuged. The cells were resuspended in FACS buffer and stained with viability dye (1:1000) and PE anti-mouse PD-L1 antibody (BioLegend) (1:100) for 30 minutes. After washing

twice with PBS, the cells were fixed with 1% PFA for 20 minutes before flow cytometry acquisition.

3.11 Statistics

When comparing untreated versus treated samples, p values were calculated using a paired student's t-test with two-tailed distribution. When comparing three or more groups, a one-way analysis of variance (ANOVA) was performed, comparing all groups to each other and correcting for multiple comparison using Dunnett's or Sidak's test. For survival experiments, the Kaplan-Meier survival curves were compared using log-rank (Mantel-Cox) test. Statistical significance was determined as follows: $*p<0.05$, $**p<0.0021$, $***p<0.0002$ and $****p<0.0001$. All statistical analysis was performed using Prism Software (GraphPad).

Chapter 4:

Effects of Maraba Virus on Melanoma Cells – *in vitro* models

4 Chapter 4: Effects of Maraba Virus on Melanoma Cells – *in vitro* models

4.1 Introduction

OVs selectively infect and replicate within tumour cells and exert a cytotoxic effect through tumour cell lysis. During their replicative cycle, OVs release amplified progeny viruses that can go on to progressively infect other tumour cells. This chapter aims to investigate the ability of MG1 to exert an oncolytic effect on murine and human malignant melanoma cell lines.

MG1 has been shown to demonstrate potent cytotoxicity across many different murine and human cancer cell lines. This includes five human melanoma cell lines from the NCI60 (US National Cancer Institute) including M14, MALME3M, SKMEL28, UACC257 and UACC6.[321] Moreover, three murine melanoma cell lines, B16, B16-F10 and B16lacZ show susceptibility to MG1 cytotoxicity. To reflect the tropic nature of MG1 to act as a tumour selective OV, the literature also reports that MG1 virulence is attenuated when tested against non-malignant human GM38 primary fibroblasts.[321]

To expand on this work, MG1 infection, replication and cytotoxicity in a wider panel of human and murine melanoma cell lines was investigated, taking into consideration the different mutational profiles that are frequently identified clinically, therefore including cells with known BRAF and NRAS mutations and their wild-type counterparts. By means of comparison, non-melanoma pancreatic cell lines were investigated, to see if any specific features could be identified to predict for cellular sensitivity or resistance to MG1.

4.2 MG1 infection of murine and human melanoma cell lines

As previously mentioned, MG1 has shown the capacity to infect a range of melanoma cell lines. Expanding on previously published studies, the ability of MG1 to infect an extended panel of human (Mel888, A375, DO4, Mel624 and

MeWo) and murine (4434 and 21015) melanoma cells, as well as the previously investigated B16 derivatives (B16-F1 and B16-F10) was investigated. To demonstrate this, fluorescence microscopy was performed at 24 and 48 hours following infection with MG1 expressing GFP at multiplicities of infection (MOI) ranging from 0.001-10. Figure 5A shows representative brightfield, GFP and merged images of murine melanoma cell lines exposed to either PBS control or MG1-GFP infected at MOI 0.1 for 24 hours. Additional images are presented from the 21015 cell line including MOI 1.0, 24 hours post infection, and MOI 10, 48 hours post infection (Figure 5B).

Of the murine melanoma cell lines tested, B16-F1, B16-F10 and 4434 were found to be sensitive to MG1 infection as GFP positive cells were detected following MG1-GFP treatment. Conversely, in the 21015 cell line, no GFP signal was detected at the same viral dose and timepoint (MOI 0.1 at 24 hours). GFP positive cells could be detected when 100-fold more virus was added (MOI 10) and at a later timepoint (48 hours post-infection), albeit at a lower frequency than the other murine cell lines, thereby indicating that this cell line was more resistant than the other murine cell lines tested. Figure 5C shows representative brightfield, GFP and merged images of human melanoma cells lines exposed to either PBS control or MG1-GFP viral infection following 24 hours and using an MOI of 0.1. GFP expression following MG1-GFP infection was evident in all the five human cell lines tested.

The images qualitatively illustrated that MG1-GFP was readily able to infect all cell lines with the exception of the murine 21015 cell line. To quantitively evaluate the differences in the susceptibility of infection across the different murine and human melanoma cell lines flow cytometry was performed. Melanoma cells were either infected with PBS control or MG1-GFP at a concentration of 0.1 MOI for 24 hours. Melanoma cells were then stained with a viability dye to distinguish between live and dead cells in order to ensure that the evaluation of GFP expression was conducted only on live cells. Figure 5D shows the mean percentage of GFP expression from viable cells from two independent experiments plotted for four murine melanoma cell lines 24 hours following either PBS or MG1-GFP MOI 0.1 infection. The mean percentage

GFP expression following MG1-GFP infection was 5.5%, 54%, 77.5% and 83.5% from the 21015, 4434, B16-F1 and B16-F10 cell lines respectively, and as expected, no GFP expression was evident in PBS controls. Given the lower mean percentage of GFP expression from the 21015 cell line, additional quantification was performed as displayed in Figure 5E. Increasing the viral dose to an MOI of 10 resulted in mean percentage GFP expression of 15% and 22.5% at 24 and 48 hours post infection respectively. These results therefore mirror the results shown in Figure 5B, indicating that 21015 cells are infectible with MG1-GFP, however, despite increasing the time and viral concentration, the percentage of cells expressing GFP remains less than observed from the other cell lines tested. Of note, the more sensitive cell lines (4434, B16-F1 and B16-F10) were also analysed following infection with a higher viral titre at 48 hours. However, increasing either of these factors resulted in the majority of cells dying (as evidenced through viability dye uptake) making any subsequent evaluation of GFP expression on the remaining live cells unreliable (data not shown).

Figure 5F presents similar data of mean percentage GFP expression from viable cells from two independent experiments plotted for five human melanoma cell lines, 24 hours following either PBS or MG1-GFP MOI 0.1 infection. The mean GFP expression was 73.5%, 74%, 84%, 72.5% and 68.5% from the Mel888, A375, DO4, Mel624 and MeWo cell lines respectively.

In summary, the qualitative fluorescence microscopy and the quantitative flow cytometry analysis of GFP expression both demonstrate a high level of sensitivity to MG1-GFP infection amongst the murine and human melanoma cell lines tested, albeit with some variation between cell lines and with the exception of 21015. These results are supportive of, and consistent with, the notion that MG1 is a potent and highly oncolytic virus that readily infects a range of tumour cells.

(A)

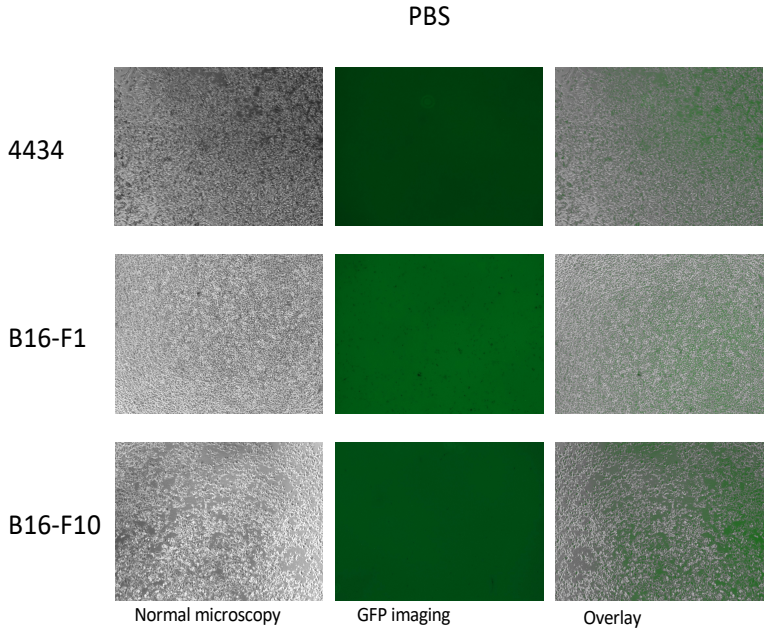
PBS
4434
B16-F1
B16-F10
Normal microscopy
GFP imaging
Overlay

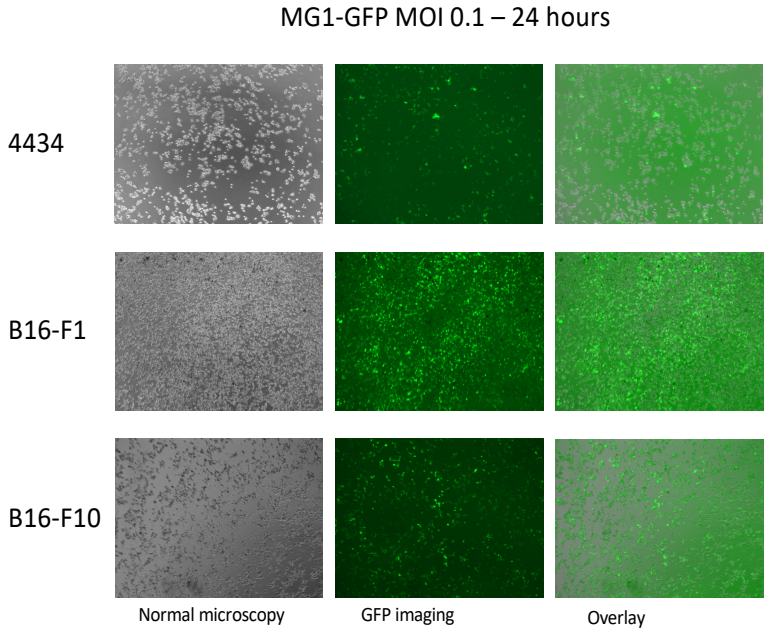
MG1-GFP MOI 0.1 – 24 hours
4434
B16-F1
B16-F10
Normal microscopy
GFP imaging
Overlay

(B)

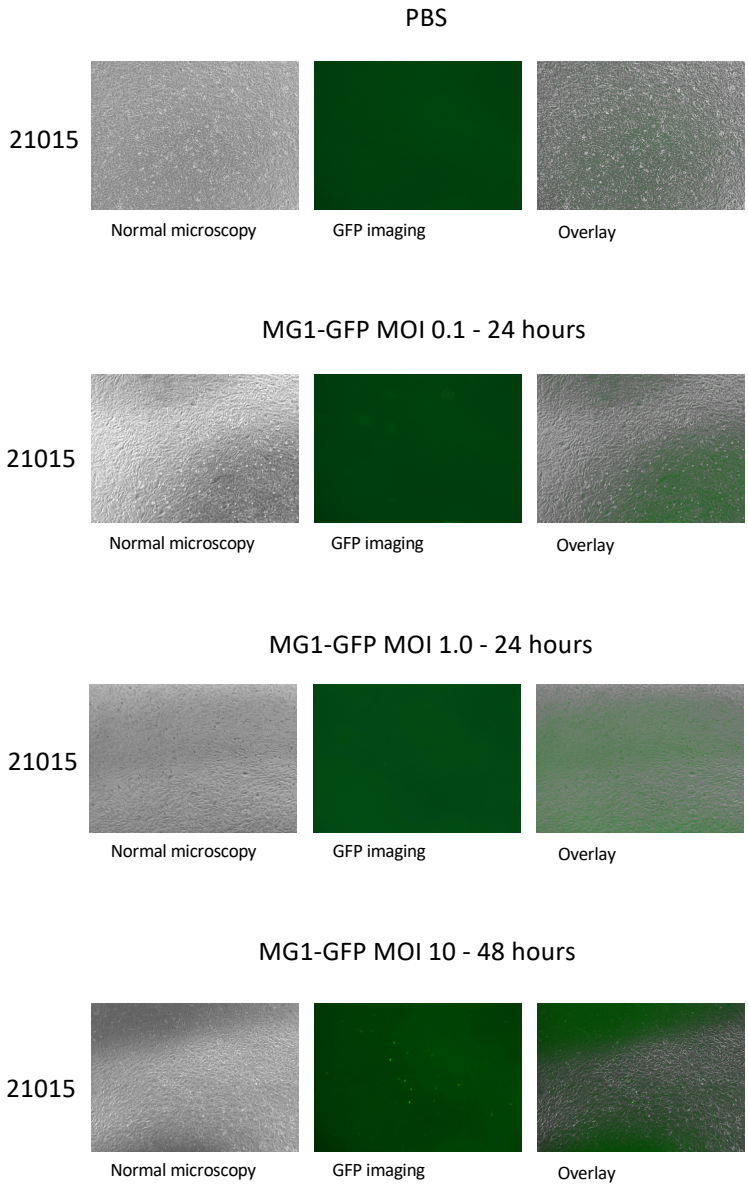
PBS
21015
Normal microscopy
GFP imaging
Overlay
MG1-GFP MOI 0.1 - 24 hours
21015
Normal microscopy
GFP imaging
Overlay
MG1-GFP MOI 1.0 - 24 hours
21015
Normal microscopy
GFP imaging
Overlay
MG1-GFP MOI 10 - 48 hours
21015
Normal microscopy
GFP imaging
Overlay

(C)

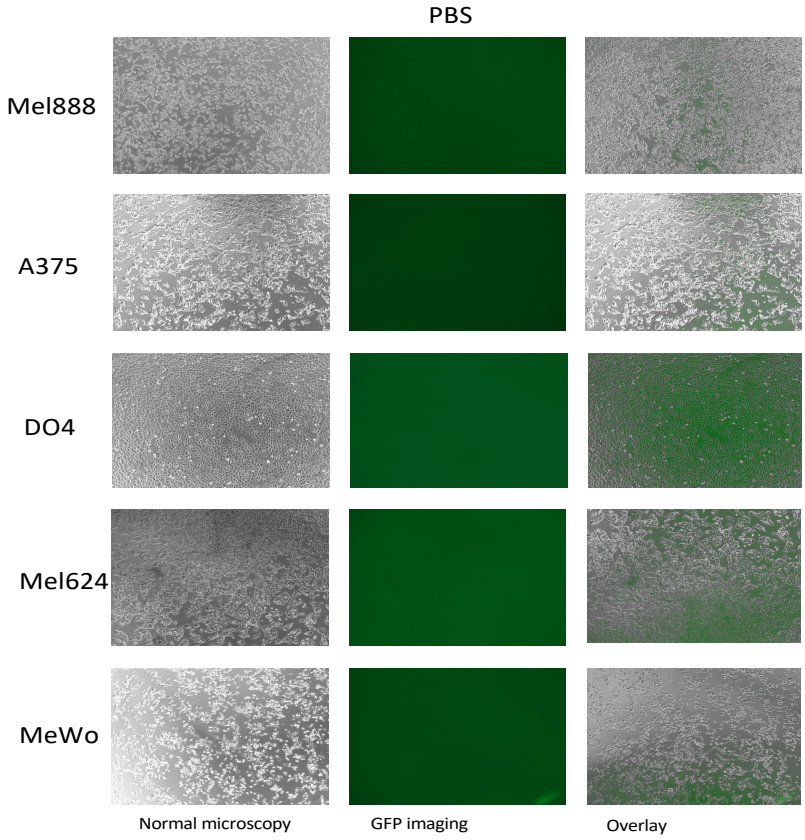
PBS
Mel888
A375
DO4
Mel624
MeWo
Normal microscopy
GFP imaging
Overlay

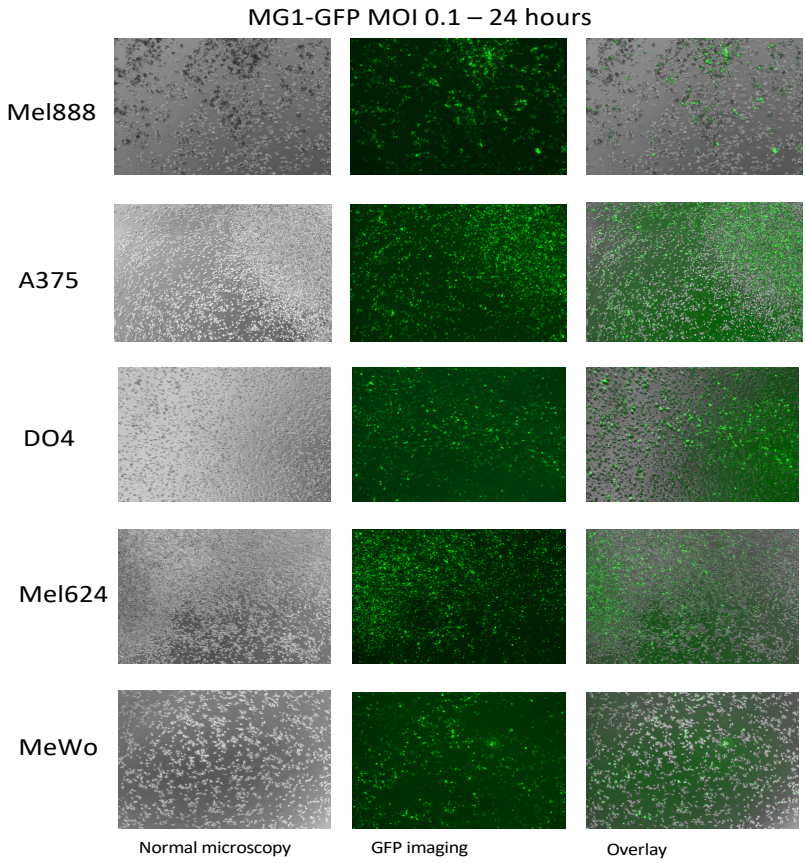
MG1-GFP MOI 0.1 – 24 hours
Mel888
A375
DO4
Mel624
MeWo
Normal microscopy
GFP imaging
Overlay

(D)

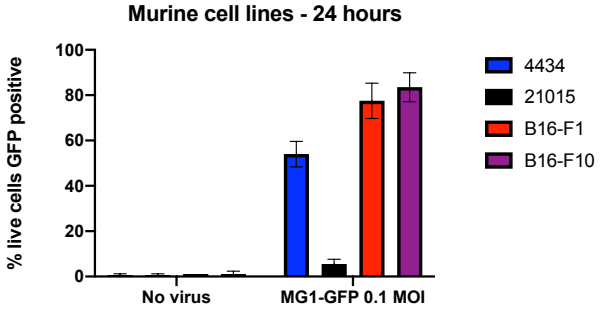

(E)

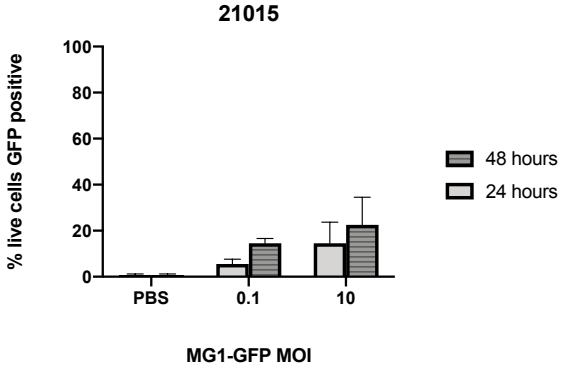

(F)

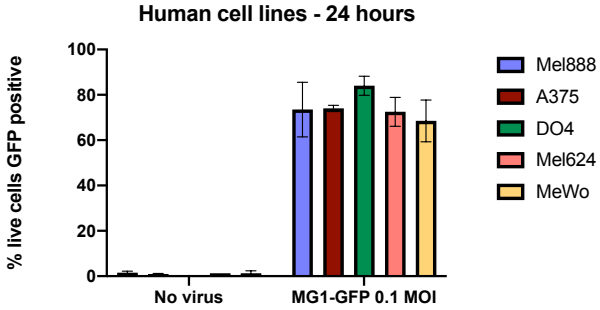

Figure 5: MG1-GFP infectivity in murine and human cell lines *in vitro*

Fluorescence microscopy was performed using EVOS cell imaging systems after cell lines were exposed to either PBS or MG1-GFP MOI 0.1 at 24 hours. Murine cell lines (A) and human cell lines (C) with additional conditions for the 21015 cell line (B). Flow cytometry analysis of cell lines infected with PBS or MG1-GFP MOI 0.1 at 24 hours displayed in bar charts showing percentage of GFP positive live cells within total population of live cells for murine cell lines (D), human cell lines (F) with additional conditions for the 21015 cell line (E). Bar charts with error bars represent the mean and SD of two independent experiments.

4.3 MG1 replication within murine melanoma cell lines

Having identified some variation in the cell line susceptibility to MG1 infection, this was validated further by evaluating the ability of MG1 to replicate within tumour cells. The four murine melanoma cell lines were selected for this objective.

4434, 21015, B16-F1 and B16-F10 cells were infected with MG1-GFP at either 0.1 or 1.0 MOI. Supernatants were harvested at 0, 4, 8, 18, 24, 48 and 72 hours following viral infection. The viral titre was established for each time point and for both viral concentrations. In addition to evaluating the absolute viral titre detected, the fold-change was calculated by comparing the baseline timepoint MG1-GFP titre with subsequent readings.

Figure 6A shows the viral output of MG1-GFP in the four murine melanoma cell lines tested at two MOIs, 0.1 or 1.0, displayed as a trend over 72 hours. Figure 6B shows the data in Figure 6A plotted as fold change in viral titre compared to baseline for each cell line. The results display the mean and standard deviation from three independent experiments.

Figure 6A displays a minimal increase in viral titre from the 21015 cell line peaking at $7x10^3$ pfu/mL with MOI 0.1 and $3x10^4$ pfu/mL with MOI 1.0, however by 48 hours the viral titre obtained returns below the input titre. The 4434 cell line demonstrates a gradual increase in viral titre peaking at 24 hours at $3.3x10^6$ pfu/mL with MOI 0.1 and at $1.6x10^6$ pfu/mL with MOI 1.0. However, the greatest increases in viral titre occurred in the B16-F1 and B16-F10 cell lines with a rapid increase even by eight hours and peaking at $4.6x10^7$ pfu/mL and $3.3x10^7$ pfu/mL respectively following MOI 0.1, and at $6x10^7$ pfu/mL and $5.3x10^7$ pfu/mL respectively following MOI 1.0.

Figure 6B demonstrates that the 21015 cell line showed a very slight increase in viral titre from baseline over the time course, maximum output was detected at 18 hours post infection at both viral doses resulting in a 4.2 and 2.8 fold increase over input at MOIs 0.1 and 1.0, respectively. By the 48 and 72 hour

time points, the viral titre was lower than input for both viral concentrations. Compared to the other cell lines tested, the mean fold increase from the 21015 cell line was notably less, in keeping with the poor level of infectivity observed previously in Figure 5.

By contrast, the other three cell lines demonstrated a peak mean fold change of 1166, 9166 and 10222 at MOI 0.1 and 133, 863 and 1244 at MOI 1.0 for the 4434, B16-F1 and B16-F10 cell lines respectively. This thereby indicates that viral replication is greater within the B16-F1 and B16-F10 cell lines as the peak mean fold increase was higher in these two cell lines when compared to the 4434 cell line.

In summary, the replication assays confirm the capacity of MG1 to replicate effectively within tumour cells including the B16-F1, B16-F10 and 4434, albeit with some variation between cell lines, and with the exception of 21015. These results are consistent with the infectivity data discussed in Section 4.2.

(A)

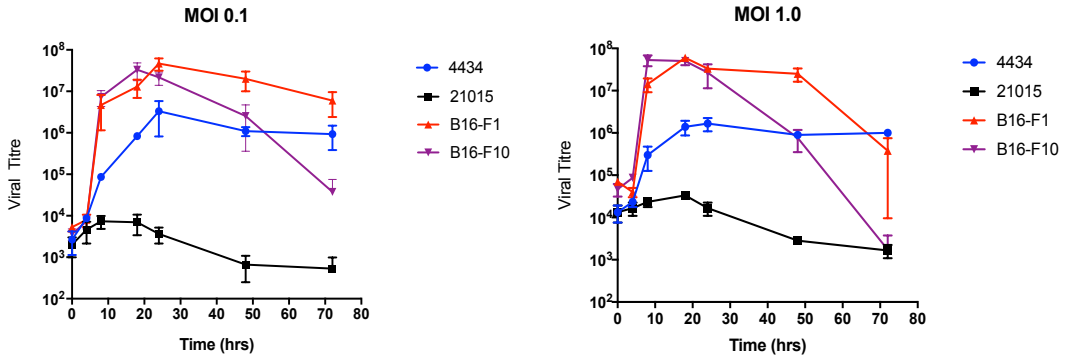
MOI 0.1
Viral Titre
Time (hrs)
4434
21015
B16-F1
B16-F10
MOI 1.0
Viral Titre
Time (hrs)
4434
21015
B16-F1
B16-F10

(B)

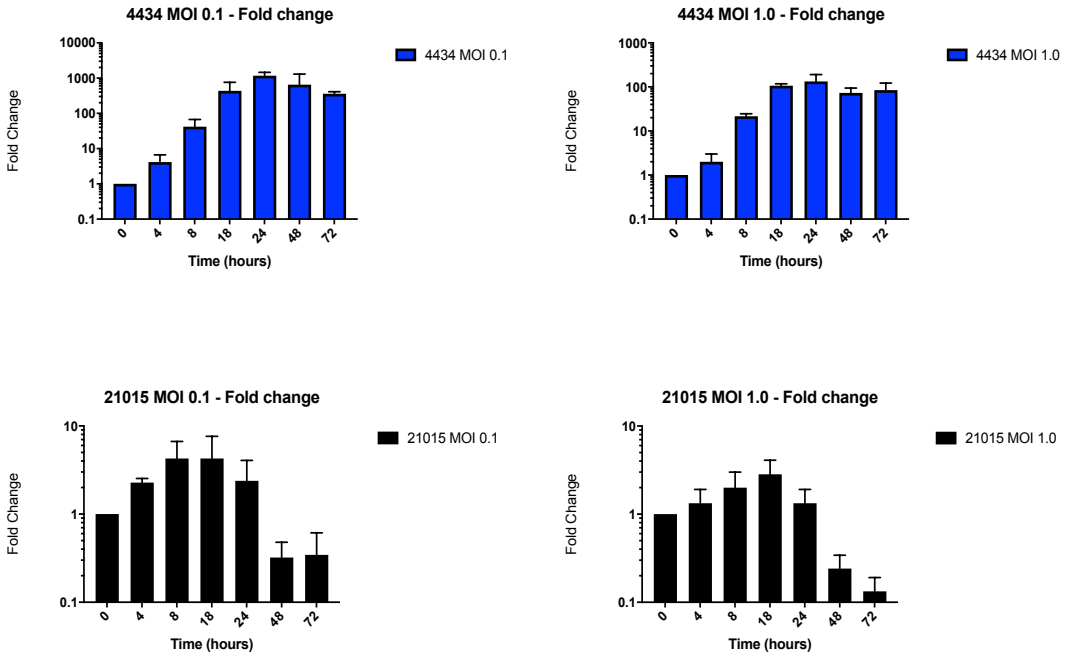
4434 MOI 0.1 - Fold change
Fold Change
Time (hours)
4434 MOI 0.1
4434 MOI 1.0 - Fold change
Fold Change
Time (hours)
4434 MOI 1.0
21015 MOI 0.1 - Fold change
Fold Change
Time (hours)
21015 MOI 0.1
21015 MOI 1.0 - Fold change
Fold Change
Time (hours)
21015 MOI 1.0

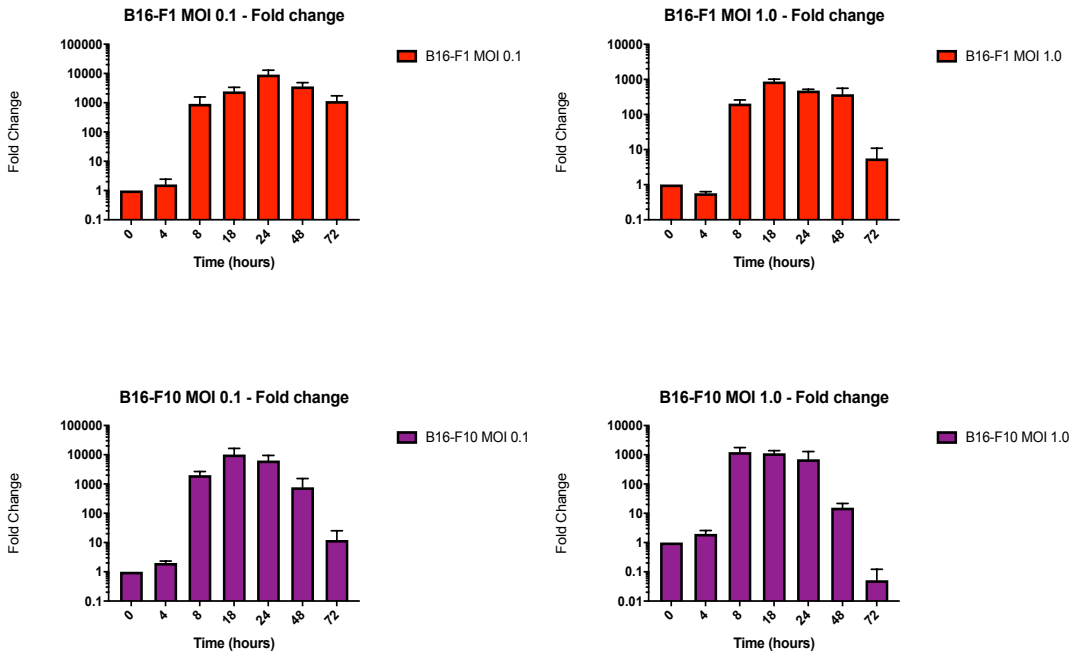

Figure 6: MG1-GFP replication within murine melanoma cell lines *in vitro*

Murine melanoma cell lines were infected with MG1-GFP at MOI 1.0 and 0.1. Supernatants were harvested and MG1-GFP titres were subsequently determined by plaque assay from a range of time points up to 72 hours (A). Fold increase was calculated as the change from the initial viral titre (B). Data with error bars presented as the mean and SD of three independent experiments.

4.4 MG1 reduces the survival of murine and human cell lines

The above sections demonstrate the ability of MG1-GFP to infect and replicate within a range of melanoma cell lines, with the exception of the 21015 cell line. It was next evaluated whether MG1-GFP infection and replication would result in tumour cell death.

MTT is a colourimetric test which relies on NAD(P)H-dependent oxidoreductase enzymes within viable cells to reduce a yellow tetrazolium salt (3-(4,5- dimethylthiazol-2-yl)-2,5-diphenyltetrazolium bromide, or MTT) to formazan. The insoluble formazan crystals are dissolved with dimethyl sulfoxide (DMSO) and the resulting purple coloured solution is quantified by measuring absorbance using a multi-well spectrophotometer. Murine and human melanoma cells were treated with PBS or MG1-GFP at MOIs ranging from 0.001 to 10 and the assessment of cell viability was conducted using an MTT assay at 24 and 48 hours post infection. The mean percentage of viable cells with standard deviation, from three independent experiments is shown in Figures 7A and 7B.

Figure 7A and Figure 7B demonstrate that, overall, MG1-GFP had a deleterious effect on the survival of all melanoma cell lines tested, and in general, this effect was time and dose-dependent.

More specifically, the 24-hour time point again suggests that the 21015 cell line is the most resistant to MG1-GFP induced cell toxicity as 92% of cells remain viable following infection at MOI 0.1, declining to 80% at an MOI of 10. By contrast, the 4434 cell line had a survival percentage of 78% with MOI 0.1 reducing to 71% at MOI 10. The B16-F1 and B16-F10 cell lines were more sensitive still, with respectively, 62% and 42% viability at MOI 0.1 and a 34% and 30% survival at MOI 10. At 48 hours after infection with MOI 0.1 and 10, the 21015 cell line had a survival percentage of 83% and 63% respectively, 4434 had 43% and 43%, B16-F1 had 19% and 19% and B16-F10 had 25% and 23%. Again, these data at 48 hours reiterate the high sensitivity of the

B16-F1 and B16-F10 cell lines, followed by the 4434 cell line and lastly the most resistance occurring in the 21015 cell line.

Following MG1 infection of human cell lines at 24 hours post infection, the MeWo cell line is most resistant to MG1-GFP cell toxicity as 87% of cells remain viable after 0.1 MOI, reducing to 80% at an MOI of 10. The Mel624 cell line appears the most sensitive with a survival percentage of 60% at 0.1 MOI and 29% at 10 MOI. The remaining three human cell lines, namely Mel888, A375 and DO4 exhibit survival percentages which lie in between the MeWo and Mel624 results. At 48 hours, again the MeWo cell line were the most resistant to viral-induced cell death as more than 50% of cells remain alive following viral dose of 0.1 MOI and 10 MOI. The Mel888, A375, DO4 and Mel624 cells display a higher sensitivity to MG1-GFP induced cell death as, in all cases, less than 40% of cells remained alive following 0.1 or 10 MOI administration.

In summary, the data obtained from the MTT assays confirm that the survival of a range of murine and human melanoma cell lines are reduced following MG1 infection, at both a range of time points and viral concentrations. Given the poor capacity of MG1 to infect and replicate within 21015, this cell line unsurprisingly was notably more resistant to MG1, as supported by the MTT results.

(A)

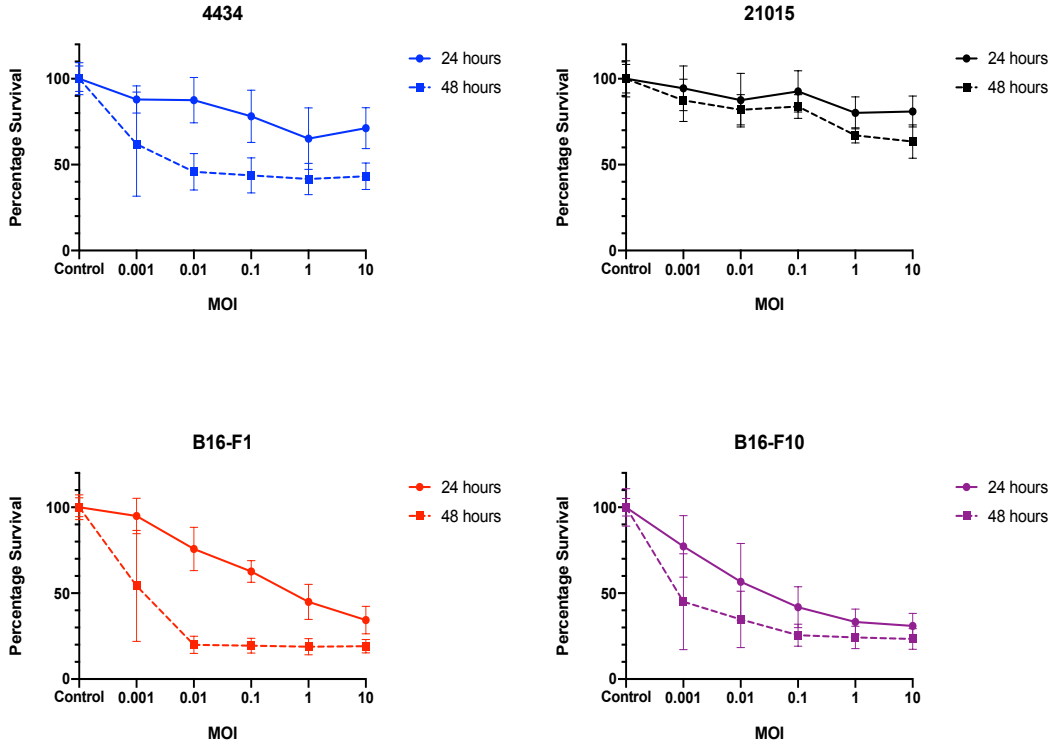
4434
21015
B16-F1
B16-F10
Percentage Survival
MOI
Control
0.001
0.01
0.1
1
10
0
50
100
24 hours
48 hours

(B)

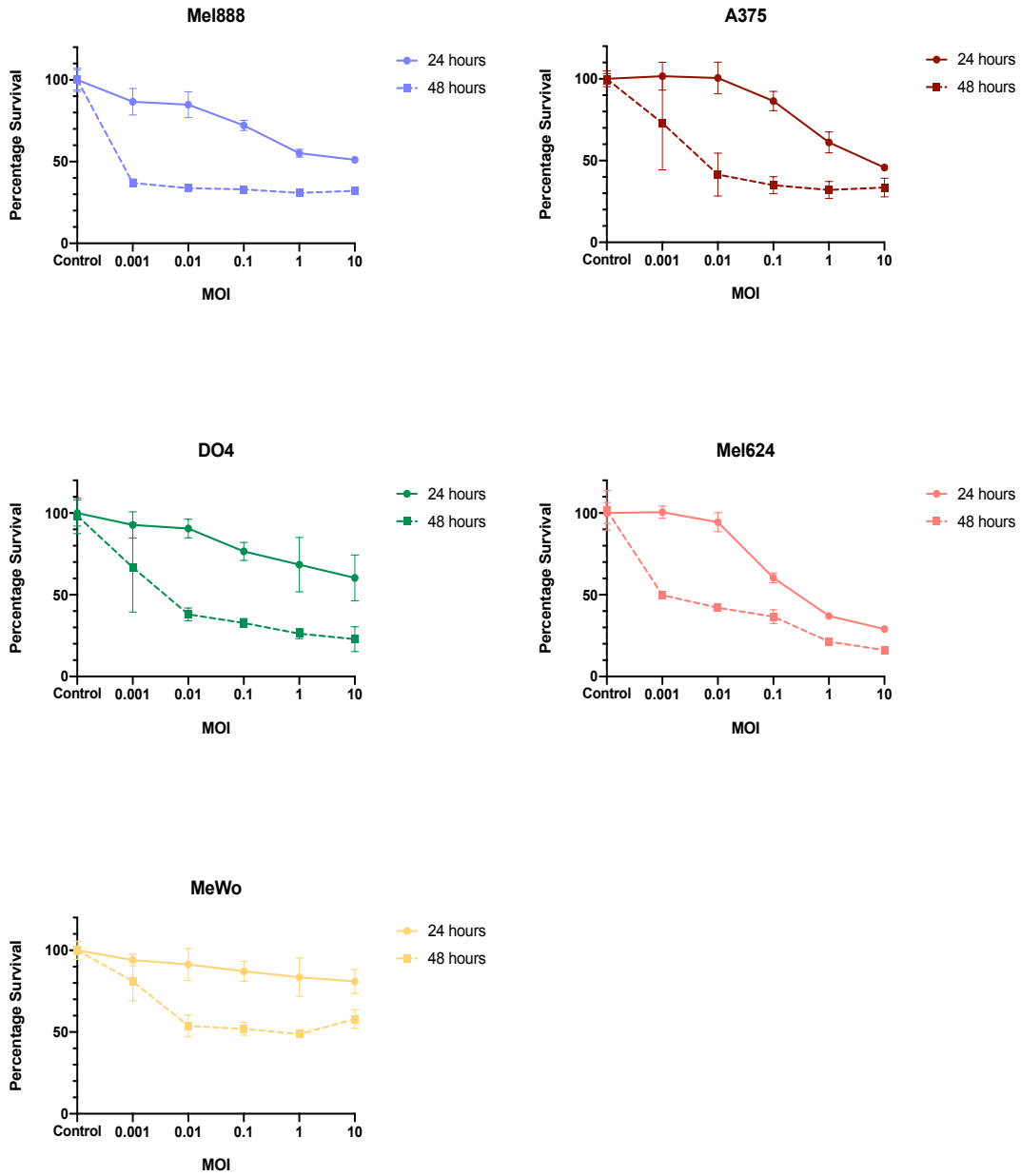

Figure 7: MG1-GFP reduces the survival of murine and human melanoma cell lines *in vitro*

Melanoma cell lines were infected with MG1-GFP at a concentration of 0.001, 0.01, 0.1, 1.0 and 10 MOI for 24 and 48 hours. MTT assay was used to determine the cell viability in murine (A) and human (B) cell lines. Data represented as the mean and SD of three independent experiments.

4.5 MG1 exerts cytotoxic, rather than cytostatic, effects on murine and human melanoma cell lines.

Given the nature of OVs, it was expected that MG1-GFP was exerting a cytotoxic rather than a cytostatic effect on the tumour cells. However, in theory, the relative decrease in survival of the infected cells measured by MTT assay in Figure 7, could be in part explained if the virus was exerting a cytostatic effect. Consequently, what would appear to be virally mediated cell death, could in fact, be from unimpeded control cell growth compared with virally mediated tumour cell stasis.

To determine this, the cell lines were infected with either PBS or MG1-GFP at a concentration of 0.1 MOI for 48 hours. The cells were collected and stained with a viability dye and analysed using flow cytometry. Figures 8A and 8B show the mean percentage of viable cells from two independent experiments plotted for the four murine and five human melanoma cell lines.

This indeed showed that MG1-GFP exerts a cytotoxic effect on tumour cells, rather than a cytostatic effect, as the viability dye measures loss of membrane integrity, signifying one of the final stages of cell death. Across all cell lines the percentage of viable cells at 48 hours following PBS administration was above 95%. Conversely, following MG1-GFP infection for 48 hours, the proportion of viable cells reduces. The murine cell lines, 4434, 21015, B16-F1 and B16-F10 cell lines had 60%, 88%, 15.5% and 21.5% viability, respectively. This therefore, further mirrored the trend identified in previous sections that the most susceptible are the B16-F1 and B16-F10 cell lines and the most resistant to viral cytotoxicity is the 21015 cell line. By means of comparison, the MTT viability percentages at the corresponding time point (48 hours) and viral dose (MOI 0.1) were 43%, 83%, 19% and 25% for the respective cell lines. The human cell lines, Mel888, A375, DO4, Mel624 and MeWo cell lines had 19.5%, 14%, 16%, 21.5% and 15% viability, respectively at the same time point. The previously presented MTT results demonstrated a 33%, 34%, 32%, 36% and 51% viability for the human cell lines.

In summary, these experiments confirm the cytotoxic, rather than cytostatic, potential of MG1-GFP against a range of both human and murine melanoma cell lines. 21015 again demonstrated the most resistance to MG1, as would be expected given the poor capacity for MG1 infection of, or replication within, the 21015 cell line. To examine the breadth of anti-tumoural effects, MG1 was investigated in cell lines from another hard-to-treat malignancy.

(A)

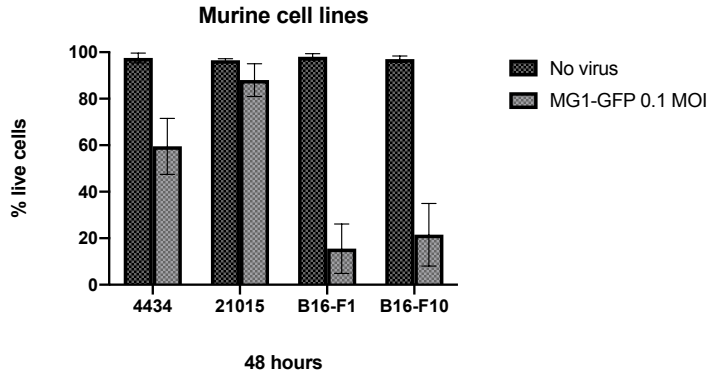

(B)

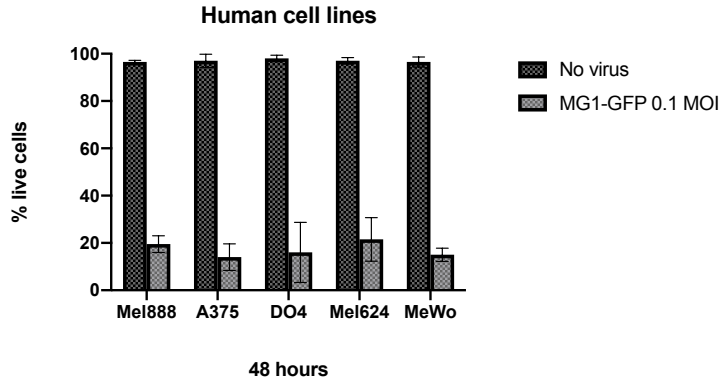

Figure 8: MG1-GFP exerts a cytotoxic effect on murine and human melanoma cell lines

Murine (A) and human (B) melanoma cell lines were infected with MG1-GFP MOI 0.1 or control, for 48 hours. Cells and supernatants were harvested, stained with a viability dye and analysed using flow cytometry to determine the live cells expressed as a percentage of the total number of cells analysed. Data and error bars represent the mean and SD of two independent experiments.

4.6 MG1 has cytotoxic potential against other malignancies including pancreatic cell lines

As previously illustrated (Table 2), a range of other tumour subtypes have been shown to exhibit sensitivity to MG1, including one human pancreatic cancer cell line, namely PANC-1. However, the effectiveness of MG1 against murine pancreatic cells has not been previously documented.[320] Therefore, the effectiveness of MG1 was tested against three murine pancreatic cell lines in order to confirm that MG1 displayed a breath of potential as an effective oncolytic agent. MG1-GFP was evaluated for its capacity to infect and kill 2334, 3275 and 7947 cells with fluorescence microscopy and MTT assay using the same techniques described previously.

Figure 9A shows representative brightfield, GFP and overlaid images of the above pancreatic cell lines at 24 and 48 hours following either PBS control or MG1-GFP viral infection using an MOI of 0.1.

This demonstrated that at an MOI of 0.1 at 24 hours, the 7947 cell line is readily infected and the 2334 cell line is infected, albeit that this is seen more clearly by 48 hours. However, in contrast, at 0.1 MOI, the 3275 cell line showed no discernible GFP expression at either 24 or 48 hours and even when using an increased viral titre of 10 MOI, GFP expression was difficult to identify, suggesting that the 3275 cells are more resistant to viral infection.

Figure 9B shows the mean percentage of viable cells with standard deviation, from three independent experiments infecting cells with PBS or MG1-GFP at MOIs ranging from 0.001 to 10 and assessing cell viability with an MTT assay following an incubation time of 24 and 48 hours.

Taking for instance the 0.1 MOI concentration, this demonstrated that the 7947 cell line has a survival percentage of 74% at 24 hours, which decreased to 55% at 48 hours after MG1-GFP administration. In the 2334 cell line, survival at 24 hours was 74% and reduced to 40% at 48 hours. The most resistant however, remained the 3275 cell line which demonstrated a survival

percentage of 72% at 24 hours and 73% at 48 hours. As with the melanoma cell lines, MG1-GFP affected to differing degrees, the survival of all pancreatic cell lines. Interestingly, despite the 3275 cells showing very little evidence of becoming infected by virus as per the GFP imaging (Figure 9A), the MTT data (Figure 9B) indicates that the 3275 cells exhibit some sensitivity. This disparity may be related to soluble factors released by the cells into the culture media in response to the presence of virus, affecting the integrity or adherence of other *in vitro* plated cells.

Finally, Figure 9C shows a chronological sequence of six-well plates using FLUC expressing 2334 (2334-FLUC) and 3275 (3275-FLUC) cells co-cultured with PBS or MG1-GFP across a range of concentrations from 0.001 to 10 and measured at 24, 48 and 72 hours post infection. This was conducted to see if virally infecting the cells would damage their ability to express FLUC luminescence, as detected with IVIS. The images from the 2334-FLUC cell line show that at 24 hours post infection, luminescence is retained at all viral concentrations, although arguably with some reduction at the highest MOI 10 concentration. However, by 48 hours, negligible luminescence is detected at any concentration above 0.001 and by 72 hours, a convincing signal of luminescence is only seen from the PBS control sample. Conversely, the 3275-FLUC cell line retains a clear luminescent signal across all viral MOI doses and even for up to 72 hours post infection, although with the suggestion that a viral MOI of 10 does reduce luminescence by 48 and 72 hours.

These data therefore confirmed that the MG1 OV has the capacity to variably infect and kill pancreatic murine cell lines *in vitro*. To our knowledge, MG1 has not previously been tested against these cell lines. These data reiterate the wide range of susceptible cell lines and therefore the breath of potential for MG1 as an oncolytic viral agent. It also recognises that certain cell lines demonstrate some resistance to MG1 activity.

In summary, it has been established that MG1 is able to infect a range of murine and human melanoma cell lines, replicate within them and have a cytotoxic effect reducing tumour cell survival. Furthermore, it was recognised

that the oncolytic potential of MG1 was not confined to melanoma alone but also applied to non-melanoma cell lines including pancreatic cancer, which traditionally usually also has a poor prognosis.

(A)

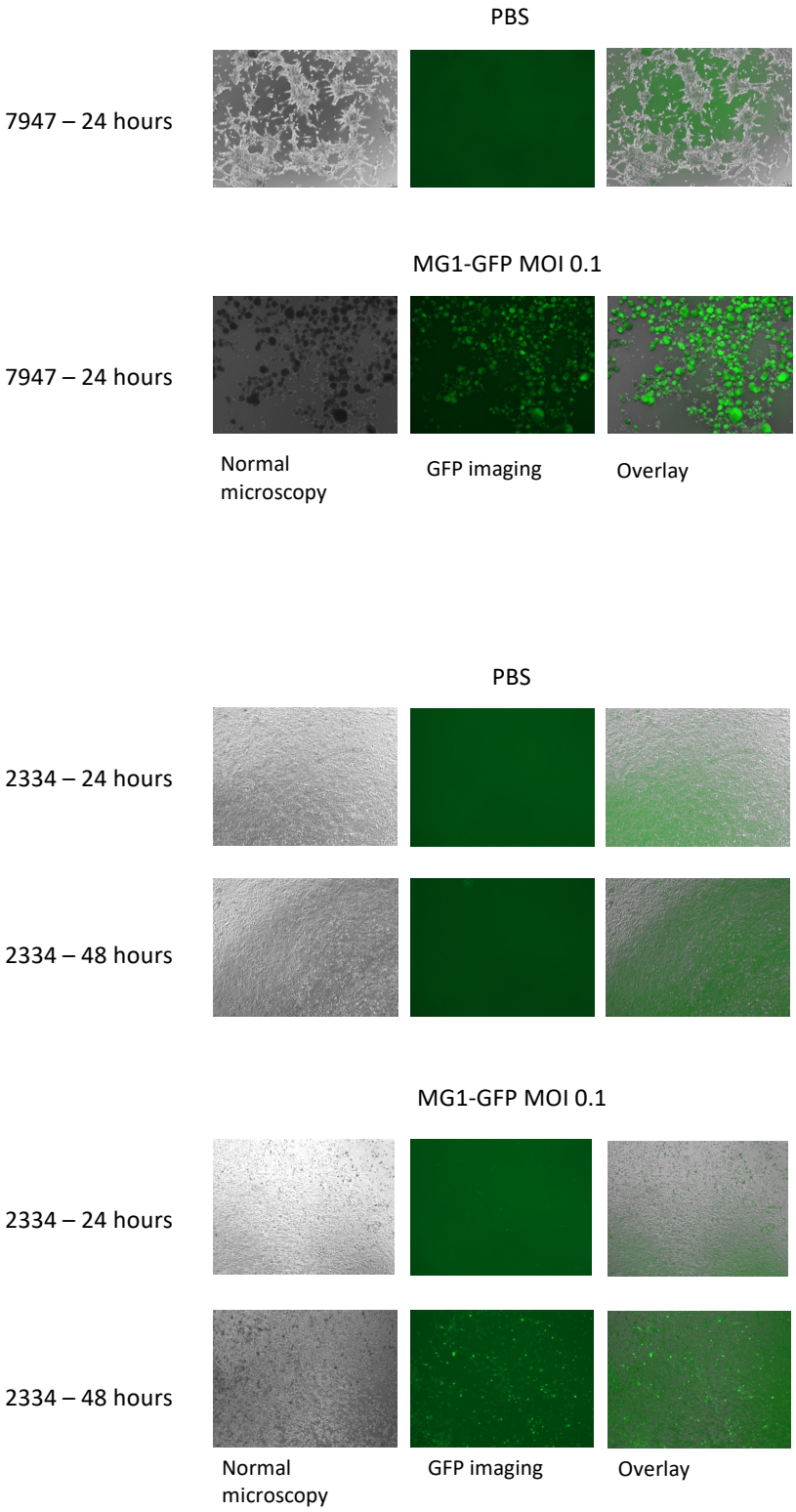
PBS
7947 – 24 hours
MG1-GFP MOI 0.1
7947 – 24 hours
Normal microscopy
GFP imaging
Overlay
PBS
2334 – 24 hours
2334 – 48 hours
MG1-GFP MOI 0.1
2334 – 24 hours
2334 – 48 hours
Normal microscopy
GFP imaging
Overlay

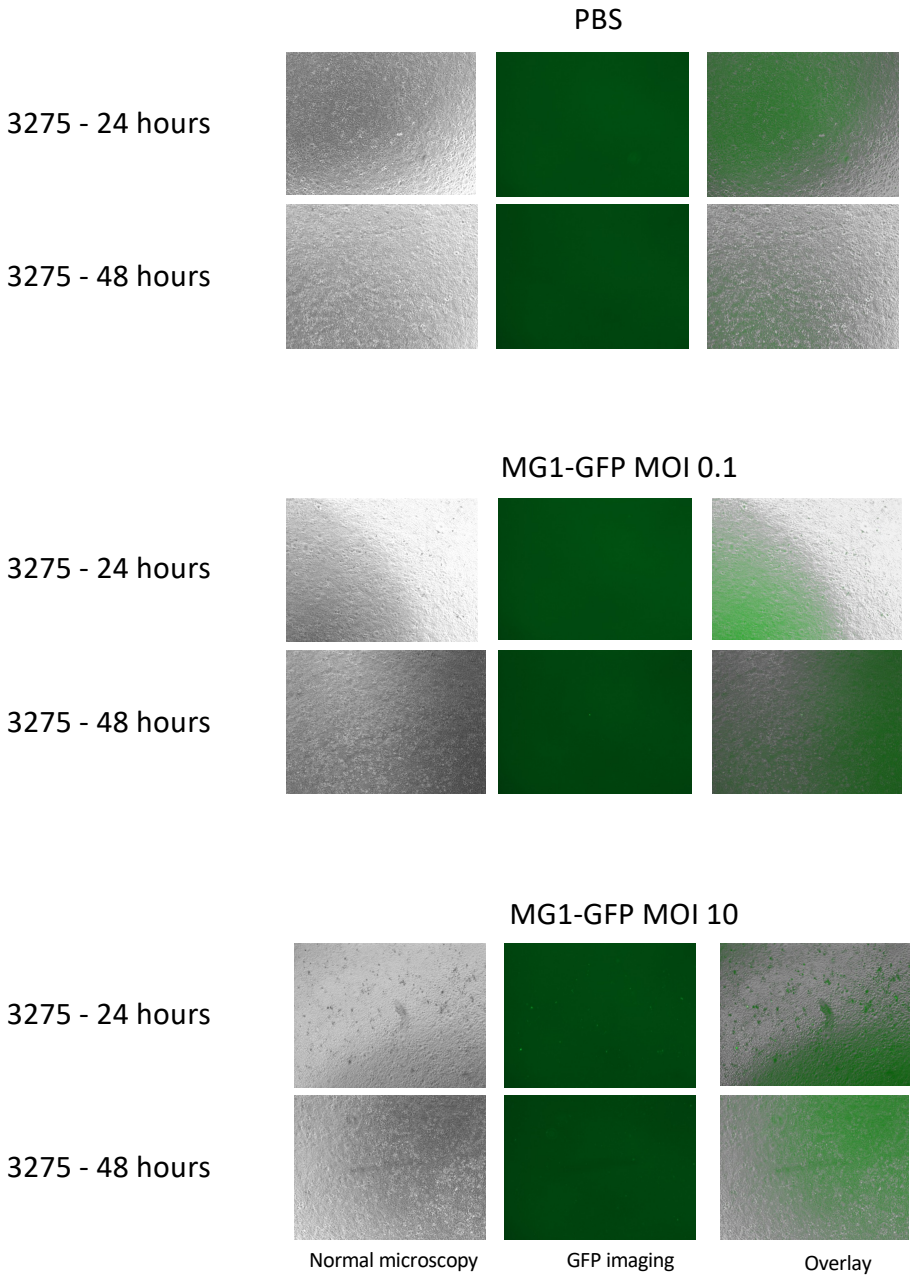
PBS
3275 - 24 hours
3275 - 48 hours
MG1-GFP MOI 0.1
3275 - 24 hours
3275 - 48 hours
MG1-GFP MOI 10
3275 - 24 hours
3275 - 48 hours
Normal microscopy
GFP imaging
Overlay

(B)

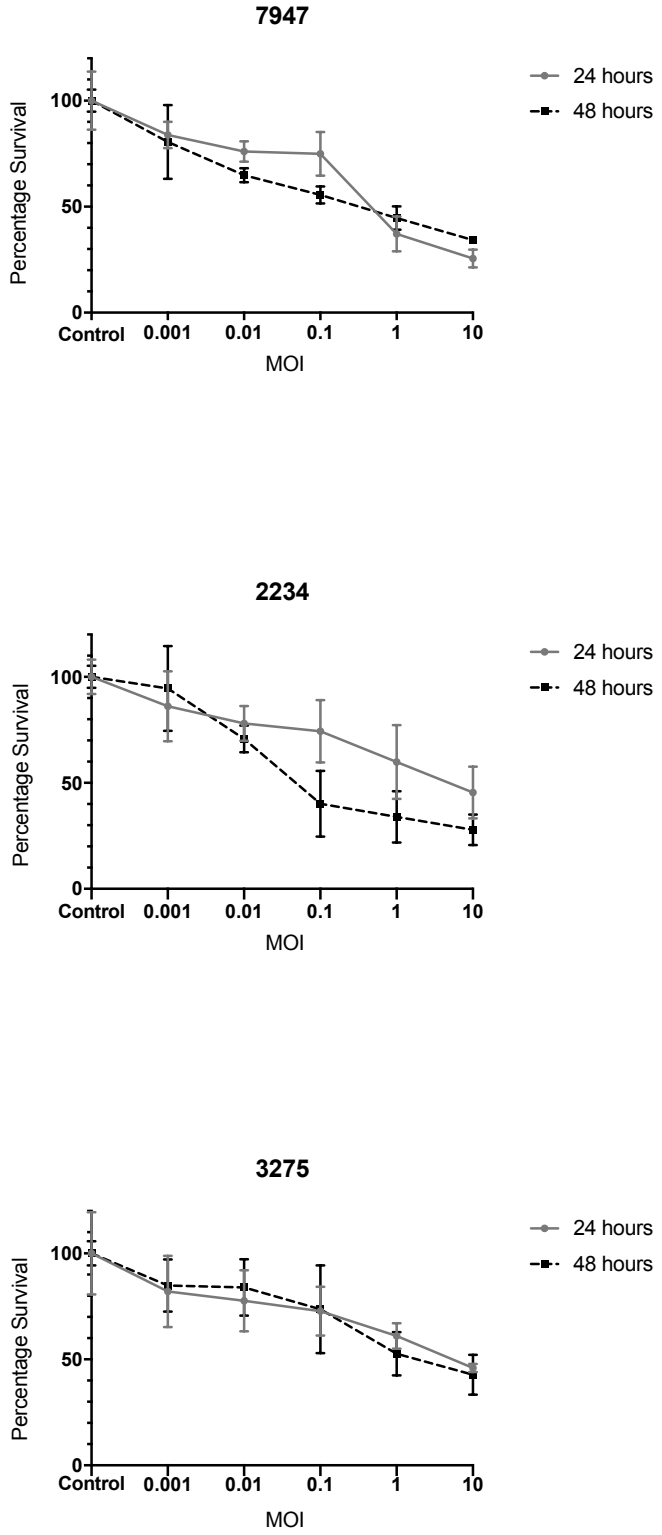
7947
Percentage Survival
100
50
0
Control
0.001
0.01
0.1
1
10
MOI
24 hours
48 hours
2234
Percentage Survival
100
50
0
Control
0.001
0.01
0.1
1
10
MOI
24 hours
48 hours
3275
Percentage Survival
100
50
0
Control
0.001
0.01
0.1
1
10
MOI
24 hours
48 hours

(C)

2234-FLUC

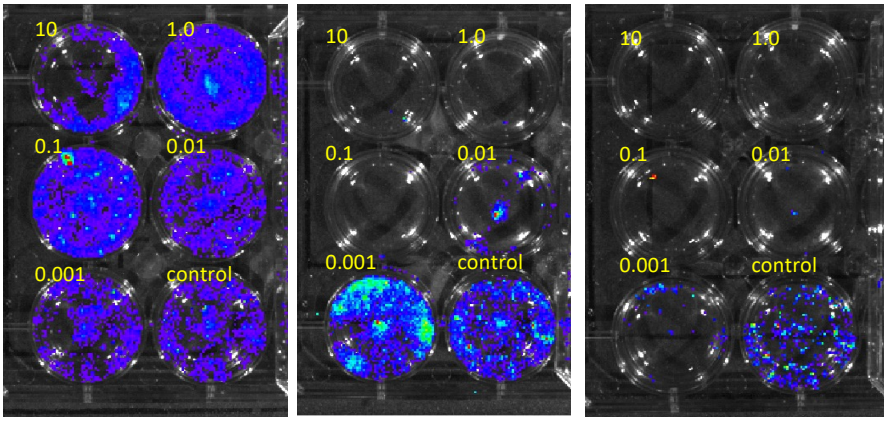

24 hrs 48 hrs 72 hrs

3275-FLUC

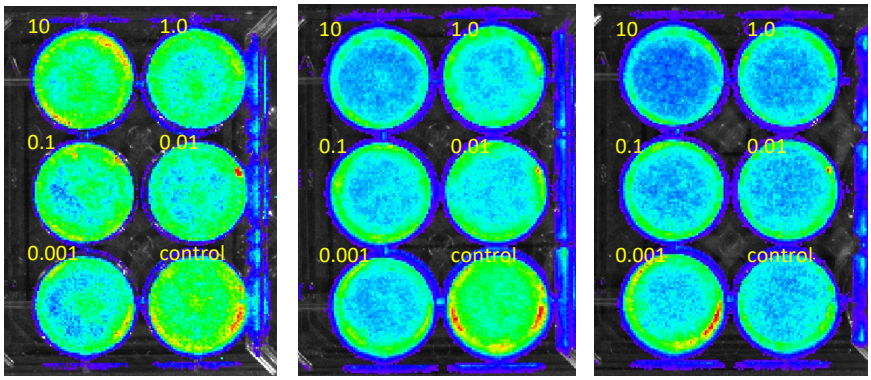

24 hrs 48 hrs 72 hrs

Figure 9: MG1-GFP infectivity and cytotoxicity in murine pancreatic cell lines

Fluorescence microscopy was performed using the EVOS cell imaging system after murine pancreatic cell lines were exposed to either PBS or MG1-GFP at varying concentrations for 24 and 48 hours (A). MTT assay was used to determine the cell viability in pancreatic cell lines following infection with MG1-GFP at 0.001, 0.01, 0.1, 1.0 and 10 MOI for 24 and 48 hours. Data represented as the mean and SD of three independent experiments (B). FLUC expressing pancreatic cells infected with MG1-GFP at a range of MOI from 0 to 10. IVIS images obtained at 24, 48 and 72 hours (C).

4.7 Discussion

Maraba is a single-stranded, negative-sense, enveloped RNA virus that derives from the vesiculovirus genus of the *Rhabdoviridae* family. It has a naturally occurring life-cycle in sandflies and is not known to be pathogenic to humans. Genetic modifications to the wild-type virus have resulted in the development of MG1, which has an enhanced capacity to replicate within tumour cells and a superior propensity to induce cancer cell death. These features support the potential use of MG1 as an oncolytic viral therapeutic agent and it is currently under investigation in three early phase clinical trials.

MG1 has shown both oncotropic and cytotoxic activity in a range of murine and human cell lines. Importantly, MG1 is highly attenuated when tested against a non-cancerous primary human skin fibroblast cell line, namely GM38, therefore highlighting its predilection to infect tumour cells whilst sparing normal cells; clearly an attractive property of any anti-cancer agent.

In this chapter, MG1 and its oncolytic potential against a broad range of both murine and human melanoma cell lines was investigated, including in previously untested cell lines. In order to represent the commonest mutational patterns found in melanoma, a panel of tumour cell lines was selected including those with either a BRAF wild type, BRAF mutant or NRAS mutant signature.

It was found that all the human melanoma cell lines tested, Mel888, A375, DO4, Mel624 and MeWo showed a susceptibility to MG1 infection. This was evidenced by the expression of the GFP viral transgene by infected cells (Figure 5C). In addition, the murine B16-F1, B16-F10 and 4434 cell lines were also readily infected by MG1 (Figure 5A). However, it was interesting to observe that the 21015 cell line showed notably more resistance to MG1 infection compared to the other cell lines. This was quantified through flow cytometry analysis of the proportion of live cells expressing GFP following viral infection which confirmed that infecting with an MOI of 0.1 for 24 hours led to

5.5% of 21015 cells expressing GFP. Under the same conditions, all other cell lines had a live cell GFP expression of at least 50% (Figure 5).

Consistent with the above, it was demonstrated that MG1 could replicate within the murine cell lines, with the greatest fold increase in MG1 progeny titre found with the B16-F1 and B16-F10 cell lines, then the 4434 cell line, and lastly the 21015 cell line. Of note, infecting with a lower MOI of 0.1 allowed for more replication and therefore a higher total fold increase compared to infecting with the higher MOI of 1.0. The most accelerated increase in MG1 titre was observed between 8 and 24 hours following initial MG1 infection. This is consistent with the published data that established Maraba and MG1 as a potential OV.[323] In summary, viral replication occurred in three of the four murine cell lines tested, mirroring the level of infection seen in Figure 5.

After demonstrating that MG1 can infect and replicate within the tumour cell lines, it was established that MG1 had a cytotoxic, rather than cytostatic, effect on cell survival. Regarding the murine cell lines, these data again showed that the 21015 cell line was the most resistant to MG1 toxicity, whereas the B16-F1 and B16-F10 cell lines were the most sensitive. In addition, regarding the human cell lines, MeWo appeared the most resistant, as compared to Mel624 which was the most sensitive.

The breadth of MG1 oncotoxicity was confirmed through the assessment of MG1 on three murine pancreatic cell lines (Figure 9). This demonstrated the sensitivity of the 7947 and 2334 cells to MG1 infection and cytotoxicity but more notable resistance from the 3275 cell line. The literature details MG1 sensitivity and out of a panel of 50 cell lines from a range of tumour types, has identified only the colorectal COLO 205, NSCLC NCI-H226 and renal TK10 cell lines show some initial resistance 48 hours following virus.[321] Therefore, the findings in the melanoma and pancreatic cell lines are consistent with existing data that supports the notion of MG1 being highly oncotoxic across a range of cell lines and tumour types with no discernible patterns to suggest any particular tumour type is more or less sensitive to MG1.

It was considered whether the underlying known mutational patterns of the different cell lines could explain the difference in sensitivity to MG1. Of interest, the more sensitive B16-F1 and B16-F10 cell lines are both BRAF wild type, whereas the 4434 and 21015 cell lines harbour a BRAF mutation. However, the least sensitive MeWo human cell line is BRAF wild-type therefore it appears unlikely that BRAF mutations alone explain differences in cell line sensitivity. Contrasting this with published material, only the sensitivity to MG1 of derivatives of the B16 murine cell line have been published. Regarding human melanoma cell lines, the literature details the results of MG1 against cell lines from the NCI 60 cell panel which includes five BRAF mutant melanoma cell lines, namely, M14, MALME-3M, SK-MEL-28, UACC-257 and UACC-62, all of which are MG1 sensitive.[321] Therefore, it is not evident that BRAF mutation status influences sensitivity to MG1.

With regards to the most resistant cell lines, namely 21015 and 3275, it would be an interesting avenue to ascertain what features render these cells less sensitive to MG1 infection, replication and toxicity. It has been previously shown that the LDL receptor (LDLR) can be differentially expressed between sensitive and resistant ovarian cancer cell lines, with a higher expression conferring increased tumour cell sensitivity to viral infection.[324, 333] It would be noteworthy to investigate the quantification of LDLR expression of the murine and human cell lines and evaluate if this correlates with the varying sensitivity of the different cell lines, both murine and human. In addition to LDLR expression, the ability of the infected tumour cell to mount an IFN response may determine the efficacy of viral replication. These elements will be explored subsequently.

In this chapter, it was identified that MG1 can infect and replicate within a range of melanoma cell lines, resulting in virally mediated tumour cell toxicity *in vitro*. The next objective was to examine whether these findings could be replicated using *in vivo* murine melanoma models.

Chapter 5:

Effects of Maraba Virus in Melanoma – *in vivo* models

5 Chapter 5: Effects of Maraba Virus in Melanoma – *in vivo* models

5.1 Introduction

Having identified a capacity to infect and replicate within tumour cells *in vitro*, it was investigated whether this was replicated using a murine *in vivo* model of melanoma. In addition, this would enable the evaluation of the tumour tropic nature of MG1 *in vivo*.

The oncolytic activity of MG1 has been demonstrated in xenograft models using human cancer cell lines of patient-derived tumours. However, whilst displaying the oncolytic potential of MG1, implanting tumours in immunodeficient mice cannot reveal the potential immunotherapeutic effect derived from OVs. Previous studies in a range of immunocompetent syngeneic tumour models have demonstrated the beneficial effect gained from MG1 treatment. This includes studies in colorectal, lung, breast and prostate cancer, sarcoma, leukaemia and melanoma.[321] Regarding the melanoma data, MG1 led to a survival benefit in the B16-F10 tumour model but only when engineered with the DCT melanoma antigen transgene and used in a prime-boost fashion along with a DCT encoded adenovirus.[323]

Therefore, there are no previous reports of MG1 used in monotherapy, leading to survival gains in immunocompetent murine models of melanoma. In addition, no previous studies have assessed MG1 on a range of *in vivo* syngeneic models with differing BRAF mutational backgrounds. In order to expand on the previously published studies, the efficacy of MG1 virotherapy to treat B16-F1 and 4434 subcutaneous tumours was investigated.

Previous reviews have highlighted the role played by neutralising antibodies (NAbs) in decreasing oncolytic viral replication and reduced anti-tumour activity in immunocompetent hosts, both in pre-clinical and early stage clinical studies.[339, 340] Strategies have sought to overcome NAbs for instance

through 'hiding' the OV within *ex vivo* infected tumour cells [341] or by using other carrier cells including mesenchymal stem cells [342, 343], T cells [344, 345] or DCs.[346, 347] Indeed, these approaches have been shown to be able to deliver the OV load to the intended tumour target, even in the presence of NAbs.

Reviewing the literature, there has been no data published that has investigated whether NAbs against MG1 virus are produced *in vivo* and what effect they have on viral delivery to the tumour. Therefore, an analysis was undertaken in order to help establish an optimal treatment regimen for future experiments.

5.2 Intravenous delivery of MG1-FLUC reaches B16-F1 and 4434 subcutaneous flank tumours *in vivo* and is tumour specific

In the early development of Maraba as an OV, it was shown that MG1 is able to reach and replicate within a subcutaneous CT26 colorectal model.[320] Subsequent to this, it was shown that the systemic administration of MG1 can reach lung metastases arising from a B16-F10 melanoma model and replicating virus can be retrieved from the metastatic tissue.[323] This project aimed to expand on this data with the use of two other syngeneic murine melanoma models, namely the 4434 and B16-F1 cell lines. This selection ensured that both a BRAF wild-type (i.e. B16-F1) and BRAF mutated (i.e. 4434) cell lines were tested *in vivo* with MG1. MG1 virus expressing firefly luciferase (MG1-FLUC) was systemically administered at a dose of $1x10^7$ plaque forming units (pfu) into four mice harbouring B16-F1 and five mice harbouring 4434 subcutaneous right flank tumours.

D-luciferin, the substrate to the virally-encoded luciferase enzyme, was then given intraperitoneally at 6, 18, 24 and 30 hours prior to imaging the anaesthetised mice using the IVIS imaging system. The mice were sacrificed

at their corresponding time point and organs were harvested for further IVIS imaging and to perform *ex vivo* plaque assays.

In the B16-F1 group, at the six hour time point, the luciferase signal was detectable through the soft tissues of the anaesthetised live mice. Following the harvesting of the brain, liver, lung, spleen and tumour, it could be seen that the bioluminescence signal was originating exclusively from the spleen, suggesting that following IV administration, the MG1-FLUC virus initially passes to the spleen, but at this early time point has not yet infected either the tumour or other organs. By the 18 hour time point, the luciferase signal remained visible through the soft tissue of the anaesthetised mouse, however, on exploring the viral biodistribution the bioluminescence signal was no longer visible from the spleen and was displayed exclusively from the tumour. This bioluminescence signal was maintained in the tumour albeit to a lesser intensity at the 24 hour time point and then by 30 hours the luciferase signal had become negligible (Figure 10A).

Similarly, in the 4434 tumour group, the spleen displayed luciferase signal six hours following MG1-FLUC viral infection. In this instance, there was also a modest bioluminescence signal from the harvested tumours. By 18 hours, the bioluminescence signal was again exclusively seen within the tumour but by the 24 hour and 48 hour time points, no further luciferase was detected (Figure 10B).

The presence of replication-competent virus was quantified in the harvested B16 F1 and 4434 flank tumours at each time point by performing *ex vivo* plaque assays. The viral titre was calculated in plaque forming units per gram (pfu/g) of tumour (Figure 10C). This demonstrated that in both cell lines, live replicating virus was recoverable from the tumour. Furthermore, in both tumour types, the amount of recoverable virus increased between six to 18 hours before decreasing by 24 hours. Specifically, from the B16-F1 tumours, no virus was identified in the six hour tumours. Subsequently, 1.3×10^4 pfu/g of live replicating virus was recovered at 18 hours before dropping to 3.2×10^3 pfu/g by 24 hours. Viral recovery from the 4434 tumours was also absent at

six hours, before increasing to $6.6x10^4$ pfu/g at 18 hours, however, no live replicating virus was identified by plaque assay at 24 hours. This early increase and rapid decrease was identified in tumours from both of the two cell lines and these data are consistent with the qualitative measure of intensity from the luciferase signal seen at the corresponding time points. *Ex vivo* plaque assays of the spleens were conducted but only demonstrated a single viral plaque ($1x10^2$ pfu/g) from the spleen of the B16-F1 bearing mouse harvested at six hours. This is consistent with the time point at which the luciferase signal is detected from the spleen. At no other time points was replicating virus recovered from the spleen. *Ex vivo* plaque assays of the other harvested organs did not reveal the presence of any replicating virus, thus further supporting the tumour tropism of MG1-FLUC (Figure 10C).

(A)

B16-F1

6 hours

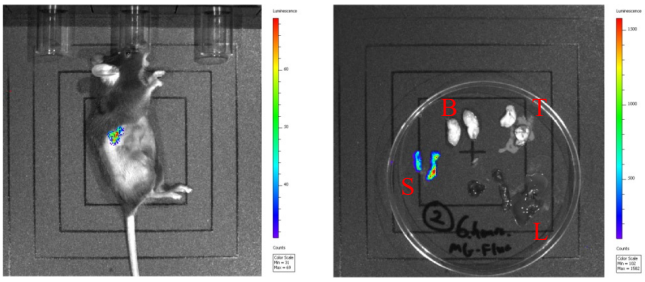

18 hours

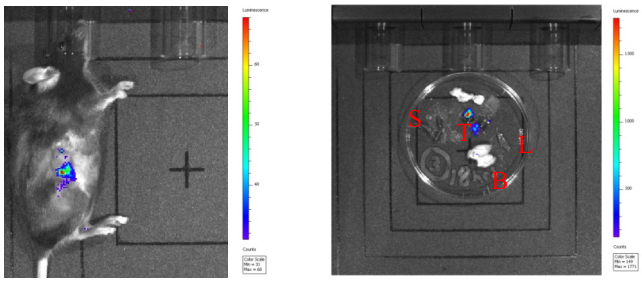

24 hours

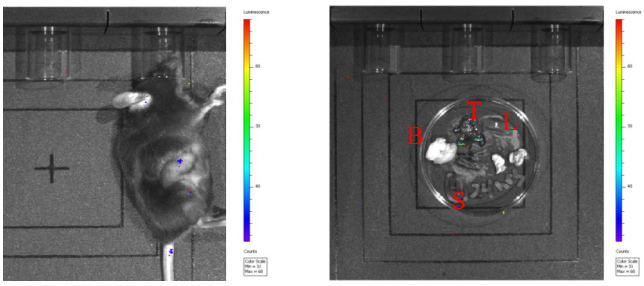

30 hours

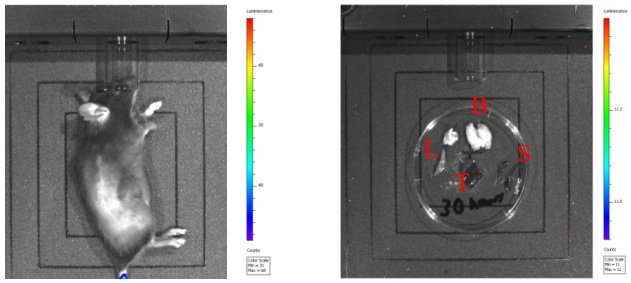

(B)

4434

6 hours

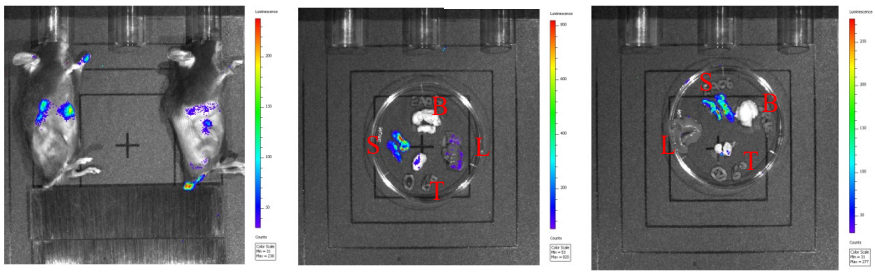

18 hours

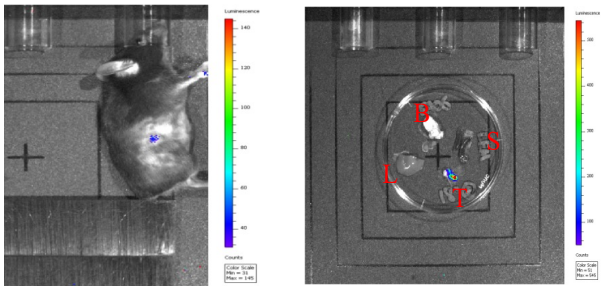

24 hours

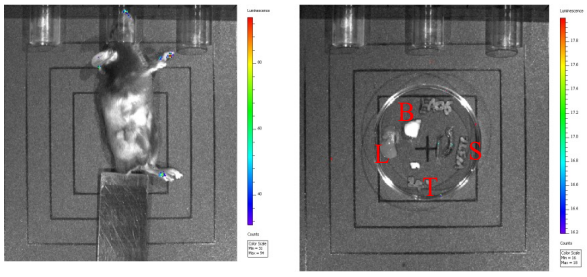

30 hours

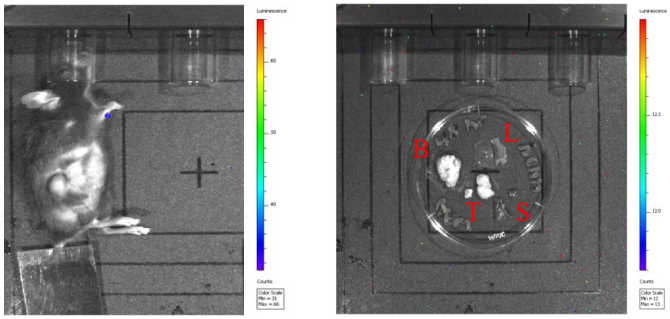

(C)

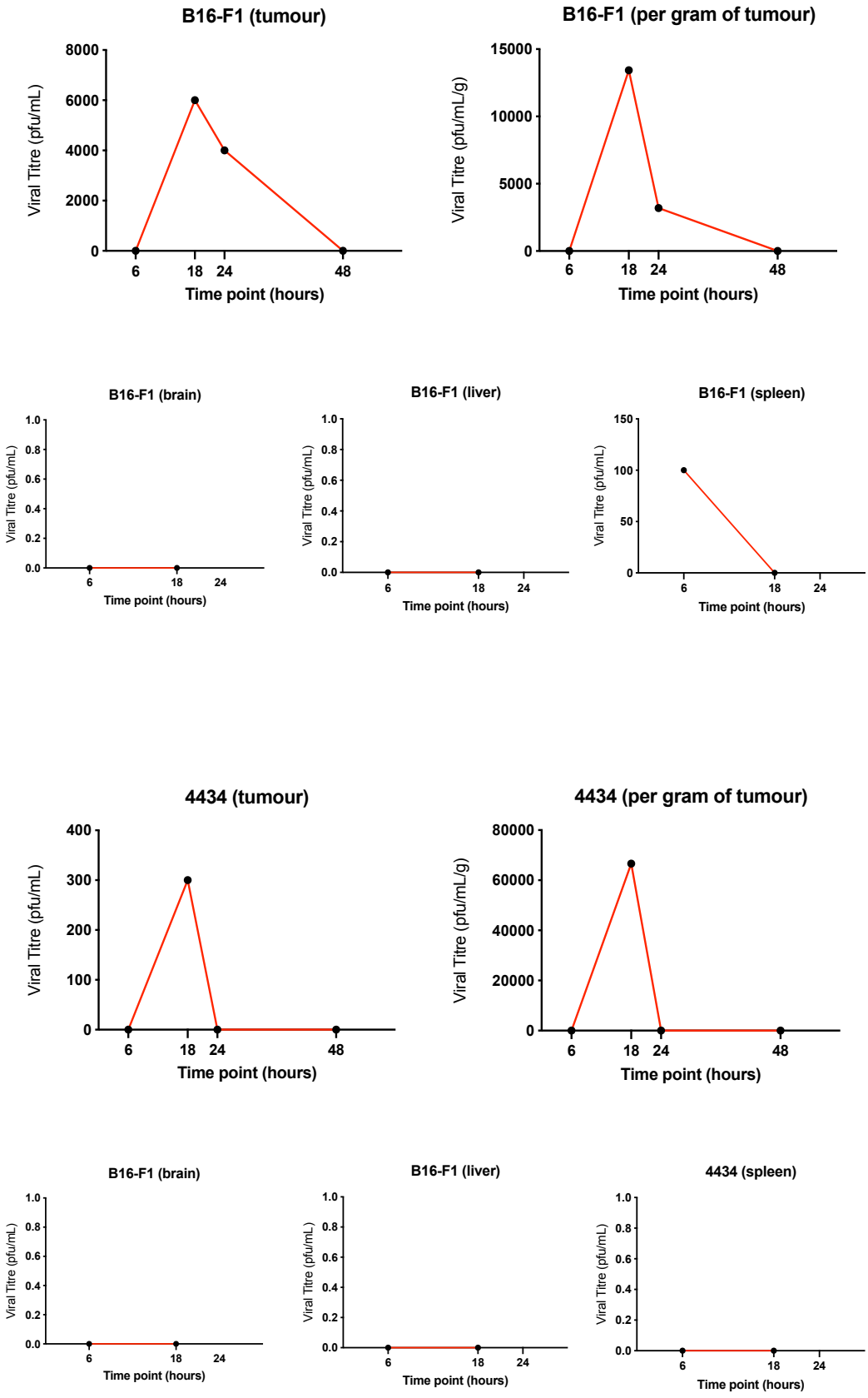
B16-F1 (tumour)
Viral Titre (pfu/mL)
8000
6000
4000
2000
0
6
18
24
48
Time point (hours)
B16-F1 (per gram of tumour)
Viral Titre (pfu/mL/g)
15000
10000
5000
0
6
18
24
48
Time point (hours)
B16-F1 (brain)
Viral Titre (pfu/mL)
1.0
0.8
0.6
0.4
0.2
0.0
6
18
24
Time point (hours)
B16-F1 (liver)
Viral Titre (pfu/mL)
1.0
0.8
0.6
0.4
0.2
0.0
6
18
24
Time point (hours)
B16-F1 (spleen)
Viral Titre (pfu/mL)
150
100
50
0
6
18
24
Time point (hours)
4434 (tumour)
Viral Titre (pfu/mL)
400
300
200
100
0
6
18
24
48
Time point (hours)
4434 (per gram of tumour)
Viral Titre (pfu/mL/g)
80000
60000
40000
20000
0
6
18
24
48
Time point (hours)
B16-F1 (brain)
Viral Titre (pfu/mL)
1.0
0.8
0.6
0.4
0.2
0.0
6
18
24
Time point (hours)
B16-F1 (liver)
Viral Titre (pfu/mL)
1.0
0.8
0.6
0.4
0.2
0.0
6
18
24
Time point (hours)
4434 (spleen)
Viral Titre (pfu/mL)
1.0
0.8
0.6
0.4
0.2
0.0
6
18
24
Time point (hours)

Figure 10: MG1 is tumour tropic and replication competent virus can be retrieved from subcutaneous tumours following systemic viral delivery

IVIS imaging of mice harbouring B16-F1 (A) and 4434 (B) subcutaneous tumours taken after MG1-FLUC virus at a dose of $1x10^7$ pfu was delivered intravenously via tail vein injection. Imaging of tumour and organs from each corresponding mouse obtained at 6, 18, 24 and 30 hours following viral injection. T – tumour, S – spleen, B – brain, L – lung. Tumour and organs homogenised and lysates analysed by plaque assay for the presence of replication competent virus, represented as both absolute viral titre and titre per gram of tumour (C).

5.3 Identification of neutralisation antibodies to MG1

Having established that IV delivery of MG1 does indeed selectively reach both subcutaneous 4434 and B16-F1 tumours, we wanted to investigate the therapeutic potential of MG1 using these two murine models. This first involved trying to establish an appropriate therapeutic regimen. As previously discussed, OV therapy may be limited by the presence of pre-existing sero-positivity to the viral agent (through previous infection or vaccination for instance). This is mitigated in the case of MG1 due to the absence of general pre-exposure to MG1 in the population. *In vivo*, or clinically in patients, this ensures that for a first dose of MG1, anti-viral neutralising antibodies are extremely unlikely to be present, however, following exposure to the first dose of MG1 treatment, NAbs could develop prior to second, third or subsequent doses of virus, potentially reducing the effective virus titre before it reaches its tumour target. Therefore, it was necessary to understand the development timeline of NAbs, in order to optimise a treatment schedule.[251]

In this instance, immunocompetent C57Bl/6 mice (bearing a non-melanoma cell line tumour in order to make use of surplus mice) were injected with IV MG1-GFP at $1x10^6$ pfu. Cardiac puncture was performed at two, three, seven and 14 days to obtain blood for the detection of NAbs. The harvested blood was centrifuged to enable plasma collection. The plasma was heat inactivated (to inactivate complement proteins) prior to undergoing serial dilutions by a factor of ten. These dilutions were repeated three times resulting in a total of four concentrations of diluted plasma for each time point: neat, 10^{-1}, 10^{-2} and 10^{-3}. Each plasma dilution was incubated with 0.1 MOI of MG1-GFP virus for four hours at 37°C, prior to using plaque assays to determine whether replication competent virus was still identifiable within the plasma, or whether it had been neutralised. MG1-GFP that had been incubated with PBS alone (i.e. not with plasma) was used as a positive control.

Figure 11A shows plaque assays of the positive control and the diluted mice serum at different time points. The positive control (top panel) shows the expected number of plaques in the absence of any neutralisation. This

demonstrates that plaques can be seen in each serial dilution, indicating the presence of replication-competent virus. At the day two time point, a similar number of plaques can be observed, thereby signifying that at this time point, there has been no discernible accumulation of NAbs in the plasma. However, by day three, no plaques were evident in the neat plasma well, and a reduced number of plaques were observed in the 10^{-1} and 10^{-2} wells when compared to the positive control and day two samples. This therefore implies the presence of NAbs in the plasma, neutralising the efficacy of MG1 to generate plaques. By day seven, there were no plaques detected in the neat or 10^{-1} sample and the number of plaques seen in the 10^{-2} and 10^{-3} samples were reduced compared to day two and three samples. This therefore suggested a further increase in the quantity of NAbs present within the plasma by this time point. Finally, at day 14, there were no plaques seen in the neat, 10^{-1} and 10^{-2} samples and only two plaques detected in the 10^{-3} sample which was considerably less than the day seven sample. Therefore, these data suggest that the development of antibodies that are effective in neutralising MG1 start to be present in sufficient quantities three days following viral administration. Whilst this may have a constraining effect on viral therapy, it does at least confer a level of safety in knowing that significant amounts of ongoing viral shedding beyond the initial days post viral administration is prevented.

After identifying the development of MG1-induced NAbs in C57Bl/6 mice, the subsequent intention was to determine, using in this case the 4434 melanoma model, whether the presence of NAbs would affect the systemic delivery of MG1 to murine tumours.

After establishing subcutaneous 4434 tumours, mice were treated either with IV PBS or MG1-GFP $1x10^7$ pfu. After five days, all mice were subsequently given an IV administration of MG1-FLUC $1x10^7$ pfu. (An intervening period of five days was selected as this gave sufficient time for NAbs to develop, and MG1-GFP was chosen as the first treatment, rather than MG1-FLUC, to ensure that any NAbs generated were to the MG1 viral capsid rather than to the transgene product). The experimental schematic is shown in Figure 11B.

Intraperitoneal D-luciferin was administered at either six or 18 hours following MG1-FLUC treatment and the tumours and organs from both the PBS-pre-treated and MG1-GFP-pre-treated groups were imaged. As shown in Figure 11C, at six hours, the group pre-treated with PBS before subsequent MG1-FLUC, demonstrated luminescence from the spleen. This is consistent with images shown previously in Figure 10. However, in those mice that had received MG1-GFP five days prior to MG1-FLUC, no luminescence was seen from the spleen (or any other site). In addition, at 18 hours post MG1-FLUC, the group pre-treated with PBS demonstrated a luminescent signal from the tumour, again consistent with Figure 10, however, no signal was seen in mice that received MG1-GFP five days prior to MG1-FLUC.

These results suggest that MG1-induced NAbs (which have been shown to be detected three days post systemic viral administration) are capable of neutralising a second dose of MG1 and preventing it reaching the tumour, when administered five days after the first viral dose.

This implies that the optimal MG1 treatment regimen for future *in vivo* experiments is likely to necessitate that either a single treatment is used or, if multiple treatments are to be given, that these are all delivered prior to day three, in order to circumvent the effect of NAbs on the ability of the virus to reach the tumour target. However, as OV therapy is not solely due to the oncolytic effect of virus, it is possible that additional MG1 doses may still serve to boost anti-tumoural immune activation, and furthermore, given it has been shown with other OVs, namely reovirus, that the immune response of DCs and T cells can indeed internalise and deliver the OV to the tumour [347] and, therefore, a multidose regimen could still be a valid therapeutic approach.

(A)

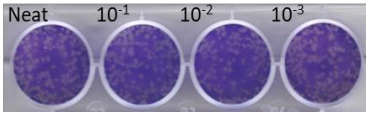

MG1-GFP MOI 0.1 alone (positive control)

2 days

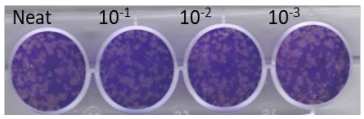

3 days

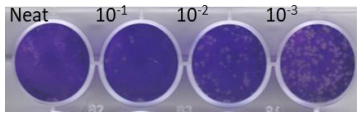

7 days

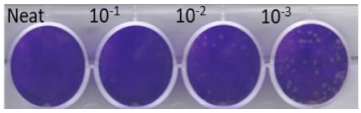

14 days

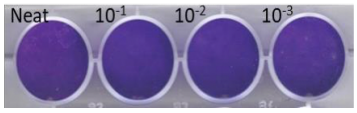

(B)

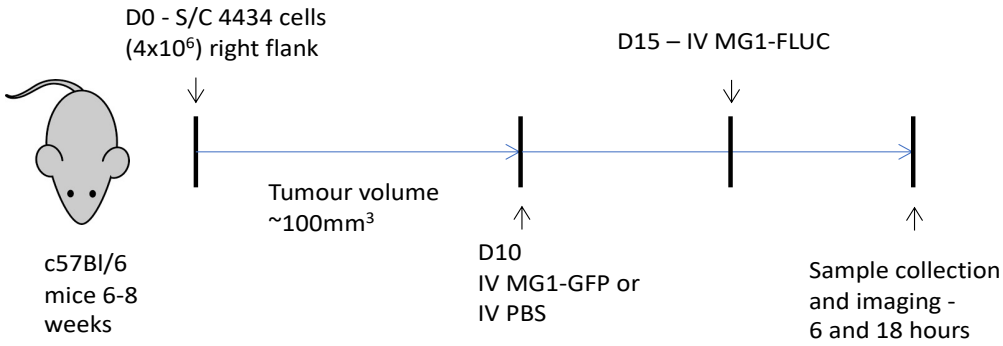

(C)

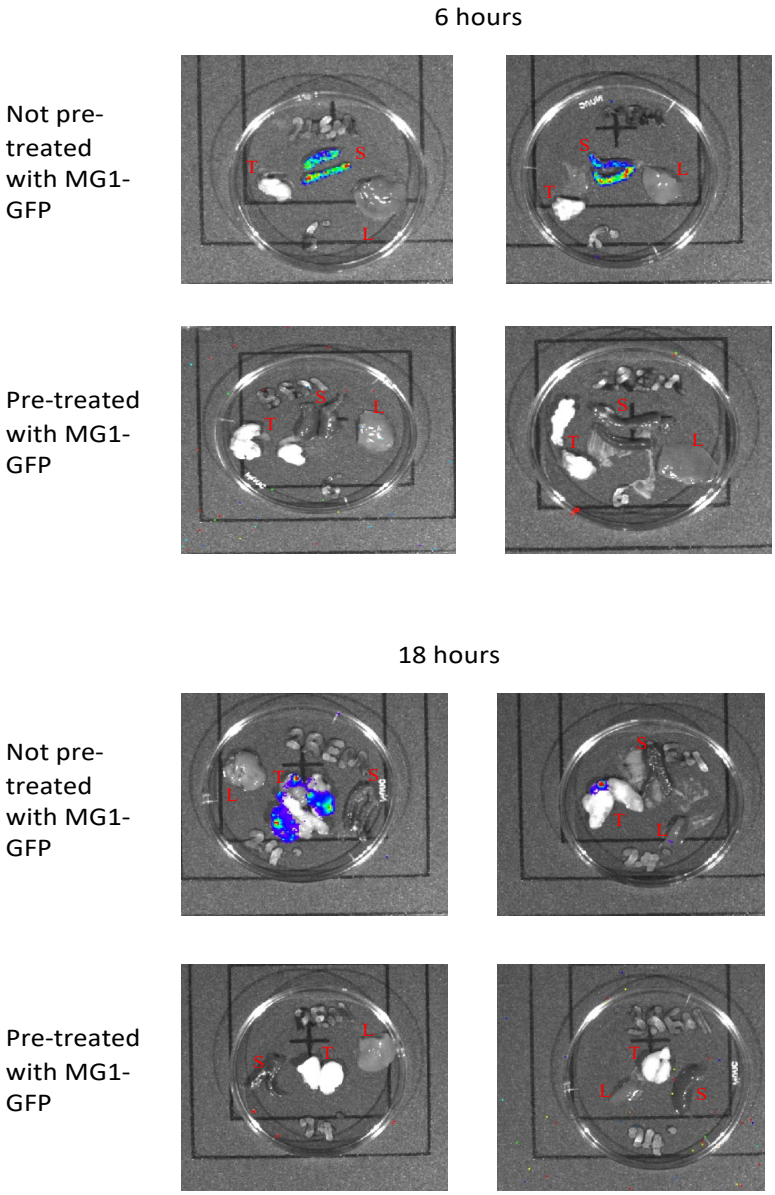

Figure 11: Intravenous MG1 induces the development of NAbs, neutralising and preventing subsequent MG1 from reaching 4434 tumours

Plaque assay of 0.1 MOI MG1-GFP as positive control and heat inactivated plasma-MG1-GFP samples at different timepoints (A). Experimental schematic for assessing systemic MG1 rechallenge in 4434 murine model (B). IVIS images of harvested tumours and organs at six and 18 hours after intravenous MG1-FLUC challenge, having been previously pre-treated, five days prior, with either PBS or MG1-GFP (2 mice per group) (C). T – tumour, S – spleen, L – liver.

5.4 MG1 efficacy against an *in vivo* B16-F1 murine melanoma model

Having identified the broad cytotoxic potential of MG1 *in vitro*, and confirming that MG1 can reach and replicate within *in vivo* tumours, the next step was to ascertain whether MG1 could limit tumour growth or improve survival *in vivo*.

C57Bl/6 mice were implanted with $5x10^5$ subcutaneous B16-F1 cells. Once the tumours were established, the mice were randomised into groups of six. Tumour bearing mice were challenged with either one dose or three alternate day doses of $1x10^7$ pfu of MG1-FLUC given via either IV or IT administration and compared with control groups that had received 50 μL of IV or IT PBS respectively.

Given the identification of the generation of NAbs and the inability of MG1 to be identified within tumours five days following a previous MG1 injection, it was considered important to deliver all MG1 doses within a five-day window.

Figure 12A illustrates the schematic of the *in vivo* experiment. Each group was comprised of six mice. PBS control group was compared with either the IV or IT administration of MG1-FLUC and also compared with either one or three administrations of virus. The average tumour size at the point of initiating treatment was between $50mm^3$ and $100mm^3$ in all cohorts. Figure 12B shows the B16 tumour growth trend for each individual mouse by treatment cohort. Figure 12C shows the median B16 tumour growth and range for each group. Despite the different regimens received, there was no significant difference in average B16 tumour growth between the PBS or viral treatment cohorts. Figure 12D plots the overall survival outcomes for each treatment cohort. The median overall survival for the IV PBS and IT PBS groups was 18 and 17 days respectively, compared to 17 days, 17 days, 19 days and 19 days for the IV x 1, IV x 3, IT x 1 and IT x 3 treatment groups respectively. As expected, given the non-significant impact on average tumour growth above, the overall survival data confirmed that there is no significant survival advantage in the B16-F1 model when treated with either IV or IT MG1-FLUC regardless of

whether given as a single treatment or three consecutive treatments, compared to PBS treated control mice. In addition, with regards to the safety of the viral treatment, some mice treated with three doses of IV MG1 displayed intermittent piloerection and weight loss, however, this was not observed in any mice following IT administration.

(A)

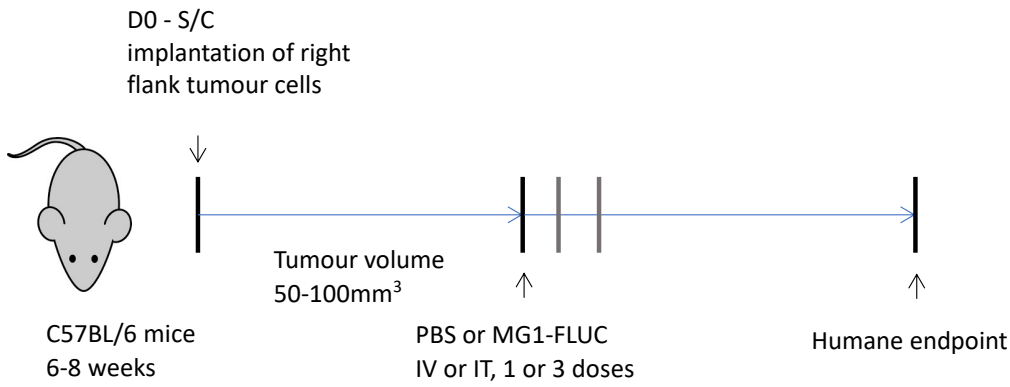
D0 - S/C
implantation of right
flank tumour cells
Tumour volume
50-100mm3
C57BL/6 mice
6-8 weeks
PBS or MG1-FLUC
IV or IT, 1 or 3 doses
Humane endpoint

(B)

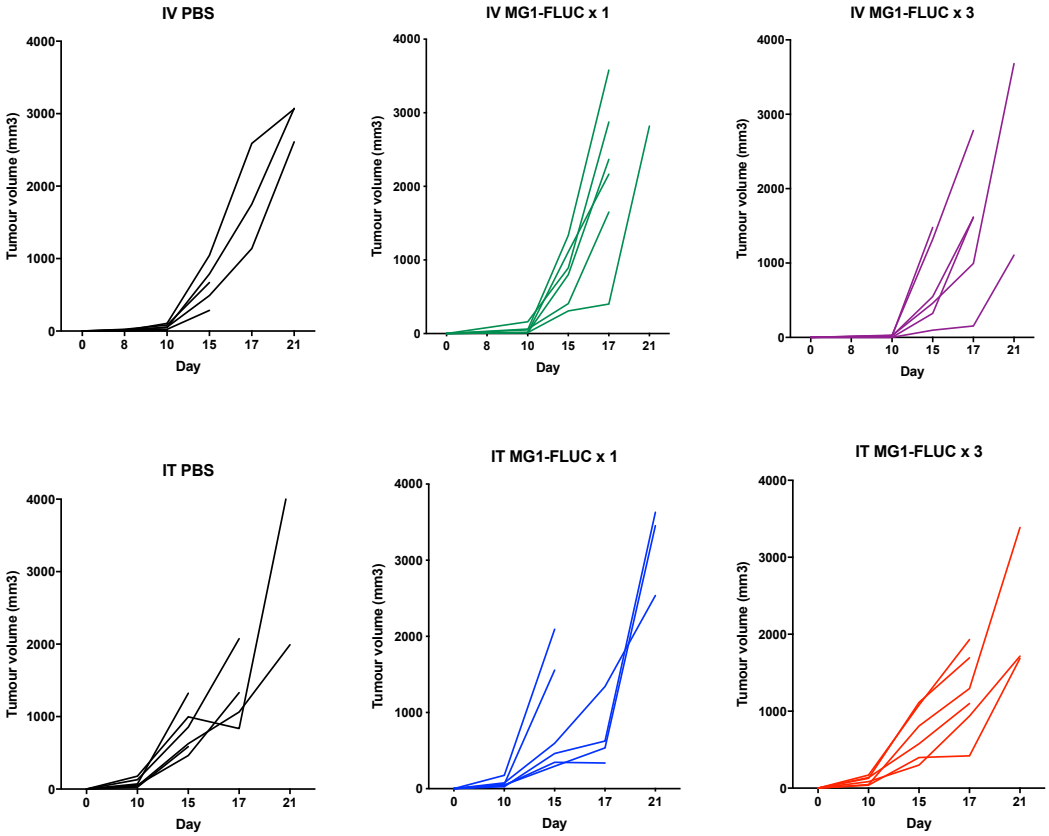
IV PBS
IV MG1-FLUC x 1
IV MG1-FLUC x 3
IT PBS
IT MG1-FLUC x 1
IT MG1-FLUC x 3
Tumour volume (mm3)
Day
0
1000
2000
3000
4000
0
8
10
15
17
21

(C)

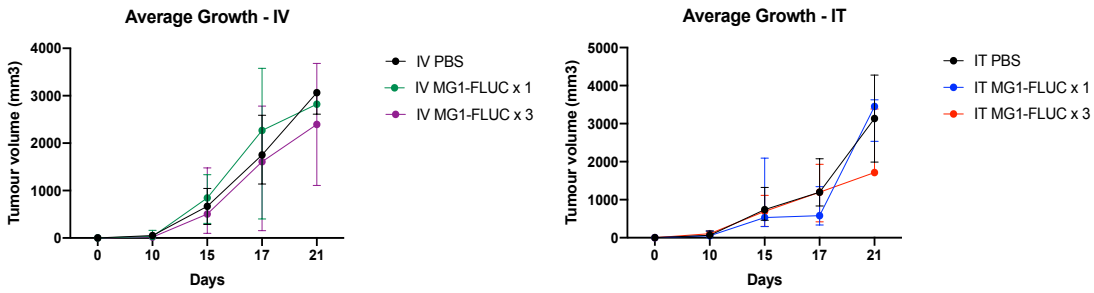

(D)

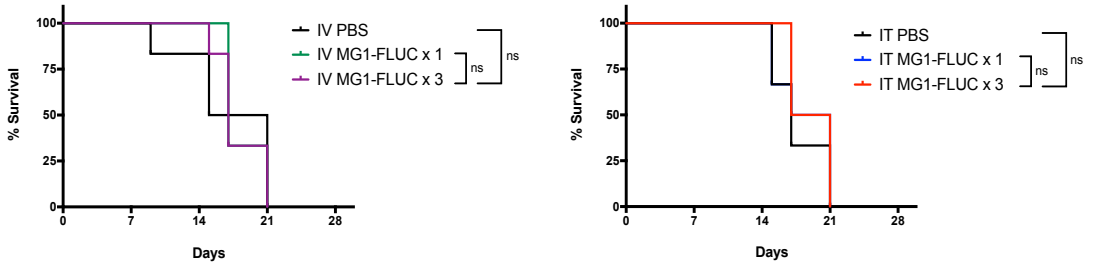

Figure 12: MG1 fails to restrict B16-F1 tumour growth and does not extend survival, regardless of IV or IT, single or multiple dose administration.

Schematic of in vivo experiment (A). Data showing B16-F1 tumour growth of individual mice in each treatment cohort (B). Graphs representing the average B16-F1 tumour growth in intravenous and intratumoural MG1-FLUC treatment groups, plotted as median and range at each time point (C). Survival curves for mice treated with intravenous and intratumoural MG1-FLUC (MG1-FLUC treated vs. control; Mantel-Cox log-rank statistical analysis) (D).

5.5 MG1 efficacy against an *in vivo* 4434 murine melanoma model

The findings above confirm previous data that indicate the lack of efficacy of MG1 in treating an *in vivo* B16 melanoma model. To investigate whether this occurred across other melanoma models, the same experiments in mice bearing the 4434 murine melanoma model were undertaken. Given the drug related side effects with three doses of IV administration described above, it was decided to use IT treatment groups alone.

The schematic for these experiments was identical to those used for investigating B16-F1 (see Figure 12A). Figure 13A shows the tumour growth trend for each individual mouse by treatment cohort, following an initial implantation of $4x10^6$ 4434 cells. Figure 13B shows the mean 4434 tumour growth for each group. The average tumour size at the point of initiating treatment in the PBS cohort was $46mm^3$ as compared to $45mm^3$ and $47mm^3$ for the IT x 1 and IT x 3 treatment groups respectively. As shown, treatment with MG1-FLUC either as a single treatment or three consecutive treatments significantly delayed tumour growth when compared to PBS. Figure 13C shows the overall survival outcomes for each treatment cohort. The median overall survival for the PBS group was 57 days, whereas it was unreached and therefore significantly longer for both the IT x 1 ($p=<0.0001$) and IT x 3 ($p=<0.0001$) treatment groups. No significant difference was identified between the administration of either one or three MG1-FLUC treatments ($p=0.32$). Of note, in total, 11 out of 12 mice in the MG1-FLUC groups achieved long-term survival.

Although these results were impressive, given the small tumour size (termed 'small' size) at the point of treatment, it was necessary to examine whether the benefits of MG1 were retained when treating larger tumours.

Therefore, the experiment was repeated in mice harbouring tumours which had been allowed to grow to two further sizes prior to treatment (termed 'medium' size and 'large' size). Given that there was no difference identified

between one or three doses of treatment, to avoid excessive use of mice with multiple groups, the use of one IT dose of virus was opted for.

Figure 13D shows the mean tumour growth for each group. The average tumour size at the point of initiating treatment in the 'medium' group was 102mm^3 and 104mm^3 in the PBS and MG1-FLUC groups respectively. The average tumour size at the point of initiating treatment in the 'large' group was 186mm^3 for both the PBS and MG1-FLUC groups. As shown, treatment of both the 'medium' and 'large' size group and with MG1-FLUC significantly delayed tumour growth when compared to PBS.

Figure 13E shows the overall survival outcomes for the 'medium' and 'large' sized tumour groups. Regarding the 'medium' group, treatment with MG1-FLUC resulted in a mOS of 57 days which was significantly longer than 47 days from the treatment with PBS ($p=0.0008$). In the 'large' tumour group mOS was 46 days in the MG1-FLUC group compared to 41 days in the PBS group ($p=0.486$). However, as shown in Figure 13F, which superimposes the outcomes from the 'small', 'medium' and 'large' treatment groups, none of the mice treated in the 'large' tumour size group resulted in long-term survival.

In summary, a single IT MG1 injection, can improve the survival of mice bearing subcutaneous 4434 flank tumours when compared to a single IT injection of PBS. The size of effect of this treatment appears to correlate with the tumour size as it is most effective in 'smaller' sized tumours then 'medium' sized tumours with the most marginal benefit seen in the 'larger' size tumour group.

(A)

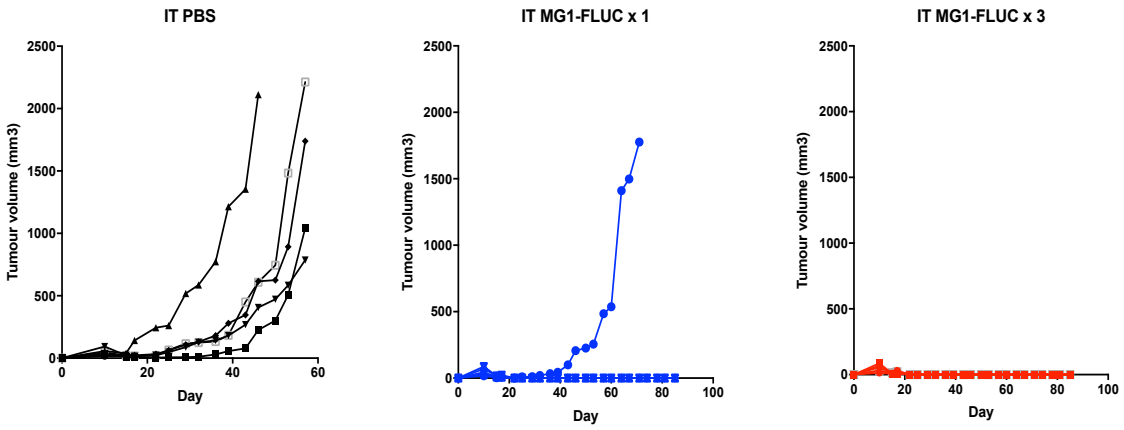
IT PBS
IT MG1-FLUC x 1
IT MG1-FLUC x 3
Tumour volume (mm3)
Day

(B)

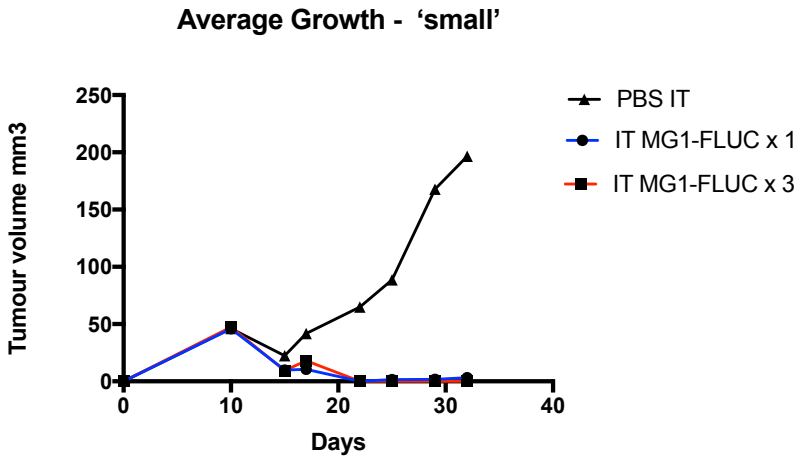
Average Growth - 'small'
Tumour volume mm3
Days
PBS IT
IT MG1-FLUC x 1
IT MG1-FLUC x 3

(C)

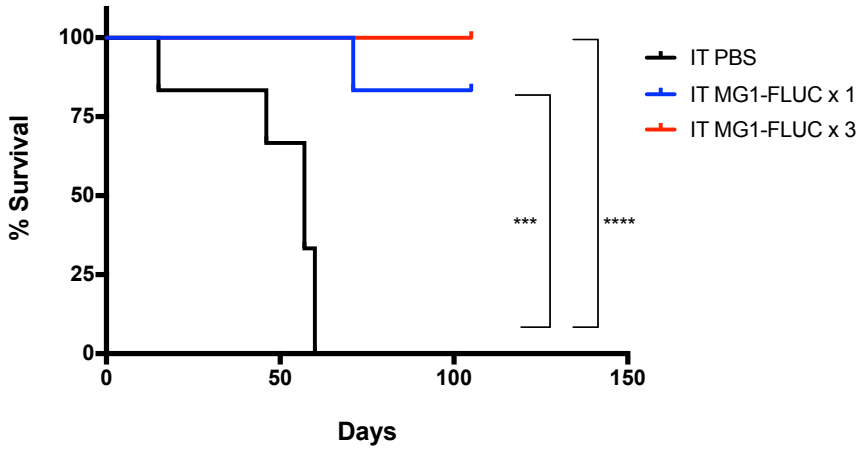
% Survival
Days
IT PBS
IT MG1-FLUC x 1
IT MG1-FLUC x 3
***
****

(D)

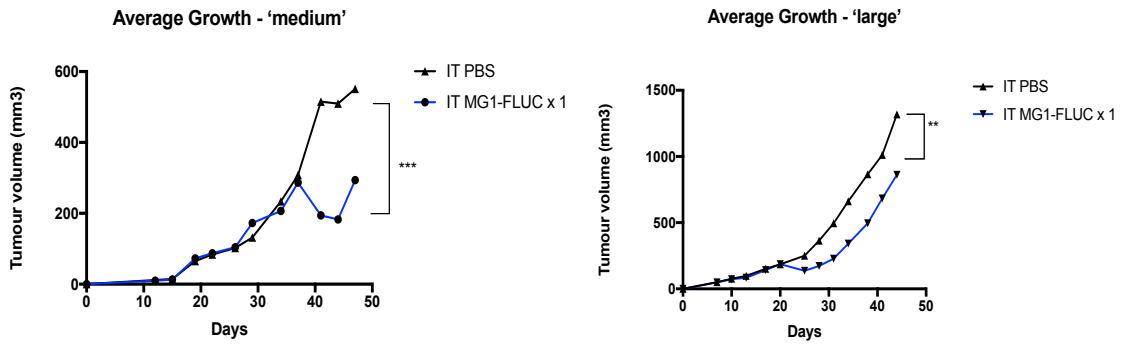

(E)

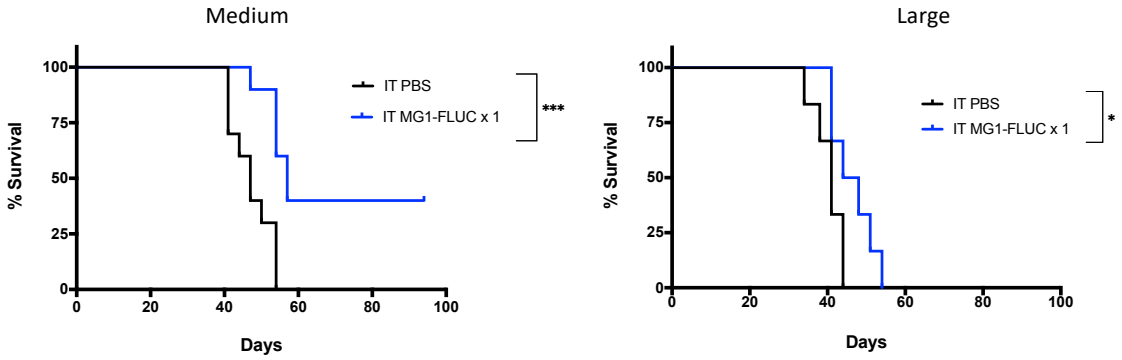

(F)

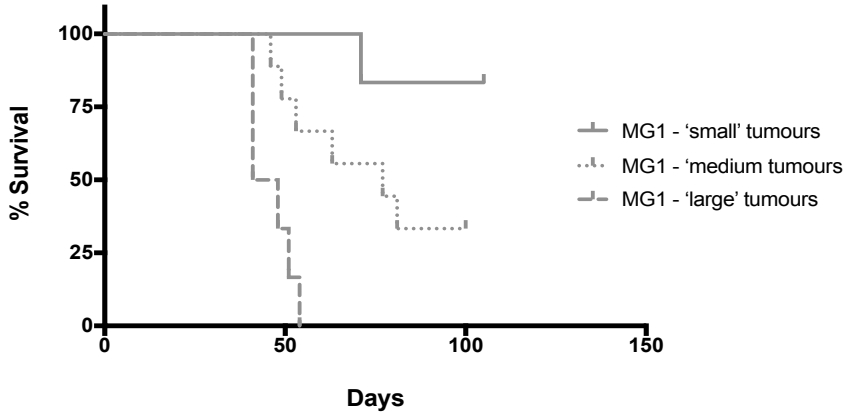

Figure 13: IT MG1 restricts tumour growth and survival in 4434, but the strength of this effect is dependent on tumour size.

Data showing 4434 tumour growth of individual mice in each treatment cohort (A). Graphs representing the average 4434 growth following intratumoural treatment in 'small' (B), 'medium' and 'large' (D) tumours (two-tailed P-value; MG1-FLUC treated vs. control; paired student T-test statistical analysis). Survival curves for mice with 'small' tumours treated with IT MG1-FLUC in 'small' (C), 'medium' and 'large' (E) 4434 tumours (MG1-FLUC treated vs. PBS control; Mantel-Cox log-rank statistical analysis). Superimposed survival curves of 'small', 'medium' and 'large' 4434 tumour groups treated with MG1-FLUC (F).

5.6 Discussion

After initially showing the sensitivity *in vitro* of a range of human and murine melanoma cells to MG1, the next approach was to evaluate whether these effects could be translated into an immunocompetent murine model of melanoma. Given the sensitivity of the B16-F1 and the 4434 cells *in vitro*, these two cell lines were selected for further *in vivo* examination.

One of the defining features of OVs is their ability to selectively replicate in tumour cells whilst sparing normal cells. In this regard, the capacity for the MG1-FLUC virus to reach the implanted tumours was assessed. The firefly luciferase bioluminescent signal could be seen emanating from the spleen at six hours following systemic viral injection and detected in the tumour at 18 hours following viral injection. Explanted evaluation of the tumour and other organs confirmed that the virus was only visibly seen within the spleen and then tumour. The reticuloendothelial system plays a role in the normal immunocompetent anti-viral response so it was unsurprising to see that a systemically administered virus could be initially sequestered within the spleen. Fortunately, virus was found to subsequently reach both the B16-F1 and the 4434 tumours and, indeed, replication competent virus was confirmed through plaque assay of the tumour lysate (Figure 10). Conversely, no replication competent virus was identified from other organs confirming the tumour tropic nature of MG1.

By 48 hours post systemic viral treatment, however, it was not possible to detect virus within the tumour, either visually or following plaque assay. This could be due to the triggering of the innate immune recognition in response to virus and will be explored in the next chapter. An additional response to the virus was explored by assessing for the generation of NAbs and how this may impact on the capacity for virus to reach and be detected from the tumour. It was observed that MG1-induced NAbs were detectable within the plasma of mice from three days following systemic MG1 administration as co-culturing MG1 virus with *ex vivo* plasma was able to prevent the generation of viral plaques on subsequent plaque assay (Figure 11). In support of this, MG1-

FLUC (given five days after initial MG1-GFP) was no longer detected by bioluminescence in the spleen at six hours, or within the tumour at 18 hours (Figure 11). Obtaining this evidence, helped to determine the treatment strategy in subsequent therapy experiments.

In these studies, no evidence of improved therapy was observed with MG1 in the B16-F1 model with the use of either IV or IT therapy (Figure 12) despite being highly sensitive *in vitro*. This was consistent with previous data testing MG1 against a B16-F10 model.[323] Conversely, the IT treatment of the subcutaneous 4434 murine melanoma model with MG1, led to an improved overall survival compared to treatment with PBS (Figure 13). This is understood to be the first time that MG1 without inserted transgenes (other than those used as reporters including GFP and FLUC) and used as monotherapy has been shown to improve survival in an immunocompetent murine model of melanoma.

The explanations for the difference in outcomes between the B16-F1 model and the 4434 model could be manifold. Firstly, in terms of their inherent differences, the B16-F1 cell line is of BRAF wild-type origin whereas the 4434 model harbours a BRAF mutation. Could this render the 4434 cell line more susceptible to viral lysis *in vivo*? The data generated in chapter four suggests otherwise, in that, *in vitro* at least, the B16-F1 cell line shows more sensitivity to viral infection, replication and cytotoxicity (Figures 5, 6, 7, 8). An attempt to analyse whether this sensitivity was determined by a difference in infectivity was performed, by assessing for IVIS measurement of luminescence from both the 4434 and B16-F1 tumours following MG1-FLUC administration. Furthermore, differences in the live replicating titre obtained from each tumour type were analysed, to see if the two cell lines resulted in differing capacity for *in vivo* viral replication. No clear differences were observed through either technique, however, making an assessment had numerous limitations. These include a difference in tumour cell pigmentation between B16-F1, which produces a dark black melanin pigment, and 4434, which does not. The differing level of pigmentation could affect the observable luminescence between the two cell lines following MG1-FLUC infection. In addition, the

tumour malleability was different between the two cell lines, with B16-F1 becoming semi-solid on explantation, compared to 4434 which retained its structure. This therefore potentially resulted in differences between how much tumour material was salvaged and furthermore, results in easier homogenisation of the B16-F1 tumours (one step in the process of releasing virus into the tumour lysate) compared to the 4434 tumours. These inherent differences make cross-tumour cell comparisons difficult. The different *in vivo* sensitivity to MG1-FLUC may also be explained by differing immunological cell profiles between the two cell lines, or be due to differing anti-viral interferon responses. And finally, the rate of tumour growth may impact the tumour outcomes. It should be noted that on average, the survival time for PBS treated B16-F1 tumours was approximately 21 days, however on average, PBS treated 4434 bearing mice survived for approximately 50 days. This being despite using just $5x10^5$ B16-F1 cells for each tumour implantation compared to $4x10^6$ cells for each 4434 tumour implantation. This underlying difference in growth speed may result from reduced immune recognition and easier immune escape by the B16-F1 tumours compared to the 4434 model. Regardless of the underlying mechanism, the more aggressive nature of B16-F1 may well have ensured that the action of MG1 virus was insufficient compared to the slower growing 4434 tumour, thereby making any like-for-like comparison of B16-F1 and 4434 tumours fraught with limitations.

In the 4434 model, we showed that treatment with MG1-FLUC can extend the overall survival compared to treatment with PBS. This held true for the smallest, medium and largest tumour sizes tested. However, the success of treatment, if measured by comparing the mOS or the number of mice achieving long-term cures, clearly shows it to be advantageous to treat the tumours at an earlier stage. In the same way as cross-trial data should not be compared from different clinical trials, the same should be said for the inherent error in comparing these three different murine experiments. Nevertheless, it would seem that a correlation exists between the size of tumour at the point of commencing treatment and the subsequent outcome.

This may be a result of the predominant mechanism of action of MG1 acting with oncolytic effects as opposed to any anti-tumour immunological effects that may be generated. To analyse this, a comparison of the levels of MG1 replication in small, medium and large tumours would be warranted. An equally possible explanation is that the MG1 initiated anti-tumoural T cell response generated at the earlier time point is more effective against a smaller tumour mass, or that the T cell response in smaller tumours is acting within a less immunosuppressive TME.

With this in mind, the subsequent objective was to explore the effects that MG1 could confer towards the tumour immune microenvironment, in order to understand whether, in addition to the oncolytic activity, anti-tumour immune generation plays a role in the outcome of MG1 treatment.

Chapter 6:

The Immunological Consequences of MG1 Infection

6 Chapter 6: The Immunological Consequences of MG1 Infection

6.1 Introduction

In addition to their oncolytic effects, OVs can induce both innate and adaptive anti-tumour immune responses and therefore have the potential to favourably alter the tumour immune microenvironment. In melanoma, this has been effectively demonstrated in human clinical trials that have compared tissue samples pre and post T-VEC OV treatment and illustrated an increase in $CD8^+$ T cells, an elevated IFN-γ gene expression and a raised PD-L1 protein expression.[266] MG1 has been shown to affect the innate immune system. It has been demonstrated that IV MG1 can reduce the number of lung metastases that develop following the IV administration of B16 tumour cells. The ability of MG1 to control lung metastases development was abrogated in NK cell depleted mice, indicating the importance of the role of NK cells in MG1 activity.[263] MG1 has also been shown to initiate an adaptive anti-tumour immune response. In a murine model of triple negative breast cancer, neoadjuvant MG1 exerted a protective effect against a subsequent postoperative tumour rechallenge.[330] To delineate factors which may be influencing the *in vivo* outcomes from MG1, this chapter aims to further explore the immunogenic properties of MG1 virus in melanoma. For *in vivo* experiments, this will predominantly be investigated using the 'medium' size of tumour (approximately $100mm^3$) as this size model most reliably enables analysis by avoiding the potential for the tumour to resolve too quickly or to grow too large prior to the timepoints needed for tumour analysis.

6.2 MG1 induces the release of type I interferon *in vitro*

A crucial component in the interplay between OVs and the tumoural immune response is the role of type I interferons (IFN), particularly IFN-α and IFN-β.[348] The natural immune response to viral infection is the production of interferons. The subsequent binding of interferons to their respective

receptors can trigger the induction of interferon stimulated genes (ISGs) through two recognised pathways. This can occur through the canonical 'classical' pathway that signals through the activation through phosphorylation of the JAK/STAT tyrosine kinase pathway as illustrated in Figure 14, or through signalling independent of this pathway, known as the non-canonical 'non-classical' pathway.[349] Both can limit viral propagation through the mediation of a wide range of viral functions including the degradation of viral RNA and the blocking of the translation of viral mRNA intracellular signalling.[350]

Figure 14: The Canonical IFN signalling pathway [349]

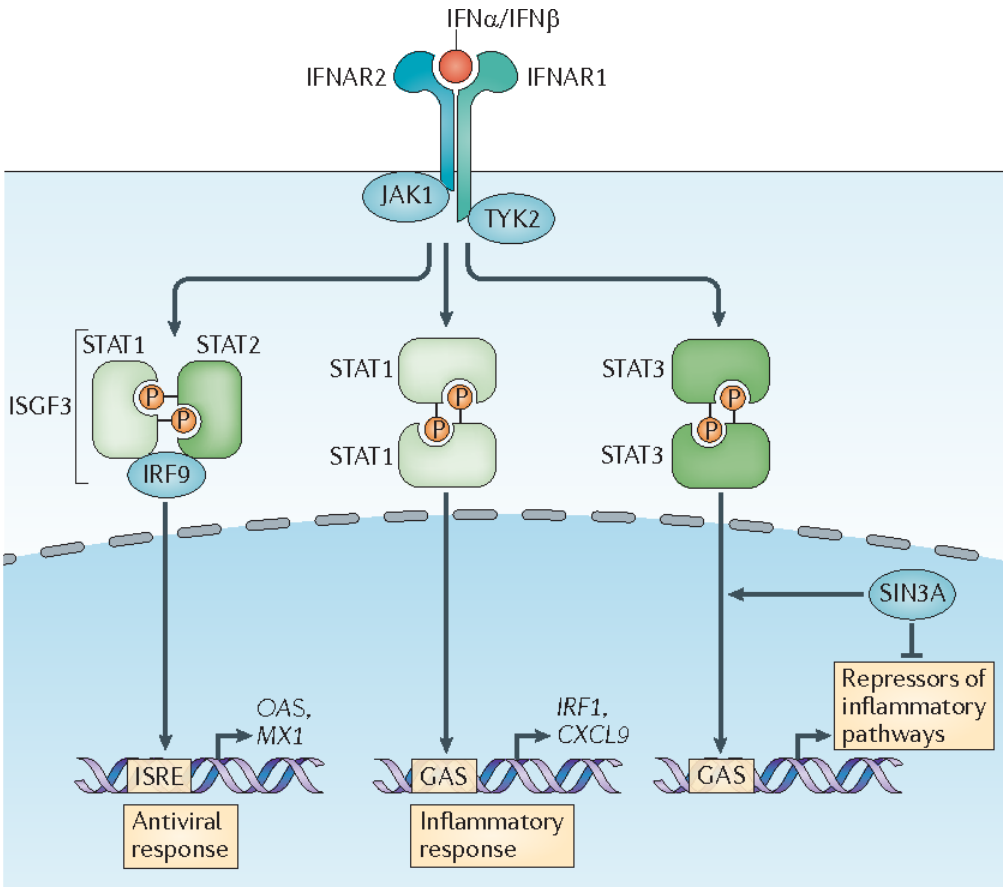

In addition to their antiviral host defence mechanisms, IFN signalling plays a significant role in inflammation and modulation of the immune TME. The production of Type I IFNs in response to OV can stimulate diverse immune cell subsets within the TME including the recruitment and cytotoxic activity of

NK cells and $CD8^+$ T cells, the secretion of pro-inflammatory cytokines by macrophages, and the cross-presentation activity of mature DCs.[348, 351]

As discussed previously, tumour cells often exhibit defective IFN signalling pathways. This feature can influence the susceptibility of the tumour cell to OV infection and replication thereby enabling the anti-tumour oncolytic effects of OVs.

To determine the capacity of MG1 to induce a type I IFN response, 4434 and B16-F1 cell lines were infected with MG1-FLUC at an MOI of 1.0 and 0.01. The supernatants were collected at eight, 24 and 48 hours following viral exposure. The samples were centrifuged to remove cellular debris and the presence of murine IFN-β was evaluated by ELISA quantification. Figure 15A shows the quantity of IFN-β released after MG1 infection compared to uninfected samples. The B16-F1 cell line showed no detectable IFN-β eight hours after viral infection. At 24 hours, 9.0 pg/mL and 31.9 pg/mL IFN-β was detected for the 0.01 and 1.0 MOI respectively. This increased further, to 23.4 pg/mL and 46.8 pg/mL by 48 hours. The 4434 cell line also showed no detectable IFN-β at the eight hour time point from the 0.01 MOI sample however 34.3 pg/mL was detected from the MOI 1.0 sample. By 24 hours, 116.1 pg/mL and 3733.7 pg/mL of IFN-β was detected which increased further to 10781.6 pg/mL and 8423.9 pg/mL respectively for the MOI 0.01 and 1.0 samples. Throughout, no IFN-β was detected from uninfected PBS control samples.

Collectively, these results show that MG1 infection stimulates the release of IFN-β from both 4434 and B16-F1 murine melanoma cell lines and that this quantity increases over time. However, at the corresponding time points and viral MOI, the quantity of IFN-β released from the 4434 cell line was markedly higher than from the B16-F1 cell line. Further sampling beyond 48 hours was not undertaken as, by this point, the majority of cells from the virally infected samples were dead. This is in keeping with the cell survival MTT data

generated in Section 4.4 which shows the high percentage of cell death by 48 hours post virus in both the 4434 and B16-F1 cell lines.

Having identified that the B16 F1 cell line release of IFN-β was notably less than from the 4434 cell line, it was considered necessary to investigate the signalling pathways involved in the B16-F1 cell line following MG1 infection. To investigate this, B16-F1 cells were infected with MG1 at an MOI of 0.001, 0.01, 0.1 and 1.0 and compared with an uninfected control. These samples were collected for western blot analysis six, 24 and 48 hours following viral exposure.

Figure 15B displays cellular pathways used to detect RNA viruses through sensing proteins including RIG-I and MDA-5. RIG-I and MDA-5 bind to the IFN-β promoter stimulator I (IPS-1) (also known as mitochondrial antiviral-signalling protein (MAVS)) on the mitochondrial outer membrane, which in turn activates (interferon regulatory factor) IRF3 and IRF7 through TRAF3, NAP1 and TBK1. IRF3 and IRF7 control the expression of type I IFNs, while NF-κB regulates the production of inflammatory cytokines. IPS-1 also interacts with FADD and RIP1 which are involved in the apoptosis pathway and the activation of the NF-κB pathway leading to the upregulation of inflammatory cytokines.[352, 353]

Figure 15C shows the western blot results for the proteins investigated including phosphorylated TBK1, phosphorylated IRF3, RIG-I and tubulin and the corresponding sample conditions. It demonstrates that the tubulin band was evident in the majority of samples but not in the 24 hour MOI 1.0 sample, or any of the samples collected at 48 hours. This suggests, or indeed confirms, that at these viral concentrations and time points, a significant proportion of cells were no longer viable, resulting in tubulin degradation and its subsequent absence on western blot detection. The viable samples demonstrated an increased expression of pTBK1 and pIRF3 compared to the uninfected control. No RIG-I protein was detected from any of the sample conditions suggesting that following MG1 viral infection, the B16-F1 cell may signal through an alternative RNA sensing protein. The limitation was that this experiment was

undertaken without a positive control and therefore limits the possible conclusions that can be drawn. However, given that RIG-I signalling has been demonstrated when using other oncolytic viruses, including reovirus, using the same antibody (data not shown) it is possible to infer that there is a lack of activity in RIG-I signalling following MG1 infection.

(A)

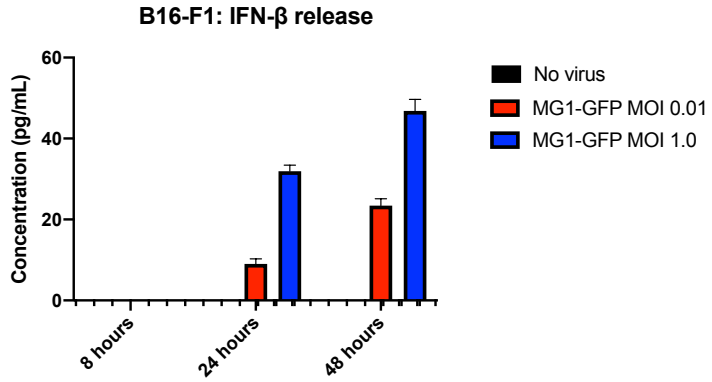
B16-F1: IFN-β release
Concentration (pg/mL)
60
40
20
0
8 hours
24 hours
48 hours
No virus
MG1-GFP MOI 0.01
MG1-GFP MOI 1.0

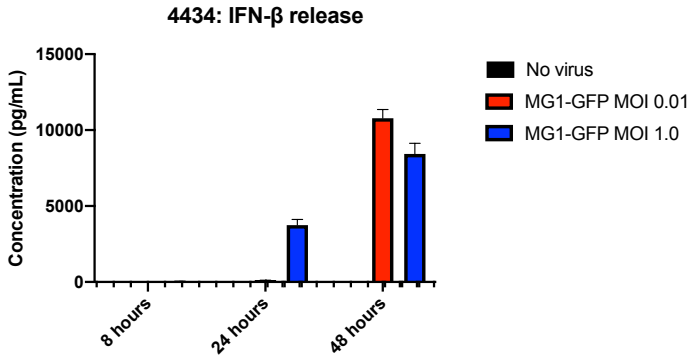
4434: IFN-β release
Concentration (pg/mL)
15000
10000
5000
0
8 hours
24 hours
48 hours
No virus
MG1-GFP MOI 0.01
MG1-GFP MOI 1.0

(B)

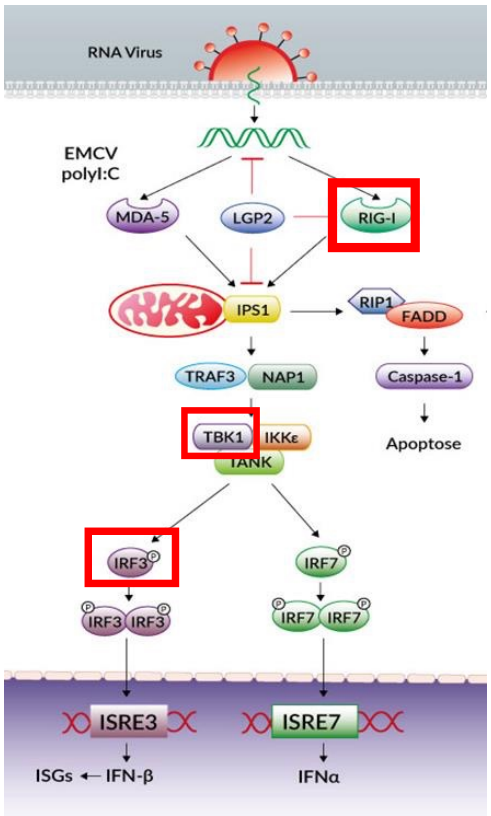
RNA Virus
EMCV
polyI:C
MDA-5
LGP2
RIG-I
IPS1
RIP1
FADD
TRAF3
NAP1
Caspase-1
TBK1
IKKε
TANK
Apoptose
IRF3
IRF7
ISRE3
ISRE7
ISGs ← IFN-β
IFNα

(C)

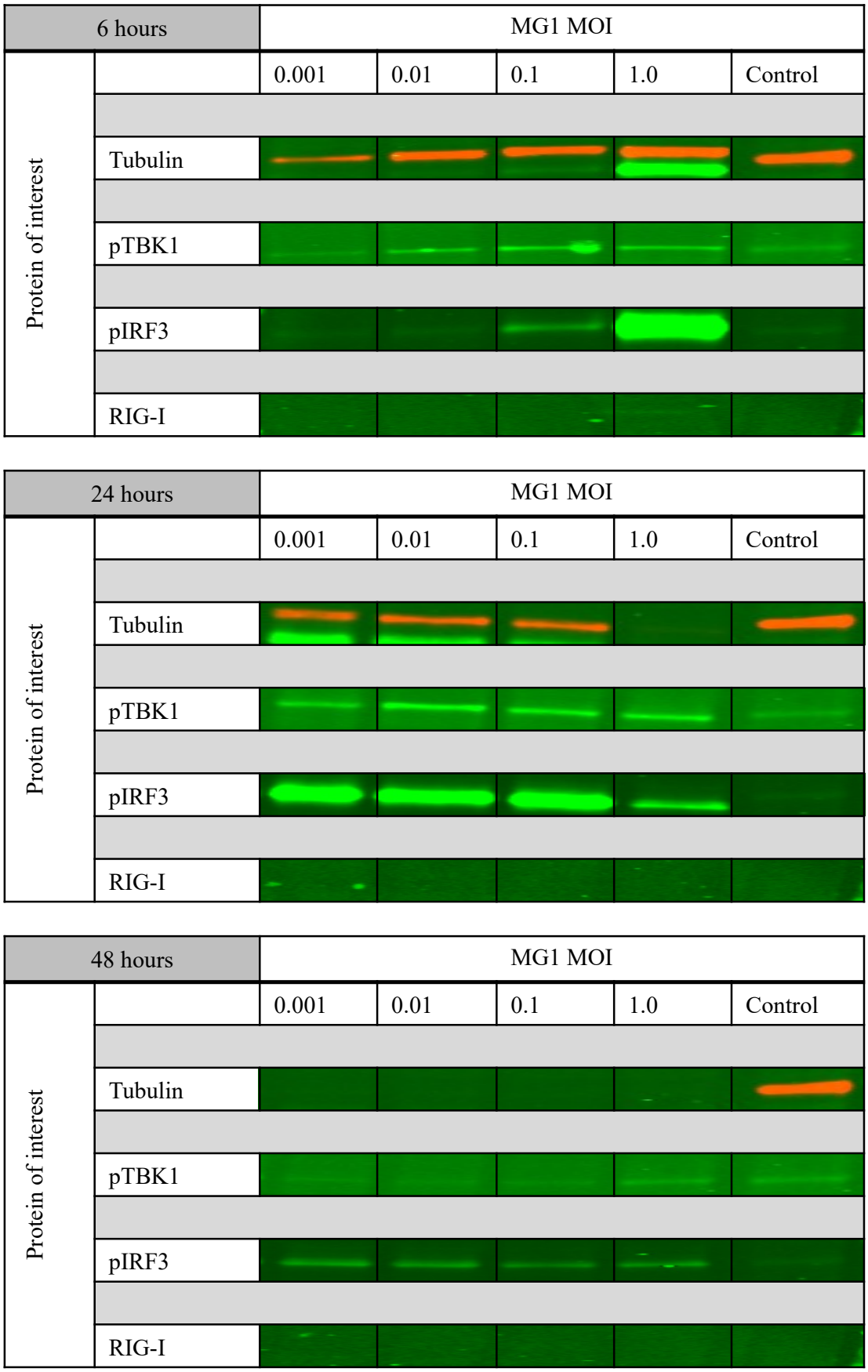
6 hours
MG1 MOI
0.001
0.01
0.1
1.0
Control
Protein of interest
Tubulin
pTBK1
pIRF3
RIG-I
24 hours
MG1 MOI
0.001
0.01
0.1
1.0
Control
Protein of interest
Tubulin
pTBK1
pIRF3
RIG-I
48 hours
MG1 MOI
0.001
0.01
0.1
1.0
Control
Protein of interest
Tubulin
pTBK1
pIRF3
RIG-I

Figure 15: MG1 infection results in IFN-β secretion from the 4434 and B16-F1 murine melanoma cell lines; and stimulates the expression of pTBK1 and pIRF3 from the B16-F1 cell line

Bar chart showing concentration of IFN-β detected via ELISA from supernatants of 4434 and B16-F1 cells infected with MG1-GFP MOI 0.1 for eight, 24 and 48 hours. Data presented are the mean plus SD of three independent experiments (A). Type I IFN signalling pathway for RNA viruses. Red boxes highlight the proteins of interest tested for in subsequent western blot experiment. Figure adapted from: Invivogen. RIG-I-Like receptors & cytosolic DNA sensors; 2012 [353] (B). Western blot analysis from B16-F1 cells of upstream proteins involved in Type I IFN signalling (pTBK1, pIRF3 and RIG-I) after infection with MG1-GFP at a range of MOI from 0.001 to 1.0 or uninfected PBS control. No positive control used. Samples collected over various time points including six, 24 and 48 hours (C).

6.3 Interferon protects melanoma cell lines from the cytotoxic effect of MG1 *in vitro*

The experiments above have demonstrated that MG1 can result in the release of IFN-β from both B16-F1 and 4434 melanoma cells *in vitro*, albeit at varying levels. Knowing that IFN-β is involved in host defence mechanisms against viral infection, the next objective was to ascertain what effect IFN-β would have on the sensitivity of melanoma cells to MG1 cytotoxicity.

To investigate this, 4434 and B16-F1 cells were infected with MG1 MOI of 0.1 or PBS control, and after 24 hours, the supernatants were collected, and a plaque assay performed to ascertain the supernatant viral titre. In order to remove progeny viruses from the sample, half of the supernatant was centrifuged through a 100 kDa filter unit (Thermo Fisher). An MTT assay was conducted using the filtered and unfiltered media to ensure that the filtration process had successfully removed progeny virus. Figure 16A shows that 24 hours after co-culturing either 4434 or B16-F1 cells with unfiltered media, there is a significant reduction in the proportion of surviving cells, when compared to both the filtered media and PBS control, indicating that the filtration process successfully removed MG1. 4434 and B16-F1 cells were then co-cultured with either the 4434 or B16-F1 supernatant conditioned media or PBS control for 24 hours prior to infecting with MG1 at an MOI of 0.1. After a further 24 hours, an MTT assay was performed on these samples. Figure 16B shows that pre-exposing the B16-F1 cells to the 4434 conditioned media confers a protective effect which mitigates the cytotoxic effects of subsequent MG1 infection. This effect of the 4434 conditioned media is also evident, but to a lesser extent, in protecting the 4434 cell line against viral exposure. However, pre-exposing B16-F1 or 4434 cells to the B16-F1 conditioned media does not lead to the same protective effect. These data suggest that components of the 4434 conditioned media are able to protect the cell lines, whereas the B16-F1 conditioned media is not. Due to the higher concentration of IFN released from MG1 infected 4434 cells it was postulated that this higher IFN-β level in the 4434 conditioned media was a protective factor against subsequent viral infection, while the levels in B16-F1 conditioned media (100-fold lower) were

insufficient to protect against viral infection. This protective effect is more notable in the B16-F1 cell line compared to the 4434 cell line ($p=0.0137$) therefore suggesting that the B16-F1 cell line is particularly responsive to IFN-β and hence, better able to attenuate the cytotoxic effects of MG1.

To ascertain whether IFN-β was indeed protecting against subsequent viral infection, 4434 and B16-F1 cells were pre-exposed to three different concentrations of exogenous IFN-β (20, 200 and 2000 pg/mL) for 24 hours prior to MG1 MOI 0.1 viral infection. After a further 24 hours, an MTT assay was performed. Figure 16C illustrates the protective effect of IFN-β, as MG1 was unable to kill B16-F1 cells that have been pre-exposed to IFN-β at all the concentrations investigated. With regards to the 4434 cells, at a concentration of 200 pg/mL IFN-β protective effects against subsequent MG1 infection can be observed. However, when this concentration is reduced to 20 pg/mL this effect is lost. If the concentration is increased to 2000 pg/mL, then the exogenous IFN-β itself compromises the cell survival regardless of the subsequent administration of virus.

(A)

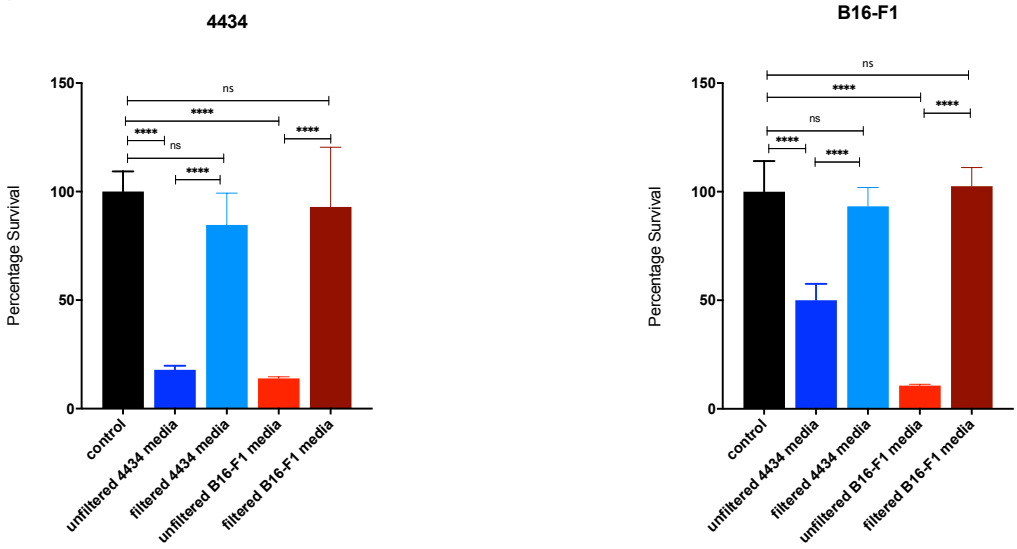
4434
B16-F1
Percentage Survival
150
100
50
0
ns
****
control
unfiltered 4434 media
filtered 4434 media
unfiltered B16-F1 media
filtered B16-F1 media

(B)

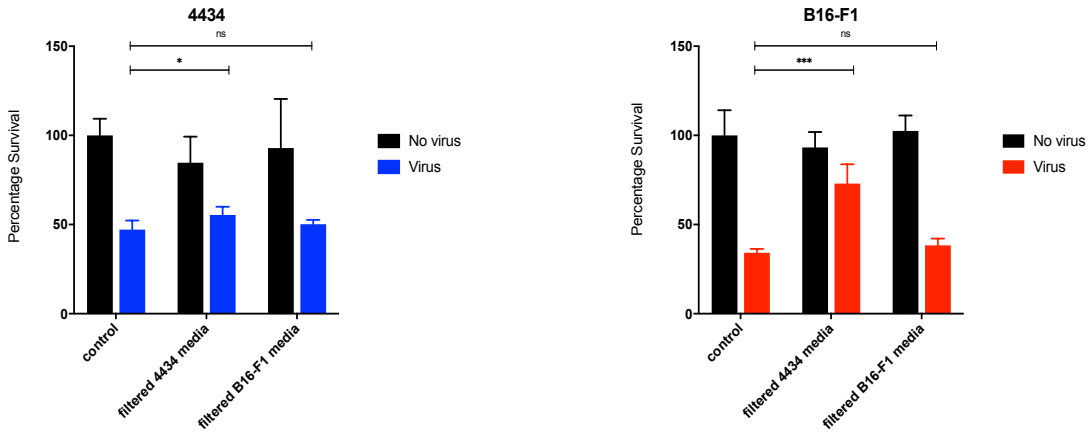
4434
B16-F1
Percentage Survival
150
100
50
0
ns
*
***
control
filtered 4434 media
filtered B16-F1 media
No virus
Virus

(C)

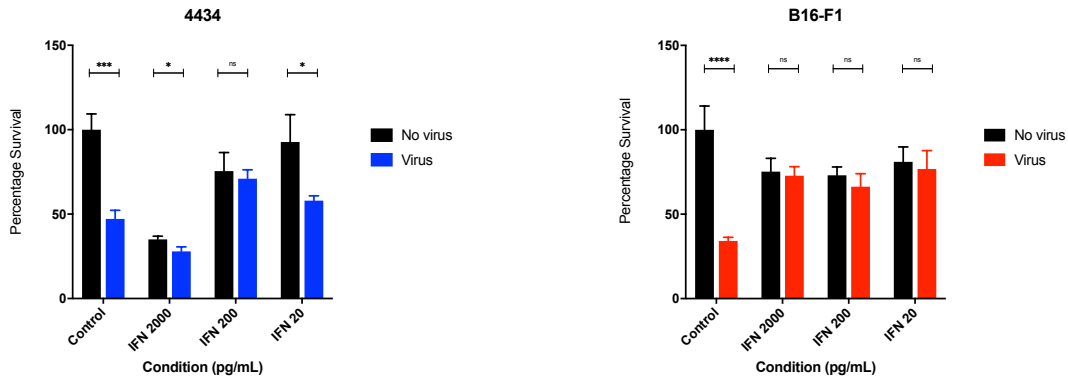
4434
B16-F1
Percentage Survival
150
100
50
0
***
*
ns
****
Control
IFN 2000
IFN 200
IFN 20
Condition (pg/mL)
No virus
Virus

Figure 16: The protective anti-viral effects of IFN-β in murine melanoma cell lines

MTT assay to determine viability of 4434 and B16-F1 cell lines co-cultured with filtered or unfiltered supernatants obtained from either infected 4434 or B16-F1 cells. Filtering infected supernatant medium through a 100 kDa filter system removes MG1 thereby preventing cytotoxicity when compared to unfiltered medium and PBS control (A). MTT assay to determine viability of 4434 and B16-F1 cell lines infected with MG1-GFP MOI 0.1, cell lines having been previously co-cultured with either 4434 or B16-F1 filtered supernatants. 4434 filtered supernatant mitigates the cytotoxic effects of MG1-GFP on both 4434 and B16-F1 cells, compared to B16-F1 filtered media which is no better than PBS (B). MTT assay to determine viability of 4434 and B16-F1 cells infected with MG1-GFP MOI 0.1 following co-culture with different concentrations of IFN-β or PBS control (C). Bar charts in each case present the mean plus SD of three independent experiments. Paired student t-test statistical analysis.

6.4 MG1 induces the release of type I interferon *in vivo*

Having identified that MG1 can lead to IFN-β release *in vitro*, the effects of MG1 on IFN-β release were explored *in vivo*. This was considered important as, compared to *in vitro*, IFN-β could be released from other cells including immune cells and connective tissue within the TME in response to MG1, not only from the tumour cells themselves. To investigate this, 4434 and B16-F1 subcutaneous tumours were implanted in the right flank of C57/Bl6 mice. 10 days post-implantation, MG1 at a dose of $1x10^7$ pfu/mL, or PBS control, was delivered by IT injection and the tumours explanted at either 24, 48 or 72 hours following viral treatment. Each time point utilised five mice. The tumours were weighed, homogenised and tumour lysates analysed by ELISA for the presence of IFN-β. Figure 17 shows the concentration of IFN-β per gram of tumour obtained for each condition at each time point. The B16-F1 tumours secreted more IFN-β following MG1 treatment at all time points compared with PBS with a significant difference at the 24 hour point. The 4434 tumours did not demonstrate any significant difference in the concentration of IFN-β released whether the tumour had been treated with MG1 or PBS.

In summary, the *in vitro* results indicate that the murine melanoma cell lines can produce IFN-β and also respond to exogenous IFN-β, with differing responses between the B16-F1 and 4434 cell lines. However, *in vivo*, when considering the TME as a whole, the difference in levels of IFN-β produced by the two cell lines appears to be inversely correlated with the *in vitro* results. This may contribute in part to the differences in the observed therapeutic efficacy of MG1 *in vivo* as seen in Chapter 5. Given the influence of Type I IFN on tumour immunogenicity and immune cell recruitment, the next approach was to assess whether MG1 could induce the production of other markers involved in immune recruitment and to stimulate immunogenic cell death (ICD).

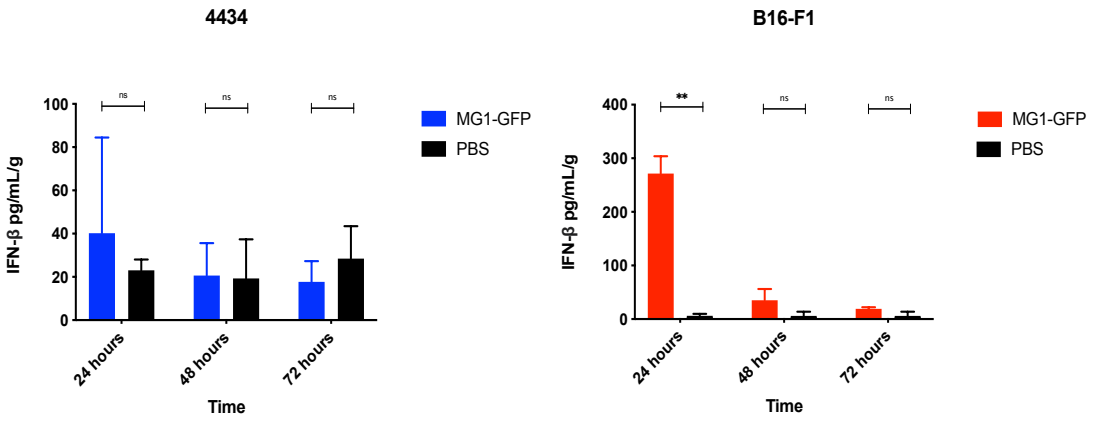

Figure 17: MG1 infection and the detection of IFN-β from 4434 and B16-F1 tumours *in vivo*

4434 and B16-F1 tumour bearing mice were injected with IT MG1-GFP 1x10^{7} pfu or PBS control. Tumours were explanted at 24, 48 or 72 hours, homogenised and lysates analysed by ELISA for the presence of IFN-β. Bar charts display mean plus SD. Multiple t-test statistical analysis corrected for multi-comparison using Holme-Sidak method.

6.5 MG1 induces immunogenic cell death (ICD)

The ICD of tumour cells represents a functionally unique response pattern that arises following the induction of cellular stress, and culminates with cell death accompanied by the exposure, active secretion, or passive release of numerous damage associated molecular patterns (DAMPs). The release of DAMPs in the course of ICD and the binding of DAMPs to specific pattern recognition receptors (PRRs) expressed by DCs initiates a cellular cascade that ultimately results in the activation of both innate and adaptive immune responses.[354]

ICD can be induced by different stressors including conventional chemotherapy and radiotherapy. In addition, intracellular pathogens can induce ICD and therefore, there is particular interest in the potential for OVs to trigger tumour cell ICD, thereby generating an anti-tumour immune response.[355, 356]

In addition to the synthesis of type I IFNs discussed previously, other DAMPs can indicate the activation of ICD. These include the endoplasmic reticulum (ER) chaperones including calreticulin (CALR) and heat-shock proteins (HSPs), which are exposed on the cell surface. These then act as an “eat-me” signal, facilitating the engulfment of dying cells by DCs, thus providing the DCs with antigenic material for presentation. In addition, the non-histone chromatin-binding protein high-mobility group box 1 (HMGB1), the cytoplasmic protein annexin A1 (ANXA1), and the small metabolite ATP are released from dying cells into the extracellular space. Extracellular ATP operates as a prominent “find-me” signal for DCs and macrophages. In short, DAMPs can be recognised by both the innate and adaptive immune systems via distinct PRRs, resulting in the chemoattraction and activation of immune cells, ultimately resulting in the cross-presentation of tumour antigens to $CD8^+$ T cells.[354, 357]

Having previously identified that type I IFN is released from melanoma cells following MG1 infection, two further markers of ICD were investigated.

Firstly, to assess for the release of HMGB1, 4434 and B16-F1 cell lines were infected with MG1-GFP at an MOI of 0.1, or PBS control. The supernatants were collected 24 and 48 hours following infection, centrifuged to remove cellular debris before analysing the concentration of HMGB1 by ELISA. Figure 18A demonstrates that compared to control, MG1 infection leads to the statistically significant release of HMGB1 from both the 4434 and B16-F1 cell lines. This occurred at both the 24 and 48 hour time points. For both cell lines, the maximum mean HMGB1 concentration occurred 48 hours following viral treatment. Of note, the 4434 cell line resulted in a higher quantity of HMGB1 release when compared to the B16-F1 cell line, both at 24 and 48 hours, albeit that the baseline from the uninfected control samples was also higher in the 4434 group.

Following this, the 4434 and B16-F1 cell lines were evaluated for the release of ATP. The cells were infected with MG1-GFP at a dose of either MOI 0.01, 1.0 or uninfected PBS control. The cells were infected for either 24 or 48 hours and at each point the supernatants were collected and centrifuged prior to being analysed for ATP using the CellTiter-Glo® Luminescent Assay. The addition of the reagent results in cell lysis and generation of a luminescent signal which is proportional to the amount of ATP present. Figure 18B demonstrates that in the B16-F1 cell line, levels of ATP were significantly increased compared to control, at both the 24 and 48 hour time points and at both viral concentrations (at 24 hours, MOI 0.01 vs PBS $p=0.0012$, MOI 1.0 vs PBS $p=0.003$; at 48 hours, MOI 0.01 vs PBS $p=0.004$, MOI 1.0 vs PBS $p=0.018$). Regarding the 4434 cell line, a significant increase was observed with an MOI of 1.0 at 24 hours ($p=0.04$) and with an MOI of 0.01 at 48 hours ($p=0.019$). Despite a clear trend towards increased ATP release at 24 hours following MOI 0.01, this did not reach significance ($p=0.17$), however, this may be due to the lower cytotoxicity of MG1-GFP MOI 0.01 towards the 4434 cell line compared to B16-F1 as shown in Figure 8. Furthermore, significance was not reached at 48 hours with an MOI of 1.0 ($p=0.12$) and this is likely due to many cells already having been killed thus reducing their capacity to secrete further ATP. This is corroborated with the B16-F1 cell line results which, albeit

that it retains significance, also shows a reduction in ATP levels between the 48 hour MOI 0.01 and MOI 1.0 results.

In summary, these results demonstrate that MG1 acting on murine melanoma cell lines can stimulate the release of HMGB1, ATP and Type I IFN. Whilst further markers could be investigated, collectively this strongly suggests that MG1 can induce a pattern of immunogenic cell death.

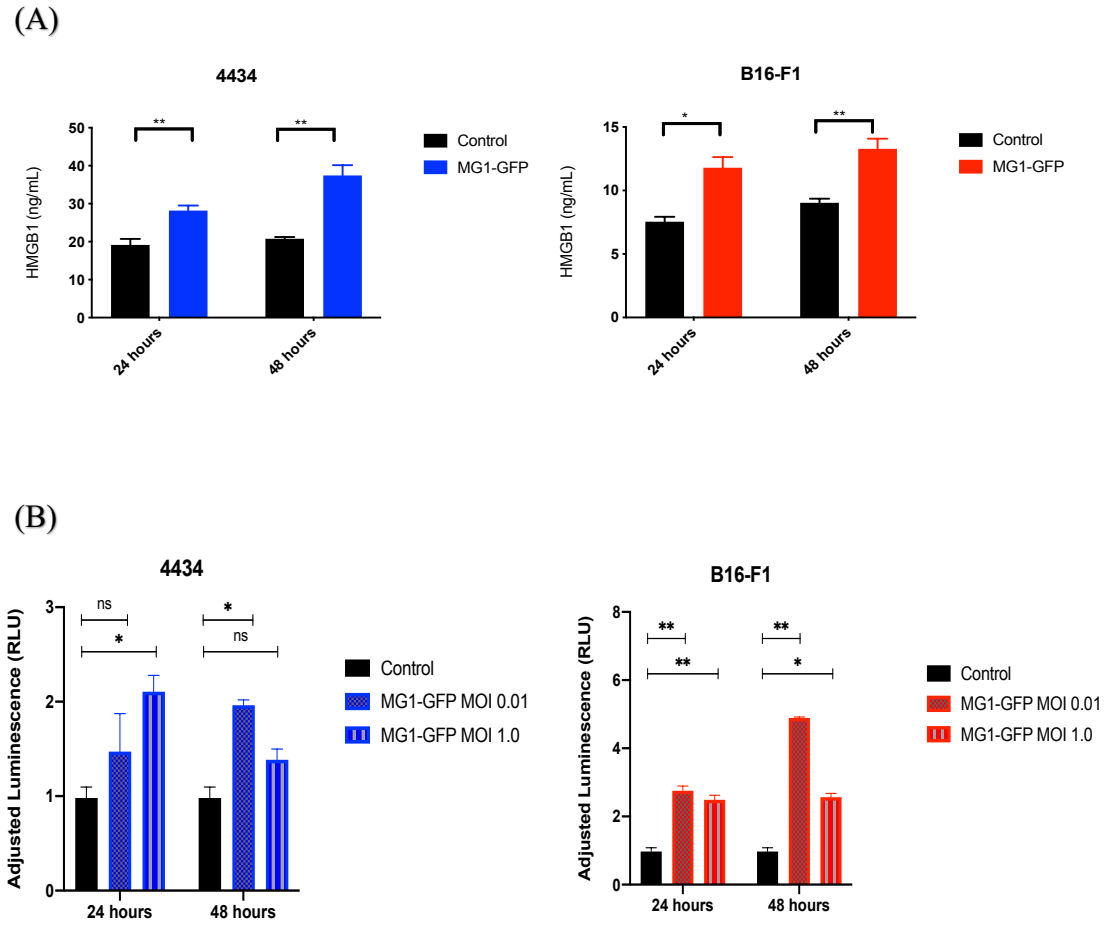

Figure 18: MG1 infection induces HMGB1 and ATP release from murine melanoma cell lines

Graph showing the concentration of HMGB1 within the supernatant of 4434 and B16-F1 cells infected with MG1 MOI 0.1 for 24 and 48 hours, as measured by ELISA. Mean plus SD displayed from three independent experiments using paired t-test statistical analysis (A). Bar chart demonstrating adjusted luminescence (RLU), which correlates with ATP quantity, following infection with MG1 MOI 0.01 or 1.0 or PBS control in 4434 and B16-F1 cell lines at either 24 and 48 hours (B). Mean plus SD of three independent experiments plotted using paired t-test statistical analysis.

6.6 MG1 modulates cytokine expression *in vivo*

The previous investigations identified that MG1 can generate components involved in an ICD response. In order to more broadly evaluate the effects of MG1 on immunological signals, an exploration of tumour cytokine secretion was conducted. Given the different survival outcomes observed *in vivo* (Figure 13), this cytokine evaluation was conducted in both small and large tumours treated with either PBS control or MG1, in order to try and identify factors which may be influencing the therapeutic survival results.

Cytokines are a general category of signalling molecules that are particularly associated with their role in modulating the immune system including the balance between humoural and cellular immune responses in addition to the regulation, maturation, expansion and responsiveness of particular immune cell populations.

With regards to MG1, it has been shown in breast cancer models that MG1 induces the cytokines CCL5 and CXCL11 and that these can enhance the migration of splenocyte immune cells through chemotaxis.[330] Furthermore, through experiments using a recombinant MG1 encoded to express the cytokine IL-12 (MG1-IL12), it has been shown that MG1-IL12 can upregulate IFN-γ and the cytokine CXCL10, thereby playing a role in enhancing NK cell activation. Moreover, MG1-IL12 has been shown to improve the outcome in murine models of peritoneal carcinomatosis.[321]

To assess the effect of MG1 on cytokine production *in vivo*, subcutaneous 4434 tumours were implanted prior to treatment on day 10 (small tumours) or 21 (large tumours) with MG1-FLUC or PBS control. After 48 hours, samples were collected and homogenised and the consequent *ex vivo* tumour lysates were processed in duplicate on a cytokine antibody array membrane (Section 3.9.2).

Figure 19A shows a heat map which includes the cytokines and their associated fold change in enrichment between small tumours treated with

MG1 or those treated with PBS. Among those cytokines which were more enriched in the MG1 treatment sample include CD257, a potent B cell recruitment and activation cytokine.[358] In addition, the monocyte chemoattractant CCL2 and the neutrophil chemoattractants CXCL1, CXCL2 and CXCL5 were elevated. Furthermore, the RAGE receptor was elevated with MG-1 treatment; this receptor has an inflammatory function in innate immunity and HMGB1 is an agonist ligand of RAGE, thereby further validating the findings of increased MG1 related ICD and immune modulation.[359] CCL5 (also known as RANTES) was elevated and is a marker of inflammation and involved in the recruitment of leukocytes and the proliferation and activation of NK cells.[360] With regards to other lymphocyte chemoattractant cytokines, CCL20 was elevated, in addition to IL-17, a proinflammatory cytokine which is released from activated T cells.[361]

CXCL9, and its closely related cytokines CXCL10 and CXCL11, also increased with MG1 treatment. These cytokines are involved in stimulating immune cells through Th1 polarization and activation which in turn leads to Th1 cell production of IFN-γ, TNF-α and IL-1 and enhanced anti-tumour immunity through the stimulation of CTLs, NK cells and macrophages.[362, 363]

Finally, IL-12 was elevated which plays a wide and important role in the growth and function of T cells. This includes the stimulation of IFN-γ and TNF-α from T cells and NK cells, the reduction of IL-4 mediated suppression of IFN-γ.[364] The increased production of IFN-γ, which was also identified in the MG1 treated sample, increases CXCL10 levels which also enables IL-12 to have an anti-angiogenic effect. In addition, IL-12 can enhance the cytotoxic activity of NK cells and $CD8^+$ T cells.[364]

Conversely, the most notable cytokines showing a decrease in enrichment between the small PBS and MG1 treated tumours include CCL17 which is involved in the recruitment of $CD4^+$ T cells to tumours, including T regs.[365] In addition, fibroblast growth factor-1 (FGF-1) reduced. This is involved in crosstalk among angiogenesis, inflammation and tumour growth, and

contributes to tumour progression.[366] Other agents promoting tumour angiogenesis, including VEGF and endoglin, were also notably reduced in the MG1 treated sample.

Whilst this is a broad evaluation and would need validating further, it does suggest that, when compared with PBS control, MG1 can lead to the enrichment of certain cytokines involved in regulating aspects of both the innate and adaptive immune system from aspects of the myeloid and lymphoid systems. In addition, some cytokines involved in immunosuppression, angiogenesis and tumour proliferation decreased in the MG1 treated tumour compared to PBS.

As displayed in Chapter 5, MG1 was able to successfully treat the majority of small 4434 tumours leading to long term survival and immune protection against tumour rechallenge (Figure 13C). However, no mice bearing larger tumours were cured with MG1 alone (Figure 13E). Therefore, differences in cytokine changes between the small and large MG1 treated tumours were also assessed to evaluate for factors which may have been contributing to these differences in MG1 efficacy (Figure 19B).

Among those cytokines which were more enriched in the larger tumours includes angiopoietin 1 and 2, endoglin and VEGF which are necessary for angiogenesis within the growing tumour.[367] Also amplified was the release of matrix metalloproteinase-3 (MMP-3) and periostin, factors involved in the breakdown of the extracellular matrix and the epithelial-mesenchymal transition, thereby enabling the growth and spread of tumours.[368] In addition, CCL17 was elevated which has been associated with both the recruitment of Tregs to the tumour and also the activation of infiltrating lymphocytes.[365] The costimulatory protein CD40 was increased and is involved in APC activation.[369] Finally, the immune signalling cytokine IL-2 was elevated.[370]

Conversely, the larger MG1 treated tumour showed a decrease in IFN-γ and IL-12 enrichment compared to the smaller MG1 treated tumour. In addition,

IL-15, which has been shown to enhance the anti-tumour immunity of $CD8^+$ T cells, was reduced.[371] Other interleukins including IL-17 and IL-22 (part of the IL-10 superfamily) also decreased, and are involved in generating an immunosuppressive TME and promoting tumour growth.[361] Furthermore, the neutrophil chemoattractants CXCL1, CXCL2, CXCL5 and G-CSF were reduced, as was the monocyte chemoattractant CCL2 and the DC growth stimulator Flt3 ligand.

Despite the caveat that this evaluation is a broad assessment of the release of many cytokines, it does indicate the changing microenvironment between smaller and larger tumours, particularly regarding factors involved in angiogenesis and connective tissue remodelling that are necessary for the growth and spread of the evolving cancer. In addition, these factors are associated with an immunosuppressive TME. This is supported by the decreased levels, in the larger tumour, of IFN-γ and IL-12 which exert anti-tumoural immune effects and therefore, may play a role in reducing the effectiveness of MG1 monotherapy in larger tumours compared to smaller tumours.

(A)

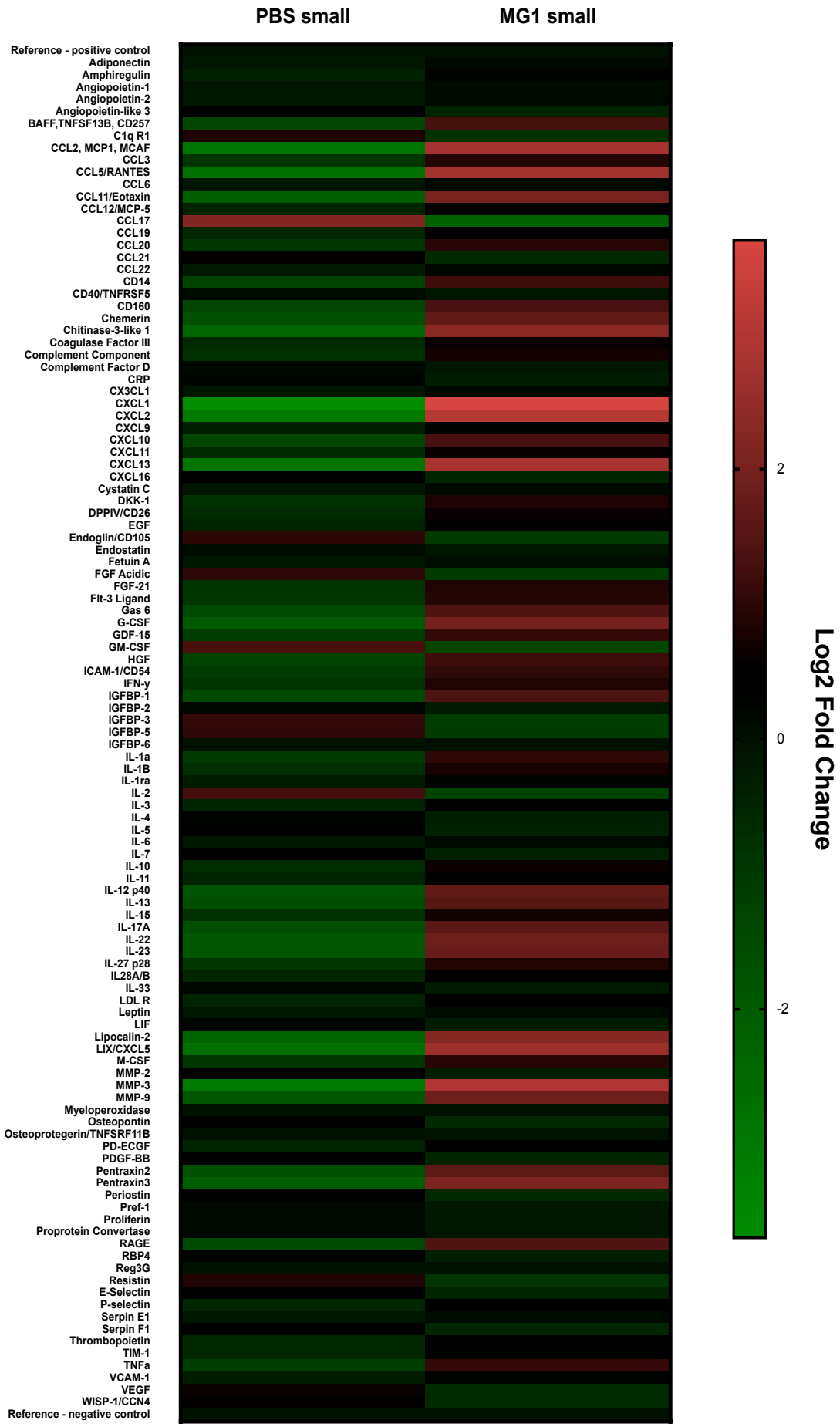
PBS small
MG1 small
Reference - positive control
Adiponectin
Amphiregulin
Angiopoietin-1
Angiopoietin-2
Angiopoietin-like 3
BAFF,TNFSF13B, CD257
C1q R1
CCL2, MCP1, MCAF
CCL3
CCL5/RANTES
CCL6
CCL11/Eotaxin
CCL12/MCP-5
CCL17
CCL19
CCL20
CCL21
CCL22
CD14
CD40/TNFRSF5
CD160
Chemerin
Chitinase-3-like 1
Coagulase Factor III
Complement Component
Complement Factor D
CRP
CX3CL1
CXCL1
CXCL2
CXCL9
CXCL10
CXCL11
CXCL13
CXCL16
Cystatin C
DKK-1
DPPIV/CD26
EGF
Endoglin/CD105
Endostatin
Fetuin A
FGF Acidic
FGF-21
Flt-3 Ligand
Gas 6
G-CSF
GDF-15
GM-CSF
HGF
ICAM-1/CD54
IFN-y
IGFBP-1
IGFBP-2
IGFBP-3
IGFBP-5
IGFBP-6
IL-1a
IL-1B
IL-1ra
IL-2
IL-3
IL-4
IL-5
IL-6
IL-7
IL-10
IL-11
IL-12 p40
IL-13
IL-15
IL-17A
IL-22
IL-23
IL-27 p28
IL28A/B
IL-33
LDL R
Leptin
LIF
Lipocalin-2
LIX/CXCL5
M-CSF
MMP-2
MMP-3
MMP-9
Myeloperoxidase
Osteopontin
Osteoprotegerin/TNFSRF11B
PD-ECGF
PDGF-BB
Pentraxin2
Pentraxin3
Periostin
Pref-1
Proliferin
Proprotein Convertase
RAGE
RBP4
Reg3G
Resistin
E-Selectin
P-selectin
Serpin E1
Serpin F1
Thrombopoietin
TIM-1
TNFa
VCAM-1
VEGF
WISP-1/CCN4
Reference - negative control
2
0
-2
Log2 Fold Change

(B)

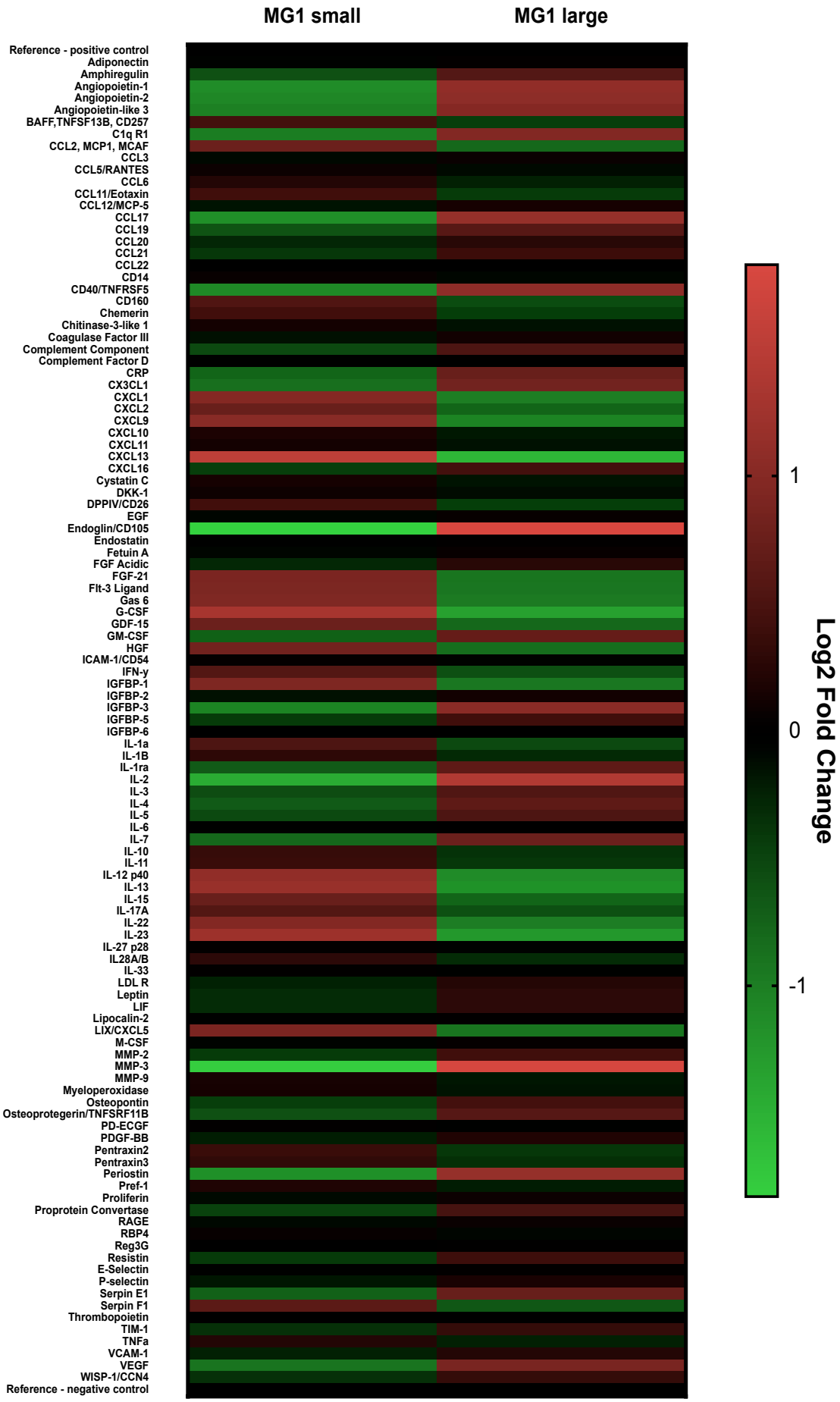
MG1 small
MG1 large
Reference - positive control
Adiponectin
Amphiregulin
Angiopoietin-1
Angiopoietin-2
Angiopoietin-like 3
BAFF,TNFSF13B, CD257
C1q R1
CCL2, MCP1, MCAF
CCL3
CCL5/RANTES
CCL6
CCL11/Eotaxin
CCL12/MCP-5
CCL17
CCL19
CCL20
CCL21
CCL22
CD14
CD40/TNFRSF5
CD160
Chemerin
Chitinase-3-like 1
Coagulase Factor III
Complement Component
Complement Factor D
CRP
CX3CL1
CXCL1
CXCL2
CXCL9
CXCL10
CXCL11
CXCL13
CXCL16
Cystatin C
DKK-1
DPPIV/CD26
EGF
Endoglin/CD105
Endostatin
Fetuin A
FGF Acidic
FGF-21
Flt-3 Ligand
Gas 6
G-CSF
GDF-15
GM-CSF
HGF
ICAM-1/CD54
IFN-y
IGFBP-1
IGFBP-2
IGFBP-3
IGFBP-5
IGFBP-6
IL-1a
IL-1B
IL-1ra
IL-2
IL-3
IL-4
IL-5
IL-6
IL-7
IL-10
IL-11
IL-12 p40
IL-13
IL-15
IL-17A
IL-22
IL-23
IL-27 p28
IL28A/B
IL-33
LDL R
Leptin
LIF
Lipocalin-2
LIX/CXCL5
M-CSF
MMP-2
MMP-3
MMP-9
Myeloperoxidase
Osteopontin
Osteoprotegerin/TNFSRF11B
PD-ECGF
PDGF-BB
Pentraxin2
Pentraxin3
Periostin
Pref-1
Proliferin
Proprotein Convertase
RAGE
RBP4
Reg3G
Resistin
E-Selectin
P-selectin
Serpin E1
Serpin F1
Thrombopoietin
TIM-1
TNFa
VCAM-1
VEGF
WISP-1/CCN4
Reference - negative control
1
0
-1
Log2 Fold Change

Figure 19: MG1 infection alters cytokine expression within the TME in 4434 tumours

Mice bearing large and small 4434 tumours were injected with IT MG1-GFP $1x10^7$ pfu or PBS control. Tumours were explanted following 48 hours, homogenised and lysates analysed for the release of a panel of cytokines using an antibody array membrane. Results normalised to reference and fold change between groups displayed as a heat-map comparison between PBS small vs MG1 small (A) and MG1 small vs MG1 large (B).

6.7 MG1 alters the differential gene expression as evaluated by RNA quantification

In addition to assessing cytokine enrichment, an evaluation of the differential gene expression between smaller and larger PBS or MG1 treated tumours was conducted through the quantification of RNA expression in each condition. This was undertaken using RNA-Seq analysis (Section 3.9.3).

With regards to MG1, the literature reports a variation in the upregulated genes between active MG1 and UV-inactivated MG1 in two *in vitro* cell line models of TNBC, namely 4T1 and EMT6. Through gene ontology analysis, this revealed that most of the top ten enriched pathways were linked to immune responses including, cytokine receptor binding, cytokine activity, chemokine receptor binding, chemokine activity, CCR binding, GPCRs binding, dsRNA binding, RNA polymerase II activity, CXCR binding and dsDNA binding.[330]

To assess the effect of MG1 on gene expression *in vivo* (Figure 20), subcutaneous 4434 tumours were implanted prior to treatment on day 10 (small tumours) or 21 (large tumours) with MG1-FLUC or PBS control. After 48 hours, the tumours were explanted and the samples stored in RNAlater solution at -80°C before subsequent processing for RNA-Seq analysis (Section 3.9.3).

The results presented (Figure 20) assessed the differences between small tumours or large tumours treated with either PBS or MG1. Results were grouped into 11 categories of gene signature: interferon, chemoattractant, HLAs, activation, NK profile, myeloid profile, T cell, coinhibitory, costimulatory, cytokine signalling and pattern recognition receptors.

Regarding the small tumours, there was a notable overall increase in gene activation, as measured by the increased z score, between the PBS and MG1 treated samples. This was prevalent across all the gene signatures, perhaps with the exception of the myeloid markers and to a lesser extent, the cytokine signalling category. Regarding the larger tumours, MG1 led to an increased

gene expression across multiple categories, although this was arguably less evident in the HLA, myeloid and coinhibitory categories. Given the difference in MG1 efficacy *in vivo* between the treatment of small and large tumours, a comparison between the small MG1 and large MG1 treated tumours was reviewed. Relative to the large tumours, the small MG1 treated tumours showed considerably greater gene enrichment across all categories. This thereby indicates that the larger tumours display an immunologically 'colder' transcriptomic environment, and this differential response may be relevant in the understanding of why MG1 can be so effective in treating smaller tumours compared to larger tumours. It should be noted that an underlying difference in gene expression was observed between the two PBS treated groups (PBS small and PBS large).

Of interest, the RNA-Seq analysis identified an upregulation of CXCL10 in the small and large MG1 treated tumours, compared to their respective PBS treated controls. CXCL10 is secreted in response to IFN-γ and is involved in immune cell chemoattraction. This result mirrors that seen in the cytokine analysis and may point towards an MG1 driven enriched 'hotter' immune TME. In addition, the FoxP3 gene, associated with immunosuppressive Tregs was decreased in both MG1 treated cohorts compared to PBS controls, whereas CD8 gene markers were increased in both MG1 treated groups compared to PBS controls, again giving further evidence to the virally mediated generation of a more favourable immune TME.

In summary, MG1 treatment leads to an increased activation of genes involved in anti-tumour immunity in both smaller and larger tumours, when compared to PBS. Potentially this difference is greater in the smaller tumours, which could be relevant to the *in vivo* efficacy results observed previously.

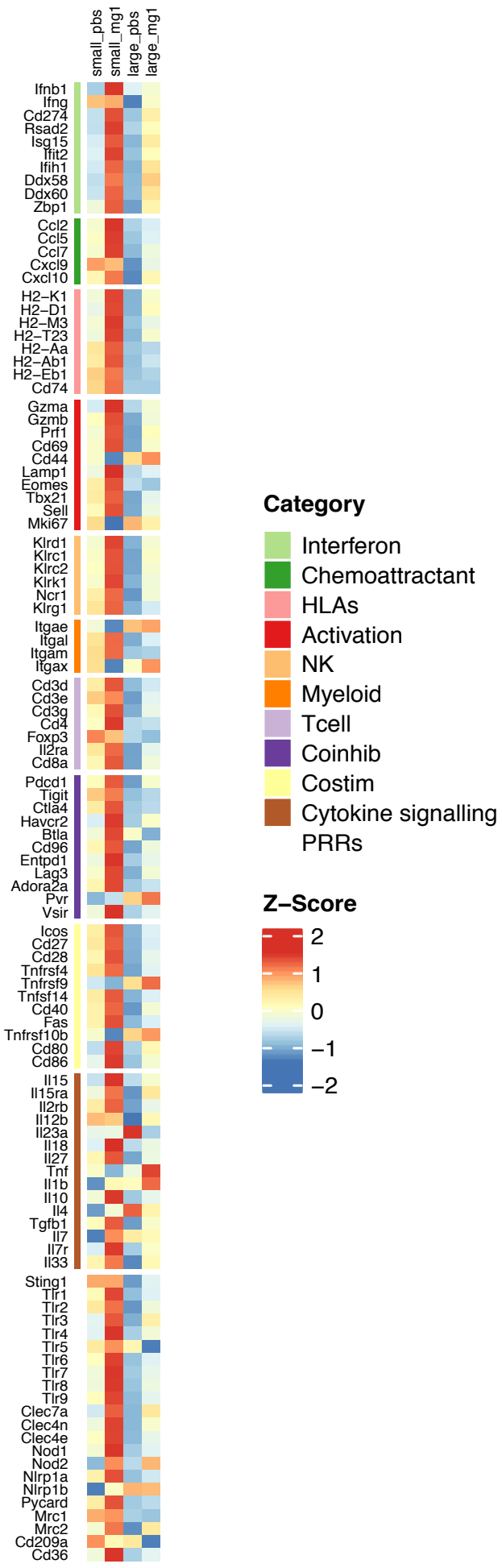
small_pbs
small_mg1
large_pbs
large_mg1
Ifnb1
Ifng
Cd274
Rsad2
Isg15
Ifit2
Ifih1
Ddx58
Ddx60
Zbp1
Ccl2
Ccl5
Ccl7
Cxcl9
Cxcl10
H2−K1
H2−D1
H2−M3
H2−T23
H2−Aa
H2−Ab1
H2−Eb1
Cd74
Gzma
Gzmb
Prf1
Cd69
Cd44
Lamp1
Eomes
Tbx21
Sell
Mki67
Klrd1
Klrc1
Klrc2
Klrk1
Ncr1
Klrg1
Itgae
Itgal
Itgam
Itgax
Cd3d
Cd3e
Cd3g
Cd4
Foxp3
Il2ra
Cd8a
Pdcd1
Tigit
Ctla4
Havcr2
Btla
Cd96
Entpd1
Lag3
Adora2a
Pvr
Vsir
Icos
Cd27
Cd28
Tnfrsf4
Tnfrsf9
Tnfsf14
Cd40
Fas
Tnfrsf10b
Cd80
Cd86
Il15
Il15ra
Il2rb
Il12b
Il23a
Il18
Il27
Tnf
Il1b
Il10
Il4
Tgfb1
Il7
Il7r
Il33
Sting1
Tlr1
Tlr2
Tlr3
Tlr4
Tlr5
Tlr6
Tlr7
Tlr8
Tlr9
Clec7a
Clec4n
Clec4e
Nod1
Nod2
Nlrp1a
Nlrp1b
Pycard
Mrc1
Mrc2
Cd209a
Cd36
Category
Interferon
Chemoattractant
HLAs
Activation
NK
Myeloid
Tcell
Coinhib
Costim
Cytokine signalling
PRRs
Z−Score
2
1
0
−1
−2

Figure 20: MG1 infection of small and large 4434 tumours alters the gene expression differential compared to PBS control

4434 tumour bearing mice were injected with IT MG1-GFP $1x10^7$ pfu or PBS control. Tumours were explanted at 48 hours, homogenised and lysates analysed for their differential gene expression profiles. Results displayed as a heat-map comparison between small and large, PBS and MG1 treated groups.

6.8 MG1 induced changes in the murine melanoma tumour immune microenvironment

Having identified that MG1 can stimulate the release of IFN-β and other cytokines involved in immunological signalling, an evaluation of the *in vivo* immunological changes occurring in a murine melanoma model was undertaken.

In a B16 model, it has previously been reported that MG1 resulted in an increase in splenic NK cells and DCs. The NK cell activation lasted up to five days post-MG1 administration and was accompanied by an enhancement of effector NKs secreting IFN-γ or granzyme B (GrzB). The selective depletion of NKs abolished tumour growth control, highlighting the importance of the acute NK cell response.[263] However, given as monotherapy, MG1 was unable to affect the survival outcome of mice with established B16 tumours (Figure 12).[323] Therefore, the 4434 murine melanoma model was examined to assess for any associated immunological changes in a tumour model in which MG1 extends survival (tumours averaging 100mm^3).

Subcutaneous 4434 tumours were implanted, and mice were randomised to treatment with IT PBS or MG1-FLUC (1x10^7 pfu). At either 48 hours or seven days post treatment, both the tumours and spleens were harvested and prepared for flow cytometry analysis. Each cohort contained six mice. The experimental schematic is shown in Figure 21A.

Viable cells were stained and phenotyped with the following markers: CD45$^+$/CD3$^-$/NK1.1$^+$ for NK cells, CD45$^+$/CD3$^+$/CD4$^+$ for helper T cells and CD45$^+$/CD3$^+$/CD8$^+$ for effector T cells. The CD3$^+$/CD4$^+$ T cells were further characterised into CD3$^+$/CD4$^+$/CD25$^+$/FoxP3$^+$ Treg cells (discussed subsequently in chapter 7). The gating strategy for flow cytometry analysis is shown in Figure 21B. These lymphocyte subsets were further stained with antibodies to detect the activation markers GrzB, CD69 and Ki67. In addition, antibodies to detect the PD-1 checkpoint protein were included.

(A)

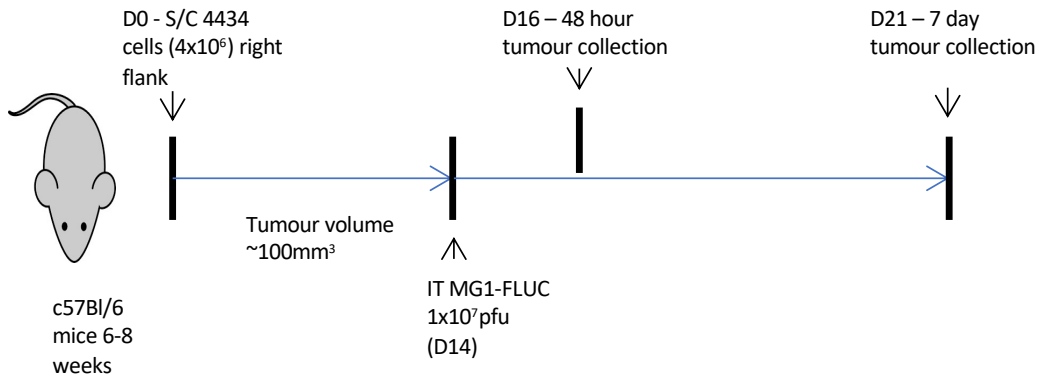
D0 - S/C 4434
cells (4x10⁶) right
flank
D16 – 48 hour
tumour collection
D21 – 7 day
tumour collection
Tumour volume
~100mm³
IT MG1-FLUC
1x10⁷pfu
(D14)
c57Bl/6
mice 6-8
weeks

(B)

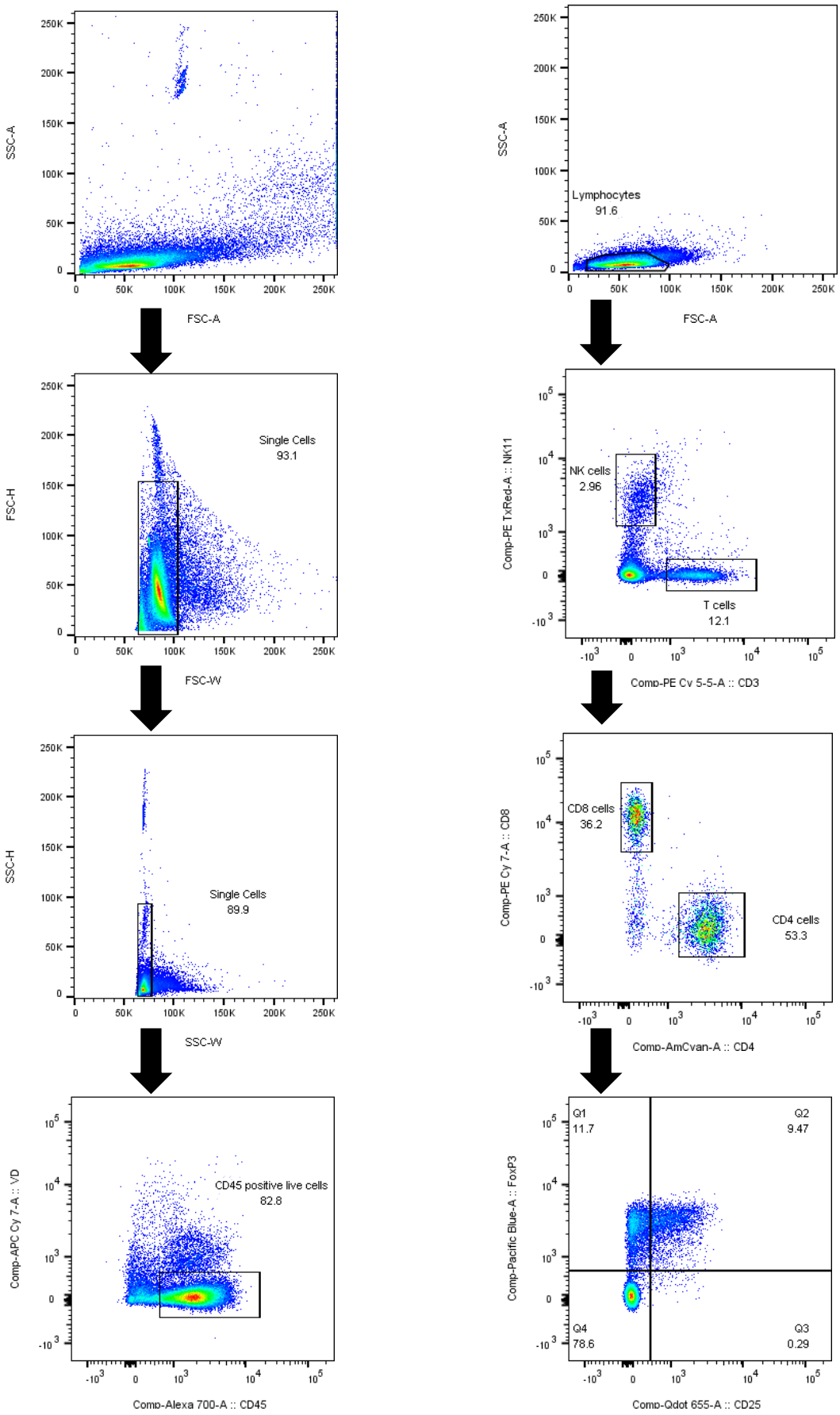
SSC-A
FSC-A
Lymphocytes
91.6
FSC-H
FSC-W
Single Cells
93.1
Comp-PE TxRed-A :: NK11
Comp-PE Cy 5-5-A :: CD3
NK cells
2.96
T cells
12.1
SSC-H
SSC-W
Single Cells
89.9
Comp-PE Cy 7-A :: CD8
Comp-AmCyan-A :: CD4
CD8 cells
36.2
CD4 cells
53.3
Comp-APC Cy 7-A :: VD
Comp-Alexa 700-A :: CD45
CD45 positive live cells
82.8
Comp-Pacific Blue-A :: FoxP3
Comp-Qdot 655-A :: CD25
Q1
11.7
Q2
9.47
Q4
78.6
Q3
0.29

Figure 21: MG1 and the tumour immune microenvironment

Schematic for in vivo experiment analysing MG1-induced immune consequences in 4434 murine model (A). Gating strategy shown by representative two-colour fluorescence dot plots identifying; all cells, single cells, $CD45^+$ live cells. These were further differentiated into $CD3^-NK1.1^+$ cells, $CD3^+CD4^+$, $CD3^+CD8^+$. $CD3^+CD4^+$ T cells were further differentiated into $CD25^+FoxP3^+$ regulatory T cells (B).

6.8.1 MG1 infection induces early immune changes in splenocytes

Figure 22A shows that, compared to PBS control, IT MG1 resulted in a significant decrease in splenic NK cells as a percentage of $CD45^+$ cells at the 48 hour time point (3.6% vs 2.1% for the PBS and MG1 treated groups respectively, p=0.0009). Despite the decrease of the NK cells overall percentage, treatment with MG1 resulted in a notable increase in splenic NK cell activation. This was demonstrated by an increase in NK cell expression of Ki67, GrzB and the early activation marker CD69 in the MG1 treated cohort compared to the PBS group. Specifically, for Ki67 the mean percentage NK cell expression increased by 14.2%, (p=0.0002). For GrzB, the mean percentage NK cell expression increased by 15.6%, (p=0.0051). Finally, the NK cell CD69 expression increased by 27.1% (1.9% to 29.0%) between the PBS group and the MG1 cohort respectively (p=0.0003).

With regards to $CD8^+$ cells, Figure 22B demonstrates the significantly lower splenocyte $CD8^+$ T cells as a percentage of $CD45^+$ cells in the MG1 group as compared to PBS control (2.95% of live $CD45^+$ cell population with MG1, 6.82% with PBS, p=<0.0001) at the 48 hour timepoint. However, despite this reduction, splenocyte $CD8^+$ T cells were found to be more activated in the MG1 cohort compared with the PBS group as CD69 expression was increased by 27% (p=<0.0001), GrzB increased by 6% (p=0.0002) and Ki67 expression increased by 10.7% (p=0.0025).

(A)

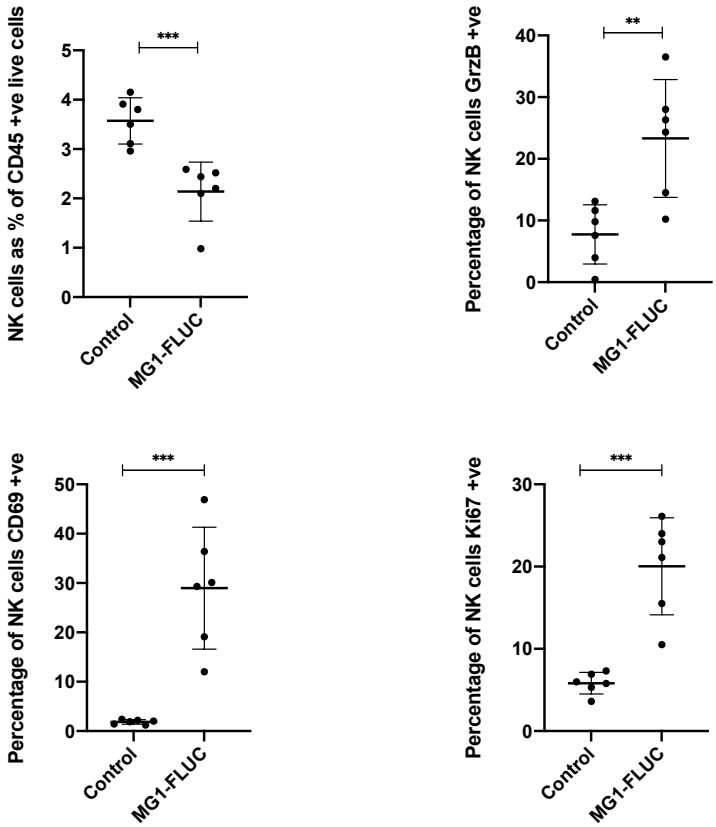
NK cells as % of CD45 +ve live cells
***
Control
MG1-FLUC
Percentage of NK cells GrzB +ve
**
Control
MG1-FLUC
Percentage of NK cells CD69 +ve
***
Control
MG1-FLUC
Percentage of NK cells Ki67 +ve
***
Control
MG1-FLUC

(B)

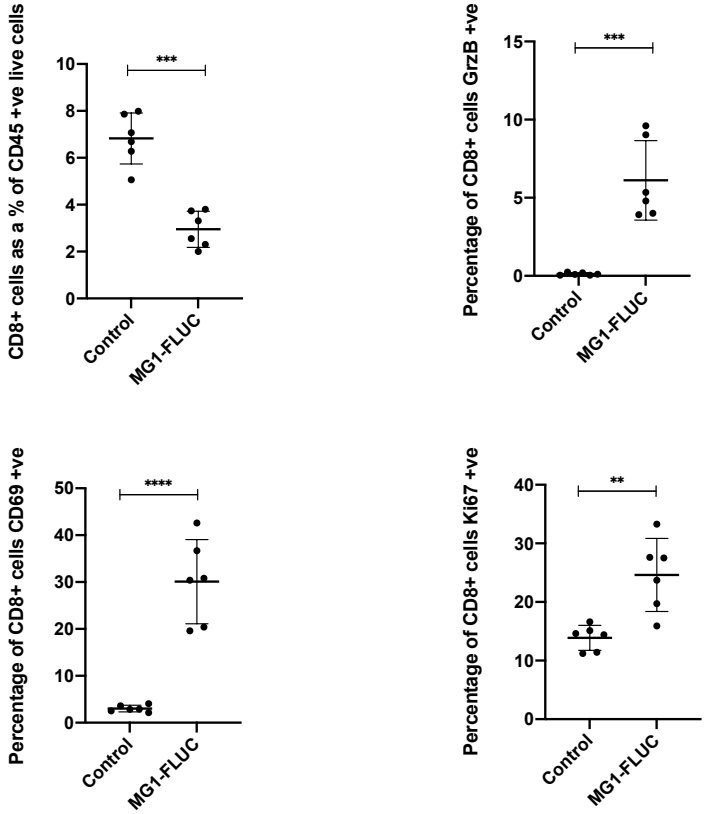
CD8+ cells as a % of CD45 +ve live cells
***
Control
MG1-FLUC
Percentage of CD8+ cells GrzB +ve
***
Control
MG1-FLUC
Percentage of CD8+ cells CD69 +ve
****
Control
MG1-FLUC
Percentage of CD8+ cells Ki67 +ve
**
Control
MG1-FLUC

Figure 22: MG1 infection induces early immune changes in splenocytes

Graphs showing percentage of NK cells out of total CD45$^+$ live cells within the spleen as well as percentage expression of GrzB, CD69 and Ki67 on splenic NK cells at the 48 hour timepoint (A). Graphs showing percentage of CD8$^+$ T cells out of total CD45$^+$ live cells within the spleen as well as percentage expression of GrzB, CD69 and Ki67 on splenic CD8$^+$ T cells at the 48 hour timepoint (B). Mean plus SD of six mice within each group. PBS control compared with MG1 using paired t-test statistical analysis.

6.8.2 MG1 infection induces early changes within the tumour immune microenvironment

Within the 4434 tumours, the NK cell population as a percentage of $CD45^+$ cells displayed no significant difference between MG1 and PBS treated mice at 48 hours, as shown in Figure 23A. Consistent with the splenocyte findings, expression of GrzB within NK cells was greater in the MG1 cohort compared to PBS controls. Specifically, a 31.3% increase in GrzB was demonstrated in the MG1 group as compared to the PBS cohort ($p=0.0005$).

With regards to the $CD8^+$ cell response, Figure 23B illustrates that MG1 treatment did not lead to any significant change in the proportion of $CD8^+$ cells within the tumours at the 48 hour time point. The number of $CD8^+$ T cells as a percentage of the $CD45^+$ population was 7.3% with PBS and 4.6% with MG1 treatment ($p=0.16$). There were also no significant changes in the activation status of these $CD8^+$ T cells in terms of GrzB expression between the two groups ($p=0.43$).

(A)

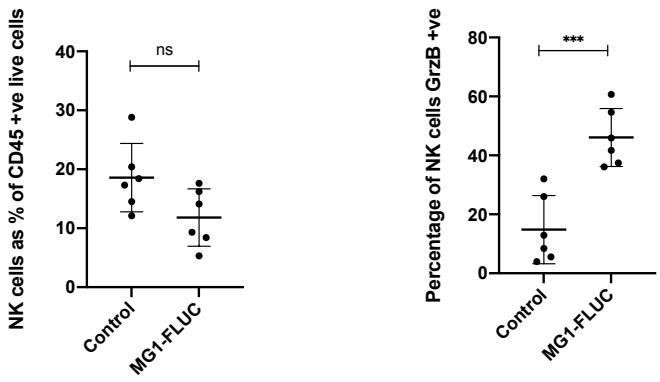

(B)

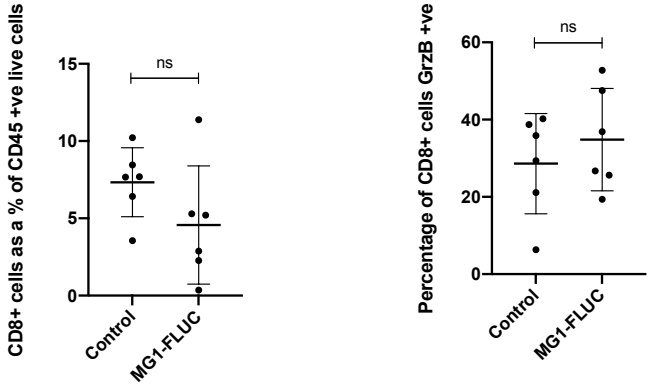

Figure 23: MG1 infection induces early immune changes within the tumour immune microenvironment

Graphs showing percentage of NK cells out of total CD45$^+$ live cells within the tumour as well as percentage expression of GrzB on tumoural NK cells at the 48 hour timepoint (A). Graphs showing percentage of CD8$^+$ T cells out of total CD45$^+$ live cells within the tumour as well as percentage expression of GrzB, CD69 and Ki67 on tumoural CD8$^+$ T cells at the 48 hour timepoint (B). Mean plus SD of six mice within each group. PBS control compared with MG1 using paired t-test statistical analysis.

6.8.3 MG1 infection alters the splenic immune microenvironment seven days following treatment

Seven days following infection, the splenic immune landscape demonstrates notable differences between the MG1 and PBS treated cohorts as shown in Figure 24A. As a percentage of $CD45^+$ cells, NK cells were elevated by 1.7% in the MG1 group when compared to PBS (p=0.0011). The proportion of NK cells expressing GrzB and CD69 activation markers remained significantly higher in the MG1 treatment cohort. Specifically, GrzB NK cell expression was increased by 8.7% (p=0.038) and $CD69^+$ cells were 1.1% higher (p=0.015) in splenocytes from the MG1 treatment group. Conversely, the Ki67 expression on NK cells was significantly lower in the MG1 treatment group (p=0.04).

Regarding the $CD8^+$ cell response (Figure 24B), by seven days, the proportion of $CD8^+$ T cells increased significantly following MG1 treatment with $CD8^+$ cells representing 7.8% of $CD45^+$ cells as compared to 5.9% following PBS treatment (p=0.02). This increase in percentage $CD8^+$ cells in the MG1 cohort is also complemented by their enhanced expression of GrzB (an increase of 6.0% expression in MG1 treatment group, p=0.0021) and Ki67 (an increase of 14.6%, p=0.0005) however the $CD8^+$ cell expression of the early activation marker CD69 decreased by 2.1%, (p=0.0034).

(A)

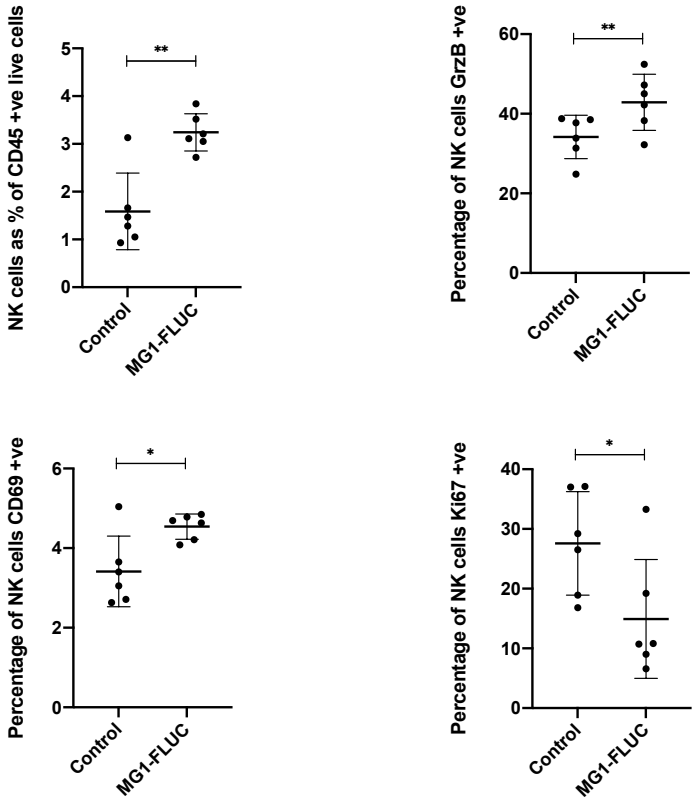
NK cells as % of CD45 +ve live cells
Percentage of NK cells GrzB +ve
Percentage of NK cells CD69 +ve
Percentage of NK cells Ki67 +ve
Control
MG1-FLUC
**
*

(B)

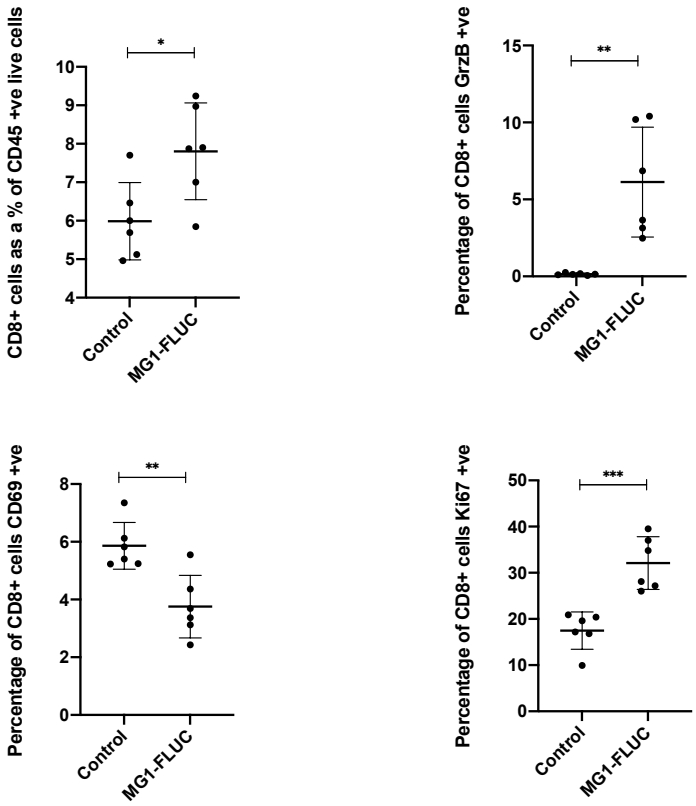
CD8+ cells as a % of CD45 +ve live cells
Percentage of CD8+ cells GrzB +ve
Percentage of CD8+ cells CD69 +ve
Percentage of CD8+ cells Ki67 +ve
Control
MG1-FLUC
*
**
***

Figure 24: MG1 infection alters the splenic immune microenvironment seven days following treatment

Graphs showing percentage of NK cells out of total CD45$^+$ live cells within the spleen as well as percentage expression of GrzB, CD69 and Ki67 on splenic NK cells at the seven day timepoint (A). Graphs showing percentage of CD8+ T cells out of total CD45$^+$ live cells within the spleen as well as percentage expression of GrzB, CD69 and Ki67 on splenic CD8$^+$ T cells at the seven day timepoint (B). Mean plus SD of six mice within each group. PBS control compared with MG1 using paired t-test statistical analysis.

6.8.4 MG1 infection alters the tumour immune microenvironment seven days following treatment

Within the tumour, at seven days following MG1 treatment (Figure 25A), there was no significant difference in the percentage of NK cells between the two groups (p=0.406) and corresponding with this, the activation markers which were initially elevated in the MG1 treatment group at 48 hours were no longer evident (difference between MG1 and PBS groups for GrzB p=0.27, CD69 p=0.37, Ki67 p=0.52).

Similarly to the splenic results, by seven days the $CD8^+$ cell component of the TME increased from 5.0% in PBS controls to 18.0% in the MG1 treated tumours (p=0.0009). However, there is no significant difference in the level of activation markers detected on $CD8^+$ cells between the two groups (difference between MG1 and PBS groups for GrzB p=0.79, CD69 p=0.74, Ki67 p=0.11) (Figure 25B).

In summary MG1 generates an early innate immune response 48 hours following MG1 treatment as evidenced particularly by the significantly increased activation of NK cells in both the spleen and tumour. The actual percentage of NK cells within the spleen reduced in the MG1 treated cohort whereas the NK cell percentage did not significantly reduce in the tumour. This may be explained if the NK cells, as early responders, relocate from the spleen towards the site of viral injection within the tumour.

As a percentage of $CD45^+$ cells, at the early 48 hour time point, the $CD8^+$ cell component did not differ between the MG1 and control groups, however were more activated. Conversely, by the later seven day time point, both the spleen and tumour demonstrated an increased percentage of $CD8^+$ T cell infiltration. This points towards a shift from the innate immune response at 48 hours, towards an adaptive response by seven days. Therefore, in conclusion it appears that the IT administration of the MG1 OV can generate phenotypic features of both an innate and adaptive immune response.

(A)

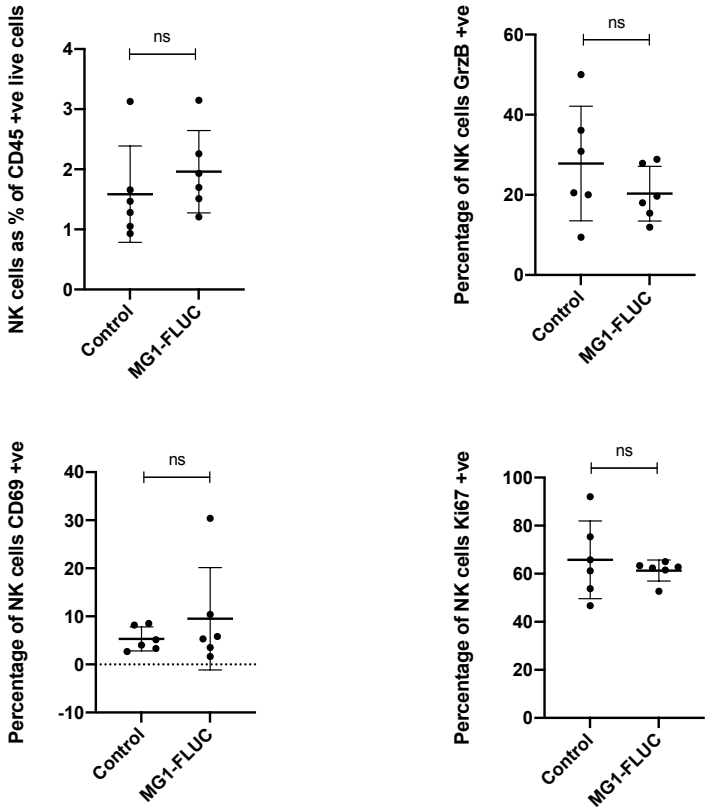
NK cells as % of CD45 +ve live cells
ns
Control
MG1-FLUC
Percentage of NK cells GrzB +ve
ns
Control
MG1-FLUC
Percentage of NK cells CD69 +ve
ns
Control
MG1-FLUC
Percentage of NK cells Ki67 +ve
ns
Control
MG1-FLUC

(B)

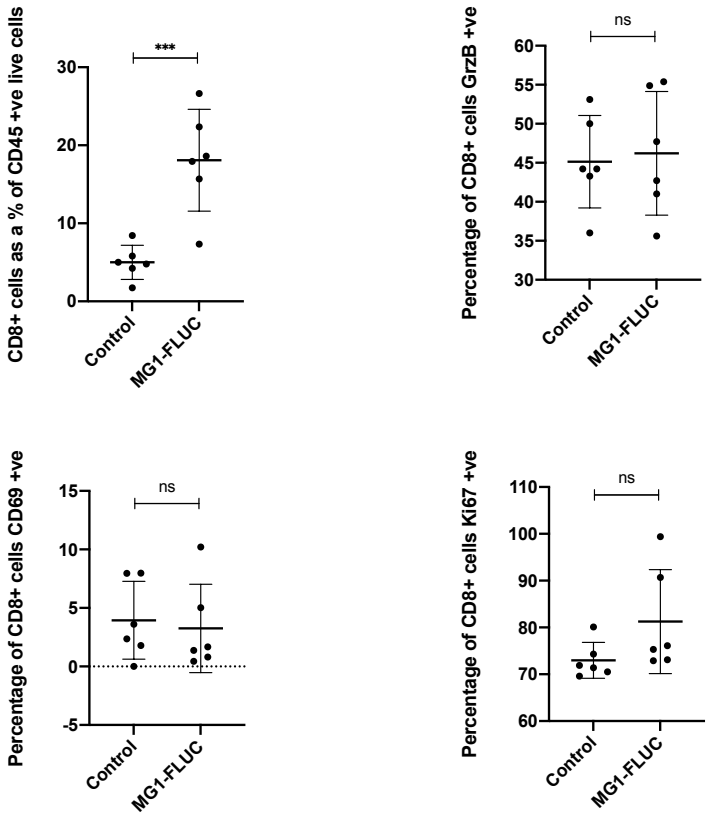
CD8+ cells as a % of CD45 +ve live cells
***
Control
MG1-FLUC
Percentage of CD8+ cells GrzB +ve
ns
Control
MG1-FLUC
Percentage of CD8+ cells CD69 +ve
ns
Control
MG1-FLUC
Percentage of CD8+ cells Ki67 +ve
ns
Control
MG1-FLUC

Figure 25: MG1 infection alters the tumour immune microenvironment seven days following treatment

Graphs showing percentage of NK cells out of total CD45$^+$ live cells within the tumour as well as percentage expression of GrzB, CD69 and Ki67 on tumoural NK cells at the seven day timepoint (A). Graphs showing percentage of CD8$^+$ T cells out of total CD45$^+$ live cells within the tumour as well as percentage expression of GrzB, CD69 and Ki67 on tumoural CD8$^+$ T cells at the seven day timepoint (B). Mean plus SD of six mice within each group. PBS control compared with MG1 using paired t-test statistical analysis.

6.9 Mice successfully treated with MG1 are immune to tumour rechallenge

Having revealed, by flow cytometry, phenotypic features to suggest an adaptive immune response, to assess *in vivo* whether MG1 could generate a functional acquired anti-tumour immune response, successfully treated mice were subjected to tumour rechallenge. A total of 10 mice bearing right flank 4434 tumours had been successfully treated with IT MG1. Six of these mice were then rechallenged with a second administration of subcutaneous 4434 tumours into the left flank, using the same number of cells in the rechallenge as used in the initial implantation (i.e. $4x10^6$ cells). The remaining four mice were rechallenged with an alternative (i.e. non-4434) cell line, namely B16-F1, in the left flank. Six naïve mice also were used as experimental controls and implanted with left flank 4434 tumours ($4x10^6$ cells). Figure 26A shows the experiment schedule. As shown, a minimum of 40 days had elapsed between initial treatment and tumour rechallenge. Figure 26B displays the average tumour growth for each group and demonstrates that previously treated 4434 bearing mice were immune to 4434 tumour rechallenge. Conversely, 4434 tumours grew in the naïve mice cohort, thereby demonstrating that the cells used in the rechallenge experiment were viable. In addition, B16-F1 tumours grew in the mice that had their 4434 tumours previously successfully treated. This signifies that the anti-tumour immunity generated was specific to the previously treated 4434 cell line. Overall, these experiments indicate that OV treated 4434 bearing mice can lead to the generation of anti-tumour immunity.

(A)

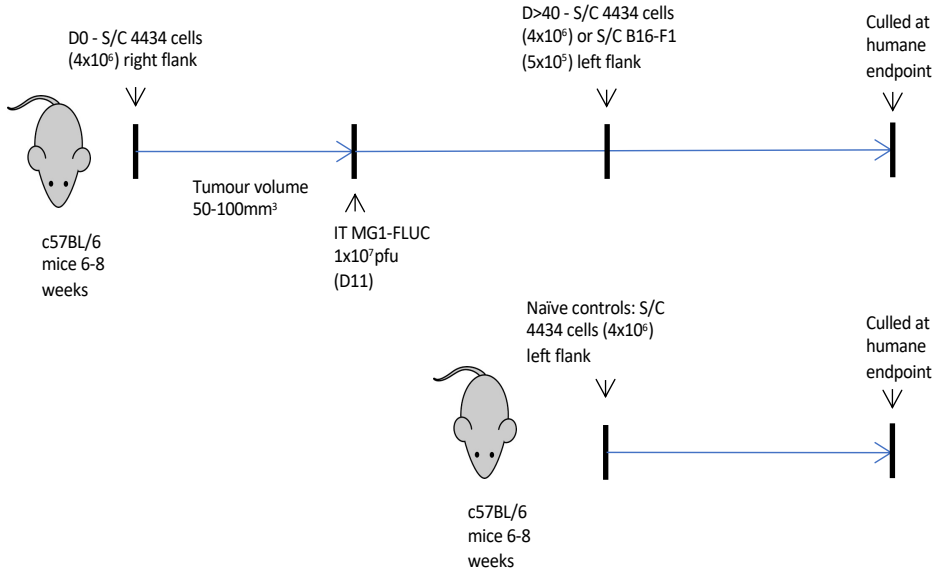

(B)

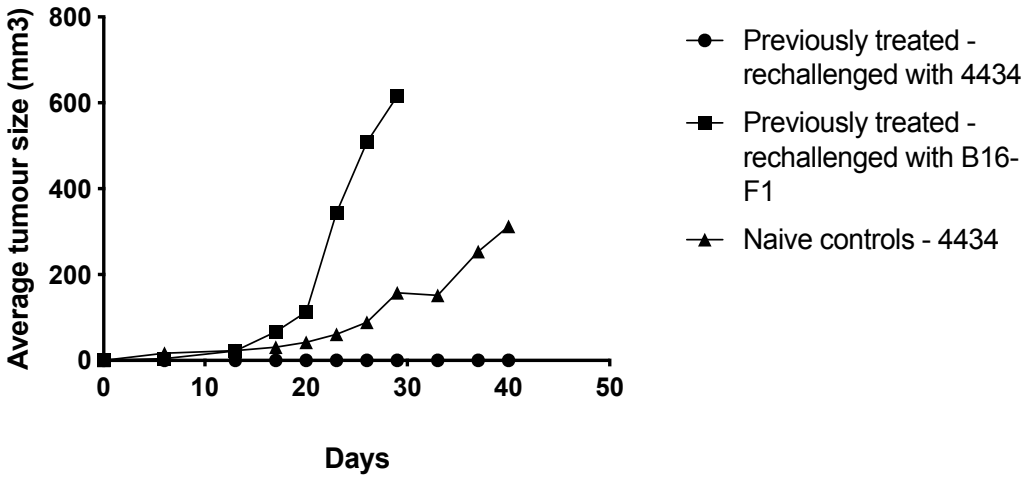

Figure 26: Mice successfully treated with MG1 are immune to tumour rechallenge

Experimental schematic for tumour rechallenge (A). Average tumour growth of left flank tumours in previously successfully treated mice rechallenged with either 4434 (six mice) or B16-F1 (four mice) and compared with 4434 tumours implanted in tumour naïve mice (six mice) (B).

6.10 Splenocytes from MG1 treated mice express greater IFN-γ following 4434 tumour cell rechallenge

To further assess the capacity for MG1 to generate acquired anti-tumour immunity, splenocyte IFN-γ release was evaluated. IFN-γ is the only member of type II IFN and is involved in both innate and adaptive immunity. IFN-γ is an inducer of the MHC class II molecule on APCs and can upregulate PD-L1 on tumour cells. IFN-γ can be released by $CD4^+$ T helper cells and by $CD8^+$ effector T cells once antigen-specific immunity develops as part of the adaptive immune response. Therefore, the release of IFN-γ by splenocytes can act as a marker of tumour antigen recognition.

IFN-γ release from splenocytes has been assessed in a murine breast cancer model. When restimulated with tumours cells, splenocyte IFN-γ release was higher in those mice treated with MG1 as compared to untreated controls. This therefore indicates that MG1 treatment has the potential to generate tumour antigens and to prime immune cells to respond to a subsequent re-exposure to tumour cells.[330]

To evaluate splenocyte IFN-γ release in a murine model of melanoma, three cohorts were compared. This included 4434 bearing mice that had been successfully treated with MG1-FLUC, in addition to untreated 4434 bearing mice, and naïve non-tumour bearing mice. Splenocytes were harvested on day 10 post treatment, counted and plated at a concentration of $5x10^5$ cells per well. Splenocytes were restimulated by co-culturing with either 4434 cells ($1x10^5$), an alternative melanoma cell line, namely B16-F1, or with PBS control. The sample supernatants were collected and centrifuged following 24 hours of co-culture and then analysed by ELISA for the presence of IFN-γ.

Figure 27A shows the concentration of IFN-γ released by each group. Negligible IFN-γ was released from splenocytes in all untreated or naïve mice, whereas IFN-γ was detected in four of six mice previously treated with MG1. The increase in IFN-γ trended towards significance ($p=0.07$). To ensure that the increase was specific to the re-exposure to 4434, splenocytes were also

exposed to either PBS or B16-F1 cells as shown in Figure 27B. Again, these two groups released negligible IFN-γ in comparison to re-exposure to 4434, and, albeit that this wasn't statistically significant, suggests that the effect is specific to the particular previously treated 4434 cell line.

(A)

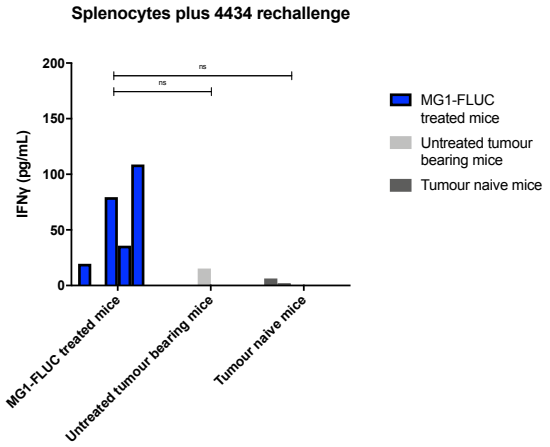

(B)

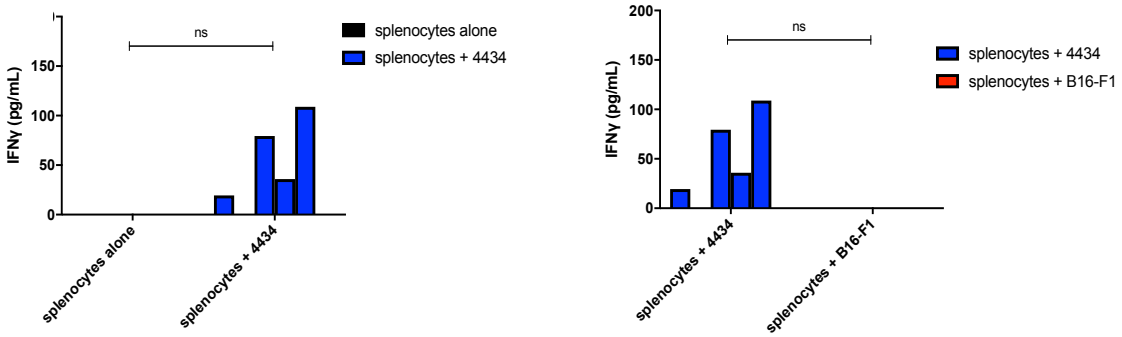

Figure 27: Splenocytes from MG1 treated mice express greater IFN-γ following 4434 tumour cell rechallenge

The spleens of successfully treated, untreated and tumour naïve mice were explanted, prepared into a single cell suspension and co-cultured with 4434 or B16-F1 cells, or PBS control. Supernatants were collected after 24 hours and analysed with ELISA for the presence of IFN-γ. Graphs display the concentration of IFN-γ obtained following rechallenge with 4434 (A), B16-F1 or PBS control (B). Graphs present the IFN-γ concentration and each bar represents the result acquired for each individual mouse, with six mice per group; multiple t test statistical analysis corrected for multi-comparison using Holme-Sidak method (A), paired student t-test analysis (B).

6.11 Discussion

OVs have been shown to have cytotoxic potential in a range of tumour cell lines including in melanoma. In addition, they have the potential to improve survival in certain tumour models as shown in the previous chapter. As with other OVs, MG1 also has the potential to foster an anti-tumour immune response.

In this chapter the immunological consequences of MG1 infection both *in vitro* and *in vivo* were explored. The type I IFN response to MG-1 infection was investigated, given its pivotal role as a molecule involved in the cellular host immune response to viral infection, as well as being involved in the recruitment and cytotoxic activity of NK and $CD8^+$ T cells, the secretion of pro-inflammatory cytokines and the cross-presentation activity of mature DCs. Moreover, deficiencies in IFN signalling in tumour cells can be exploited by OVs to enable their replication. In this chapter, the important interaction between MG1 and IFN was demonstrated in several ways. MG1 infecting two murine melanoma cell lines, B16-F1 and 4434, resulted in the release of IFN-β. *In vitro* the concentration obtained was notably higher from the 4434 cell line compared to the B16-F1 cell line (Figure 15A). Given the lower IFN-β level released by the B16-F1 cell line, a western blot analysis investigated the IFN signalling pathway and confirmed that the upstream proteins to type I IFN, pIRF3 and pTBK1, showed an increase in expression after virus infection (Figure 15C). Unfortunately, expression of the RIG-I protein was not detected following MG1 infection thereby suggesting that RNA viral sensing could be through an alternative pathway. Therefore, future experiments could investigate other viral sensing receptors including melanoma differentiation-associated gene 5 (MDA5). In addition, assessment of both viral sensing pathways via western blot could be conducted, for comparison, in the 4434 murine melanoma cell line and furthermore, type I IFN production could also be measured by ELISA from the human melanoma cell lines that were found previously to be sensitive to MG1 infection (Chapter 4).

This chapter also explored the potential of MG1 to induce ICD. ICD promotes anti-tumour immunity through the release of DAMP signals which are detected by PRRs, especially on DCs, resulting in the cross-presentation of tumour antigens to $CD8^+$ T cells. The capacity to induce ICD has been shown in OVs including adenovirus, VV and Semliki Forest virus.[372] This chapter established that, compared to uninfected controls, MG1 infection in murine melanoma cell lines could induce hallmarks of ICD including the release of both ATP and HMGB1 (Figure 18).

Giving further credence to the immunogenic potential of MG1 infection, this chapter explored the release of a panel of cytokines following IT treatment of 4434 tumours (Figure 19). This confirmed an elevation, compared to uninfected control, of cytokines involved in chemoattracting a range of cell types from both the innate and adaptive arms of the immune system. Moreover, larger tumours were associated with increases in immunosuppressive angiogenic factors, perhaps contributing to the difference in efficacy outcomes using MG1 to treat small and large tumours. Whilst this panel was a useful broad initial oversight of what cytokine changes appear to occur, this requires confirmation through assessing cytokine levels via ELISA and the use of more animals in order to be statistically significant. In addition, an assessment of the functionality of these changes would be necessary, for instance through splenocyte immune cell migratory experiments, to assess that the change in cytokine expression exerts a functional effect on the migration of immune cells. Nevertheless, it provided useful information with which to analyse the *in vivo* immune changes that occur following MG1 infection.

Analysis of the transcriptome through mRNA analysis by RNA-Seq further supported the immune modifying effect generated by MG1 (Figure 20). Of interest, larger tumours from both PBS control treated and MG1 treated groups were less immunogenic ('colder') than their smaller tumour counterparts from each respective treatment cohort. These data were therefore consistent with the results from the cytokine assessment. The data also demonstrated an increase in IFN-β mRNA expression in MG1 treated cohorts, consistent with

the increased concentration of IFN-β released by MG1 infected cells as determined by ELISA (Figure 15). RNA-Seq clearly identified the notable effect exerted by MG1 in modifying the immune TME across the spectrum of the immune landscape, from the lymphoid and myeloid systems and also costimulatory, coinhibitory and activation molecules.

It may be intuitive that larger tumours are more difficult to treat than smaller tumours, especially if using the same dose of virus, as the higher number of tumour cells present requires greater oncolysis per viral particle delivered. However, the cytokine and RNA-Seq data sets validate that this is not simply due to the reduced oncolytic effect of the virus in larger tumours, but is also related to the evolution of an increasingly immunosuppressive TME.

Through flow cytometry experiments in the 4434 melanoma model, this chapter identified that, when compared to PBS control treatment, MG1 can lead to changes in the TME and spleen, indicative of both innate and adaptive immune responses. At the earlier time point, the proportion of NK cells decreased, but became significantly more activated (Figures 22 and 23). These findings were only partially consistent with previous data by Zhang *et al*. which investigated the activity of MG1 in the B16 model and showed an increase in the proportion of splenic NK cells.[263] This study also reported an initial splenomegaly which resulted from a local increase in dendritic cells and NK cells following viral treatment. However, it should be noted that in this study by Zhang *et al*., MG1 was administered via IV injection and therefore the quantity of virus reaching the spleen systemically is likely to be considerably greater than via the IT method. Indeed, IT administration may explain why the proportion of splenic NK cells decreases as NK cells may relocate from the spleen to where the virus is located. It was observed that despite IT injection of virus, even splenic NK cells show increased activation, presumably through either partial systemic leak of virus or through the circulating nature of immune cells.

The level of early splenic NK cell activation seems similar between both the B16 model reported by Zhang *et al*. (samples taken at day three) and from this

4434 model (samples taken at 48 hours). Findings in the B16 model reported around a 20-fold increase in percentage of CD69+ expression, compared to PBS treatment, whereas this increase was 15-fold in the 4434 model. Regarding splenic NK cell GrzB expression, there was a three-fold increase in both the B16 model and the 4434 model. This three-fold increase in GrzB expression was also observed in tumoural NK cells 48 hours following MG1 IT administration.

In the B16 model, Zhang *et al*. reported that NK cell activation persisted up to five days post-MG1 administration. This was consistent in the 4434 model (Figure 24) where it was found that at seven days there continued to be some evidence of NK cell activation. Splenic NK cell GrzB expression in MG1 treated mice compared to PBS controls was 1.2-fold higher ($p=0.038$), CD69 expression was 1.3-fold higher ($p=0.015$) whereas, unexpectedly, Ki67 expression was in fact 1.9-fold lower in the MG1 group ($p=0.04$). Within the tumour, there was no difference in levels of NK cell activation at seven days following MG1 treatment (Figure 25). As the fold change between the MG1 and PBS control groups was notably closer, compared to the differences at 48 hours, this suggests that by seven days, the early innate NK cell activation is waning within the TME.

The reduced activation of the innate immune system at the seven day time point contrasted with the increasing features of an adaptive immune response as evidenced by the increasing proportion of CD8+ T cells in both the spleen and tumour in the MG1 group compared to controls at seven days (Figures 24 and 25). In support of these data, rechallenging successfully treated mice with a subsequent tumour implantation showed the presence of immunological memory preventing 4434 tumour growth (Figure 26). This demonstrates that in addition to the phenotypic changes seen within the flow cytometry data, a functional anti-tumour immunity exists.

This was further reinforced by restimulating the splenocytes of cured mice with a re-exposure to the 4434 cell line *ex vivo*. Whilst the results showed some variation between each individual mouse and were therefore not statistically

significant with the small number of mice utilised, the overall trend appears to support the notion that splenocytes from successfully treated mice release a higher concentration of IFN-γ when re-exposed to tumour cells, thereby suggesting the generation of anti-tumour immune recognition and response (Figure 27).

Thus far, it has been demonstrated that MG1 has tumour tropic effects *in vitro* and *in vivo* and can successfully treat smaller, but not larger 4434 tumours. This chapter has displayed the capacity of MG1 to induce ICD and to stimulate both innate and adaptive aspects of the immune response, leading to functional immunological memory in previously treated mice. However, despite these changes, larger 4434 tumours escape the oncolytic and immunostimulatory effects of MG1. Therefore, the next chapter will explore novel but rational MG1 combinations with the aim of enhancing the therapeutic outcomes observed.

Chapter 7:

MG1 in Combination with Novel Immunotherapeutic Approaches

7 Chapter 7: MG1 in Combination with Novel Immunotherapeutic Approaches

7.1 Introduction

As demonstrated, OVs including MG1 have both oncolytic and immunomodulatory effects on models of melanoma, leading to the successful treatment of smaller 4434 tumours. In addition, they offer the potential for a tumour tropic and well tolerated treatment. However, when administered as a monotherapy, the clinical efficacy of OV treatment appears to be limited, in part due to the generation of anti-viral host immunity. Therefore, greater therapeutic gains may come through delivering OVs as combinatorial treatment.[220] This has been the approach taken thus far with the early clinical development of MG1 which, as discussed, is being utilised with an adenoviral adjunct in a prime-boost strategy.[321] In addition, given their ability to alter the immune TME, another rational approach is to integrate the use of OVs, including MG1, with other immune modifying therapies.[220]

Previous chapters have demonstrated that MG1 has a more pronounced benefit when treating smaller, as supposed to larger, 4434 melanoma tumours. Whilst MG1 may exert an oncolytic effect on these larger tumours, it is likely that they escape immunological control, thereby avoiding a long-term survival benefit. Therefore, the next chapter will explore novel but rational combinations in conjunction with MG1, with the aim of having beneficial immunomodulatory effects which lead to enhanced therapeutic outcomes.

7.2 MG1 in combination with an Fc-optimised anti-CD25 tumour infiltrating regulatory T cell depleting antibody

As discussed in section 2.1.7.2.1.6, $FoxP3^{+}$ $CD25^{+}$ Tregs have been associated with poorer prognostic data and therefore, they have been targeted in an attempt to improve outcomes.[87]

In preclinical murine models, the anti-CD25 antibody clone PC-61 was shown to partially deplete Treg cells in the blood and peripheral lymphoid organs and has the capacity to inhibit tumour growth and improve survival when administered before or soon after tumour implantation.[120, 124] However, the use of anti-CD25 antibodies to reduce Tregs as a therapeutic intervention against established tumours has generally failed to delay tumour growth or prolong survival as they have been unable to selectively reduce the Treg cells within the TME.[120, 121] However, the recently developed antibody, αCD25-m2a, was optimised to bind to the Treg FcγR and through ADCC resulted in superior intratumoural Treg depletion. In murine models this optimised antibody had a greater therapeutic effect compared to its unoptimised counterpart.[121]

These promising data led to the exploration of the role of Tregs in the 4434 tumour model and whether the therapeutic effects of MG1 could be enhanced with the selective depletion of Tregs in the TME. To determine this, subcutaneous 4434 tumours were implanted, and mice were randomised to treatment with IT PBS or MG1-FLUC with an MOI of $1x10^7$ pfu. At either 48 hours or seven days post treatment, both the tumours and spleens were harvested and prepared for flow cytometry analysis. Each cohort contained six mice. The experimental schematic has been shown previously in Figure 21A.

Cells were stained and phenotyped into live $CD45^+/CD3^-/NK1.1^+$ NK cells, $CD45^+/CD3^+/CD4^+$ T cells and live $CD45^+/CD3^+/CD8+$ T cells. The $CD3^+/CD4^+$ T cells were further characterised into $CD3^+/CD4^+/CD25^+/FoxP3^+$ Treg cells. The gating strategy for flow cytometry analysis has been shown previously in Figure 21B.

7.2.1 MG1 infection alters Tregs within the spleen

As shown in Figure 28A, the percentage of Treg cells as a percentage of total $CD4^+$ cells within the spleen does not alter 48 hours following MG1 treatment. Treg cells from the control group measured 10.8% of total $CD4^+$ cells

compared to 12.6% following MG1 therapy (p=0.19). However, the ratio of $CD8^+$:Treg cells reduces from 6.0 $CD8^+$ cells to every Treg in the control group, compared to 3.2 $CD8^+$ cells to every Treg in the MG1 treated cohort. This is supportive of the previous findings in Figure 22 which demonstrated a reduction in the percentage of $CD8^+$ cells as a percentage of the total $CD45^+$ live cells therefore the reduced $CD8^+$:Treg ratio is likely related to a reduced $CD8^+$ cell component rather than an increase in Treg cells.

At the seven day time point (Figure 28B), the percentage of Treg cells as a percentage of total $CD4^+$ cells increases significantly from the control group to the MG1 treated group (p=0.0076), albeit that the absolute mean change between the two cohorts is just 1%. With regards to the $CD8^+$:Treg ratio, in contrast to the 48 hour time point, the ratio of $CD8^+$ cells to Treg cells increases from 4.0 in the control group to 5.2 in the MG1 treated group (p=0.0125). This is again consistent with the previously illustrated (Figure 24) increase in $CD8^+$ cells as a percentage of $CD45^+$ cells within the spleen seven days following MG1 treatment.

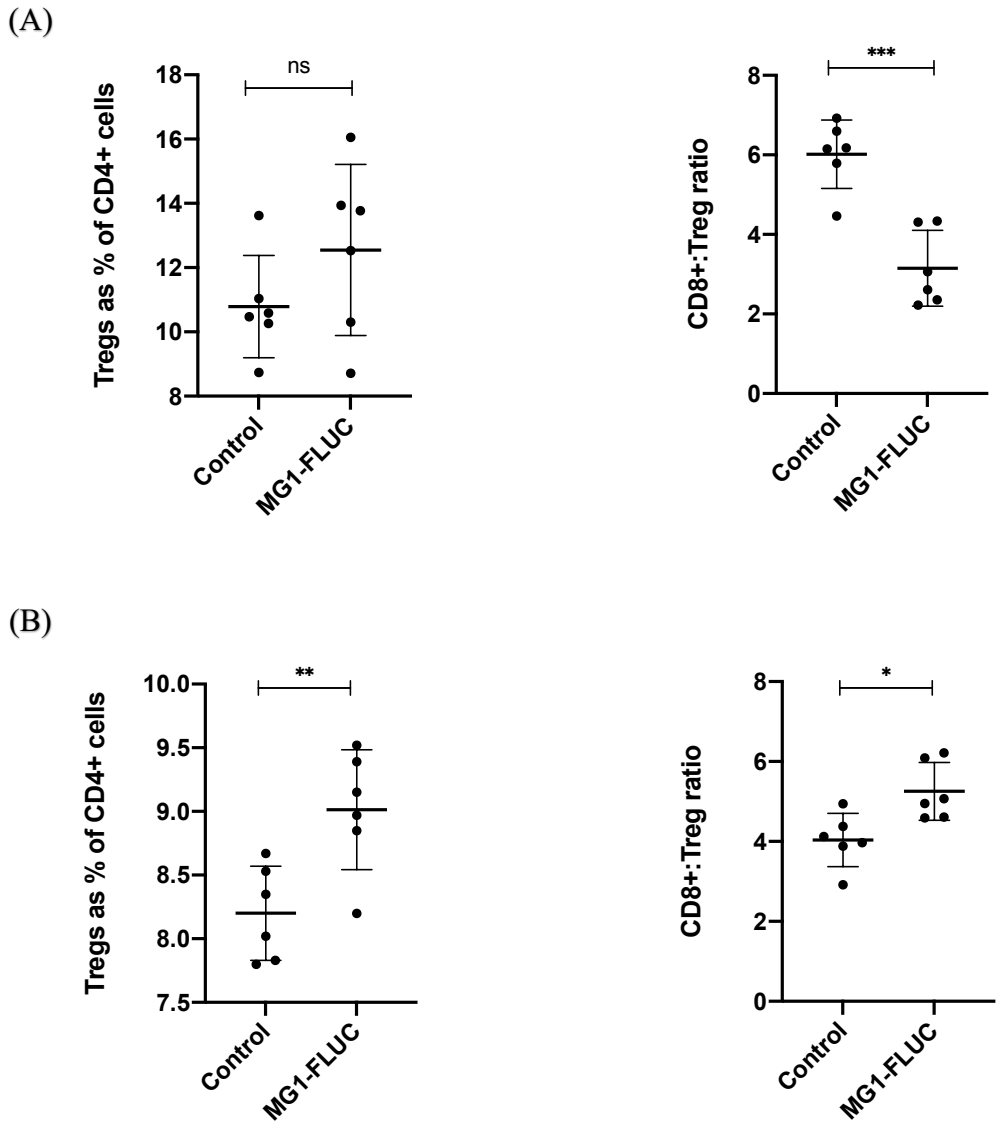

Figure 28: MG1 infection alters Tregs within the spleen

Graphs showing percentage of Treg cells out of total CD4⁺ live cells, as well as the CD8⁺:Treg ratio within the spleen at the 48 hour (A) and seven day (B) timepoint. Mean plus SD of six mice within each group. PBS control compared with MG1 using paired t-test statistical analysis.

7.2.2 MG1 infection does not alter Tregs within the TME

Consistent with the splenic results at 48 hours, Figure 29A demonstrates that the level of Tregs as a percentage of $CD4^+$ cells within the tumour is not significantly different between the control or MG1 cohorts (p=0.18). Furthermore, there was no significant change in the $CD8^+$:Treg ratio (p=0.21) in tumours treated with either PBS or MG1. This is consistent with the previous finding that at the 48-hour time point, tumoural $CD8^+$ cells as a percentage of $CD45^+$ cells were not significantly altered between control and MG1 treated groups (Figure 23).

In contrast to the day seven splenic results, Tregs were unaltered in the tumour following MG1 treatment. The Treg percentage of $CD4^+$ cells was 7.0% in the PBS treated cohort as compared to 10.3% in the MG1 treated group, however this increase was not significant (p=0.39). Furthermore, there was no significant difference in the $CD8^+$:Treg ratio between the two treatment groups (p=0.51) (Figure 29B).

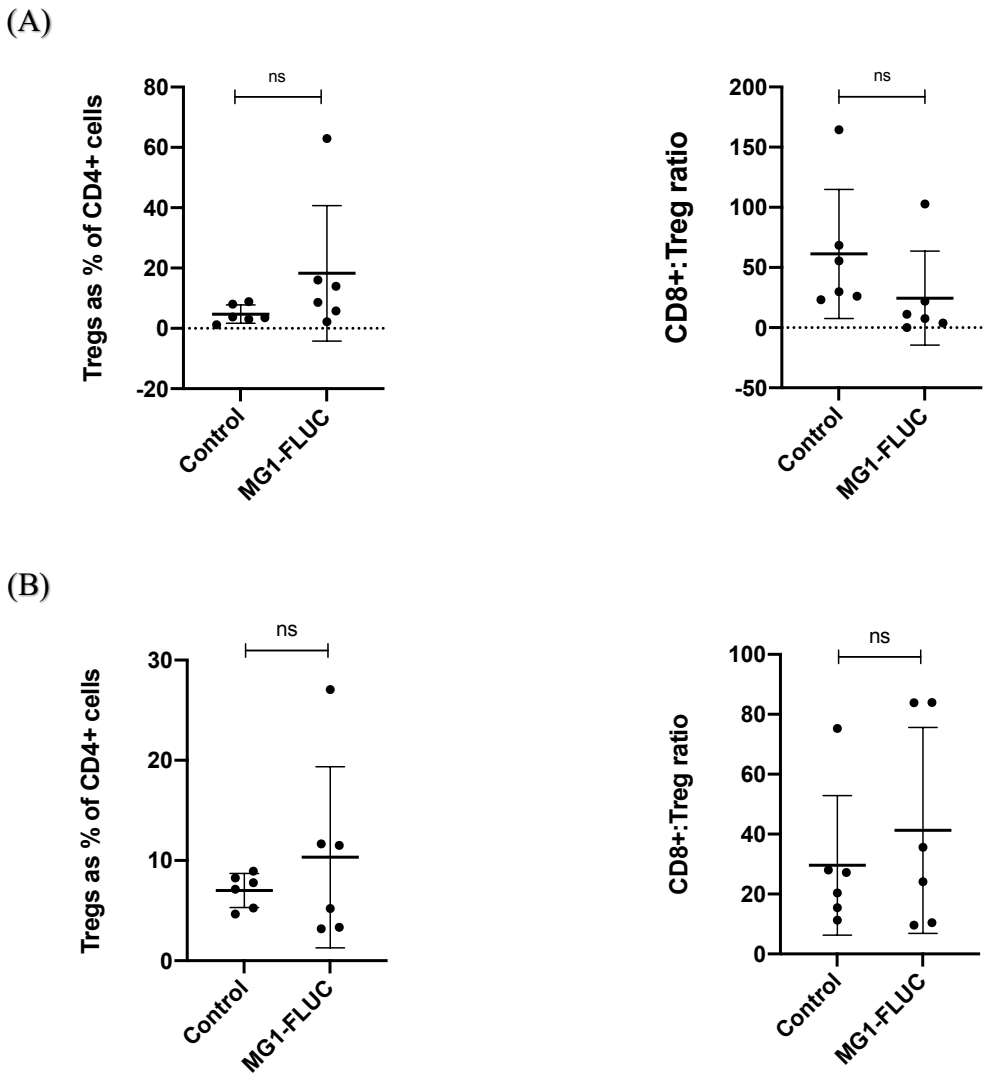

Figure 29: MG1 does not alter Tregs within the TME

Graphs showing percentage of Treg cells out of total CD4⁺ live cells, as well as the CD8⁺:Treg ratio within the TME at the 48 hour (A) and seven day (B) timepoint. Mean plus SD of six mice within each group. PBS control compared with MG1 using paired t-test statistical analysis.

7.2.3 Selectively depleting tumoural Tregs fails to improve MG1 therapeutic outcomes

MG1 infection did not significantly alter the percentage of Tregs or the $CD8^+$:Treg ratio in the TME, however, Tregs are clearly present within the TME of the 4434 tumours. Therefore, it was hypothesised that selectively depleting tumoural Tregs may lead to favourable therapeutic outcomes in the 4434 model. A recent study evaluating the effectiveness of Treg depletion in a MCA205 murine fibrosarcoma model identified a baseline level of $FoxP3^+$ cells as a percentage of $CD4^+$ cells of approximately 47% which could be depleted to approximately 10% with the optimised aCD25 Ab which, in turn, increased the tumoural $CD8^+$:Treg ratio and also resulted in 15% of mice achieving long term survival. With regards to melanoma, in a B16 model, 14.5% of $CD4^+$ cells were Tregs which could be depleted to 5.2% using the PC61 aCD25 Ab.[124] However, no published data exists describing the effects of Treg depletion in a 4434 melanoma model.

To determine whether the optimised depletion of intratumoural Tregs positively affected survival, medium sized murine subcutaneous 4434 tumours were established (average 100 mm^3). On day 12, the mice were treated with 100 μL of either IP PBS or 200 μg IP anti-CD25 antibody (aCD25 Ab) and this was continued twice weekly for up to four weeks. 48 hours later (day 14), the tumours were injected with 50 μL of either IT PBS or IT MG1 $1x10^7$ pfu. Tumour growth was monitored, and mice were sacrificed at a humane end point. The experimental schedule is illustrated in Figure 30A.

Figure 30B further demonstrates the survival advantage from a single IT administration of MG1 in comparison to PBS treatment as the median survival in these two groups was 39 days following IT PBS and 77 days following MG1-FLUC ($p=0.0028$). However, the addition of aCD25 depleting antibody failed to improve the therapeutic outcome, either as a single therapy (median survival PBS control 39 days versus aCD25 Ab 49 days, $p=0.3380$) or when given in combination with MG1 (median survival MG1-FLUC 77 days versus MG1-FLUC with aCD25 Ab 63 days, $p=0.8247$).

(A)

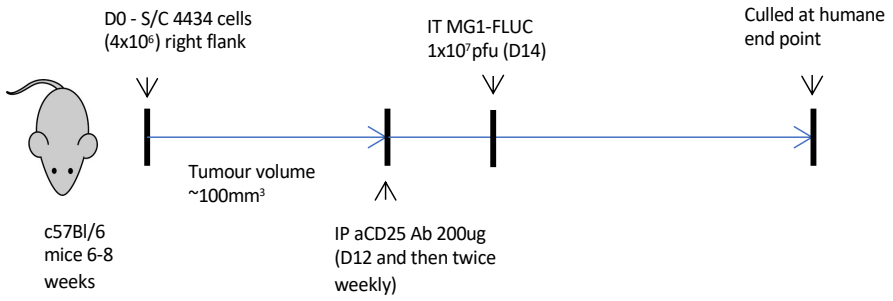

(B)

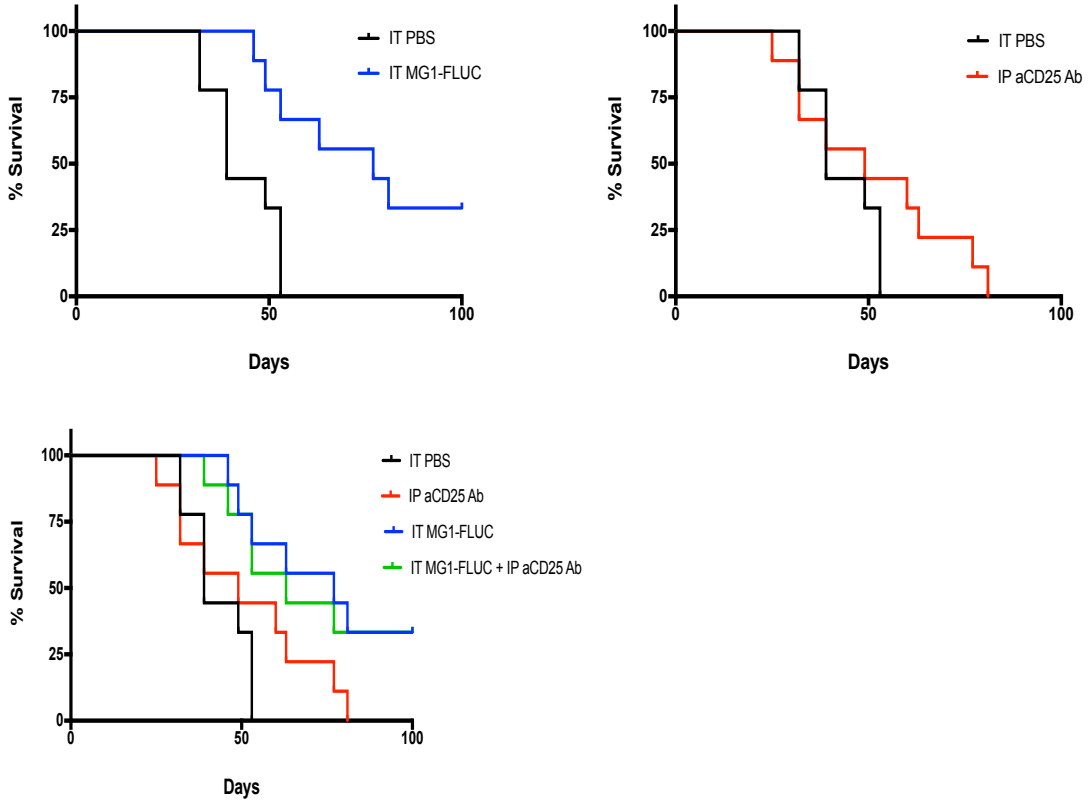

Figure 30: The selective depletion of tumoural Tregs fails to improve MG1 therapeutic outcomes

Experimental schematic of experiment investigating MG1 in combination with anti-CD25 antibody (A). Kaplan-Meier survival curves of 4434 tumour bearing mice (six mice per group) following IT PBS control vs IT MG1 alone and vs IP aCD25 Ab alone and IT MG1 with IP aCD25 Ab in combination (B).

7.3 MG1 and the PD-1/PD-L1 axis

As discussed previously, the advent of ICIs has transformed the treatment landscape for patients with malignant melanoma both in the advanced and adjuvant treatment settings. Nevertheless, many patients still fail to respond or develop resistance to ICI treatment.

When deployed with ICIs, OVs may increase the response to, and reverse the resistance to, ICB and to favourably alter components of the anti-tumour immune response.[220] A comprehensive review of the pre-clinical and clinical studies combining ICB with oncolytic viruses has been recently published by our group.[314]

With regards to Maraba virus, as presented previously, using a murine model of TNBC, Bourgeois-Daigneault *et al*. found that neo-adjuvant treatment with MG1 led to reduction in size and number of subsequent lung metastases and improved survival. Furthermore, MG1 infection resulted in increased levels of tumour cell PD-L1 expression. In addition, following neo-adjuvant MG1, using a post-operative treatment regimen combining anti-CTLA-4 and anti-PD-1 antibodies, resulted in a significantly improved survival compared to both untreated mice and those receiving either ICI or MG1 therapy alone.[330] To our knowledge, the effects of combination therapies of MG1 with checkpoint inhibition in a melanoma model has not been demonstrated and was therefore a logical avenue to explore in the 4434 murine *in vivo* tumour model. This rationale was supported by findings from the RNA-Seq analysis which showed an upregulation in PD-1 in both small and large MG1 treated tumours compared to PBS control (Figure 20).

7.3.1 MG1 alters the expression of PD-L1 on murine melanoma cell lines *in vitro*

To determine the effect of MG1 infection on melanoma cell PD-L1 expression, murine (4434 and B16-F1) melanoma cells were plated and infected with MG1-GFP at an MOI of 0.01 or PBS control. 24 hours later, cells were

collected and prepared for flow cytometry analysis. Cells were stained with a viability dye and an a fluorescently conjugated antibody to detect the PD-L1 cell surface protein.

Figure 31 demonstrates that the percentage of live cells expressing PD-L1 increases following the addition of MG1-GFP in the 4434 murine cell line. Mean PD-L1 expression with PBS control was 1.4%, increasing significantly to 4.2% in the MG1-GFP treatment group ($p=0.0223$). Of note, 86% of PD-L1 expressing cells in the MG1 group expressed GFP (data not shown), therefore implying that viral infection of the tumour cell was involved in the increased PD-L1 expression. Regarding the B16-F1 cell line, despite having greater sensitivity to MG1 infection (section 4.2) there was no significant difference between the PBS control group and the MG1-GFP cohort (mean PD-L1 expression 1.8% vs 1.1% respectively, $p=0.1380$).

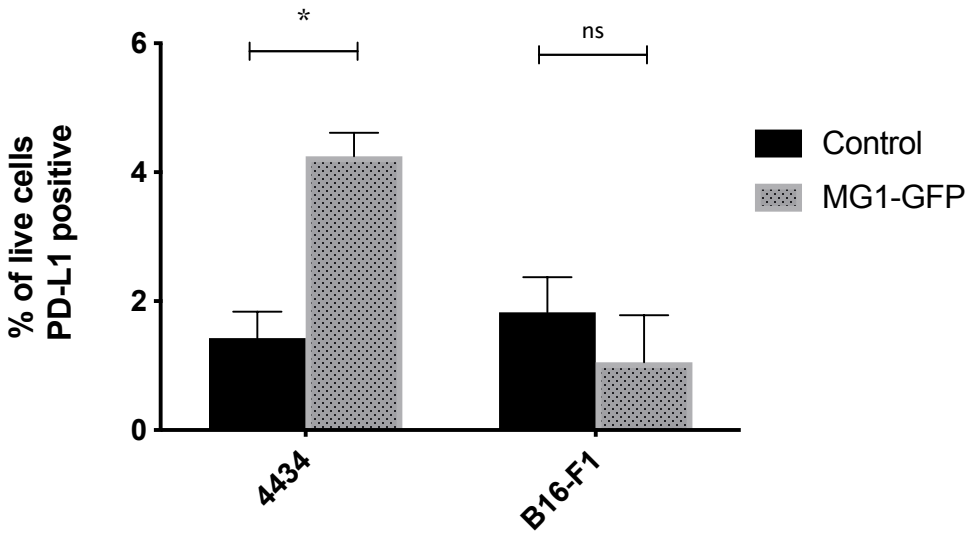

Figure 31: MG1 infection alters the expression of PD-L1 on murine melanoma cell lines *in vitro*

Cell surface programmed death ligand 1 (PD-L1) expression on live 4434 and B16-F1 cells after 24 hours of incubation with 0.01 MOI MG1-GFP or PBS control. Mean PD-L1 expression plus SD from three independent experiments. Paired Student T-test statistical analysis.

7.3.2 MG1 alters the expression of PD-1 on CD8+ T cells *in vivo*

Having shown that MG1 can enhance the PD-L1 expression in the 4434 cell line, the effects of PD-1 and PD-L1 expression *in vivo* were investigated. This was to further investigate the previously presented findings (Figure 20) showing that MG1 increases PD-1 RNA expression in both small and large 4434 tumours. To analyse this further, murine 4434 tumours and spleens from PBS and IT MG1-FLUC ($1x10^7$ pfu) treatment groups were harvested at 48 hours and seven day timepoints, prepared and analysed using flow cytometry as per section 6.8.

Figure 32A demonstrates the expression of PD-1 on $CD8^+$ T cells at 48 hours following MG1 or PBS control treatment. 3% of splenic $CD8^+$ cells treated with PBS had PD-1 expression which increased slightly to 3.4% following MG1 treatment, although this did not reach significance (p=0.10). Regarding tumoural $CD8^+$ T cells the mean percentage expressing PD-1 did not significantly alter between the PBS (68% PD-1^+) or MG1 (64% PD-1^+) treated groups (p=0.60), however, it was notable that the intra-tumoural $CD8^+$ T cells expressed a greater percentage of PD-1 when compared to splenic $CD8^+$ T cells in both the PBS and MG-1 cohorts.

Regarding the later seven day time point, the percentage of splenic $CD8^+$ cells expressing PD-1 increased from 8.5% to 22.8% between the control and MG1 treatment cohorts respectively; a mean increase of 14.3% (p=<0.0001) as shown in Figure 32B. However, this was not replicated in the findings from tumoural $CD8^+$ cells where the mean PD-1 expression reduced by 4.9% (p=0.01) between the control and MG1 treated cohorts. However, the mean absolute percentage of PD-1 expression on the tumoural $CD8^+$ cells was high at 97.5% in the PBS and 92.6% in the MG1 cohort.

In summary, whilst MG1 itself fails to increase the percentage of tumoural $CD8^+$ cells that express PD-1 compared to PBS control, there appears to be a general increase in PD-1 expression between the 48 hour and seven day time

points in both the PBS and MG1 groups. Given the high PD-1^{+} percentages observed in T cells, this gave credence to evaluating the therapeutic potential of incorporating an anti-PD-1 Ab into the treatment paradigm.

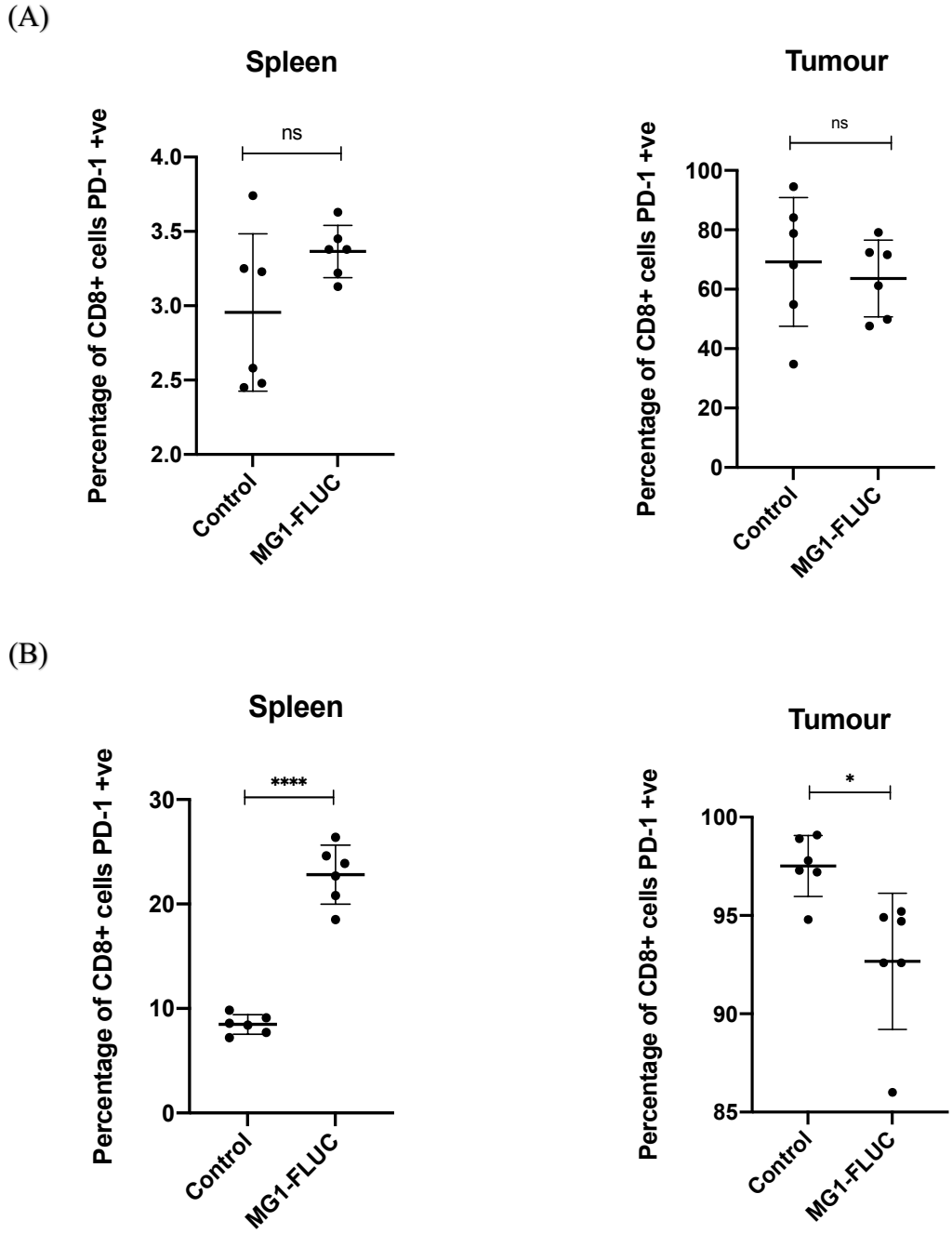

Figure 32: MG1 alters the expression of PD-1 on CD8+ T cells *in vivo*

4434 tumour bearing mice injected with IT MG1-FLUC 1x10^7 or PBS control. Tumours explanted after 48 hours (A) or seven days (B), processed and analysed using flow cytometry. Graphs showing percentage of live CD8$^+$ T cells expressing PD-1 from within the spleen and tumour. Mean plus SD of six mice within each group. PBS control compared with MG1 using paired student t-test statistical analysis.

7.3.3 MG1 in combination with anti-PD-1 antibody improves survival in an *in vivo* murine 4434 melanoma model

The previous sections identified that MG1 infection can increase PD-L1 expression on melanoma tumour cell lines *in vitro* and increases PD-1 expression levels on splenic $CD8^+$ T cells following IT delivery. Furthermore, the mean percentage of PD-1 expression increases at seven days compared to the 48 hour time point, both regarding splenic and tumoural T cells, reaching a particularly high mean of greater than 90% $PD\text{-}1^+$ in both PBS and MG1 treated tumoural T cells. In addition, as shown in chapter 6, the immunological changes generated from MG1 infection implied both an innate and adaptive response and therefore, the rational subsequent experiment was to determine whether the addition of anti-PD-1 antibody to IT MG1 therapy in the 4434 *in vivo* model could enhance therapeutic outcomes and lead to improved overall survival.

It was previously demonstrated in Chapter 5 that MG1 monotherapy could improve survival in 4434 tumours, leading to some mice displaying long term survivorship in the small and medium sized tumours. However, despite a minimal improvement in the treatment of larger sized tumours, MG1 failed to achieve any long-term tumour control. In addition, section 6.6 revealed changes in the quantities of cytokines (including the angiogenic factors angiopoietin 1 and 2, endoglin and VEGF and both CCL17 and IL-2 which can develop and recruit Tregs) released between smaller and larger tumours that potentially could be constricting the immunogenic potential of MG1. Therefore, it was hypothesised that the combination of anti-PD-1 antibody with IT MG1 may improve the outcomes in larger tumours compared to either therapy given alone.

Figure 33A illustrates the experimental schematic, showing that mice were implanted with subcutaneous 4434 tumours, which were allowed to grow until reaching approximately $150mm^3$. At this point, mice were randomised into four treatment groups: IT PBS with IP anti-PD-1 isotype, IT PBS with IP anti-PD-1 Ab, IT MG1-FLUC ($1x10^7$ pfu) with anti-PD-1 isotype, combination of IT

MG1-FLUC with anti-PD-1 Ab. IT treatment (either IT MG1-FLUC or IT PBS) was administered once only whereas IP treatment (IP anti-PD-1 Ab or IP anti-PD-1 isotype) was given twice weekly for four weeks. The anti-PD-1 antibody chosen for use was the commercially available InVivoMab rat anti-mouse PD-1 (CD279), clone RMP1-14, IgG2a-κ (2BScientific) given that this was the antibody used in previously published pre-clinical checkpoint inhibitor and MG1 combination experiments.[330]

Figure 33B demonstrates the overall survival for each treatment arm. Median survival was 41, 38, 46 and 77 days respectively for the four treatment groups. There was no significant difference in survival between the control group and anti-PD-1 monotherapy. The MG1 monotherapy group showed a marginally improved survival (p=0.0486) compared to PBS control. However, most notably, the combination group showed an improved survival when compared to both the anti-PD-1 Ab (p=0.0015) and the MG1 (p=0.0078) monotherapy groups, in addition to the control cohort (p=0.0008). Despite these survival gains, treatment did not lead to the long-term survival of any mice.

(A)

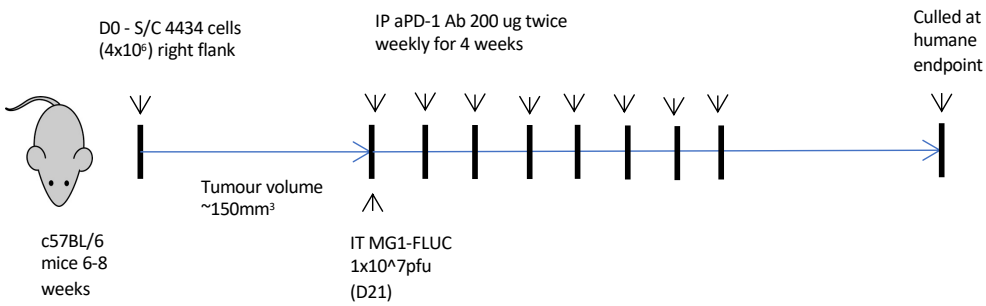

(B)

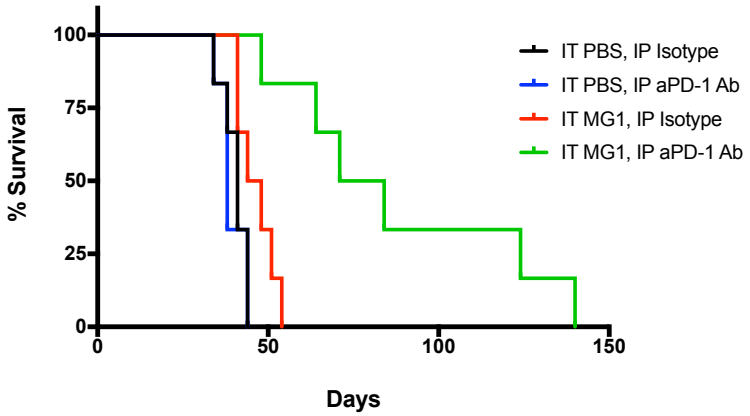

Figure 33: MG1 in combination with anti-PD-1 antibody improves survival in an *in vivo* murine 4434 melanoma model

4434 tumours that had grown to an average size of 150mm^3 were injected with IT MG1-FLUC 1x10^7 or PBS control. In addition, at the same time point they received either IP anti-PD-1 antibody or isotype which was continued twice weekly for four weeks, as shown in the experimental schematic (A). Kaplan-Meier survival curves of 4434 tumour bearing mice (six mice per group) following IT PBS control vs IT MG1, vs IP aPD-1 Ab and vs both treatments in combination (B).

7.3.4 Splenocytes from mice treated with MG1 in combination with anti-PD-1 antibody express greater IFN-γ following 4434 tumour cell rechallenge

The success of using combination MG1 with anti-PD-1 Ab in 'large' tumours, resulted in an interest to measure whether anti-tumour immune effects were involved in contributing to these survival gains.

Four murine treatment cohorts were investigated in a method similar to that described previously in section 6.10 with four mice per group. 10 days after establishing subcutaneous 4434 tumours, mice were treated in four differing groups with either IT MG1 ($1x10^7$ pfu) in combination with twice weekly IP anti-PD-1 antibody (200μg in 100 μL), either therapy given alone as monotherapy, or control with IT PBS and IP isotype antibody.

In section 7.3.2, it was shown that splenic $CD8^+$ cells increased their expression of PD-1 seven days, but not 48 hours, after MG1 treatment when compared to PBS control. Therefore, it was decided to ensure that sufficient time had elapsed, following treatment, to allow for splenic $CD8^+$ cells to increase their expression of PD-1. A 10 day time point was decided upon, which also allowed for practicalities of the experimental protocol. At this 10 day post-treatment time point, spleens from each mouse were harvested and processed into a single cell suspension and co-cultured alongside either PBS control or either 4434 or B16-F1 cells as described in section 6.10. Following a further 24 and 48 hours, sample supernatants were collected and analysed by ELISA for the presence of IFN-γ.

Figure 34A illustrates the concentration of IFN-γ measured from each treatment cohort at the 24-hour time point. It demonstrates that negligible IFN-γ is produced from the splenocytes alone group and from splenocytes exposed to B16-F1 cells. In the cohort re-exposed to 4434 cells, there was no significant difference in the quantity of IFN-γ released between the mice treated with PBS control or either anti-PD-1 antibody or MG1 alone, and IFN-γ released from these groups was minimal. However, splenocytes from the

mice treated with combination of MG1 with anti-PD-1 antibody resulted in a mean IFN-γ concentration of 138 pg/mL which was a significant increase when compared to PBS control (p=0.0097), anti-PD-1 antibody monotherapy (p=0.0097) and MG1 monotherapy (p=0.0107).

The 48-hour time point (Figure 34B), continued to show negligible IFN-γ release from splenocytes cultured alone. This was also the case with splenocytes from the PBS or anti-PD-1 alone treatment groups exposed *ex vivo* to B16-F1 cells. However, in the MG1 alone and the combination treatment groups, IFN-γ was released from splenocytes of two out of the four mice co-cultured with B16-F1 cells (perhaps suggesting some level of cross-presentation between different melanoma cell lines) however, there was no significant difference in IFN-γ release between any of the groups within the B16-F1 cohort. In contrast, splenocytes re-exposed to 4434 cells released a mean IFN-γ concentration of 3.8 pg/mL, 3.5 pg/mL, 38.3 pg/mL and 212 pg/mL from the PBS control, anti-PD-1 alone, MG1 alone and doublet combination treatment groups respectively. Treating mice with either MG1 alone or combination therapy led to a significant subsequent increase in IFN-γ (p=0.0492 and p=0.0005 respectively) when compared to PBS treatment control. Furthermore, the combination therapy treatment of MG1 with anti-PD-1 antibody resulted in splenocytes releasing significantly more IFN-γ compared to either MG1 or anti-PD-1 treatment given as monotherapy (p=0.0005 and p=0.0004 respectively).

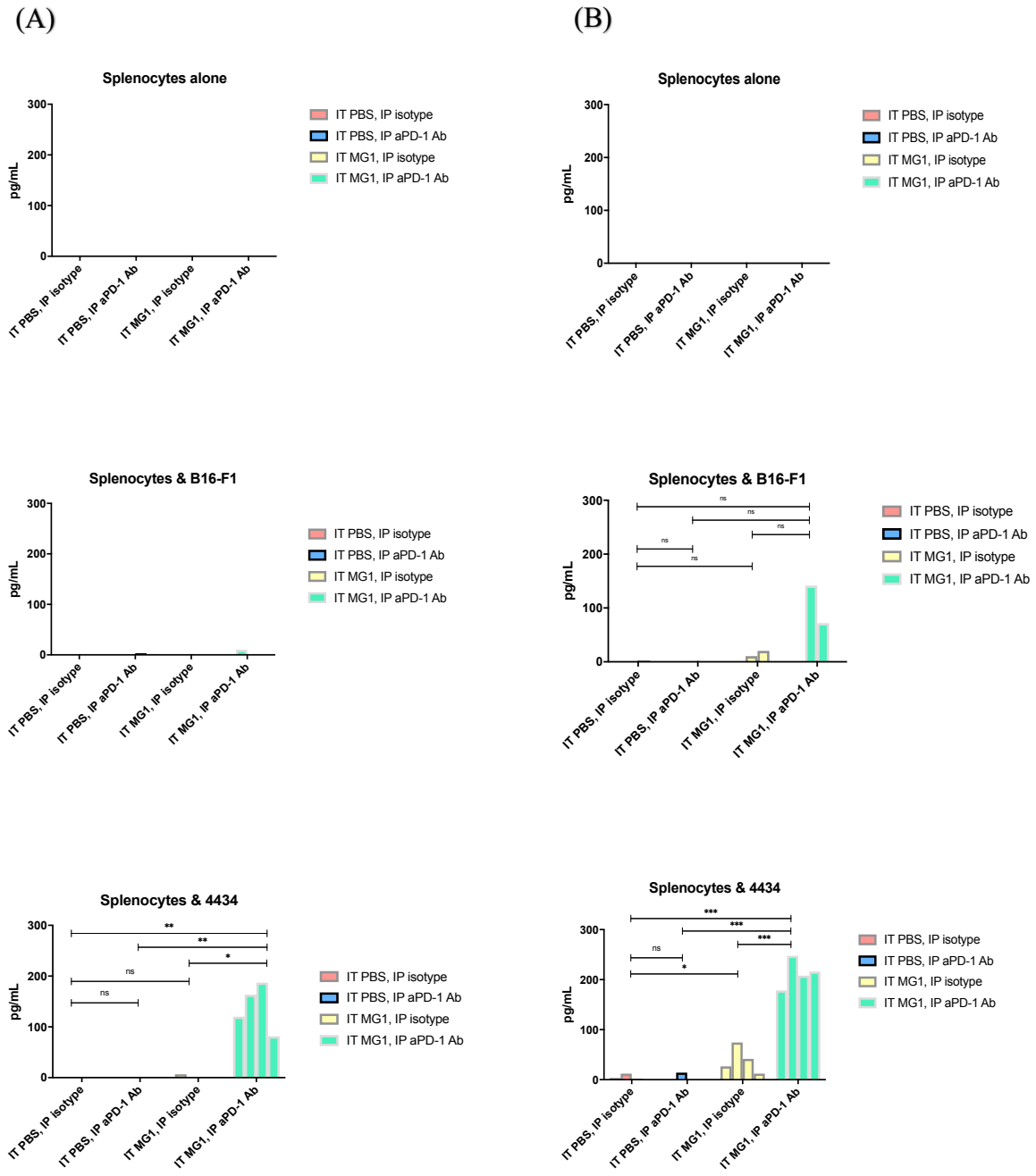

Figure 34: Splenocytes from mice treated with MG1 in combination with aPD-1 Ab express greater IFN-γ following 4434 tumour cell rechallenge.

4434 tumour bearing mice were treated with PBS control, IP aPD-1 Ab, IT MG1-FLUC or doublet combination. After 10 days, the spleens of each animal were explanted, prepared into a single cell suspension and co-cultured with 4434 or B16-F1 cells, or PBS control. Supernatants were collected after 24 hours (A) and 48 hours (B) and analysed with ELISA for the presence of IFN-γ. Graphs display the concentration of IFN-γ obtained following rechallenge. Graphs present the mean plus SD from four mice per group; multiple t-test statistical analysis corrected for multi-comparison using Holme-Sidak method.

7.4 Discussion

OVs are well recognised for their ability to infect, replicate in and kill tumour cells. More recently recognised is their role in effecting anti-tumour immunity. As shown earlier, MG1 possesses strong oncolytic properties and can generate signals indicative of ICD and subsequent innate and adaptive immune responses, consequently leading to successful therapy in a murine 4434 model. However, these *in vivo* benefits were observed predominantly in smaller tumours, with long-term survival gains being lost in a cohort of mice bearing larger tumours, implying either that the oncolytic effect of MG1 was insufficient and/or that tumours were able to escape the immunogenic changes induced by MG1 infection. Given the clinical challenges in treating patients with a greater burden of disease, and the aim of realising therapies that result in longer term control, this chapter has therefore explored combination treatments with MG1 in an attempt to enhance its beneficial anti-tumour effects.

The options for OV combination partners are numerous, however this chapter focused on OV immunotherapy combinations given the importance of ICIs as a standard of care in current melanoma management. Furthermore, OVs have demonstrated a capacity to convert the TME from immunologically “cold” to “hot”, with increases in infiltrating effector cells, thereby creating an environment for treatment synergy with ICB. Indeed, in several pre-clinical models, this has already translated *in vivo* into successful treatment outcomes using OV with immune checkpoint inhibitor combinations.[314] In melanoma models, combinations with ICB have been successful with several OVs including HSV, adenovirus, myxoma virus, reovirus, measles virus, VSV, NDV, coxsackievirus, poliovirus and Semliki Forest virus.[314] This approach has been taken forward into several combination clinical trials in melanoma including with HSV, adenovirus, coxsackievirus, poliovirus and MG1.[314] Pre-clinically, MG1 has been shown to increase tumour cell PD-L1 expression in a TNBC murine model and has improved therapeutic results when given in the neoadjuvant setting followed by postoperative combination anti-CTLA-4 and anti-PD-1 immune checkpoint blockade.[330]

In addition to ICI therapy, another rational OV combination partner involves modifying the TME through the depletion of the immunosuppressive Tregs, a novel approach which has recently shown promise.[121]

Evaluating the effects of MG1 on Tregs identified mixed effects within the spleen. Specifically, at the earlier 48-hour time point there was no change in the percentage of Treg cells, however, subsequently at seven days the percentage of Treg cells in the spleen increased (Figure 28). Within the tumour, no significant changes in the percentage of Tregs was observed between the control and MG1 treatment cohorts (Figure 29). Of note however, whilst absolute percentages may not have changes, MG1 may have altered the activation status of the Tregs present, however, this was not investigated.

Although, in itself, MG1 did not alter tumour Treg levels, it was hoped that depleting the tumoural Tregs may have resulted in a favourable TME, leading to enhanced MG1 activity. However, unfortunately no significant benefit was observed with anti-CD25 antibody above that seen with MG1 alone. The lack of MG1 related tumoural Treg changes may have explained the failure of the combination treatment to improve subsequent therapeutic outcomes. In addition, other more influential immunosuppressive factors, other than Tregs alone, such as inhibitory checkpoint activity, or the surrounding ECM, may have had a greater influence on MG1 treatment outcomes. Furthermore, it was possible that in this 4434 tumour model, the anti-CD25 Ab may not have significantly depleted the intratumoural Tregs, hence resulting in no observable difference between treatment groups. Whilst this should ideally have been confirmed (proving successful Treg depletion was complicated by the possibility that the depletion Ab was blocking the binding site for the FACS immunofluorescence CD25 detection Ab), it was felt that this was unlikely given the proven effectiveness of this anti-CD25 Ab, both within the published literature from another research group [121] and also from colleagues using the 4434 model within the Harrington-Melcher laboratory group.[129]

In contrast to the findings with anti-CD25 antibody, this project identified that combining MG1 with anti-PD-1 Ab in 'large' tumours led to improved survival outcomes above that seen with either virus or antibody therapy alone. The initial *in vitro* evaluation of this pathway observed that MG1 infection increased PD-L1 expression on 4434 tumour cells 24 hours following viral infection. It must be noted that these results were obtained from an *in vitro* model and therefore may not have been representative of the changes seen *in vivo*. Nevertheless, these *in vitro* results were in keeping with previous findings using MG1 in a TNBC model [330] and upregulating PD-L1 has also been observed in the clinical setting in matched pre- and post-T-VEC biopsy samples.[266]

The effect of MG1 on effector T cell expression of PD-1 was also assessed *in vivo*. At 48 hours following viral treatment, no significant differences were seen between groups. This time point was likely too early to see the effect of MG1, as by the seven day time point, PD-1 expression had significantly increased in splenic T cells in the MG1 group compared to PBS control. Meanwhile, within the tumour, the mean percentage of PD-1 expression was above 60% at 48 hours in both groups and above 90% in both groups at seven days. With such a high baseline tumoural T cell PD-1 expression at seven days, it was perhaps unsurprising there was no significant increase, unlike the seven day splenic results, as a result of the addition of MG1.

One limitation with these results is the time points used for evaluation. Two points were selected, 48 hours and seven days, in part due to the logistical aspects of the experimental protocol, but also as this was deemed a reasonable option for evaluating early and adaptive immune changes. However, choosing two finite time points results in major uncertainty with regards to any immune changes that may be occurring at any other time point, which are potentially more critical in matching the immune changes with the murine survival outcomes. In addition, no analysis was made of the tumour draining lymph node which may have been a more accurate surrogate for what lymphoid changes were taking place in the tumour vicinity.

The *ex vivo* experiment replicated that seen in section 6.10 although on this occasion, splenocyte IFN-γ release was assessed in mice that had received both MG1 alone and combination therapy. It revealed that at 24 hours, the combination treatment of MG1 with anti-PD-1 resulted in higher IFN-γ than either single agent alone or control (Figure 34A). By 48 hours following 4434 re-exposure, both the MG1 monotherapy group and the combination group had elevated IFN-γ detected, with the combination group significantly higher than the MG1 monotherapy cohort (Figure 34B). This significant finding was suggestive that the combination treatment is more effective in priming splenocytes before subsequent tumour re-exposure. Thereby, this gave strong support to the generation of anti-tumour immunological memory as a mechanistic process underpinning the observed survival benefits seen with combination therapy.

The combination of MG1 with anti-PD-1 therapy led to a survival advantage compared to either therapy given alone (Figure 33). Assessing survival with combination therapy was performed in larger tumours as the benefits of MG1 monotherapy were less pronounced with this tumour size. As mentioned, larger tumours are arguably less likely to be cleared solely from the oncolytic effects of an OV and therefore the therapeutic gain from combination therapy was likely due to added anti-tumour immune effects. Unfortunately, the combination did not lead to long-term survival of any of the treated mice. This may be due to the tumour developing immune escape mechanisms including the loss of MHC class I antigen presentation. In addition, alternative barriers to long-term immune tumour clearance may exist including immunosuppressive factors from tumoural Tregs or cells within the extracellular matrix. As shown in section 6.6, the larger tumours expressed higher quantities of cytokines involved in angiogenesis and ECM remodelling. Given these signals are known to be immunosuppressive, they are therefore potentially limiting the gains from the ICI. Larger tumours are more likely to display regions of hypoxia, in which T cells will be less effective. In addition, in a murine model, it was recently shown that heat inactivated OV (in this case a modified vaccinia virus) was more effective than its replication competent

counterpart in generating pro-inflammatory cytokines and type I IFN release *in vitro*, through signalling via the cGAS/STING pathway, and when in combination with ICB *in vivo* could eradicate tumour models of melanoma and lymphoma.[373] Therefore paradoxically, it is possible that the highly replicative and lytic MG1 may in fact be lessening the activity of ICB through reduced immunogenicity compared to an equivalent non-replicating virus. It would therefore be prudent and interesting to explore the effects of combining anti-PD-1 therapy with a heat or UV inactivated non-replicating MG1. However, it should be noted that the anti-PD-1 antibody given alone did not result in any observable benefit compared to PBS control, therefore potentially implying that the 4434 tumour model harbours a significant baseline level of resistance to ICB treatment, that MG1 was able to improve but not reverse adequately to result in tumour immune eradication. Therefore, as one dose of virus was sufficient to treat smaller tumours, it would be interesting to investigate whether an increased number of viral doses could result in improved therapy in larger tumours when combined with anti-PD-1. In addition, it may be that due to the tumour architecture and extracellular matrix that is established as the tumour grows larger, the anti-PD-1 antibody is unable to penetrate, migrate through and reach the intratumoural T cells without the oncolytic, destructive and inflammatory effects of the combination with MG1. To address this, the effectiveness of anti-PD-1 could be investigated in smaller tumours, both without, and in combination with, MG1.

To analyse these outcomes further, subsequent experiments could include an evaluation of the immunological structural landscape, and how this changes within larger tumours treated with PBS, MG1 and/or anti-PD-1 Ab, through for example, immunofluorescence microscopy. In addition, given the results from combining MG1 with both anti-PD-1 and anti-CTLA-4 antibodies in a TNBC model, it would be interesting to evaluate whether this doublet checkpoint blockade with MG1 leads to long term survival in the 4434 melanoma model. Furthermore, there may be additional mechanisms of immune modulation, through manipulating the MG1 genome with transgenes or with alternative exogenous antibody combinations, or through combinations with anti-angiogenic agents that enhance therapeutic outcomes.

Nevertheless, the combination treatment did improve murine survival outcomes and is an important addition to the literature as this has shown, for the first time, that MG1 in combination with anti-PD-1 checkpoint inhibition can enhance survival in a 4434 murine model of melanoma.

Chapter 8:

Discussion

8 Chapter 8: Discussion

8.1 Conclusions

The results presented within this project have analysed the therapeutic potential of the MG1 OV in models of melanoma. *In vitro*, it was demonstrated that MG1 can infect a range of murine and human cell lines that span the most common mutations found clinically in melanoma patients. In addition, it was demonstrated that MG1 can successfully replicate within tumour cells and exert a cytotoxic effect. These data were backed up by results with pancreatic cell lines and has therefore demonstrated, and added to our understanding of, the breadth of the potential oncolytic effects exerted by MG1.

T-VEC, the first widely approved OV is delivered by IT injection and one of the challenges in OV research is to develop OVs which can be administered systemically whilst delivering the virus to tumour sites not easily accessible by IT injection. In the data presented, following systemic delivery, MG1 demonstrates tumour tropism *in vivo*, as identified through both fluorescence imaging and by the identification of live replicating virus from *ex vivo* harvested tumours, sparing normal tissue. These properties indicate the potential suitability for MG1 in the treatment of patients with metastatic disease.

As a biological agent, ensuring safety is crucial, especially with systemic delivery, and in this regard, the MG1 *ex vivo* viral titres obtained diminish by 48 hours following viral treatment and coincide with the development of anti-MG1 neutralising antibodies. This therefore ensures that MG1 viral replication within host tumours does not proceed unchecked, thereby mitigating the potential for excess viral toxicity, again supporting the appropriateness of MG1 as a potential clinical agent.

Oncolysis alone is unlikely to be a sufficient mechanism for cancer elimination, hence there is interest in the potential for OV generated anti-tumour immunity. In addition to its tumour tropic and oncolytic effects, MG1 can also initiate ICD, a characteristic of MG1 that has not been reported previously. Furthermore,

MG1 infection resulted in the increased production of IFN-β from melanoma cell lines both *in vitro* and *in vivo*. Additionally, analysis of tumour cytokine and mRNA production demonstrated features involved in immune signalling upregulation in response to MG1 infection.

These findings warranted further flow cytometry exploration of the immune TME following IT MG1 in the 4434 murine melanoma model. MG1 engaged the innate immune response as seen in the significantly increased activation status of NK cells within both the spleen and tumour 48 hours following viral treatment. Furthermore, MG1 led to an expansion in both the percentage of, and the level of activation of, $CD8^+$ T cells within the spleen, and increased the percentage of $CD8^+$ T cells within the TME.

Evidence for the capacity of MG1 to engage the adaptive immune system was supported by findings from *ex vivo* splenocytes of MG1 treated mice releasing the highest concentration of IFN-γ when rechallenged with 4434 cells. Furthermore, 4434 tumours failed to establish when given as a rechallenge in mice successfully treated previously with MG1. These findings have not been reported previously and are indicative of the immunogenic potential of MG1 in the treatment of melanoma.

The interplay between the oncolytic and immunogenic effects from MG1 were borne out in the *in vivo* therapy experiments. IT MG1 extended the survival of mice bearing 4434 tumours; 'small' tumours were almost all successfully eliminated, the growth of 'large' tumours was delayed but with no long-term survival, and the treatment of 'medium sized' tumours resulted in a mixed picture of delayed growth with some tumours eliminated. These results pointed primarily to the oncolytic properties of MG1 as the success of MG1 treatment was proportional to the tumour size at the point of treatment.

An explanation for the failure to eliminate larger 4434 tumours through oncolysis alone is likely to be due to the anti-viral immune responses that clear the virus following infection. In addition to the early development of

neutralising antibodies, the upregulation of tumoural IFN-β in response to the presence of MG1 causes nearby cells to heighten their anti-viral defence. In addition to mitigating the oncolytic effects of MG1, the cytokine and RNA-Seq data comparing small with large tumours also suggest an immune explanation for the failure of MG1 to eliminate large tumours. These data indicated that larger tumours are immunologically 'colder' than smaller tumours, and that MG1 treatment is more effective in generating a favourable immune TME in smaller tumours compared to larger tumours.

Having identified both oncolytic and immunogenic effects of MG1, the project analysed combinatorial approaches to enhancing the anti-tumour immune response, in an attempt to improve therapy. Firstly, MG1 was noted not to alter the percentage of tumoural Tregs and therefore it was proposed that depleting these immunosuppressive cells may impact treatment results. Unfortunately however, the MG1 and anti-CD25 antibody combination treatment failed to improve therapeutic outcomes. In contrast, MG1 was noted to upregulate PD-L1 receptors on 4434 cells *in vitro*. Additionally, RNA-Seq analysis identified that MG1 increased PD-1 RNA expression in both small and large tumours. Furthermore, MG1 led to an increase in IFN-γ released from splenocytes from mice treated with MG1 and anti-PD-1 combination compared to other cohorts, and improved the treatment outcomes in mice bearing larger tumours above that previously seen with MG1 monotherapy.

These final results indicated that as well as an oncolytic effect, the immune changes observed following MG1 infection can be harnessed with combination treatment and result in an increased survival beyond that observed with either treatment given alone. This is the first time that MG1 in combination with ICB has been shown to improve outcomes in a model of melanoma, and therefore gives credence to translating this approach into the clinical arena.

8.2 Improving experimental studies

In vivo studies, in particular, could be improved in order to gain greater confidence in the statistical results. Primarily, to avoid excessive use of mice,

in vivo studies were conducted only once per experiment. Ideally, these would be repeated in order to improve their validity. This could also be improved by repeating the experiments with an increased number of mice per group and to increase or adjust the time points at which tumours were harvested for immunological phenotyping by flow cytometry.

Immunological panels were constrained by the number of laser channels available within the flow cytometer and an increased spectrum of immune cells, particularly myeloid cells, and changes in additional immune checkpoints could have been investigated.

8.3 Future Studies

One notable disparity observed was the survival outcome data between the MG1 treated 4434 and B16-F1 tumours. The greater success achieved in treating the 4434 model led to an experimental focus on that tumour model. The different *ex vivo* quantity of IFN-β observed between the two models may in part have contributed to the distinct outcomes between the B16-F1 and 4434 models. However, as discussed, multiple other variables may underpin these differences and understanding these factors would have been an interesting area for exploration as this may have identified factors that determine the success of OV treatment and how to modulate these differences for therapeutic gain.

As the 4434 model harbours a *BRAF* V600E mutation, a further avenue of exploration could investigate the result of combining BRAF targeted therapy with MG1 to assess for a synergistic or additional benefit with these treatments in combination.

Treatment outcomes in the 4434 model varied between smaller and larger tumours following one dose of MG1. In future *in vivo* therapy experiments, an increased number of viral doses could be administered to see if this alters outcomes in larger tumours. Furthermore, UV inactivated MG1 could be

assessed to evaluate if this leads to a greater immune stimulating, rather than oncolytic, effect and how this might impact on therapeutic success.

In addition to the differences in treatment outcomes between small and large tumours, differences in the cytokine profiles between these cohorts were identified using the Protein Profiler. The RNA-Seq data also identified a 'colder' immune environment in the larger tumours compared to smaller tumours. Furthermore, MG1 treatment of both small and large tumours resulted in the smaller tumours becoming immunologically 'hotter' than the larger tumours. To support these results, analysis of the changing immune phenotypes by flow cytometry between smaller and larger tumours may have identified different characteristics that could have been targeted in future experiments. Future flow cytometry experiments could also look specifically at other immune cells including myeloid populations, particularly given the myeloid changes identified in mRNA expression from the RNA-Seq analysis data.

Immune phenotyping by flow cytometry highlighted the MG1-induced early upregulation of NK cell activity. To evaluate whether the activation of NK cells also occurs in a human melanoma model, the levels of degranulation of human NK cells in response to exposure to human melanoma cell lines or MG1 could be evaluated. In addition, regarding the murine 4434 model, to conclude that the innate immune changes observed within the spleen and tumour are contributing to tumour elimination and delaying tumour growth, a repeat experiment to assess if these therapeutic gains are negated following the depletion of NK cells, would be appropriate. Furthermore, given the expanded percentage of $CD8^+$ T cells at the later time point, a similar protocol depleting $CD8^+$ T cells should be conducted to evaluate their role in survival outcomes secondary to the development of an adaptive anti-tumour response.

The combination of MG1 with anti-PD-1 antibody improved outcomes in larger tumours, however, analysing these treatment groups by flow cytometry would assist in understanding which immunological changes may be responsible for these improved outcomes. In addition, to improve longer term outcomes using

MG1 together with immune checkpoint inhibition, alternative MG1 combinations with other ICBs could be considered. Finally, modifications to the MG1 genetic backbone could be incorporated in order to enhance the capacity for MG1 to mount an immune response, thereby enabling MG1 to comprise both potent oncolytic and immunogenic anti-tumour potential.

Chapter 9:

Appendix

9 Chapter 9: Appendix

9.1 Melanoma staging

(T, N and M descriptors adapted from: AJCC Melanoma of the Skin Staging - 8th Edition)

Primary Tumour (T)		
Tx	Primary tumour cannot be assessed	
T0	No evidence of primary tumour	
Tis	Melanoma *in situ*	
T1	Melanoma 1.0 mm or less in thickness	
T2	Melanoma 1.1 - 2.0 mm	
T3	Melanoma 2.1 – 4.0 mm	
T4	Melanoma >4.0 mm	
Note	a and b subcategories of T are assigned based on ulceration and thickness	
T1	≤1.0 mm	a: Breslow <0.8 mm without ulceration b: Breslow 0.8 – 1.0 mm without ulceration or ≤ 1.0 mm with ulceration
T2	1.1 – 2.0 mm	a: without ulceration b: with ulceration
T3	2.1 – 4.0 mm	a: without ulceration b: with ulceration
T4	>4.0 mm	a: without ulceration b: with ulceration

Regional Lymph Nodes (N)		
Nx	Regional LNs cannot be assessed	
N0	No regional metastasis detected	
N1-3	Regional metastases based on the number of metastatic nodes, number of palpable metastatic nodes on clinical exam, and presence or absence of microsatellite invasion (MSI)	
Note	N1-3 and a-c subcategories assigned as shown below:	
N1	0-1 node	a: clinically occult, no MSI b: clinically detected, no MSI c: 0 nodes, MSI present
N2	1-3 nodes	a: 2-3 nodes clinically occult, no MSI b: 2-3 nodes clinically detected, no MSI c: 1 node clinical or occult, MSI present
N3	>1 nodes	a: >3 nodes, all clinically occult, no MSI b: >3 nodes, ≥1 clinically detected or matted, no MSI c: >1 nodes clinical or occult, MSI present

Distant Metastasis (M)	
M0	No detectable evidence of distant metastases
M1a	Metastases to skin, subcutaneous, or distant LNs
M1b	Metastases to lung
M1c	Metastases to all over visceral sites
M1d	Metastases to brain
Note	Serum LDH is incorporated into the M category as shown below:
M1a-d	LDH not assessed
M1a-d(0)	LDH normal
M1a-d(1)	LDH elevated

Pathological Staging			
Stage	**T**	**N**	**M**
0	Tis	N0	M0
IA	T1a	N0	M0
IB	T1b	N0	M0
	T2a		
IIA	T2b	N0	M0
	T3a		
IIB	T3b	N0	M0
	T4a		
IIC	T4b	N0	M0
IIIA	T1-2a	N1a	M0
	T1-2a	N2a	
IIIB	T0	N1b-c	M0
	T1-2a	N1b-c	
	T1-2a	N2b	
	T2b-3a	N1a-2b	
IIIC	T0	N2b-c	M0
	T0	N3b-c	
	T1a-3a	N2c-3c	
	T3b-4a	Any N	
	T4b	N1a-2c	
IIID	T4b	N3a-c	M0
IV	Any T	Any N	M1

9.2 Western blot antibodies

Antibody	Primary/ Secondary	Species of origin	Dilution	Supplier	Catalogue reference
RIG-I (D14G6)	Primary	Rabbit	1:1000	Cell signalling	#3743
pTBK1 (ser172)	Primary	Rabbit	1:1000	Cell signalling	#5483
pIRF3 (Ser396)	Primary	Rabbit	1:1000	Cell signalling	#3743
Tubulin	Primary	Mouse	1:1000	Sigma	T5168
Goat anti-mouse IgG, Alexa Fluor 680	Secondary	Goat	1:10000	Invitrogen	A-21058
IRDye® 800CW Goat anti-Rabbit IgG	Secondary	Goat	1:10000	LI-COR	926-32211

9.3 Flow cytometry antibodies

Target	Clone	Conjugate	Cat. Number	Dilution
CD4	RM4.4	V500	560783 (BD Bioscience)	1:300
CD8	53-6.7	Pe-Cy7	100722	1:300
CD8	53-6.7	BV650	100742	1:300
CD3	17A2	PerCp Cy5.5	100218	1:100
CD45	30-F11	AF700	103128	1:300
CD25	PC61	BV650	102037	1:100
CD25	PC61	APC	102011	1:100
NK1.1	PK136	PE-Dazzle594	108748	1:100
CD69	H1.2F3	FITC	104506	1:100
FoxP3	FJK-16s	eFluor 450	48-5773-82 (Thermo Fisher)	1:100
Ki67	16A8	PE	652404	1:100
GrzB	GB11	AF647	515406	1:100
CTLA-4	UC10-489	PE	106306	1:100
PD-1	29F.1A12	Pe-Cy7	135216	1:100
Hamster IgG	HTK888	PE	400907	1:100
Rat IgG2a κ	RTK2758	PE	400507	1:100
Rat IgG2a κ	RTK2758	PE-Cy7	400521	1:100
Rat IgG2a κ	eBR2a	Pacific Blue	48-4321-80 (Thermo Fisher)	1:100
Rat IgG2a κ	MOPC-21	APC	400135	1:100
Biotin Rat anti-mouse CD16/CD32	2.4G2	FITC	553143 (BD biosciences)	1:100

Chapter 10:

References

10 Chapter 10: References

1. (CRUK), C.R.U. [cited 2021; Available from: https://www.cancerresearchuk.org/health-professional/cancer-statistics/statistics-by-cancer-type/melanoma-skin-cancer.
2. Wolchok, J.D., et al., *Development of ipilimumab: a novel immunotherapeutic approach for the treatment of advanced melanoma.* Annals of the New York Academy of Sciences, 2013. **1291**(1): p. 1-13.
3. Ajani, J.A., *In H, Sano T, et al. Stomach.* AJCC Cancer staging manual. 8th ed. New York: Springer-Verlag, 2016.
4. Garbe, C., et al., *Systematic review of medical treatment in melanoma: current status and future prospects.* Oncologist, 2011. **16**(1): p. 5-24.
5. Eggermont, A.M. and J.M. Kirkwood, *Re-evaluating the role of dacarbazine in metastatic melanoma: what have we learned in 30 years?* Eur J Cancer, 2004. **40**(12): p. 1825-36.
6. Eggermont, A.M. and D. Schadendorf, *Melanoma and immunotherapy.* Hematol Oncol Clin North Am, 2009. **23**(3): p. 547-64, ix-x.
7. *Genomic Classification of Cutaneous Melanoma.* Cell, 2015. **161**(7): p. 1681-96.
8. Davies, H., et al., *Mutations of the BRAF gene in human cancer.* Nature, 2002. **417**(6892): p. 949-54.
9. Davis, E.J., et al., *Melanoma: What do all the mutations mean?* Cancer, 2018. **124**(17): p. 3490-3499.
10. Bardeesy, N., et al., *Role of epidermal growth factor receptor signaling in RAS-driven melanoma.* Molecular and cellular biology, 2005. **25**(10): p. 4176-4188.
11. Sullivan, R.J. and K. Flaherty, *MAP kinase signaling and inhibition in melanoma.* Oncogene, 2013. **32**(19): p. 2373-9.
12. Chapman, P.B., et al., *Improved survival with vemurafenib in melanoma with BRAF V600E mutation.* N Engl J Med, 2011. **364**(26): p. 2507-16.
13. Flaherty, K.T., et al., *Improved survival with MEK inhibition in BRAF-mutated melanoma.* N Engl J Med, 2012. **367**(2): p. 107-14.
14. Long, G.V., et al., *Combined BRAF and MEK inhibition versus BRAF inhibition alone in melanoma.* N Engl J Med, 2014. **371**(20): p. 1877-88.
15. Dummer, R., et al., *Overall survival in patients with BRAF-mutant melanoma receiving encorafenib plus binimetinib versus vemurafenib or encorafenib (COLUMBUS): a multicentre, open-label, randomised, phase 3 trial.* Lancet Oncol, 2018. **19**(10): p. 1315-1327.
16. Larkin, J., et al., *Combined vemurafenib and cobimetinib in BRAF-mutated melanoma.* N Engl J Med, 2014. **371**(20): p. 1867-76.
17. Long, G.V., et al., *Adjuvant Dabrafenib plus Trametinib in Stage III BRAF-Mutated Melanoma.* N Engl J Med, 2017. **377**(19): p. 1813-1823.

18. Dumaz, N., et al., *In melanoma, RAS mutations are accompanied by switching signaling from BRAF to CRAF and disrupted cyclic AMP signaling.* Cancer Res, 2006. **66**(19): p. 9483-91.
19. Nazarian, R., et al., *Melanomas acquire resistance to B-RAF(V600E) inhibition by RTK or N-RAS upregulation.* Nature, 2010. **468**(7326): p. 973-7.
20. Nicola, N. *NRAS in melanoma: ESMA biomarker factsheet* . 2015; Available from: https://oncologypro.esmo.org/education-library/factsheets-on-biomarkers/nras-in-melanoma.
21. Devitt, B., et al., *Clinical outcome and pathological features associated with NRAS mutation in cutaneous melanoma.* Pigment Cell Melanoma Res, 2011. **24**(4): p. 666-72.
22. Curtin, J.A., et al., *Distinct sets of genetic alterations in melanoma.* N Engl J Med, 2005. **353**(20): p. 2135-47.
23. Jakob, J.A., et al., *NRAS mutation status is an independent prognostic factor in metastatic melanoma.* Cancer, 2012. **118**(16): p. 4014-23.
24. Ellerhorst, J.A., et al., *Clinical correlates of NRAS and BRAF mutations in primary human melanoma.* Clin Cancer Res, 2011. **17**(2): p. 229-35.
25. Dummer, R., et al., *Binimetinib versus dacarbazine in patients with advanced NRAS-mutant melanoma (NEMO): a multicentre, open-label, randomised, phase 3 trial.* Lancet Oncol, 2017. **18**(4): p. 435-445.
26. Kiuru, M. and K.J. Busam, *The NF1 gene in tumor syndromes and melanoma.* Laboratory investigation; a journal of technical methods and pathology, 2017. **97**(2): p. 146-157.
27. Cirenajwis, H., et al., *NF1-mutated melanoma tumors harbor distinct clinical and biological characteristics.* Mol Oncol, 2017. **11**(4): p. 438-451.
28. Curtin, J.A., et al., *Somatic activation of KIT in distinct subtypes of melanoma.* J Clin Oncol, 2006. **24**(26): p. 4340-6.
29. Guo, J., et al., *Phase II, open-label, single-arm trial of imatinib mesylate in patients with metastatic melanoma harboring c-Kit mutation or amplification.* J Clin Oncol, 2011. **29**(21): p. 2904-9.
30. Hodi, F.S., et al., *Imatinib for melanomas harboring mutationally activated or amplified KIT arising on mucosal, acral, and chronically sun-damaged skin.* J Clin Oncol, 2013. **31**(26): p. 3182-90.
31. Meng, D. and R.D. Carvajal, *KIT as an Oncogenic Driver in Melanoma: An Update on Clinical Development.* Am J Clin Dermatol, 2019. **20**(3): p. 315-323.
32. Delyon, J., C. Lebbe, and N. Dumaz, *Targeted therapies in melanoma beyond BRAF: targeting NRAS-mutated and KIT-mutated melanoma.* Curr Opin Oncol, 2020. **32**(2): p. 79-84.
33. Carvajal, R.D., et al., *Phase II Study of Nilotinib in Melanoma Harboring KIT Alterations Following Progression to Prior KIT Inhibition.* Clin Cancer Res, 2015. **21**(10): p. 2289-96.
34. Guo, J., et al., *Efficacy and safety of nilotinib in patients with KIT-mutated metastatic or inoperable melanoma: final results from the global, single-arm, phase II TEAM trial.* Ann Oncol, 2017. **28**(6): p. 1380-1387.

35. Kalinsky, K., et al., *A phase 2 trial of dasatinib in patients with locally advanced or stage IV mucosal, acral, or vulvovaginal melanoma: A trial of the ECOG-ACRIN Cancer Research Group (E2607).* Cancer, 2017. **123**(14): p. 2688-2697.
36. Lee, S.J., et al., *Phase II Trial of Nilotinib in Patients With Metastatic Malignant Melanoma Harboring KIT Gene Aberration: A Multicenter Trial of Korean Cancer Study Group (UN10-06).* Oncologist, 2015. **20**(11): p. 1312-9.
37. Carvajal, R.D., et al., *Effect of selumetinib vs chemotherapy on progression-free survival in uveal melanoma: a randomized clinical trial.* Jama, 2014. **311**(23): p. 2397-405.
38. Nathan, P., et al., *Overall Survival Benefit with Tebentafusp in Metastatic Uveal Melanoma.* New England Journal of Medicine, 2021. **385**(13): p. 1196-1206.
39. Alexandrov, L.B., et al., *Signatures of mutational processes in human cancer.* Nature, 2013. **500**(7463): p. 415-421.
40. Attrill, G.H., et al., *The tumour immune landscape and its implications in cutaneous melanoma.* Pigment Cell Melanoma Res, 2020.
41. Schumacher, T.N. and R.D. Schreiber, *Neoantigens in cancer immunotherapy.* Science, 2015. **348**(6230): p. 69-74.
42. Hanahan, D. and R.A. Weinberg, *Hallmarks of cancer: the next generation.* Cell, 2011. **144**(5): p. 646-74.
43. Coley, W.B., *II. Contribution to the Knowledge of Sarcoma.* Ann Surg, 1891. **14**(3): p. 199-220.
44. McCarthy, E.F., *The toxins of William B. Coley and the treatment of bone and soft-tissue sarcomas.* The Iowa orthopaedic journal, 2006. **26**: p. 154-158.
45. Sharma, P., et al., *Primary, Adaptive, and Acquired Resistance to Cancer Immunotherapy.* Cell, 2017. **168**(4): p. 707-723.
46. Ehrlich, P., *Ueber den jetzigen Stand der Karzinomforschung*. 1908.
47. Burnet, M., *Cancer: a biological approach. III. Viruses associated with neoplastic conditions. IV. Practical applications.* Br Med J, 1957. **1**(5023): p. 841-7.
48. Thomas, L. and H. Lawrence, *Cellular and humoral aspects of the hypersensitive states.* New York: Hoeber-Harper, 1959: p. 529-32.
49. Rygaard, J. and C.O. Povlsen, *The mouse mutant nude does not develop spontaneous tumours. An argument against immunological surveillance.* Acta Pathol Microbiol Scand B Microbiol Immunol, 1974. **82**(1): p. 99-106.
50. Stutman, O., *Tumor development after 3-methylcholanthrene in immunologically deficient athymic-nude mice.* Science, 1974. **183**(4124): p. 534-6.
51. Dunn, G.P., et al., *Cancer immunoediting: from immunosurveillance to tumor escape.* Nat Immunol, 2002. **3**(11): p. 991-8.
52. Lavin, Y., et al., *Regulation of macrophage development and function in peripheral tissues.* Nat Rev Immunol, 2015. **15**(12): p. 731-44.
53. Noy, R. and J.W. Pollard, *Tumor-associated macrophages: from mechanisms to therapy.* Immunity, 2014. **41**(1): p. 49-61.

54. Gonzalez, H., C. Hagerling, and Z. Werb, *Roles of the immune system in cancer: from tumor initiation to metastatic progression.* Genes Dev, 2018. **32**(19-20): p. 1267-1284.
55. Fridman, W.H., et al., *The immune contexture in human tumours: impact on clinical outcome.* Nat Rev Cancer, 2012. **12**(4): p. 298-306.
56. Shojaei, F., et al., *Role of myeloid cells in tumor angiogenesis and growth.* Trends Cell Biol, 2008. **18**(8): p. 372-8.
57. O'Sullivan, C., et al., *Secretion of epidermal growth factor by macrophages associated with breast carcinoma.* Lancet, 1993. **342**(8864): p. 148-9.
58. Mantovani, A., et al., *Tumour-associated macrophages as treatment targets in oncology.* Nat Rev Clin Oncol, 2017. **14**(7): p. 399-416.
59. Tham, M., et al., *Melanoma-initiating cells exploit M2 macrophage TGFβ and arginase pathway for survival and proliferation.* Oncotarget, 2014. **5**(23): p. 12027-42.
60. Wang, T., et al., *BRAF Inhibition Stimulates Melanoma-Associated Macrophages to Drive Tumor Growth.* Clin Cancer Res, 2015. **21**(7): p. 1652-64.
61. Kolaczkowska, E. and P. Kubes, *Neutrophil recruitment and function in health and inflammation.* Nat Rev Immunol, 2013. **13**(3): p. 159-75.
62. Donskov, F., *Immunomonitoring and prognostic relevance of neutrophils in clinical trials.* Semin Cancer Biol, 2013. **23**(3): p. 200-7.
63. Keizman, D., et al., *The association of pre-treatment neutrophil to lymphocyte ratio with response rate, progression free survival and overall survival of patients treated with sunitinib for metastatic renal cell carcinoma.* Eur J Cancer, 2012. **48**(2): p. 202-8.
64. Jensen, T.O., et al., *Intratumoral neutrophils and plasmacytoid dendritic cells indicate poor prognosis and are associated with pSTAT3 expression in AJCC stage I/II melanoma.* Cancer, 2012. **118**(9): p. 2476-85.
65. Li, Y.W., et al., *Intratumoral neutrophils: a poor prognostic factor for hepatocellular carcinoma following resection.* J Hepatol, 2011. **54**(3): p. 497-505.
66. Motzer, R.J., et al., *Nivolumab plus Ipilimumab versus Sunitinib in Advanced Renal-Cell Carcinoma.* New England Journal of Medicine, 2018. **378**(14): p. 1277-1290.
67. Jamieson, T., et al., *Inhibition of CXCR2 profoundly suppresses inflammation-driven and spontaneous tumorigenesis.* J Clin Invest, 2012. **122**(9): p. 3127-44.
68. Fridlender, Z.G., et al., *Polarization of tumor-associated neutrophil phenotype by TGF-beta: "N1" versus "N2" TAN.* Cancer Cell, 2009. **16**(3): p. 183-94.
69. Governa, V., et al., *The Interplay Between Neutrophils and CD8(+) T Cells Improves Survival in Human Colorectal Cancer.* Clin Cancer Res, 2017. **23**(14): p. 3847-3858.
70. Takeshima, T., et al., *Key role for neutrophils in radiation-induced antitumor immune responses: Potentiation with G-CSF.* Proc Natl Acad Sci U S A, 2016. **113**(40): p. 11300-11305.
71. Hurt, B., et al., *Cancer-promoting mechanisms of tumor-associated neutrophils.* Am J Surg, 2017. **214**(5): p. 938-944.

72. Houghton, A.M., et al., *Neutrophil elastase-mediated degradation of IRS-1 accelerates lung tumor growth.* Nat Med, 2010. **16**(2): p. 219-23.
73. Wang, T.T., et al., *Tumour-activated neutrophils in gastric cancer foster immune suppression and disease progression through GM-CSF-PD-L1 pathway.* Gut, 2017. **66**(11): p. 1900-1911.
74. Wculek, S.K. and I. Malanchi, *Neutrophils support lung colonization of metastasis-initiating breast cancer cells.* Nature, 2015. **528**(7582): p. 413-7.
75. Nabizadeh, J.A., et al., *The Complement C3a Receptor Contributes to Melanoma Tumorigenesis by Inhibiting Neutrophil and CD4+ T Cell Responses.* J Immunol, 2016. **196**(11): p. 4783-92.
76. Albanesi, M., et al., *Neutrophils mediate antibody-induced antitumor effects in mice.* Blood, 2013. **122**(18): p. 3160-4.
77. Cerwenka, A. and L.L. Lanier, *Natural killer cell memory in infection, inflammation and cancer.* Nat Rev Immunol, 2016. **16**(2): p. 112-23.
78. Marcus, A., et al., *Recognition of tumors by the innate immune system and natural killer cells.* Adv Immunol, 2014. **122**: p. 91-128.
79. Coca, S., et al., *The prognostic significance of intratumoral natural killer cells in patients with colorectal carcinoma.* Cancer, 1997. **79**(12): p. 2320-8.
80. Ishigami, S., et al., *Prognostic value of intratumoral natural killer cells in gastric carcinoma.* Cancer, 2000. **88**(3): p. 577-83.
81. Al-Shibli, K., et al., *The prognostic value of intraepithelial and stromal innate immune system cells in non-small cell lung carcinoma.* Histopathology, 2009. **55**(3): p. 301-12.
82. Chevrier, S., et al., *An Immune Atlas of Clear Cell Renal Cell Carcinoma.* Cell, 2017. **169**(4): p. 736-749.e18.
83. Villegas, F.R., et al., *Prognostic significance of tumor infiltrating natural killer cells subset CD57 in patients with squamous cell lung cancer.* Lung Cancer, 2002. **35**(1): p. 23-8.
84. Voskoboinik, I., M.J. Smyth, and J.A. Trapani, *Perforin-mediated target-cell death and immune homeostasis.* Nat Rev Immunol, 2006. **6**(12): p. 940-52.
85. Erdag, G., et al., *Immunotype and immunohistologic characteristics of tumor-infiltrating immune cells are associated with clinical outcome in metastatic melanoma.* Cancer Res, 2012. **72**(5): p. 1070-80.
86. Kaufman, K.L., et al., *Surface antigen profiles of leukocytes and melanoma cells in lymph node metastases are associated with survival in AJCC stage III melanoma patients.* Clin Exp Metastasis, 2014. **31**(4): p. 407-21.
87. Jacquelot, N., et al., *Immunophenotyping of Stage III Melanoma Reveals Parameters Associated with Patient Prognosis.* J Invest Dermatol, 2016. **136**(5): p. 994-1001.
88. Vivier, E., et al., *Innate or adaptive immunity? The example of natural killer cells.* Science (New York, N.Y.), 2011. **331**(6013): p. 44-49.
89. Lee, H., et al., *Integrated molecular and immunophenotypic analysis of NK cells in anti-PD-1 treated metastatic melanoma patients.* Oncoimmunology, 2019. **8**(2): p. e1537581.

90. Lee, Y.S. and K.J. Radford, *The role of dendritic cells in cancer.* Int Rev Cell Mol Biol, 2019. **348**: p. 123-178.
91. Roberts, E.W., et al., *Critical Role for CD103(+)/CD141(+) Dendritic Cells Bearing CCR7 for Tumor Antigen Trafficking and Priming of T Cell Immunity in Melanoma.* Cancer Cell, 2016. **30**(2): p. 324-336.
92. Labidi-Galy, S.I., et al., *Quantitative and functional alterations of plasmacytoid dendritic cells contribute to immune tolerance in ovarian cancer.* Cancer Res, 2011. **71**(16): p. 5423-34.
93. Nsengimana, J., et al., *β-Catenin-mediated immune evasion pathway frequently operates in primary cutaneous melanomas.* J Clin Invest, 2018. **128**(5): p. 2048-2063.
94. Mukherji, B., et al., *Induction of antigen-specific cytolytic T cells in situ in human melanoma by immunization with synthetic peptide-pulsed autologous antigen presenting cells.* Proc Natl Acad Sci U S A, 1995. **92**(17): p. 8078-82.
95. Nestle, F.O., et al., *Vaccination of melanoma patients with peptide- or tumor lysate-pulsed dendritic cells.* Nat Med, 1998. **4**(3): p. 328-32.
96. Wilgenhof, S., et al., *Phase II Study of Autologous Monocyte-Derived mRNA Electroporated Dendritic Cells (TriMixDC-MEL) Plus Ipilimumab in Patients With Pretreated Advanced Melanoma.* J Clin Oncol, 2016. **34**(12): p. 1330-8.
97. Clemente, C.G., et al., *Prognostic value of tumor infiltrating lymphocytes in the vertical growth phase of primary cutaneous melanoma.* Cancer, 1996. **77**(7): p. 1303-10.
98. Azimi, F., et al., *Tumor-infiltrating lymphocyte grade is an independent predictor of sentinel lymph node status and survival in patients with cutaneous melanoma.* J Clin Oncol, 2012. **30**(21): p. 2678-83.
99. Dieu-Nosjean, M.C., et al., *Long-term survival for patients with non-small-cell lung cancer with intratumoral lymphoid structures.* J Clin Oncol, 2008. **26**(27): p. 4410-7.
100. Tosolini, M., et al., *Clinical impact of different classes of infiltrating T cytotoxic and helper cells (Th1, th2, treg, th17) in patients with colorectal cancer.* Cancer Res, 2011. **71**(4): p. 1263-71.
101. Kondo, T., et al., *Favorable prognosis of renal cell carcinoma with increased expression of chemokines associated with a Th1-type immune response.* Cancer Sci, 2006. **97**(8): p. 780-6.
102. Zhang, L., et al., *Intratumoral T cells, recurrence, and survival in epithelial ovarian cancer.* N Engl J Med, 2003. **348**(3): p. 203-13.
103. Stanton, S.E. and M.L. Disis, *Clinical significance of tumor-infiltrating lymphocytes in breast cancer.* J Immunother Cancer, 2016. **4**: p. 59.
104. Liakou, C.I., et al., *Focus on TILs: Prognostic significance of tumor infiltrating lymphocytes in human bladder cancer.* Cancer Immun, 2007. **7**: p. 10.
105. Ling, A., et al., *The intratumoural subsite and relation of CD8(+) and FOXP3(+) T lymphocytes in colorectal cancer provide important prognostic clues.* Br J Cancer, 2014. **110**(10): p. 2551-9.
106. Gebhardt, T., et al., *Tissue-resident memory T cells in tissue homeostasis, persistent infection, and cancer surveillance.* Immunol Rev, 2018. **283**(1): p. 54-76.

107. Edwards, J., et al., *Prevalence and Cellular Distribution of Novel Immune Checkpoint Targets Across Longitudinal Specimens in Treatment-naïve Melanoma Patients: Implications for Clinical Trials.* Clin Cancer Res, 2019. **25**(11): p. 3247-3258.
108. Van Acker, H.H., et al., *CD56 in the Immune System: More Than a Marker for Cytotoxicity?* Front Immunol, 2017. **8**: p. 892.
109. Malik, B.T., et al., *Resident memory T cells in the skin mediate durable immunity to melanoma.* Sci Immunol, 2017. **2**(10).
110. Park, S.L., et al., *Tissue-resident memory CD8(+) T cells promote melanoma-immune equilibrium in skin.* Nature, 2019. **565**(7739): p. 366-371.
111. Veatch, J.R., et al., *Tumor-infiltrating BRAFV600E-specific CD4+ T cells correlated with complete clinical response in melanoma.* J Clin Invest, 2018. **128**(4): p. 1563-1568.
112. Shankaran, V., et al., *IFNgamma and lymphocytes prevent primary tumour development and shape tumour immunogenicity.* Nature, 2001. **410**(6832): p. 1107-11.
113. Kalams, S.A. and B.D. Walker, *The critical need for CD4 help in maintaining effective cytotoxic T lymphocyte responses.* J Exp Med, 1998. **188**(12): p. 2199-204.
114. Galon, J., et al., *Type, density, and location of immune cells within human colorectal tumors predict clinical outcome.* Science, 2006. **313**(5795): p. 1960-4.
115. Halim, L., et al., *An Atlas of Human Regulatory T Helper-like Cells Reveals Features of Th2-like Tregs that Support a Tumorigenic Environment.* Cell Rep, 2017. **20**(3): p. 757-770.
116. De Monte, L., et al., *Intratumor T helper type 2 cell infiltrate correlates with cancer-associated fibroblast thymic stromal lymphopoietin production and reduced survival in pancreatic cancer.* J Exp Med, 2011. **208**(3): p. 469-78.
117. Grotz, T.E., et al., *Evidence of Th2 polarization of the sentinel lymph node (SLN) in melanoma.* Oncoimmunology, 2015. **4**(8): p. e1026504.
118. Muranski, P., et al., *Tumor-specific Th17-polarized cells eradicate large established melanoma.* Blood, 2008. **112**(2): p. 362-73.
119. Mahnke, K., T. Bedke, and A.H. Enk, *Regulatory conversation between antigen presenting cells and regulatory T cells enhance immune suppression.* Cell Immunol, 2007. **250**(1-2): p. 1-13.
120. Jones, E., et al., *Depletion of CD25+ regulatory cells results in suppression of melanoma growth and induction of autoreactivity in mice.* Cancer Immun, 2002. **2**: p. 1.
121. Arce Vargas, F., et al., *Fc-Optimized Anti-CD25 Depletes Tumor-Infiltrating Regulatory T Cells and Synergizes with PD-1 Blockade to Eradicate Established Tumors.* Immunity, 2017. **46**(4): p. 577-586.
122. Shang, B., et al., *Prognostic value of tumor-infiltrating FoxP3+ regulatory T cells in cancers: a systematic review and meta-analysis.* Sci Rep, 2015. **5**: p. 15179.
123. Campbell, D.J., *Control of Regulatory T Cell Migration, Function, and Homeostasis.* J Immunol, 2015. **195**(6): p. 2507-13.

124. Quezada, S.A., et al., *Limited tumor infiltration by activated T effector cells restricts the therapeutic activity of regulatory T cell depletion against established melanoma.* J Exp Med, 2008. **205**(9): p. 2125-38.
125. Jacobs, J.F., et al., *Dendritic cell vaccination in combination with anti-CD25 monoclonal antibody treatment: a phase I/II study in metastatic melanoma patients.* Clin Cancer Res, 2010. **16**(20): p. 5067-78.
126. Rech, A.J., et al., *CD25 blockade depletes and selectively reprograms regulatory T cells in concert with immunotherapy in cancer patients.* Sci Transl Med, 2012. **4**(134): p. 134ra62.
127. Peggs, K.S., et al., *Principles and use of anti-CTLA4 antibody in human cancer immunotherapy.* Current opinion in immunology, 2006. **18**(2): p. 206-213.
128. Quezada, S.A., et al., *CTLA4 blockade and GM-CSF combination immunotherapy alters the intratumor balance of effector and regulatory T cells.* J Clin Invest, 2006. **116**(7): p. 1935-45.
129. Bozhanova, G., et al., *Abstract 3415: Mutant BRAF small molecule inhibition enhances oncolytic herpes virus immunotherapy through increased immune cell recruitment and activation in melanoma.* Cancer Research, 2020. **80**(16 Supplement): p. 3415.
130. Wouters, M.C.A. and B.H. Nelson, *Prognostic Significance of Tumor-Infiltrating B Cells and Plasma Cells in Human Cancer.* Clin Cancer Res, 2018. **24**(24): p. 6125-6135.
131. Kroeger, D.R., K. Milne, and B.H. Nelson, *Tumor-Infiltrating Plasma Cells Are Associated with Tertiary Lymphoid Structures, Cytolytic T-Cell Responses, and Superior Prognosis in Ovarian Cancer.* Clin Cancer Res, 2016. **22**(12): p. 3005-15.
132. Cipponi, A., et al., *Neogenesis of lymphoid structures and antibody responses occur in human melanoma metastases.* Cancer Res, 2012. **72**(16): p. 3997-4007.
133. Bosisio, F.M., et al., *Plasma cells in primary melanoma. Prognostic significance and possible role of IgA.* Mod Pathol, 2016. **29**(4): p. 347-58.
134. Somasundaram, R., et al., *Tumor-associated B-cells induce tumor heterogeneity and therapy resistance.* Nat Commun, 2017. **8**(1): p. 607.
135. Ribas, A. and J.D. Wolchok, *Cancer immunotherapy using checkpoint blockade.* Science, 2018. **359**(6382): p. 1350-1355.
136. Allison, J.P. and M.F. Krummel, *The Yin and Yang of T cell costimulation.* Science, 1995. **270**(5238): p. 932-3.
137. Alegre, M.L., K.A. Frauwirth, and C.B. Thompson, *T-cell regulation by CD28 and CTLA-4.* Nat Rev Immunol, 2001. **1**(3): p. 220-8.
138. Pardoll, D.M., *The blockade of immune checkpoints in cancer immunotherapy.* Nature Reviews Cancer, 2012. **12**(4): p. 252-264.
139. Freeman, G.J., et al., *Engagement of the PD-1 immunoinhibitory receptor by a novel B7 family member leads to negative regulation of lymphocyte activation.* J Exp Med, 2000. **192**(7): p. 1027-34.
140. Baumeister, S.H., et al., *Coinhibitory Pathways in Immunotherapy for Cancer.* Annu Rev Immunol, 2016. **34**: p. 539-73.

141. Ishida, Y., et al., *Induced expression of PD-1, a novel member of the immunoglobulin gene superfamily, upon programmed cell death.* Embo j, 1992. **11**(11): p. 3887-95.
142. Hodi, F.S., et al., *Improved survival with ipilimumab in patients with metastatic melanoma.* N Engl J Med, 2010. **363**(8): p. 711-23.
143. Robert, C., et al., *Ipilimumab plus dacarbazine for previously untreated metastatic melanoma.* N Engl J Med, 2011. **364**(26): p. 2517-26.
144. Robert, C., et al., *Nivolumab in previously untreated melanoma without BRAF mutation.* N Engl J Med, 2015. **372**(4): p. 320-30.
145. Robert, C., et al., *Pembrolizumab versus Ipilimumab in Advanced Melanoma.* N Engl J Med, 2015. **372**(26): p. 2521-32.
146. Robert, C., et al., *Pembrolizumab versus ipilimumab in advanced melanoma (KEYNOTE-006): post-hoc 5-year results from an open-label, multicentre, randomised, controlled, phase 3 study.* Lancet Oncol, 2019. **20**(9): p. 1239-1251.
147. Larkin, J., et al., *Combined Nivolumab and Ipilimumab or Monotherapy in Untreated Melanoma.* N Engl J Med, 2015. **373**(1): p. 23-34.
148. Wolchok, J.D., et al., *Overall Survival with Combined Nivolumab and Ipilimumab in Advanced Melanoma.* N Engl J Med, 2017. **377**(14): p. 1345-1356.
149. Larkin, J., et al., *Five-Year Survival with Combined Nivolumab and Ipilimumab in Advanced Melanoma.* N Engl J Med, 2019. **381**(16): p. 1535-1546.
150. Atkins, M.B. and J. Larkin, *Immunotherapy Combined or Sequenced With Targeted Therapy in the Treatment of Solid Tumors: Current Perspectives.* J Natl Cancer Inst, 2016. **108**(6): p. djv414.
151. Eggermont, A.M., et al., *Adjuvant ipilimumab versus placebo after complete resection of high-risk stage III melanoma (EORTC 18071): a randomised, double-blind, phase 3 trial.* Lancet Oncol, 2015. **16**(5): p. 522-30.
152. Weber, J., et al., *Adjuvant Nivolumab versus Ipilimumab in Resected Stage III or IV Melanoma.* N Engl J Med, 2017. **377**(19): p. 1824-1835.
153. Ascierto, P.A., et al., *Adjuvant nivolumab versus ipilimumab in resected stage IIIB-C and stage IV melanoma (CheckMate 238): 4-year results from a multicentre, double-blind, randomised, controlled, phase 3 trial.* Lancet Oncol, 2020. **21**(11): p. 1465-1477.
154. Eggermont, A.M.M., et al., *Adjuvant Pembrolizumab versus Placebo in Resected Stage III Melanoma.* N Engl J Med, 2018. **378**(19): p. 1789-1801.
155. Luke, J.J., et al., *KEYNOTE-716: Phase III study of adjuvant pembrolizumab versus placebo in resected high-risk stage II melanoma.* Future Oncol, 2020. **16**(3): p. 4429-4438.
156. Gide, T.N., et al., *Primary and Acquired Resistance to Immune Checkpoint Inhibitors in Metastatic Melanoma.* Clin Cancer Res, 2018. **24**(6): p. 1260-1270.
157. Chen, P.-L., et al., *Analysis of immune signatures in longitudinal tumor samples yields insight into biomarkers of response and mechanisms*

of resistance to immune checkpoint blockade. Cancer discovery, 2016. **6**(8): p. 827-837.
158. Liu, C., et al., *BRAF inhibition increases tumor infiltration by T cells and enhances the antitumor activity of adoptive immunotherapy in mice.* Clin Cancer Res, 2013. **19**(2): p. 393-403.
159. Huang, H., et al., *VEGF suppresses T-lymphocyte infiltration in the tumor microenvironment through inhibition of NF-κB-induced endothelial activation.* The FASEB Journal, 2015. **29**(1): p. 227-238.
160. Ni, K. and H.C. O'Neill, *The role of dendritic cells in T cell activation.* Immunol Cell Biol, 1997. **75**(3): p. 223-30.
161. Ladányi, A., et al., *Density of DC-LAMP(+) mature dendritic cells in combination with activated T lymphocytes infiltrating primary cutaneous melanoma is a strong independent prognostic factor.* Cancer Immunol Immunother, 2007. **56**(9): p. 1459-69.
162. Gabrilovich, D.I., et al., *Production of vascular endothelial growth factor by human tumors inhibits the functional maturation of dendritic cells.* Nat Med, 1996. **2**(10): p. 1096-103.
163. Ohm, J.E. and D.P. Carbone, *VEGF as a mediator of tumor-associated immunodeficiency.* Immunol Res, 2001. **23**(2-3): p. 263-72.
164. Parsa, A.T., et al., *Loss of tumor suppressor PTEN function increases B7-H1 expression and immunoresistance in glioma.* Nat Med, 2007. **13**(1): p. 84-8.
165. Peng, W., et al., *Loss of PTEN Promotes Resistance to T Cell-Mediated Immunotherapy.* Cancer Discov, 2016. **6**(2): p. 202-16.
166. Gajewski, T.F., H. Schreiber, and Y.X. Fu, *Innate and adaptive immune cells in the tumor microenvironment.* Nat Immunol, 2013. **14**(10): p. 1014-22.
167. Holmgaard, R.B., et al., *Tumor-Expressed IDO Recruits and Activates MDSCs in a Treg-Dependent Manner.* Cell Rep, 2015. **13**(2): p. 412-24.
168. Holmgaard, R.B., et al., *Indoleamine 2, 3-dioxygenase is a critical resistance mechanism in antitumor T cell immunotherapy targeting CTLA-4.* Journal of Experimental Medicine, 2013. **210**(7): p. 1389-1402.
169. Hugo, W., et al., *Genomic and Transcriptomic Features of Response to Anti-PD-1 Therapy in Metastatic Melanoma.* Cell, 2016. **165**(1): p. 35-44.
170. Gao, J., et al., *Loss of IFN-γ Pathway Genes in Tumor Cells as a Mechanism of Resistance to Anti-CTLA-4 Therapy.* Cell, 2016. **167**(2): p. 397-404.e9.
171. Zaretsky, J.M., et al., *Mutations Associated with Acquired Resistance to PD-1 Blockade in Melanoma.* N Engl J Med, 2016. **375**(9): p. 819-29.
172. Liakou, C.I., et al., *CTLA-4 blockade increases IFNgamma-producing CD4+ICOShi cells to shift the ratio of effector to regulatory T cells in cancer patients.* Proc Natl Acad Sci U S A, 2008. **105**(39): p. 14987-92.
173. Shin, D.S., et al., *Primary Resistance to PD-1 Blockade Mediated by JAK1/2 Mutations.* Cancer Discov, 2017. **7**(2): p. 188-201.

174. Antonia, S.J., et al., *Overall Survival with Durvalumab after Chemoradiotherapy in Stage III NSCLC.* N Engl J Med, 2018. **379**(24): p. 2342-2350.
175. Bellmunt, J., et al., *Pembrolizumab as Second-Line Therapy for Advanced Urothelial Carcinoma.* N Engl J Med, 2017. **376**(11): p. 1015-1026.
176. Reck, M., et al., *Pembrolizumab versus Chemotherapy for PD-L1-Positive Non-Small-Cell Lung Cancer.* N Engl J Med, 2016. **375**(19): p. 1823-1833.
177. Madore, J., et al., *PD-L1 negative status is associated with lower mutation burden, differential expression of immune-related genes, and worse survival in stage III melanoma.* Clinical Cancer Research, 2016. **22**(15): p. 3915-3923.
178. Gabrilovich, D.I., *Myeloid-Derived Suppressor Cells.* Cancer Immunol Res, 2017. **5**(1): p. 3-8.
179. Yang, L., et al., *Expansion of myeloid immune suppressor Gr+CD11b+ cells in tumor-bearing host directly promotes tumor angiogenesis.* Cancer Cell, 2004. **6**(4): p. 409-21.
180. Bronte, V., et al., *L-arginine metabolism in myeloid cells controls T-lymphocyte functions.* Trends Immunol, 2003. **24**(6): p. 302-6.
181. Tcyganov, E., et al., *Plasticity of myeloid-derived suppressor cells in cancer.* Curr Opin Immunol, 2018. **51**: p. 76-82.
182. Chen, J., et al., *Suppression of T cells by myeloid-derived suppressor cells in cancer.* Hum Immunol, 2017. **78**(2): p. 113-119.
183. Diaz-Montero, C.M., J. Finke, and A.J. Montero, *Myeloid-derived suppressor cells in cancer: therapeutic, predictive, and prognostic implications.* Semin Oncol, 2014. **41**(2): p. 174-84.
184. Diaz-Montero, C.M., et al., *Increased circulating myeloid-derived suppressor cells correlate with clinical cancer stage, metastatic tumor burden, and doxorubicin-cyclophosphamide chemotherapy.* Cancer Immunol Immunother, 2009. **58**(1): p. 49-59.
185. Montero, A.J., et al., *Myeloid-derived suppressor cells in cancer patients: a clinical perspective.* J Immunother, 2012. **35**(2): p. 107-15.
186. Solito, S., et al., *A human promyelocytic-like population is responsible for the immune suppression mediated by myeloid-derived suppressor cells.* Blood, 2011. **118**(8): p. 2254-65.
187. Sinha, P., et al., *Cross-talk between myeloid-derived suppressor cells and macrophages subverts tumor immunity toward a type 2 response.* J Immunol, 2007. **179**(2): p. 977-83.
188. Meyer, C., et al., *Frequencies of circulating MDSC correlate with clinical outcome of melanoma patients treated with ipilimumab.* Cancer Immunol Immunother, 2014. **63**(3): p. 247-57.
189. Hu, W., et al., *Tumor-associated macrophages in cancers.* Clin Transl Oncol, 2016. **18**(3): p. 251-8.
190. Kuang, D.M., et al., *Activated monocytes in peritumoral stroma of hepatocellular carcinoma foster immune privilege and disease progression through PD-L1.* J Exp Med, 2009. **206**(6): p. 1327-37.
191. Ruffell, B., et al., *Macrophage IL-10 blocks CD8+ T cell-dependent responses to chemotherapy by suppressing IL-12 expression in intratumoral dendritic cells.* Cancer Cell, 2014. **26**(5): p. 623-37.

192. Gajewski, T.F., *Identifying and overcoming immune resistance mechanisms in the melanoma tumor microenvironment.* Clinical Cancer Research, 2006. **12**(7): p. 2326s-2330s.
193. Jandus, C., et al., *Selective accumulation of differentiated FOXP3(+) CD4 (+) T cells in metastatic tumor lesions from melanoma patients compared to peripheral blood.* Cancer Immunol Immunother, 2008. **57**(12): p. 1795-805.
194. Viehl, C.T., et al., *Depletion of CD4+CD25+ regulatory T cells promotes a tumor-specific immune response in pancreas cancer-bearing mice.* Ann Surg Oncol, 2006. **13**(9): p. 1252-8.
195. Hong, M., et al., *Chemotherapy induces intratumoral expression of chemokines in cutaneous melanoma, favoring T-cell infiltration and tumor control.* Cancer research, 2011. **71**(22): p. 6997-7009.
196. Kuo, P.T., et al., *The Role of CXCR3 and Its Chemokine Ligands in Skin Disease and Cancer.* Front Med (Lausanne), 2018. **5**: p. 271.
197. Harlin, H., et al., *Chemokine expression in melanoma metastases associated with CD8+ T-cell recruitment.* Cancer research, 2009. **69**(7): p. 3077-3085.
198. Highfill, S.L., et al., *Disruption of CXCR2-mediated MDSC tumor trafficking enhances anti-PD1 efficacy.* Sci Transl Med, 2014. **6**(237): p. 237ra67.
199. Lippitz, B.E., *Cytokine patterns in patients with cancer: a systematic review.* Lancet Oncol, 2013. **14**(6): p. e218-28.
200. Lin, R.L. and L.J. Zhao, *Mechanistic basis and clinical relevance of the role of transforming growth factor-β in cancer.* Cancer Biol Med, 2015. **12**(4): p. 385-93.
201. Teicher, B.A. and S.P. Fricker, *CXCL12 (SDF-1)/CXCR4 pathway in cancer.* Clin Cancer Res, 2010. **16**(11): p. 2927-31.
202. Lebrun, J.J., *The Dual Role of TGFβ in Human Cancer: From Tumor Suppression to Cancer Metastasis.* ISRN Mol Biol, 2012. **2012**: p. 381428.
203. Wargo, J.A., et al., *Association of the diversity and composition of the gut microbiome with responses and survival (PFS) in metastatic melanoma (MM) patients (pts) on anti-PD-1 therapy*. 2017, American Society of Clinical Oncology.
204. Vétizou, M., et al., *Anticancer immunotherapy by CTLA-4 blockade relies on the gut microbiota.* Science, 2015. **350**(6264): p. 1079-1084.
205. Baruch, E.N., et al., *Fecal microbiota transplant promotes response in immunotherapy-refractory melanoma patients.* Science, 2021. **371**(6529): p. 602-609.
206. Restifo, N.P., et al., *Loss of functional beta 2-microglobulin in metastatic melanomas from five patients receiving immunotherapy.* J Natl Cancer Inst, 1996. **88**(2): p. 100-8.
207. Koller, B.H., et al., *Normal development of mice deficient in beta 2M, MHC class I proteins, and CD8+ T cells.* Science, 1990. **248**(4960): p. 1227-30.
208. Zijlstra, M., et al., *Beta 2-microglobulin deficient mice lack CD4-8+ cytolytic T cells.* Nature, 1990. **344**(6268): p. 742-6.
209. He, Y., et al., *TIM-3, a promising target for cancer immunotherapy.* Onco Targets Ther, 2018. **11**: p. 7005-7009.

210. Anderson, A.C., N. Joller, and V.K. Kuchroo, *Lag-3, Tim-3, and TIGIT: Co-inhibitory Receptors with Specialized Functions in Immune Regulation.* Immunity, 2016. **44**(5): p. 989-1004.
211. Tawbi, H.A., et al., *Relatlimab and Nivolumab versus Nivolumab in Untreated Advanced Melanoma.* N Engl J Med, 2022. **386**(1): p. 24-34.
212. Dupuytren, G., *De la gangrène spontanée générale et partielle des tumeurs cancéreuses du sein.* J Hebdom Med, 1829. **4**: p. 38-41.
213. Lecoq, H., *[Discovery of the first virus, the tobacco mosaic virus: 1892 or 1898?].* C R Acad Sci III, 2001. **324**(10): p. 929-33.
214. Dock, G., *The influence of complicating diseases upon leukaemia.* The American Journal of the Medical Sciences (1827-1924), 1904. **127**(4): p. 563.
215. De Pace, N., *Sulla scomparsa di un enorme cancro vegetante del collo dell'utero senza cura chirurgica.* 1912.
216. Levaditi, C. and S. Nicolau, *Sur le culture du virus vaccinal dans les neoplasmes epithelieux.* CR Soc Biol, 1922. **86**: p. 928.
217. Hoster, H.A., R.P. Zanes, and E. von Haam, *Studies in Hodgkin's Syndrome: IX. The Association of "Viral" Hepatitis and Hodgkin's Disease (A Preliminary Report).* Cancer research, 1949. **9**(8): p. 473-480.
218. Kelly, E. and S.J. Russell, *History of oncolytic viruses: genesis to genetic engineering.* Molecular therapy, 2007. **15**(4): p. 651-659.
219. Alberts, P., et al., *The advent of oncolytic virotherapy in oncology: The Rigvir® story.* European Journal of Pharmacology, 2018. **837**: p. 117-126.
220. Harrington, K., et al., *Optimizing oncolytic virotherapy in cancer treatment.* Nat Rev Drug Discov, 2019. **18**(9): p. 689-706.
221. Russell, L., et al., *Oncolytic Viruses: Priming Time for Cancer Immunotherapy.* BioDrugs, 2019. **33**(5): p. 485-501.
222. Maroun, J., et al., *Designing and building oncolytic viruses.* Future virology, 2017. **12**(4): p. 193-213.
223. Kelly, E. and S.J. Russell, *History of oncolytic viruses: genesis to genetic engineering.* Mol Ther, 2007. **15**(4): p. 651-9.
224. Buijs, P.R., et al., *Oncolytic viruses: From bench to bedside with a focus on safety.* Hum Vaccin Immunother, 2015. **11**(7): p. 1573-84.
225. Lawler, S.E., et al., *Oncolytic viruses in cancer treatment: a review.* JAMA oncology, 2017. **3**(6): p. 841-849.
226. Newcombe, N.G., et al., *Enterovirus capsid interactions with decay-accelerating factor mediate lytic cell infection.* Journal of virology, 2004. **78**(3): p. 1431-9.
227. Shafren, D.R., et al., *Oncolysis of human ovarian cancers by echovirus type 1.* International journal of cancer. Journal international du cancer, 2005. **115**(2): p. 320-8.
228. Anderson, B.D., et al., *High CD46 receptor density determines preferential killing of tumor cells by oncolytic measles virus.* Cancer research, 2004. **64**(14): p. 4919-26.
229. Ochiai, H., et al., *Targeted therapy for glioblastoma multiforme neoplastic meningitis with intrathecal delivery of an oncolytic recombinant poliovirus.* Clin Cancer Res, 2006. **12**(4): p. 1349-54.

230. Kohlhapp, F.J. and H.L. Kaufman, *Molecular Pathways: Mechanism of Action for Talimogene Laherparepvec, a New Oncolytic Virus Immunotherapy.* Clin Cancer Res, 2016. **22**(5): p. 1048-54.
231. Kanerva, A., et al., *Targeting adenovirus to the serotype 3 receptor increases gene transfer efficiency to ovarian cancer cells.* Clinical cancer research : an official journal of the American Association for Cancer Research, 2002. **8**(1): p. 275-80.
232. Dmitriev, I., et al., *An adenovirus vector with genetically modified fibers demonstrates expanded tropism via utilization of a coxsackievirus and adenovirus receptor-independent cell entry mechanism.* Journal of virology, 1998. **72**(12): p. 9706-13.
233. Thomson, B.J., *Viruses and apoptosis.* Int J Exp Pathol, 2001. **82**(2): p. 65-76.
234. Bischoff, J.R., et al., *An adenovirus mutant that replicates selectively in p53-deficient human tumor cells.* Science, 1996. **274**(5286): p. 373-6.
235. Balachandran, S. and G.N. Barber, *Defective translational control facilitates vesicular stomatitis virus oncolysis.* Cancer cell, 2004. **5**(1): p. 51-65.
236. Fiola, C., et al., *Tumor selective replication of Newcastle disease virus: association with defects of tumor cells in antiviral defence.* International journal of cancer. Journal international du cancer, 2006. **119**(2): p. 328-38.
237. Hummel, J.L., E. Safroneeva, and K.L. Mossman, *The role of ICP0-Null HSV-1 and interferon signaling defects in the effective treatment of breast adenocarcinoma.* Mol Ther, 2005. **12**(6): p. 1101-10.
238. Hummel, J.L., E. Safroneeva, and K.L. Mossman, *The role of ICP0-Null HSV-1 and interferon signaling defects in the effective treatment of breast adenocarcinoma.* Molecular therapy : the journal of the American Society of Gene Therapy, 2005. **12**(6): p. 1101-10.
239. Bergmann, M., et al., *A genetically engineered influenza A virus with ras-dependent oncolytic properties.* Cancer research, 2001. **61**(22): p. 8188-93.
240. Symons, J.A., A. Alcami, and G.L. Smith, *Vaccinia virus encodes a soluble type I interferon receptor of novel structure and broad species specificity.* Cell, 1995. **81**(4): p. 551-60.
241. Strong, J.E., et al., *The molecular basis of viral oncolysis: usurpation of the Ras signaling pathway by reovirus.* The EMBO journal, 1998. **17**(12): p. 3351-62.
242. Coffey, M.C., et al., *Reovirus therapy of tumors with activated Ras pathway.* Science, 1998. **282**(5392): p. 1332-4.
243. He, B., M. Gross, and B. Roizman, *The gamma(1)34.5 protein of herpes simplex virus 1 complexes with protein phosphatase 1alpha to dephosphorylate the alpha subunit of the eukaryotic translation initiation factor 2 and preclude the shutoff of protein synthesis by double-stranded RNA-activated protein kinase.* Proceedings of the National Academy of Sciences of the United States of America, 1997. **94**(3): p. 843-8.
244. Martuza, R.L., *Conditionally replicating herpes vectors for cancer therapy.* J Clin Invest, 2000. **105**(7): p. 841-6.

245. Perez, O.D., et al., *Design and selection of Toca 511 for clinical use: modified retroviral replicating vector with improved stability and gene expression.* Mol Ther, 2012. **20**(9): p. 1689-98.
246. Kawashima, T., et al., *Telomerase-specific replication-selective virotherapy for human cancer.* Clin Cancer Res, 2004. **10**(1 Pt 1): p. 285-92.
247. Ruiz, A.J. and S.J. Russell, *MicroRNAs and oncolytic viruses.* Curr Opin Virol, 2015. **13**: p. 40-8.
248. Russell, S.J. and K.W. Peng, *Viruses as anticancer drugs.* Trends Pharmacol Sci, 2007. **28**(7): p. 326-33.
249. Nande, R., C.M. Howard, and P.P. Claudio, *Ultrasound-mediated oncolytic virus delivery and uptake for increased therapeutic efficacy: state of art.* Oncolytic Virother, 2015. **4**: p. 193-205.
250. Smith, H.G., et al., *PD-1 Blockade Following Isolated Limb Perfusion with Vaccinia Virus Prevents Local and Distant Relapse of Soft-tissue Sarcoma.* Clin Cancer Res, 2019. **25**(11): p. 3443-3454.
251. Russell, S.J., K.W. Peng, and J.C. Bell, *Oncolytic virotherapy.* Nat Biotechnol, 2012. **30**(7): p. 658-70.
252. Tesfay, M.Z., et al., *Vesiculovirus neutralization by natural IgM and complement.* J Virol, 2014. **88**(11): p. 6148-57.
253. Peng, K.W., et al., *Using clinically approved cyclophosphamide regimens to control the humoral immune response to oncolytic viruses.* Gene Ther, 2013. **20**(3): p. 255-61.
254. Miest, T.S., et al., *Envelope-chimeric entry-targeted measles virus escapes neutralization and achieves oncolysis.* Mol Ther, 2011. **19**(10): p. 1813-20.
255. Lee, J., et al., *The Antiviral Apparatus: STING and Oncolytic Virus Restriction.* Mol Ther Oncolytics, 2019. **13**: p. 7-13.
256. Gujar, S., et al., *Antitumor Benefits of Antiviral Immunity: An Underappreciated Aspect of Oncolytic Virotherapies.* Trends Immunol, 2018. **39**(3): p. 209-221.
257. Bommareddy, P.K., et al., *Oncolytic virus immunotherapy induces immunogenic cell death and overcomes STING deficiency in melanoma.* Oncoimmunology, 2019. **8**(7): p. 1591875.
258. Galluzzi, L., et al., *Immunogenic cell death in cancer and infectious disease.* Nat Rev Immunol, 2017. **17**(2): p. 97-111.
259. Donnelly, O.G., et al., *Measles virus causes immunogenic cell death in human melanoma.* Gene Ther, 2013. **20**(1): p. 7-15.
260. Prestwich, R.J., et al., *Tumor infection by oncolytic reovirus primes adaptive antitumor immunity.* Clin Cancer Res, 2008. **14**(22): p. 7358-66.
261. Toda, M., et al., *Herpes simplex virus as an in situ cancer vaccine for the induction of specific anti-tumor immunity.* Hum Gene Ther, 1999. **10**(3): p. 385-93.
262. Burke, S., et al., *Oncolytic Newcastle disease virus activation of the innate immune response and priming of antitumor adaptive responses in vitro.* Cancer Immunol Immunother, 2020. **69**(6): p. 1015-1027.
263. Zhang, J., et al., *Maraba MG1 virus enhances natural killer cell function via conventional dendritic cells to reduce postoperative metastatic disease.* Mol Ther, 2014. **22**(7): p. 1320-1332.

264. Errington, F., et al., *Reovirus activates human dendritic cells to promote innate antitumor immunity.* J Immunol, 2008. **180**(9): p. 6018-26.
265. López, C.B., et al., *Sendai virus infection induces efficient adaptive immunity independently of type I interferons.* J Virol, 2006. **80**(9): p. 4538-45.
266. Ribas, A., et al., *Oncolytic Virotherapy Promotes Intratumoral T Cell Infiltration and Improves Anti-PD-1 Immunotherapy.* Cell, 2017. **170**(6): p. 1109-1119.e10.
267. van Vloten, J.P., et al., *Critical Interactions between Immunogenic Cancer Cell Death, Oncolytic Viruses, and the Immune System Define the Rational Design of Combination Immunotherapies.* J Immunol, 2018. **200**(2): p. 450-458.
268. Sattentau, Q., *Avoiding the void: cell-to-cell spread of human viruses.* Nat Rev Microbiol, 2008. **6**(11): p. 815-26.
269. Bateman, A.R., et al., *Viral fusogenic membrane glycoproteins kill solid tumor cells by nonapoptotic mechanisms that promote cross presentation of tumor antigens by dendritic cells.* Cancer Res, 2002. **62**(22): p. 6566-78.
270. Ayala-Breton, C., et al., *Faster replication and higher expression levels of viral glycoproteins give the vesicular stomatitis virus/measles virus hybrid VSV-FH a growth advantage over measles virus.* J Virol, 2014. **88**(15): p. 8332-9.
271. Fu, X., et al., *Expression of a fusogenic membrane glycoprotein by an oncolytic herpes simplex virus potentiates the viral antitumor effect.* Mol Ther, 2003. **7**(6): p. 748-54.
272. Simpson, G.R. and R.S. Coffin, *Construction and characterization of an oncolytic HSV vector containing a fusogenic glycoprotein and prodrug activation for enhanced local tumor control.* Methods Mol Biol, 2009. **542**: p. 551-64.
273. Middleton, M.R., et al., *An open-label, single-arm, phase II clinical trial of RP1, an enhanced potency oncolytic herpes virus, combined with nivolumab in four solid tumor types: Initial results from the skin cancer cohorts.* Journal of Clinical Oncology, 2020. **38**(15_suppl): p. e22050-e22050.
274. Yun, C.O., *Overcoming the extracellular matrix barrier to improve intratumoral spread and therapeutic potential of oncolytic virotherapy.* Curr Opin Mol Ther, 2008. **10**(4): p. 356-61.
275. Guedan, S., et al., *Hyaluronidase expression by an oncolytic adenovirus enhances its intratumoral spread and suppresses tumor growth.* Mol Ther, 2010. **18**(7): p. 1275-83.
276. Kim, J.H., et al., *Relaxin expression from tumor-targeting adenoviruses and its intratumoral spread, apoptosis induction, and efficacy.* J Natl Cancer Inst, 2006. **98**(20): p. 1482-93.
277. Corban-Wilhelm, H., et al., *Cytosine deaminase versus thymidine kinase: a comparison of the antitumor activity.* Clin Exp Med, 2003. **3**(3): p. 150-6.
278. Cloughesy, T.F., et al., *Effect of Vocimagene Amiretrorepvec in Combination With Flucytosine vs Standard of Care on Survival Following Tumor Resection in Patients With Recurrent High-Grade*

Glioma: A Randomized Clinical Trial. JAMA Oncol, 2020. **6**(12): p. 1939-1946.
279. Barton, K.N., et al., *Phase I study of noninvasive imaging of adenovirus-mediated gene expression in the human prostate.* Mol Ther, 2008. **16**(10): p. 1761-9.
280. Russell, S.J., et al., *Remission of disseminated cancer after systemic oncolytic virotherapy.* Mayo Clin Proc, 2014. **89**(7): p. 926-33.
281. Curtsinger, J.M., et al., *Cutting edge: type I IFNs provide a third signal to CD8 T cells to stimulate clonal expansion and differentiation.* The Journal of Immunology, 2005. **174**(8): p. 4465-4469.
282. Willmon, C.L., et al., *Expression of IFN-beta enhances both efficacy and safety of oncolytic vesicular stomatitis virus for therapy of mesothelioma.* Cancer Res, 2009. **69**(19): p. 7713-20.
283. Willmon, C.L., et al., *Expression of IFN-beta enhances both efficacy and safety of oncolytic vesicular stomatitis virus for therapy of mesothelioma.* Cancer research, 2009. **69**(19): p. 7713-20.
284. Choi, I.K., et al., *Oncolytic adenovirus co-expressing IL-12 and IL-18 improves tumor-specific immunity via differentiation of T cells expressing IL-12Rbeta2 or IL-18Ralpha.* Gene therapy, 2011. **18**(9): p. 898-909.
285. Chang, D.Z., et al., *Granulocyte-macrophage colony stimulating factor: an adjuvant for cancer vaccines.* Hematology, 2004. **9**(3): p. 207-15.
286. Liu, B.L., et al., *ICP34.5 deleted herpes simplex virus with enhanced oncolytic, immune stimulating, and anti-tumour properties.* Gene therapy, 2003. **10**(4): p. 292-303.
287. McLaughlin, J.P., et al., *Immunization with a syngeneic tumor infected with recombinant vaccinia virus expressing granulocyte-macrophage colony-stimulating factor (GM-CSF) induces tumor regression and long-lasting systemic immunity.* Journal of immunotherapy, 1997. **20**(6): p. 449-59.
288. Mack, M., G. Riethmüller, and P. Kufer, *A small bispecific antibody construct expressed as a functional single-chain molecule with high tumor cell cytotoxicity.* Proceedings of the National Academy of Sciences, 1995. **92**(15): p. 7021-7025.
289. Offner, S., et al., *Induction of regular cytolytic T cell synapses by bispecific single-chain antibody constructs on MHC class I-negative tumor cells.* Molecular immunology, 2006. **43**(6): p. 763-771.
290. Yu, F., et al., *T-cell engager-armed oncolytic vaccinia virus significantly enhances antitumor therapy.* Molecular Therapy, 2014. **22**(1): p. 102-111.
291. Speck, T., et al., *Targeted BiTE Expression by an Oncolytic Vector Augments Therapeutic Efficacy Against Solid Tumors.* Clin Cancer Res, 2018. **24**(9): p. 2128-2137.
292. Porter, C.E., et al., *Oncolytic Adenovirus Armed with BiTE, Cytokine, and Checkpoint Inhibitor Enables CAR T Cells to Control the Growth of Heterogeneous Tumors.* Mol Ther, 2020. **28**(5): p. 1251-1262.
293. Zheng, M., et al., *Oncolytic Viruses for Cancer Therapy: Barriers and Recent Advances.* Mol Ther Oncolytics, 2019. **15**: p. 234-247.

294. DiPaola, R.S., et al., *A phase I trial of pox PSA vaccines (PROSTVAC-VF) with B7-1, ICAM-1, and LFA-3 co-stimulatory molecules (TRICOM) in patients with prostate cancer.* J Transl Med, 2006. **4**: p. 1.
295. Zamarin, D., et al., *Intratumoral modulation of the inducible co-stimulator ICOS by recombinant oncolytic virus promotes systemic anti-tumour immunity.* Nat Commun, 2017. **8**: p. 14340.
296. Zamarin, D. and J.D. Wolchok, *Potentiation of immunomodulatory antibody therapy with oncolytic viruses for treatment of cancer.* Mol Ther Oncolytics, 2014. **1**: p. 14004.
297. Calmels, B., et al., *Bypassing tumor-associated immune suppression with recombinant adenovirus constructs expressing membrane bound or secreted GITR-L.* Cancer Gene Ther, 2005. **12**(2): p. 198-205.
298. Holay, N., et al., *Sharpening the Edge for Precision Cancer Immunotherapy: Targeting Tumor Antigens through Oncolytic Vaccines.* Frontiers in immunology, 2017. **8**: p. 800-800.
299. Lichty, B.D., et al., *Going viral with cancer immunotherapy.* Nature Reviews Cancer, 2014. **14**(8): p. 559-567.
300. Liu, B.L., et al., *ICP34.5 deleted herpes simplex virus with enhanced oncolytic, immune stimulating, and anti-tumour properties.* Gene Ther, 2003. **10**(4): p. 292-303.
301. Andtbacka, R.H., et al., *Talimogene Laherparepvec Improves Durable Response Rate in Patients With Advanced Melanoma.* J Clin Oncol, 2015. **33**(25): p. 2780-8.
302. Andtbacka, R.H.I., et al., *Final analyses of OPTiM: a randomized phase III trial of talimogene laherparepvec versus granulocyte-macrophage colony-stimulating factor in unresectable stage III-IV melanoma.* J Immunother Cancer, 2019. **7**(1): p. 145.
303. Kaufman, H.L., et al., *Local and distant immunity induced by intralesional vaccination with an oncolytic herpes virus encoding GM-CSF in patients with stage IIIc and IV melanoma.* Ann Surg Oncol, 2010. **17**(3): p. 718-30.
304. Xia, Z.J., et al., *[Phase III randomized clinical trial of intratumoral injection of E1B gene-deleted adenovirus (H101) combined with cisplatin-based chemotherapy in treating squamous cell cancer of head and neck or esophagus].* Ai Zheng, 2004. **23**(12): p. 1666-70.
305. Garber, K., *China Approves World's First Oncolytic Virus Therapy For Cancer Treatment.* JNCI: Journal of the National Cancer Institute, 2006. **98**(5): p. 298-300.
306. Lang, F.F., et al., *Phase I Study of DNX-2401 (Delta-24-RGD) Oncolytic Adenovirus: Replication and Immunotherapeutic Effects in Recurrent Malignant Glioma.* J Clin Oncol, 2018. **36**(14): p. 1419-1427.
307. Heo, J., et al., *Randomized dose-finding clinical trial of oncolytic immunotherapeutic vaccinia JX-594 in liver cancer.* Nat Med, 2013. **19**(3): p. 329-36.
308. Park, S.H., et al., *Phase 1b Trial of Biweekly Intravenous Pexa-Vec (JX-594), an Oncolytic and Immunotherapeutic Vaccinia Virus in Colorectal Cancer.* Mol Ther, 2015. **23**(9): p. 1532-40.

309. Abou-Alfa, G.K., et al., *PHOCUS: A phase 3 randomized, open-label study comparing the oncolytic immunotherapy Pexa-Vec followed by sorafenib (SOR) vs SOR in patients with advanced hepatocellular carcinoma (HCC) without prior systemic therapy*. 2016, American Society of Clinical Oncology.
310. Singh, P., et al., *Development of PROSTVAC immunotherapy in prostate cancer.* Future Oncol, 2015. **11**(15): p. 2137-48.
311. Madan, R.A., et al., *Ipilimumab and a poxviral vaccine targeting prostate-specific antigen in metastatic castration-resistant prostate cancer: a phase 1 dose-escalation trial.* Lancet Oncol, 2012. **13**(5): p. 501-8.
312. Viralytics. *Final data from CALM: A phase II study of Coxsackievirus A21 (CVA21) oncolytic virus immunotherapy in patients with advanced melanoma*. 2015; Available from: https://viralytics.com/wp-content/uploads/2015/03/150601-AmSocClinOnc-CALM-Poster.pdf.
313. Desjardins, A., et al., *Recurrent Glioblastoma Treated with Recombinant Poliovirus.* N Engl J Med, 2018. **379**(2): p. 150-161.
314. Chiu, M., et al., *Combination therapy with oncolytic viruses and immune checkpoint inhibitors.* Expert Opin Biol Ther, 2020. **20**(6): p. 635-652.
315. Puzanov, I., et al., *Talimogene Laherparepvec in Combination With Ipilimumab in Previously Untreated, Unresectable Stage IIIB-IV Melanoma.* J Clin Oncol, 2016. **34**(22): p. 2619-26.
316. Chesney, J., et al., *Randomized, Open-Label Phase II Study Evaluating the Efficacy and Safety of Talimogene Laherparepvec in Combination With Ipilimumab Versus Ipilimumab Alone in Patients With Advanced, Unresectable Melanoma.* J Clin Oncol, 2018. **36**(17): p. 1658-1667.
317. Ribas, A., et al., *Association of response to programmed death receptor 1 (PD-1) blockade with pembrolizumab (MK-3475) with an interferon-inflammatory immune gene signature*. 2015, American Society of Clinical Oncology.
318. Ribas, A., et al., *1037O MASTERKEY-265: A phase III, randomized, placebo (Pbo)-controlled study of talimogene laherparepvec (T) plus pembrolizumab (P) for unresectable stage IIIB–IVM1c melanoma (MEL).* Annals of Oncology, 2021. **32**: p. S868-S869.
319. Travassos da Rosa, A.P., et al., *Carajas and Maraba viruses, two new vesiculoviruses isolated from phlebotomine sand flies in Brazil.* Am J Trop Med Hyg, 1984. **33**(5): p. 999-1006.
320. Brun, J., et al., *Identification of genetically modified Maraba virus as an oncolytic rhabdovirus.* Mol Ther, 2010. **18**(8): p. 1440-9.
321. Pol, J.G., et al., *Development and applications of oncolytic Maraba virus vaccines.* Oncolytic virotherapy, 2018. **7**: p. 117-128.
322. Lichty, B.D., et al., *Vesicular stomatitis virus: re-inventing the bullet.* Trends Mol Med, 2004. **10**(5): p. 210-6.
323. Pol, J.G., et al., *Maraba virus as a potent oncolytic vaccine vector.* Mol Ther, 2014. **22**(2): p. 420-429.
324. Tong, J.G., et al., *Evidence for differential viral oncolytic efficacy in an in vitro model of epithelial ovarian cancer metastasis.* Mol Ther Oncolytics, 2015. **2**: p. 15013.

325. Atherton, M.J., et al., *Customized Viral Immunotherapy for HPV-Associated Cancer.* Cancer Immunol Res, 2017. **5**(10): p. 847-859.
326. Le Boeuf, F., et al., *Oncolytic Maraba Virus MG1 as a Treatment for Sarcoma.* Int J Cancer, 2017. **141**(6): p. 1257-1264.
327. Atherton, M.J., et al., *Transforming the prostatic tumor microenvironment with oncolytic virotherapy.* Oncoimmunology, 2018. **7**(7): p. e1445459.
328. Alkayyal, A.A., et al., *NK-Cell Recruitment Is Necessary for Eradication of Peritoneal Carcinomatosis with an IL12-Expressing Maraba Virus Cellular Vaccine.* Cancer Immunol Res, 2017. **5**(3): p. 211-221.
329. Bourgeois-Daigneault, M.C., et al., *Combination of Paclitaxel and MG1 oncolytic virus as a successful strategy for breast cancer treatment.* Breast Cancer Res, 2016. **18**(1): p. 83.
330. Bourgeois-Daigneault, M.C., et al., *Neoadjuvant oncolytic virotherapy before surgery sensitizes triple-negative breast cancer to immune checkpoint therapy.* Sci Transl Med, 2018. **10**(422).
331. Mahoney, D.J., et al., *Virus-tumor interactome screen reveals ER stress response can reprogram resistant cancers for oncolytic virus-triggered caspase-2 cell death.* Cancer Cell, 2011. **20**(4): p. 443-56.
332. Conrad, D.P., et al., *Leukemia cell-rhabdovirus vaccine: personalized immunotherapy for acute lymphoblastic leukemia.* Clin Cancer Res, 2013. **19**(14): p. 3832-43.
333. Tong, J.G., et al., *Spatial and temporal epithelial ovarian cancer cell heterogeneity impacts Maraba virus oncolytic potential.* BMC Cancer, 2017. **17**(1): p. 594.
334. Atherton, M.J., et al., *Preclinical development of peptide vaccination combined with oncolytic MG1-E6E7 for HPV-associated cancer.* Vaccine, 2018. **36**(16): p. 2181-2192.
335. Kim, R., *Effects of surgery and anesthetic choice on immunosuppression and cancer recurrence.* J Transl Med, 2018. **16**(1): p. 8.
336. Tai, L.H., et al., *Preventing postoperative metastatic disease by inhibiting surgery-induced dysfunction in natural killer cells.* Cancer Res, 2013. **73**(1): p. 97-107.
337. Jonker, D.J., et al., *Phase I study of oncolytic virus (OV) MG1 maraba/MAGE-A3 (MG1MA3), with and without transgenic MAGE-A3 adenovirus vaccine (AdMA3) in incurable advanced/metastatic MAGE-A3-expressing solid tumours: CCTG IND. 214*. 2017, American Society of Clinical Oncology.
338. Workman, P., et al., *Guidelines for the welfare and use of animals in cancer research.* British Journal of Cancer, 2010. **102**(11): p. 1555-1577.
339. Filley, A.C. and M. Dey, *Immune System, Friend or Foe of Oncolytic Virotherapy?* Front Oncol, 2017. **7**: p. 106.
340. Jayawardena, N., et al., *Virus-Receptor Interactions and Virus Neutralization: Insights for Oncolytic Virus Development.* Oncolytic virotherapy, 2020. **9**: p. 1-15.

341. Power, A.T. and J.C. Bell, *Taming the Trojan horse: optimizing dynamic carrier cell/oncolytic virus systems for cancer biotherapy.* Gene Ther, 2008. **15**(10): p. 772-9.
342. García-Castro, J., et al., *Treatment of metastatic neuroblastoma with systemic oncolytic virotherapy delivered by autologous mesenchymal stem cells: an exploratory study.* Cancer Gene Ther, 2010. **17**(7): p. 476-83.
343. Mader, E.K., et al., *Mesenchymal stem cell carriers protect oncolytic measles viruses from antibody neutralization in an orthotopic ovarian cancer therapy model.* Clin Cancer Res, 2009. **15**(23): p. 7246-55.
344. Ong, H.T., et al., *Evaluation of T cells as carriers for systemic measles virotherapy in the presence of antiviral antibodies.* Gene Ther, 2007. **14**(4): p. 324-33.
345. Qiao, J., et al., *Loading of oncolytic vesicular stomatitis virus onto antigen-specific T cells enhances the efficacy of adoptive T-cell therapy of tumors.* Gene Ther, 2008. **15**(8): p. 604-16.
346. Ilett, E.J., et al., *Internalization of oncolytic reovirus by human dendritic cell carriers protects the virus from neutralization.* Clin Cancer Res, 2011. **17**(9): p. 2767-76.
347. Ilett, E.J., et al., *Dendritic cells and T cells deliver oncolytic reovirus for tumour killing despite pre-existing anti-viral immunity.* Gene Ther, 2009. **16**(5): p. 689-99.
348. Achard, C., et al., *Lighting a Fire in the Tumor Microenvironment Using Oncolytic Immunotherapy.* EBioMedicine, 2018. **31**: p. 17-24.
349. Ivashkiv, L.B. and L.T. Donlin, *Regulation of type I interferon responses.* Nature Reviews Immunology, 2014. **14**(1): p. 36-49.
350. Geoffroy, K. and M.-C. Bourgeois-Daigneault, *The pros and cons of interferons for oncolytic virotherapy.* Cytokine & Growth Factor Reviews, 2020. **56**: p. 49-58.
351. Zitvogel, L., et al., *Type I interferons in anticancer immunity.* Nature Reviews Immunology, 2015. **15**(7): p. 405-414.
352. Kawai, T., et al., *IPS-1, an adaptor triggering RIG-I- and Mda5-mediated type I interferon induction.* Nat Immunol, 2005. **6**(10): p. 981-8.
353. Invivogen. *RIG-I-Like Receptors & Cytosolic DNA Sensors*. 2012; Available from: https://www.invivogen.com/review-rlr.
354. Fucikova, J., et al., *Detection of immunogenic cell death and its relevance for cancer therapy.* Cell Death & Disease, 2020. **11**(11): p. 1013.
355. Bommareddy, P.K., M. Shettigar, and H.L. Kaufman, *Integrating oncolytic viruses in combination cancer immunotherapy.* Nat Rev Immunol, 2018. **18**(8): p. 498-513.
356. Pol, J., et al., *Trial Watch: Immunogenic cell death inducers for anticancer chemotherapy.* Oncoimmunology, 2015. **4**(4): p. e1008866.
357. Krysko, D.V., et al., *Immunogenic cell death and DAMPs in cancer therapy.* Nat Rev Cancer, 2012. **12**(12): p. 860-75.
358. Mackay, F. and J.L. Browning, *BAFF: a fundamental survival factor for B cells.* Nat Rev Immunol, 2002. **2**(7): p. 465-75.
359. Sims, G.P., et al., *HMGB1 and RAGE in inflammation and cancer.* Annu Rev Immunol, 2010. **28**: p. 367-88.

360. Schall, T.J., *Biology of the RANTES/SIS cytokine family.* Cytokine, 1991. **3**(3): p. 165-83.
361. Mombelli, S., et al., *IL-17A and its homologs IL-25/IL-17E recruit the c-RAF/S6 kinase pathway and the generation of pro-oncogenic LMW-E in breast cancer cells.* Scientific Reports, 2015. **5**(1): p. 11874.
362. Schoenborn, J.R. and C.B. Wilson, *Regulation of Interferon-γ During Innate and Adaptive Immune Responses*, in *Advances in Immunology*. 2007, Academic Press. p. 41-101.
363. Tokunaga, R., et al., *CXCL9, CXCL10, CXCL11/CXCR3 axis for immune activation - A target for novel cancer therapy.* Cancer Treat Rev, 2018. **63**: p. 40-47.
364. Tugues, S., et al., *New insights into IL-12-mediated tumor suppression.* Cell Death & Differentiation, 2015. **22**(2): p. 237-246.
365. Hirata, A., et al., *Intratumoral IFN-α gene delivery reduces tumor-infiltrating regulatory T cells through the downregulation of tumor CCL17 expression.* Cancer Gene Therapy, 2019. **26**(9): p. 334-343.
366. Turner, N. and R. Grose, *Fibroblast growth factor signalling: from development to cancer.* Nature Reviews Cancer, 2010. **10**(2): p. 116-129.
367. Goel, H.L. and A.M. Mercurio, *VEGF targets the tumour cell.* Nature Reviews Cancer, 2013. **13**(12): p. 871-882.
368. Quintero-Fabián, S., et al., *Role of Matrix Metalloproteinases in Angiogenesis and Cancer.* Frontiers in Oncology, 2019. **9**(1370).
369. Singh, M., et al., *Intratumoral CD40 activation and checkpoint blockade induces T cell-mediated eradication of melanoma in the brain.* Nature Communications, 2017. **8**(1): p. 1447.
370. Liao, W., J.-X. Lin, and W.J. Leonard, *IL-2 family cytokines: new insights into the complex roles of IL-2 as a broad regulator of T helper cell differentiation.* Current opinion in immunology, 2011. **23**(5): p. 598-604.
371. Teague, R.M., et al., *Interleukin-15 rescues tolerant CD8+ T cells for use in adoptive immunotherapy of established tumors.* Nat Med, 2006. **12**(3): p. 335-41.
372. Ma, J., et al., *Characterization of virus-mediated immunogenic cancer cell death and the consequences for oncolytic virus-based immunotherapy of cancer.* Cell Death & Disease, 2020. **11**(1): p. 48.
373. Wang, W., et al., *Elucidating mechanisms of antitumor immunity mediated by live oncolytic vaccinia and heat-inactivated vaccinia.* Journal for immunotherapy of cancer, 2021. **9**(9): p. e002569.